

Towards fully computable error bounds for the
incompressible Navier-Stokes equations

Alejandro Ignacio Allendes Flores

Department of Mathematics and Statistics

University of Strathclyde

Glasgow, UK

March 2012

This thesis is submitted to the University of Strathclyde for the
degree of Doctor of Philosophy in the Faculty of Science.

The copyright of this thesis belongs to the author under the terms of the United Kingdom Copyright Acts as qualified by University of Strathclyde Regulation 3.50. Due acknowledgement must always be made of the use of any material in, or derived from, this thesis.

To Sole & Emma.

Acknowledgements

I would first like to express my deepest thanks to my supervisors, Dr. Gabriel Barrenechea and Professor Mark Ainsworth for all your guidance, support and motivation through this process. Also, a special thanks to Dr. Richard Rankin for your continuous support and contributions to my work.

Thanks also to all my friends Franck, Zafar, Wee Ping, Omer, Jill, Gaelle, Fabien, Luis, Ernesto, Puri, Brais, Enrique, Dante, José, Rodrigo and Liset for all your support and make me feel at home.

I would also like to express my gratitude to the members of the staff of the Department of Mathematics and Statistics of the University of Strathclyde.

The support of the Faculty of Science of the University of Strathclyde and Comisión Nacional de Investigación Científica y Tecnológica - CONICYT (Chile).

To my family, your love and support has made this possible.

Thank you all.

Abstract

We obtain fully computable constant free a posteriori error bounds on simplicial meshes for: a nonconforming finite element approximations for a Stokes problem and a low-order conforming and low-order stabilized conforming finite element approximations for Poisson, Stokes and Advection-Reaction-Diffusion problems. All the estimators are completely free of unknown constants and provide guaranteed numerical bounds on natural norms, in terms of a lower bound for the inf-sup constant of the underlying continuous problem in the Stokes case. These estimators are also shown to provide a lower bound for the natural norms of the error up to a constant and higher order data oscillation terms. In the Stokes problem, the adaptive selection of the stabilization parameter appears as an application. Numerical results are presented illustrating the theory and the performance of the error estimators.

Contents

1	Introduction	1
2	Preliminaries.	8
2.1	Notation.	8
2.1.1	Finite element nomenclature.	9
2.1.2	Some preliminary results.	12
3	Computable error bounds for nonconforming Fortin–Soulie finite element approximation of the Stokes problem.	19
3.1	The model problem.	21
3.2	Nonconforming finite element approximation.	22
3.2.1	A Projection Operator.	23
3.3	The error equation.	25
3.4	Solution of the Neumann problem.	29
3.5	An orthogonal decomposition of the error.	30
3.6	A guaranteed upper bound for the error.	32
3.7	Efficiency of the estimator.	35
3.8	Nonhomogeneous boundary data.	41
3.8.1	A posteriori analysis for the nonhomogeneous problem.	43
3.8.2	The extension operator $E(\mathbf{d} - \mathcal{J}(\mathbf{d}))$ is an oscillation.	46
3.9	An explicit formula to compute the norm of the solution of the Neumann problem.	47
3.10	Numerical Results.	51
3.11	Conclusions	55

4	A review of the equilibrated residual method applied to a simple Poisson problem.	58
4.1	The error equation.	59
4.2	Equilibrated fluxes on regular partitions.	61
4.2.1	Procedure for the resolution of the boundary fluxes.	63
4.3	Solution of the Neumann problem.	66
4.4	A guaranteed upper bound for the error.	67
4.5	Efficiency of the estimator.	68
4.6	An explicit formula to compute the norm of the solution of the Neumann problem.	71
4.7	A numerical result.	73
4.8	Conclusions	75
5	Application of the equilibrated residual method to the Stokes problem using stabilized conforming finite element approximations.	77
5.1	Stabilized finite element methods.	78
5.1.1	Pressure-Stabilization.	79
5.1.2	Pressure-Velocity-Stabilization.	80
5.2	The error equation.	82
5.3	Construction of the equilibrated boundary fluxes.	83
5.4	Solution of the Neumann problem.	85
5.5	A guaranteed upper bound for the errors.	86
5.6	Efficiency of the estimator.	89
5.7	An explicit formula to compute the norm of the solution of the Neumann problem.	92
5.8	Numerical results.	96
5.9	An alternative guaranteed upper bound for the error.	99
5.10	Conclusions	101
6	On the adaptive selection of the parameter in stabilized finite element approximations.	103
6.1	An algorithm for selecting the stabilization parameter on a given mesh.	105
6.2	Selection of the stabilization parameter on a sequence of adaptively refined meshes.	114
6.3	Conclusions	119

7	Application of the equilibrated residual method to an Advection-Reaction-Diffusion problem.	120
7.1	Preliminaries.	121
7.2	The model problem.	128
7.3	A Stabilized finite element method (SUPG).	128
7.4	The error equation.	129
7.5	Construction of the equilibrated boundary fluxes in 3D.	130
7.6	Solution of the Neumann problem.	132
7.7	A guaranteed upper bound for the error.	133
7.8	Efficiency of the estimator.	134
7.9	An explicit formula to compute the norm of the solution of the Neumann problem.	138
7.10	Numerical results.	141
7.11	Conclusions.	147
8	Conclusions and future work.	149

Chapter 1

Introduction

The finite element method is a numerical procedure that allows one to obtain an approximation to the solution of an ordinary or partial differential equation under appropriate initial and boundary conditions. The finite element method has a solid theoretical foundation (see [40, 43, 52, 69, 74, 93, 95]) and has become one of the most used techniques in the approximation of differential equations. The efficiency of the finite element method relies on two distinct ingredients: the approximation capability of finite elements and the ability of the user to approximate his model in a proper mathematical setting.

At the very beginning, the analysis of the finite element method was developed in the framework of *a priori* analysis, which implies existence and uniqueness of a solution, regularity estimates and rate convergence estimates for sequence of approximations (cf. [52]). This process only gives information on the asymptotic behaviour of the approximation error. This drawback opened the door for new type of error estimation, called *a posteriori* error analysis and adaptive solution algorithms. The basic idea was to apply a mesh-adaptive procedure that modifies the finite dimensional space in order to control and reduce the error. Since the pioneering work of Babuška and Rheinboldt [26], the *a posteriori* error estimates technique together with related topics such as mesh refinement and adaptivity for standard conforming finite element approximation has reached a degree of maturity, as is shown in the following books and surveys [11, 28, 30, 68, 96, 103]. The literature on *a posteriori* error estimation for finite element approximation is vast, so in what follows we will present primarily the key references and work having a direct influence on our exposition.

Let us suppose our problem is posed on a domain Ω , in which a conforming regular partition \mathcal{P} is given. The aim of an adaptive finite element scheme is to identify the elements of \mathcal{P} in which the solution is poorly resolved, and then derive an appropriate procedure to refine such elements. A key ingredient in an adaptive finite element algorithm is the availability of an a posteriori error indicator η_K for the error over an individual element K . The analysis of adaptive methods is based on two main properties of the indicator. Firstly, the sum of the local indicators should provide a reliable upper bound for the total error $\|e\|_\Omega$ measured in a user-specified norm. This means that there exists a positive constant C which is independent of any mesh size, such that

$$\|e\|_\Omega^2 \leq C\eta^2 := C \sum_{K \in \mathcal{P}} \eta_K^2. \quad (1.1)$$

Secondly, the error indicator should be efficient in the sense that there exists a positive constant c , again independent of any mesh size, such that

$$c \eta_K^2 \leq \|e\|_{\tilde{K}}, \quad (1.2)$$

where \tilde{K} denotes a patch consisting of the element K together with neighbouring elements sharing a common node with it. In practice however, it is not always possible to show that the indicator is less than some positive constant multiple of the norm of the error since the data from the differential problem may belong to an infinite dimensional space. Instead we settle for the indicator being less than a positive constant multiple of the norm of the error plus terms which are expected to decrease at a rate faster than the error, provided that the data is sufficiently smooth, as the mesh is refined.

One of the most common types of error indicators are residual-based indicators. Residual-based indicators involve residuals of the discrete solution on the element and edges of the partition. From the early works in [26, 27] a wide variety of analysis has been performed to derive residual-based a posteriori error indicators for finite element approximations of two and three-dimensional problems. A great disadvantage of many of the available error estimators so far is that they present an unknown constant in the upper bound (like in (1.1)) on the error. Even when estimates (1.1) and (1.2) are sufficient to guarantee robust convergence of the adaptive algorithm (see [65, 89, 101]), the error estimator is often called upon to provide a stopping criterion for the adaptive procedure for which knowledge of the actual value of the constant C appearing in the upper bound is required. Ideally, we would like to have a fully computable upper bound

of the form

$$\|e\|^2 \leq \eta^2 := \sum_{K \in \mathcal{P}} \eta_K^2. \quad (1.3)$$

If the error indicator η is known to provide an estimate for the error of this type, then we shall say that η is an a posteriori error estimator.

Among all the different problems in which the a posteriori finite element analysis is being applied, one of the most challenging are the ones where the phenomena can be modeled as an advection-reaction-diffusion problem. One of the most representative examples in this area are the Navier-Stokes equations. In the quest of obtaining realistic error estimates for this problem, the first objective is to develop a discretization technique that is able to handle its two major difficulties, namely: (1) singular behaviours, and (2) saddle point structures.

The analysis of the full non-linear problem is a daunting task. Therefore, we treat each of these two difficulties separately. Namely, the study shall be conducted for the incompressible Stokes problem,

$$(1) \left\{ \begin{array}{l} -\nu \Delta \mathbf{u} + \nabla p = \mathbf{f} \quad \text{in } \Omega, \\ \nabla \cdot \mathbf{u} = 0 \quad \text{in } \Omega, \\ \mathbf{u} = \mathbf{0} \quad \text{on } \partial\Omega, \end{array} \right. \quad (1.4)$$

and the advection-reaction-diffusion problem,

$$(2) \left\{ \begin{array}{l} -\nu \Delta u + \mathbf{a} \cdot \nabla u + \kappa u = f \quad \text{in } \Omega, \\ u = 0 \quad \text{on } \partial\Omega. \end{array} \right. \quad (1.5)$$

The numerical approximation of the Stokes problem (1.4), generally follows one of two complementary approaches. The first consists of using discrete velocity-pressure spaces satisfying a discrete inf-sup condition (cf. [42]). Many such methods are available in the literature (see [10, 20] for extensive reviews).

In the family of inf-sup stable nonconforming approximations to (1.4) the first order Crouzeix–Raviart [58] and the second order Fortin–Soulie [71] finite element schemes have become very popular. One of the first works to address a posteriori estimation for the first order nonconforming Crouzeix–Raviart scheme was the important paper of Dari et al. [60] who obtained two sided bounds on the error measured in an broken energy norm up to generic constants using a technique based on a Helmholtz decomposition. These ideas were later extended to nonconforming mixed finite element approximation of Stokes flow [59], not only obtained for the Crouzeix–Raviart

finite element approximation but for the second order nonconforming Fortin–Soulie finite element approximation as well. Subsequently, it was shown in [2] and [66] how computable upper bounds can be derived for the Crouzeix–Raviart scheme for a linear second order elliptic problem and a Stokes flow, respectively. More recently, in [13] and [14] the authors provide a fully computable a posteriori error bound on the broken energy norm of the error in the nonconforming finite element approximation on triangles of arbitrary order of a linear second order elliptic problem. As a first result is this work, in Chapter 3, which is based on [6], we combined all the previous reference techniques to obtain a fully computable a posteriori error estimator for a Fortin–Soulie finite element approximation for the Stokes flow.

One perceived drawback of the inf-sup stable approach is the well known fact that low-order combinations of finite element spaces do not satisfy the inf-sup condition. To eliminate this constraint so that more natural finite element spaces can be used, one may add so-called stabilizing terms to the discrete formulation. These stabilizing terms can depend on residuals of the equation at the element level, or can simply be based on compensating for the inf-sup deficiency of the pressure approximation. In the last two decades, a few residual-based a posteriori error estimator have been developed for different conforming and conforming stabilized methods for the Stokes problem (see [20, 83, 108]).

In a counter intuitive manner, deriving computable error bounds for conforming finite element approximations needs to follow a totally and more involved different approach from the one of nonconforming schemes. One choice to derive computable error estimator for conforming methods is the equilibrated residual method [10, 11]. In this method edgewise contributions, which sum up to zero, are added to the residual equation such that the residuals are in equilibrium over each element. The estimator then is given explicitly as the solution of a local Neumann problem, which allows one to obtain a fully computable a posteriori error estimator. This technique, has been applied to linear second order elliptic, singularly perturbed reaction-diffusion, and linear elasticity problems in [5, 9, 12, 15–17].

As a second part of this work, in Chapters 5 and 6, which are based on [8], we provide an actual computable numerical bound on the error in a natural norm for the Stokes problem, which can be applied to a wide family of conforming stabilized finite element methods. This estimator was obtained by combining the Helmholtz decomposition from the nonconforming setting and the equilibrated residual method in conjunction with an explicit solution of the related local Neumann problem. We also present a procedure to compute near-optimal values for

stabilization parameters presented in stabilized methods. We mention that similar results were obtained in [75], where a unified framework to obtain computable a posteriori error estimators was given for a Stokes flow, but in the case of low-order conforming stabilized finite element methods the authors only consider three stabilized methods with stabilization only in the mass conservation equation with fixed stabilization parameters.

The advection-reaction-diffusion problem (1.5) is much more complicated. Since the standard Galerkin finite element formulation usually yields inaccurate approximate solutions to this problem, due to loss of stability and it can not approximate solutions inside layers, many different finite element schemes have been proposed in order to achieve robustness with respect to the physical parameters, which guide the behaviour of the solution. Finite element schemes such as mixed, discontinuous Galerkin, nonconforming and stabilized methods are a few of the many available techniques in the literature. We mention [98] as representative of the work. Now, from the a posteriori point of view, for mixed and discontinuous Galerkin approximations in [106] and [70], the authors developed fully computable error bounds for the error measured in an energy norm, being semi-robust in the sense that local lower error bounds depends on the local Péclet number and they achieved robustness if the error is measured in an augmented norm consisting of the energy (semi)norm and a dual norm. For nonconforming and stabilized finite element approximations a posteriori error estimators have been proposed in [19, 24, 36, 99, 105], but, as far as we are aware of, the majority of these estimators are not actually computable since they involve either a generic unknown constant in the upper bound on the error or they are based on the solution of local infinite-dimensional problems.

As a third part of this work, following the same steps as in [8] and based on the generalization of the equilibrated residual method for the three dimensional case in [16], in Chapter 7 we provide a fully computable a posteriori error estimator for the advection-reaction-diffusion problem approximated using a stabilized SUPG (cf. [46]) finite element method in two and three space dimensions.

A crucial step in the development of fully computable error estimators is to rewrite the residual functional related to the equation that is satisfied by the errors in the finite element approximation (the error equation) as the following local Neumann problem,

$$\begin{aligned} -\mathbf{div} \boldsymbol{\sigma}_K &= p_K && \text{on } K \\ \boldsymbol{\sigma}_K \cdot \mathbf{n} &= p_{\gamma,K} && \text{in } \partial K, \end{aligned} \tag{1.6}$$

for given data p_K and $p_{\gamma,K}$, being polynomial functions defined on the element and each edge of the element, respectively, being related to element and edge residuals of the equation. As we will show in later sections, this rewriting of the residual functional can be used for a Poisson, Stokes and Advection-Reaction-Diffusion problems, using nonconforming and conforming (conforming stabilized) finite element approximations. In order to guarantee the existence of a solution to (1.6), it is well known that the problem data need to satisfy a compatibility condition. To ensure that this condition is satisfied, for nonconforming schemes a suitable projection operator can be constructed which can be incorporated into the error equation leading to the desired compatibility. For conforming schemes the construction in the equilibrated residual method for the edge contributions is done to guarantee this compatibility (cf. [11]). Finally, following the ideas from [94] explicit solutions can be obtained for such problem.

The aim of this work is to obtain fully computable a posteriori error estimator, first for a Stokes problem using a second order nonconforming Fortin-Soulie finite element approximation and also using low-order stabilized finite element approximations. The analysis will be developed only in the two dimensional case for the Stokes case. Later, we will provide a fully computable a posteriori error estimator for the advection-reaction-diffusion problem, but now the analysis will be given in the two and three dimensional case. In the latter case our error estimator is not fully robust with respect to the physical parameters of the equation, but is still useful for practical computations.

The remainder of this thesis is organised as follows. In Chapter 2 we define some notation of the partitioning of the domain over which the model problems are posed, then define the common notation and present some standard results which we use throughout this thesis. The chapter is concluded with an important result which will allow us to obtain explicit solutions to the Neumann problem (1.6). In Chapter 3 we perform the a posteriori error analysis which will provide a fully computable a posteriori error estimator for the Stokes problem using a second order nonconforming Fortin-Soulie finite element approximation. In Chapter 4 we provide a review of the equilibrated residual method from [11], in order to clarify how the edge contributions, that allows one to satisfy the compatibility condition of the Neumann problem, can be obtained for conforming methods on regular partitions of the domain. In Chapter 5 we perform the a posteriori error analysis which will also provide a fully computable a posteriori error estimator for the Stokes problem using now a wide family of conforming stabilized finite element approximations and in Chapter 6 we present a procedure to approximate the optimal value of the stabilization

parameter for also a wide variety of conforming stabilized methods. Finally in Chapter 7, we present a generalization of the a posteriori analysis for a stabilized finite element approximation of a three-dimensional advection-reaction-diffusion problem.

Chapter 2

Preliminaries.

The aim of this section is to introduce notation and present some standard results, which will be used throughout the manuscript, for which we follow the standard theory of finite element analysis as described in the books of Brenner and Scott [40], Ciarlet [52] and Ern and Guermond [69].

2.1 Notation.

Let $G \subseteq \mathbb{R}^d$, where $d = 1, 2$, be a bounded open domain. We denote by \overline{G} the closure of G . The Lebesgue space of square integrable functions over G is denoted by $L^2(G)$, $L_0^2(G)$ represents functions belonging to $L^2(G)$ with zero average in G and $L^\infty(G)$ denotes the space of essentially bounded functions, i.e.

$$L^2(G) = \left\{ v : \int_G |v(x)|^2 dx =: \|v\|_{L^2(G)}^2 < \infty \right\},$$

$$L_0^2(G) = \left\{ v \in L^2(G) : \int_G v \, dx = 0 \right\},$$

and

$$L^\infty(G) = \{ v : \text{ess sup}_{x \in G} |v(x)| =: \|v\|_{L^\infty(G)} < \infty \}.$$

For any two scalar functions $u, v \in L^2(G)$ or vector-valued functions $\mathbf{u}, \mathbf{v} \in L^2(G)^2$ or matrix-valued functions $\underline{\mathbf{u}}, \underline{\mathbf{v}} \in L^2(G)^{2 \times 2}$, we choose $(\cdot, \cdot)_G$ to denote:

$$\begin{aligned}
(u, v)_G &= \int_G uv \, dx && \text{the inner product in } L^2(G) \times L^2(G), \\
(\mathbf{u}, \mathbf{v})_G &= \int_G \mathbf{u} \cdot \mathbf{v} \, dx && \text{the inner product in } L^2(G)^2 \times L^2(G)^2, \\
(\underline{\underline{\mathbf{u}}}, \underline{\underline{\mathbf{v}}})_G &= \int_G \underline{\underline{\mathbf{u}}} : \underline{\underline{\mathbf{v}}} \, dx = \sum_{i,j=1}^2 \int_G u_{ij} v_{ij} \, dx && \text{the inner product in } L^2(G)^{2 \times 2} \times L^2(G)^{2 \times 2}.
\end{aligned}$$

For scalar functions $v = v(x, y)$, we let the gradient and curl operators to be defined by

$$\nabla v = \left(\frac{\partial v}{\partial x}, \frac{\partial v}{\partial y} \right) \quad \text{and} \quad \text{curl } v = \left(\frac{\partial v}{\partial y}, -\frac{\partial v}{\partial x} \right),$$

respectively. For vector valued functions $\mathbf{v} = [v_1(x, y), v_2(x, y)]$, we let the divergence, gradient and curl operators be defined by

$$\begin{aligned}
\mathbf{div } \mathbf{v} &= \nabla \cdot \mathbf{v} = \frac{\partial v_1}{\partial x} + \frac{\partial v_2}{\partial y}, \\
\nabla \mathbf{v} &= \begin{bmatrix} \frac{\partial v_1}{\partial x} & \frac{\partial v_1}{\partial y} \\ \frac{\partial v_2}{\partial x} & \frac{\partial v_2}{\partial y} \end{bmatrix} \quad \text{and} \quad \text{curl } \mathbf{v} = \begin{bmatrix} \frac{\partial v_1}{\partial y} & -\frac{\partial v_1}{\partial x} \\ \frac{\partial v_2}{\partial y} & -\frac{\partial v_2}{\partial x} \end{bmatrix},
\end{aligned}$$

respectively. For a matrix valued function $\underline{\underline{\mathbf{A}}} = [A_{ij}(x, y)]_{2 \times 2}$, the divergence of $\underline{\underline{\mathbf{A}}}$ is the vector valued function

$$\mathbf{div } \underline{\underline{\mathbf{A}}} = \left[\frac{\partial A_{11}}{\partial x} + \frac{\partial A_{12}}{\partial y}, \frac{\partial A_{21}}{\partial x} + \frac{\partial A_{22}}{\partial y} \right].$$

We shall constantly use Lebesgue and Sobolev spaces (cf. [1, 86, 90]): The space $H^1(G)$ is the usual Sobolev space, $H_0^1(G)$ denotes the subspace of $H^1(G)$ consisting of functions whose trace is zero on the boundary of G and $H^{-1}(\Omega)$ denote the dual of $H_0^1(\Omega)$ with respect to the $L^2(\Omega)$ inner product. The space $\mathbf{H}(\mathbf{div}, G)$ denotes the space of square integrable vector fields whose divergence is also a square integrable function.

The norm of the space $H^1(G)$ is denoted by $\|\cdot\|_{H^1(G)}$ while $|\cdot|_{H^1(G)}$ is used to denote the semi-norm.

We use bold letters to denote the vector-valued counterparts of the Sobolev and Lebesgue spaces, e.g., $\mathbf{H}_0^1(G) = H_0^1(G) \times H_0^1(G)$, and use an extra under accent to denote their matrix-valued counterparts, e.g. $\underline{\underline{\mathbf{L}}}^2(G) = L^2(G)^{2 \times 2}$.

2.1.1 Finite element nomenclature.

For convenience, we shall summarise all the notations used throughout the manuscript related to the triangulation of the domain.

Let $\Omega \subset \mathbb{R}^2$ be an open simple polygonal domain with boundary Γ . Let $\{\mathcal{P}\}$ be a family of regular triangulations of Ω , in the sense described in Ciarlet [52].

For a fixed triangulation \mathcal{P} let:

- \mathcal{E} denote the set of all edges;
- $\mathcal{E}_I \subset \mathcal{E}$ denote the set of internal edges;
- $\mathcal{E}_\Gamma \subset \mathcal{E}$ denote the set of boundary edges;
- \mathcal{V} index the set $\{\mathbf{x}_n\}_{n \in \mathcal{V}}$ of all element vertices;
- \mathcal{N} denote the set of all element vertices and edge midpoints;
- \mathcal{N}_Γ denote the element vertices and midpoints located on the boundary Γ ;
- \mathcal{G}_I index the set $\{\mathbf{x}_n\}_{n \in \mathcal{G}_I}$ consisting of the two Gauss–Legendre points on each edge $\gamma \in \mathcal{E}_I$;
- \mathcal{G}_Γ index the set $\{\mathbf{x}_n\}_{n \in \mathcal{G}_\Gamma}$ consisting of the two Gauss–Legendre points that lie on an edge $\gamma \in \mathcal{E}_\Gamma$;
- $\Omega_n = \{K \in \mathcal{P} : \mathbf{x}_n \in \overline{K} \text{ for a fixed } n \in \mathcal{V}\}$ is the patch consisting of elements for which \mathbf{x}_n is a vertex;
- $\mathcal{E}_n = \{\gamma \in \mathcal{E} : \mathbf{x}_n \in \overline{\gamma} \text{ for a fixed } n \in \mathcal{V}\}$;
- λ_n denote the function which is piecewise linear on \mathcal{P} and vanishes at all the vertices in \mathcal{P} , except \mathbf{x}_n , where it takes the value one, i.e.

$$\lambda_n(\mathbf{x}_m) = \delta_{nm} \quad n, m \in \mathcal{V} \text{ where } \delta_{nm} \text{ denote the Kronecker symbol,}$$

and we also define the vector-valued counterpart as follows

$$\boldsymbol{\lambda}_n^{(1)} = [\lambda_n, 0], \quad \boldsymbol{\lambda}_n^{(2)} = [0, \lambda_n].$$

For the fixed partition \mathcal{P} let $H^1(\mathcal{P}) = \{v : v|_K \in H^1(K)\}$ denote the broken space which consists of functions whose restriction to an individual element K are locally $H^1(K)$.

For an element $K \in \mathcal{P}$ let:

- $\mathbb{P}_n(K)$ denote the space of polynomials on K of total degree at most n ;
- \mathcal{E}_K denote the set containing the individual edges of the element K ;

- \mathcal{V}_K index the set $\{\mathbf{x}_n\}_{n \in \mathcal{V}_K}$ of all vertices of the element K ;
- \mathcal{N}_K denote the set of all element vertices and edge midpoints of the element K ;
- $\tilde{\Omega}_K = \{K' \in \mathcal{P} : \overline{K'} \cap \overline{K} \neq \emptyset\}$;
- $\Omega_K = \{K' \in \mathcal{P} : \mathcal{E}_K \cap \mathcal{E}_{K'} \neq \emptyset\}$;
- $|K|$ denote the area of K ;
- h_K denote the length of the longest edge of element K ;
- $\hat{\mathbf{n}}_\gamma^K$ denote the unit exterior normal vector to edge $\gamma \in \mathcal{E}_K$.
- $\bar{v}_K = \frac{1}{|K|} \int_K v \, dx$ denote the mean value of v on the element K and for a vector-valued function $\mathbf{v} = [v_1, v_2]$, then $\bar{\mathbf{v}}_K = [\bar{v}_{1K}, \bar{v}_{2K}]$.
- $v|_K$ denote the restriction of v to the element K .
- $\bar{\mathbf{x}}_K = \frac{1}{3} \sum_{i \in \mathcal{V}_K} \mathbf{x}_i$.

For an edge $\gamma \in \mathcal{E}$ let:

- $\mathbb{P}_n(\gamma)$ denote the space of polynomials on γ of total degree at most n ;
- $\mathcal{V}_\gamma = \{n \in \mathcal{V} : \mathbf{x}_n \in \overline{\gamma}\}$ denote the set of endpoints of an edge γ ;
- $\Omega_\gamma = \{K \in \mathcal{P} : \gamma \in \mathcal{E}_K\}$;
- $|\gamma|$ denote the length of γ ;
- $\bar{v}_\gamma = \frac{1}{|\gamma|} \int_\gamma v \, ds$ denote the mean value of v on the edge γ and for a vector-valued function $\mathbf{v} = [v_1, v_2]$, then $\bar{\mathbf{v}}_\gamma = [\bar{v}_{1\gamma}, \bar{v}_{2\gamma}]$.
- s_γ denote the arc length parameter on the edge γ ;
- $\hat{\mathbf{n}}_\gamma$ denote a unit normal vector to the edge γ , oriented such that, in case of an exterior edge $\gamma \in \mathcal{E}_\Gamma$ the vector $\hat{\mathbf{n}}_\gamma$ is always taken to be the unit exterior normal on Γ , denoted by $\hat{\mathbf{n}}_\Gamma$;
- $\hat{\mathbf{t}}_\gamma$ denote the corresponding unit tangent vector associated with $\hat{\mathbf{n}}_\gamma$, rotated ninety degrees anti clockwise with respect to $\hat{\mathbf{n}}_\gamma$;

- $v|_\gamma$ denote the restriction of v to the edge γ .

The normal and tangent vectors for an element satisfy the identities $\mathbf{n}_\gamma^K = |\gamma|\hat{\mathbf{n}}_\gamma^K$ and $\mathbf{t}_\gamma^K = |\gamma|\hat{\mathbf{t}}_\gamma^K$.

Finally, in the rest of the manuscript we denote by c or C any constant which does not depend on any mesh size or any physical parameter related to any of the problems that we will present and \mathbf{I} will denote the two by two identity matrix.

2.1.2 Some preliminary results.

In this section we will present some standard results, that we will frequently use through all the manuscript.

Let $\Pi_K : L^2(K) \rightarrow \mathbb{P}_1(K)$ be a projection operator, characterized as

$$(\phi - \Pi_K(\phi), p)_K = 0 \quad \forall p \in \mathbb{P}_1(K). \quad (2.1)$$

Now, $\mathbf{\Pi}_K$ will denote its vector counter-part. We will also frequently use the following result.

Theorem 2.1.1. (*Optimal Poincaré inequality for convex domains, see [33, 92]*).

Let $K \in \mathcal{P}$. Then

$$\|v - \bar{v}_K\|_{L^2(K)} \leq \frac{d}{\pi} \|\nabla v\|_{L^2(K)} \quad \text{for all } v \in H^1(K). \quad (2.2)$$

where d is the diameter of K .

An important role will be played by locally supported, nonnegative functions that are commonly referred to as bubble functions, and it will be useful to consider the effect of choosing these functions as a test function on equations related to the error in the finite element approximation.

The next result shows that an interior bubble function $\beta_K = \prod_{n \in \mathcal{V}_K} \lambda_n \in H_0^1(K)$, preserves the norm up to a constant.

Theorem 2.1.2. Let $\beta_K = \prod_{n \in \mathcal{V}_K} \lambda_n \in H_0^1(K)$. Then for any $p \in \mathbb{P}_n(K)$ with $n \geq 0$, there exists a constant C such that

$$\|\beta_K p\|_{L^2(K)} \leq \|p\|_{L^2(K)} \leq C \left\| \beta_K^{1/2} p \right\|_{L^2(K)},$$

and

$$\|\nabla(\beta_K p)\|_{L^2(K)} \leq C h_K^{-1} \|p\|_{L^2(K)},$$

where the constant C is independent of p and h_K .

The following result is to extend quantities defined on $\gamma \in \mathcal{E}_I$ (element interfaces), to the pair of elements sharing the interface by using edge bubble functions and state that the extension preserves norms, again up to a constant.

Theorem 2.1.3. *Let $\beta_\gamma = \prod_{n \in \mathcal{V}_\gamma} \lambda_n \in H_0^1(K \cup K')$ and $\beta_{\gamma|\gamma} \in H_0^1(\gamma)$ with γ being an edge share by elements $K, K' \in \mathcal{P}$. Then, for any $p \in \mathbb{P}_n(\gamma)$ with $n \geq 0$, there exists a constant C such that*

$$\|\beta_\gamma p\|_{L^2(\gamma)} \leq \|p\|_{L^2(\gamma)} \leq C \left\| \beta_\gamma^{1/2} p \right\|_{L^2(\gamma)},$$

and

$$h_K^{-1/2} \|\beta_\gamma p\|_{L^2(K)} + h_K^{1/2} \|\nabla(\beta_\gamma p)\|_{L^2(K)} \leq C \|p\|_{L^2(\gamma)},$$

where the constant C is independent of p and h_K .

More details about these results can be found in Section 2.3.1 in [11], Section 10.1.1 in [69] and Section 1.1 in [103]. Each one of the three previous results has an obvious extension to the vector-valued case.

For $K \in \mathcal{P}$, throughout we shall make use of the following formula:

$$(\lambda_i^l \lambda_j^m \lambda_k^n, 1)_K = \frac{2(l!m!n!)}{(l+m+n+2)!} |K|, \quad (2.3)$$

for $l, m, n \geq 0$ and $\mathcal{V}_K = \{i, j, k\}$ and, with $\mathcal{V}_\gamma = \{l, r\}$, for $m, n \geq 0$,

$$(\lambda_l^m, \lambda_r^n)_\gamma = \frac{m!n!}{(m+n+1)!} |\gamma|. \quad (2.4)$$

The following result presents a basis to polynomial functions of degree one defined on edges of the partition.

Lemma 2.1.4. *Any polynomial function $p \in \mathbb{P}_1(\gamma)$ can be written as*

$$p = (p, \lambda_l)_\gamma \frac{2}{|\gamma|} (2\lambda_l - \lambda_r) + (p, \lambda_r)_\gamma \frac{2}{|\gamma|} (2\lambda_r - \lambda_l), \quad (2.5)$$

where $\{l, r\} = \mathcal{V}_\gamma$.

Proof. Let $p = \alpha_l \lambda_l + \alpha_r \lambda_r$, where α_l and α_r are constants to be determined. Now, the unknowns satisfy the conditions

$$(\lambda_l, \lambda_l)_\gamma \alpha_l + (\lambda_l, \lambda_r)_\gamma \alpha_r = (p, \lambda_l)_\gamma \quad (2.6)$$

$$(\lambda_r, \lambda_l)_\gamma \alpha_l + (\lambda_r, \lambda_r)_\gamma \alpha_r = (p, \lambda_r)_\gamma \quad (2.7)$$

Equally well,

$$\mathbf{M}_\gamma \begin{bmatrix} \alpha_l \\ \alpha_r \end{bmatrix} = \begin{bmatrix} (p, \lambda_l)_\gamma \\ (p, \lambda_r)_\gamma \end{bmatrix}$$

where \mathbf{M}_γ is the mass matrix for the basis functions on the edge γ . A simple computation using (2.4) shows that

$$\mathbf{M}_\gamma = \frac{|\gamma|}{6} \begin{bmatrix} 2 & 1 \\ 1 & 2 \end{bmatrix},$$

and hence

$$\alpha_l = \frac{2}{|\gamma|} (2(p, \lambda_l)_\gamma - (p, \lambda_r)_\gamma) \quad \text{and} \quad \alpha_r = \frac{2}{|\gamma|} (2(p, \lambda_r)_\gamma - (p, \lambda_l)_\gamma).$$

Finally the actual function can be written as

$$\begin{aligned} p &= \frac{2}{|\gamma|} \left((2(p, \lambda_l)_\gamma - (p, \lambda_r)_\gamma) \lambda_l + (2(p, \lambda_r)_\gamma - (p, \lambda_l)_\gamma) \lambda_r \right) \\ &= (p, \lambda_l)_\gamma \left(\frac{2}{|\gamma|} (2\lambda_l - \lambda_r) \right) + (p, \lambda_r)_\gamma \left(\frac{2}{|\gamma|} (2\lambda_r - \lambda_l) \right), \end{aligned}$$

and the result follows. \square

In trying to obtain a fully computable quantity being equivalent to the error (up to higher order terms), in different problems, we will frequently need to solve, for each $K \in \mathcal{P}$, a local Neumann problem of the form: *Find $\boldsymbol{\sigma}_K$ such that,*

$$\begin{aligned} -\mathbf{div} \boldsymbol{\sigma}_K &= p_K \quad \text{in } K \\ \boldsymbol{\sigma}_K \cdot \hat{\mathbf{n}}_\gamma^K &= p_{\gamma,K} \quad \text{on each } \gamma \in \mathcal{E}_K, \end{aligned} \tag{2.8}$$

for given $p_K \in \mathbb{P}_1(K)$ and $p_{\gamma,K} \in \mathbb{P}_1(\gamma)$. This problem was first studied in [94], where a solution is given in terms of a Raviart–Thomas space, also in the scalar case, but in here we will present a different construction of such a function. To be able to obtain such solutions, the following functions will be useful. Let the edges, vertices, tangent vectors and unit normal vectors of an element $K \in \mathcal{P}$ be labelled as in Figure 2.1. The normal and tangent vectors for the element K satisfy, for $i \in \mathcal{V}_K = \{1, 2, 3\}$,

$$\begin{aligned} \mathbf{t}_i \cdot \mathbf{n}_i &= 0, \\ \mathbf{t}_1 \cdot \mathbf{n}_2 &= \mathbf{t}_2 \cdot \mathbf{n}_3 = \mathbf{t}_3 \cdot \mathbf{n}_1 = 2|K|, \\ \mathbf{t}_1 \cdot \mathbf{n}_3 &= \mathbf{t}_2 \cdot \mathbf{n}_1 = \mathbf{t}_3 \cdot \mathbf{n}_2 = -2|K|, \end{aligned} \tag{2.9}$$

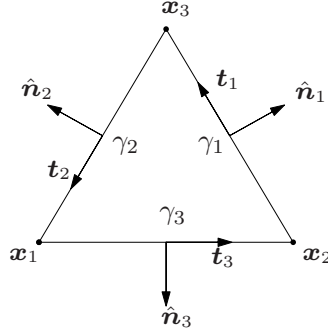


Figure 2.1: The labelling and orientation of the edges, vertices, tangents and unit normal vectors of elements K .

with $\mathbf{n}_i = |\gamma_i| \hat{\mathbf{n}}_i$, $\mathbf{t}_i = |\gamma_i| \hat{\mathbf{t}}_i$ and the linear functions λ_i restricted to the element K and on edges of K satisfy

$$\begin{aligned} \sum_{i \in \mathcal{V}_K} \lambda_i &= 1, & \sum_{i \in \mathcal{V}_\gamma} \lambda_i|_\gamma &= 1, \\ \nabla \lambda_i &= -\frac{1}{2|K|} \mathbf{n}_i, & \text{curl } \lambda_i &= \frac{1}{2|K|} \mathbf{t}_i. \end{aligned} \quad (2.10)$$

For the element K , let

$$\begin{aligned} \psi_{\lambda_2}^{(\gamma_1)} &= \frac{1}{2|K|} ((2\lambda_3 - 3\lambda_2 - \lambda_1)\lambda_3 \mathbf{t}_2 + (4\lambda_2 - \lambda_3 - 7\lambda_1)\lambda_2 \mathbf{t}_3), \\ \psi_{\lambda_3}^{(\gamma_1)} &= \frac{-1}{2|K|} ((4\lambda_3 - \lambda_2 - 7\lambda_1)\lambda_3 \mathbf{t}_2 + (2\lambda_2 - 3\lambda_3 - \lambda_1)\lambda_2 \mathbf{t}_3), \\ \tilde{\psi}_{\lambda_2}^{(\gamma_1)} &= \frac{1}{2|K|} ((2\lambda_3 + 3\lambda_3(\lambda_2 - \lambda_1))\mathbf{t}_2 + (4\lambda_2 + 3\lambda_2(\lambda_3 - \lambda_1))\mathbf{t}_3), \\ \tilde{\psi}_{\lambda_3}^{(\gamma_1)} &= \frac{-1}{2|K|} ((4\lambda_3 + 3\lambda_3(\lambda_2 - \lambda_1))\mathbf{t}_2 + (2\lambda_2 + 3\lambda_2(\lambda_3 - \lambda_1))\mathbf{t}_3). \end{aligned} \quad (2.11)$$

with $\psi_{\lambda_3}^{(\gamma_2)}$, $\psi_{\lambda_1}^{(\gamma_2)}$, $\psi_{\lambda_1}^{(\gamma_3)}$, $\psi_{\lambda_2}^{(\gamma_3)}$, $\tilde{\psi}_{\lambda_3}^{(\gamma_2)}$, $\tilde{\psi}_{\lambda_1}^{(\gamma_2)}$, $\tilde{\psi}_{\lambda_1}^{(\gamma_3)}$ and $\tilde{\psi}_{\lambda_2}^{(\gamma_3)}$ being defined by permuting the indices in an anticlockwise sense, i.e.

$$\begin{aligned} \psi_{\lambda_3}^{(\gamma_2)} &= \frac{1}{2|K|} ((2\lambda_1 - 3\lambda_3 - \lambda_2)\lambda_1 \mathbf{t}_3 + (4\lambda_3 - \lambda_1 - 7\lambda_2)\lambda_3 \mathbf{t}_1), \\ \psi_{\lambda_1}^{(\gamma_2)} &= \frac{-1}{2|K|} ((4\lambda_1 - \lambda_3 - 7\lambda_2)\lambda_1 \mathbf{t}_3 + (2\lambda_3 - 3\lambda_1 - \lambda_2)\lambda_3 \mathbf{t}_1), \end{aligned} \quad (2.12)$$

etc. Also let

$$\begin{aligned} \psi_K &= \frac{1}{2|K|} ((\lambda_2 \lambda_3 - \lambda_3 \lambda_1) \mathbf{t}_2 + (\lambda_2 \lambda_3 - \lambda_1 \lambda_2) \mathbf{t}_3), \\ \psi_K^{(1)} &= \frac{\lambda_1}{3|K|} (\lambda_3 \mathbf{t}_2 - \lambda_2 \mathbf{t}_3), \end{aligned} \quad (2.13)$$

with $\psi_K^{(2)}$ and $\psi_K^{(3)}$ being defined permuting the indices. Now, if we adopt the convention that $\lambda_4 = \lambda_1$ and $\lambda_5 = \lambda_2$, then for $i, j, k \in \mathcal{V}_K = \{1, 2, 3\}$ using (2.3), (2.4), (2.9) and (2.10), we

deduce that

$$\begin{aligned}
\left(\psi_{\lambda_{i+1}}^{(\gamma_i)}\right)_{|\gamma_k} \cdot \hat{\mathbf{n}}_k &= \frac{2}{|\gamma_i|} (3\lambda_{i+1} - 1) \delta_{ik}, & \left(\psi_{\lambda_{i+1}}^{(\gamma_i)} \cdot \hat{\mathbf{n}}_k, \lambda_j\right)_{\gamma_k} &= \delta_{i \ k} \delta_{i+1 \ j}, \\
\left(\psi_{\lambda_{i+2}}^{(\gamma_i)}\right)_{|\gamma_k} \cdot \hat{\mathbf{n}}_k &= \frac{2}{|\gamma_i|} (3\lambda_{i+1} - 1) \delta_{ik}, & \left(\psi_{\lambda_{i+2}}^{(\gamma_i)} \cdot \hat{\mathbf{n}}_k, \lambda_j\right)_{\gamma_k} &= \delta_{i \ k} \delta_{i+2 \ j}, \\
\left(\tilde{\psi}_{\lambda_{i+1}}^{(\gamma_i)}\right)_{|\gamma_k} \cdot \hat{\mathbf{n}}_k &= \frac{2}{|\gamma_i|} (3\lambda_{i+1} - 1) \delta_{ik}, & \left(\tilde{\psi}_{\lambda_{i+1}}^{(\gamma_i)} \cdot \hat{\mathbf{n}}_k, \lambda_j\right)_{\gamma_k} &= \delta_{i \ k} \delta_{i+1 \ j}, \\
\left(\tilde{\psi}_{\lambda_{i+2}}^{(\gamma_i)}\right)_{|\gamma_k} \cdot \hat{\mathbf{n}}_k &= \frac{2}{|\gamma_i|} (3\lambda_{i+1} - 1) \delta_{ik}, & \left(\tilde{\psi}_{\lambda_{i+2}}^{(\gamma_i)} \cdot \hat{\mathbf{n}}_k, \lambda_j\right)_{\gamma_k} &= \delta_{i \ k} \delta_{i+2 \ j}, \\
\left(\psi_K\right)_{|\gamma_k} \cdot \hat{\mathbf{n}}_k &= 0, & \left(\psi_K^{(i)}\right)_{|\gamma_k} \cdot \hat{\mathbf{n}}_k &= 0, \\
-\operatorname{div} \left(\tilde{\psi}_{\lambda_{i+1}}^{(\gamma_i)}\right) &= -\frac{1}{|K|}, & \left(-\operatorname{div} \psi_{\lambda_{i+1}}^{(\gamma_i)}, \lambda_j\right)_K &= \delta_{i+1 \ j}, \\
-\operatorname{div} \left(\tilde{\psi}_{\lambda_{i+2}}^{(\gamma_i)}\right) &= -\frac{1}{|K|}, & \left(-\operatorname{div} \psi_{\lambda_{i+2}}^{(\gamma_i)}, \lambda_j\right)_K &= \delta_{i+2 \ j}. \\
-\operatorname{div} \left(\psi_K\right) &= 0, & -\operatorname{div} \left(\psi_K^{(i)}\right) &= \frac{1}{|K|} \left(\lambda_i - \frac{1}{3}\right),
\end{aligned} \tag{2.14}$$

and

$$\begin{aligned}
\left\|\tilde{\psi}_{\lambda_{i+1}}^{(\gamma_i)}\right\|_{\mathbf{L}^2(K)} \leq C, \quad \left\|\tilde{\psi}_{\lambda_{i+2}}^{(\gamma_i)}\right\|_{\mathbf{L}^2(K)} \leq C, \quad \left\|\psi_{\lambda_{i+1}}^{(\gamma_i)}\right\|_{\mathbf{L}^2(K)} \leq C, \quad \left\|\psi_{\lambda_{i+2}}^{(\gamma_i)}\right\|_{\mathbf{L}^2(K)} \leq C, \\
\left\|\psi_K^{(i)}\right\|_{\mathbf{L}^2(K)} \leq C.
\end{aligned} \tag{2.15}$$

where the constant C do not depend on any size of the element K . With these functions we can give some explicit solutions to the Neumann problem (2.8), if the element and boundary data satisfy the following compatibility condition

$$(p_K, c)_K + \sum_{\gamma \in \mathcal{E}_K} (p_{\gamma, K}, c) = 0 \quad \text{for any } c \in \mathbb{R}. \tag{2.16}$$

In certain cases the data will also satisfy

$$(p_K, q)_K + \sum_{\gamma \in \mathcal{E}_K} (p_{\gamma, K}, q) = 0 \quad \text{for any } q \in \mathbb{P}_1(K). \tag{2.17}$$

The next result provide some particular solutions to (2.8) based on the functions previously presented.

Theorem 2.1.5. *Let $p_K \in \mathbb{P}_1(K)$ and $p_{\gamma, K} \in \mathbb{P}_1(\gamma)$ for each $\gamma \in \mathcal{E}_K$ be given. Then, if p_K and $p_{\gamma, K}$ satisfy (2.16),*

$$\boldsymbol{\sigma}_K = \sum_{i=1}^3 \left((p_{\gamma_i, K}, \lambda_{i+1})_{\gamma_i} \tilde{\psi}_{\lambda_{i+1}}^{(\lambda_i)} + (p_{\gamma_i, K}, \lambda_{i+2})_{\gamma_i} \tilde{\psi}_{\lambda_{i+1}}^{(\lambda_i)} + (|K| \nabla(p_K) \cdot (\mathbf{x}_i - \bar{\mathbf{x}}_K)) \psi_K^{(i)} \right) \tag{2.18}$$

is a solution to (2.8) and

$$\|\boldsymbol{\sigma}_K\|_{\mathbf{L}^2(K)} \leq C \left(h_K \|p_K\|_{L^2(K)} + \sum_{\gamma \in \mathcal{E}_K} h_K^{1/2} \|p_{\gamma, K}\|_{L^2(\gamma)} \right). \tag{2.19}$$

If p_K and $p_{\gamma,K}$ satisfy (2.17), then

$$\boldsymbol{\sigma}_K = \sum_{i=1}^3 \left((p_{\gamma_i,K}, \lambda_{i+1})_{\gamma_i} \boldsymbol{\psi}_{\lambda_{i+1}}^{(\lambda_i)} + (p_{\gamma_i,K}, \lambda_{i+2})_{\gamma_i} \boldsymbol{\psi}_{\lambda_{i+1}}^{(\lambda_i)} \right) \quad (2.20)$$

is a solution to (2.8) and

$$\|\boldsymbol{\sigma}_K\|_{\mathbf{L}^2(K)} \leq C \left(\sum_{\gamma \in \mathcal{E}_K} h_K^{1/2} \|p_{\gamma,K}\|_{L^2(\gamma)} \right) \quad (2.21)$$

where $i \in \mathcal{V}_K = \{1, 2, 3\}$, the indices are to be understood modulo 3 and the constant C is independent of h_K , p_K and $p_{\gamma,K}$.

Proof. Let $i, k \in \mathcal{V}_K = \{1, 2, 3\}$, then for any $\gamma_k \in \mathcal{E}_K$, let us restrict $\boldsymbol{\sigma}_K$, given by (2.18) or (2.20), to the edge γ_k to then be multiplied by $\hat{\mathbf{n}}_{\gamma_k}^K$, then

$$\begin{aligned} & \boldsymbol{\sigma}_K|_{\gamma} \cdot \hat{\mathbf{n}}_{\gamma_k}^K \\ &= \sum_{i=1}^3 \left((p_{\gamma_i,K}, \lambda_{i+1})_{\gamma_i} \tilde{\boldsymbol{\psi}}_{\lambda_{i+1}}^{(\gamma_i)} \cdot \hat{\mathbf{n}}_{\gamma_k}^K + (p_{\gamma_i,K}, \lambda_{i+2})_{\gamma_i} \tilde{\boldsymbol{\psi}}_{\lambda_{i+2}}^{(\gamma_i)} \cdot \hat{\mathbf{n}}_{\gamma_k}^K \right) \\ &= \sum_{i=1}^3 \left((p_{\gamma_i,K}, \lambda_{i+1})_{\gamma_i} \boldsymbol{\psi}_{\lambda_{i+1}}^{(\gamma_i)} \cdot \hat{\mathbf{n}}_{\gamma_k}^K + (p_{\gamma_i,K}, \lambda_{i+2})_{\gamma_i} \boldsymbol{\psi}_{\lambda_{i+2}}^{(\gamma_i)} \cdot \hat{\mathbf{n}}_{\gamma_k}^K \right) \\ &= \sum_{i=1}^3 \left((p_{\gamma_i,K}, \lambda_{i+1})_{\gamma_i} \frac{2}{|\gamma_i|} (3\lambda_{i+1} - 1) \delta_{ik} + (p_{\gamma_i,K}, \lambda_{i+2})_{\gamma_i} \frac{2}{|\gamma_i|} (3\lambda_{i+2} - 1) \delta_{ik} \right) \\ &= (p_{\gamma_k,K}^l, \lambda_{k+1})_{\gamma_k} \frac{2}{|\gamma_k|} (3\lambda_{k+1} - (\lambda_{k+1} + \lambda_{k+2})) \\ &\quad + (p_{\gamma_k,K}, \lambda_{k+2})_{\gamma_k} \frac{2}{|\gamma_k|} (3\lambda_{k+2} - (\lambda_{k+1} + \lambda_{k+2})) \\ &= (p_{\gamma_k,K}, \lambda_{k+1})_{\gamma_k} \frac{2}{|\gamma_k|} (2\lambda_{k+1} - \lambda_{k+2}) + (p_{\gamma_k,K}, \lambda_{k+2})_{\gamma_k} \frac{2}{|\gamma_k|} (2\lambda_{k+2} - \lambda_{k+1}) \\ &= p_{\gamma_k,K}, \end{aligned}$$

upon using (2.14), the fact that $(\lambda_{k+1} + \lambda_{k+2})|_{\gamma_k} = 1$ and Lemma 2.1.4, where the indices are to be understood modulo 3. Regarding the divergence, if $\boldsymbol{\sigma}_K$ is given by (2.18), again using the properties of the functions $\tilde{\boldsymbol{\psi}}_{\lambda}^{(\cdot)}$ and $\boldsymbol{\psi}_K^{(\cdot)}$ it follows that

$$\begin{aligned} -\operatorname{div} \boldsymbol{\sigma}_K &= \sum_{i=1}^3 \left(-\frac{1}{|K|} (p_{\gamma_i,K}, 1)_{\gamma_i} + (\nabla(p_K) \cdot (\mathbf{x}_i - \bar{\mathbf{x}}_K)) \left(\lambda_i - \frac{1}{3} \right) \right) \\ &= \sum_{i=1}^3 \left(-\frac{1}{|K|} (p_{\gamma_i,K}, 1)_{\gamma_i} + \nabla(p_K) \cdot (\mathbf{x} - \bar{\mathbf{x}}_K) \right) \\ &= \frac{1}{|K|} (p_K, 1)_K + \nabla(p_K) \cdot (\mathbf{x} - \bar{\mathbf{x}}_K) \\ &= p_K, \end{aligned}$$

upon using (2.16) and the fact that p_K is an affine function. Now, if $\boldsymbol{\sigma}_K$ is given by (2.20) it follows that

$$\begin{aligned} & (-\mathbf{div} \boldsymbol{\sigma}_K, \lambda_j)_K \\ &= \sum_{i=1}^3 \left((p_{\gamma_i, K}, \lambda_{i+1})_{\gamma_i} \left(-\mathbf{div} \boldsymbol{\psi}_{\lambda_{i+1}}^{(\gamma_i)}, \lambda_j \right) + (p_{\gamma_i, K}, \lambda_{i+2})_{\gamma_i} \left(-\mathbf{div} \boldsymbol{\psi}_{\lambda_{i+2}}^{(\gamma_i)}, \lambda_j \right) \right) \\ &= \sum_{i=1}^3 (p_{\gamma_i, K}, \lambda_j)_{\gamma_i} = (p_K, \lambda_j)_K \quad \text{for all } j \in \mathcal{V}_K = \{1, 2, 3\}, \end{aligned}$$

upon using (2.17) and (2.14), hence $-\mathbf{div} \boldsymbol{\sigma}_K = p_K$. Now, for the norm of $\boldsymbol{\sigma}_K$, we obtain

$$\begin{aligned} & \|\boldsymbol{\sigma}_K\|_{L^2(K)}^2 \\ & \leq C \sum_{i=1}^3 |K|^2 |\nabla(p_K)|^2 |\mathbf{x}_i - \bar{\mathbf{x}}_K|^2 + |\gamma_i| \|p_{\gamma_i, K}\|_{L^2(\gamma_i)}^2 \\ & \leq C \left(|K|^2 \frac{1}{|K|} \|\nabla(p_K)\|_{L^2(K)}^2 h_K^2 + \sum_{i=1}^3 |\gamma_i| \|p_{\gamma_i, K}\|_{L^2(\gamma_i)}^2 \right) \\ & \leq C \left(|K|^2 \frac{h_K^{-2}}{|K|} \|p_K\|_{L^2(K)}^2 h_K^2 + \sum_{i=1}^3 h_K \|p_{\gamma_i, K}\|_{L^2(\gamma_i)}^2 \right) \\ & \leq C \left(h_K^2 \|p_K\|_{L^2(K)}^2 + \sum_{i=1}^3 h_K \|p_{\gamma_i, K}\|_{L^2(\gamma_i)}^2 \right), \end{aligned}$$

upon using the regularity of the mesh, (2.15), the Cauchy–Schwarz inequality and an inverse estimate (see Lemma 1.138 in [69]). Hence, (2.19) and (2.21) follow. \square

Chapter 3

Computable error bounds for nonconforming Fortin–Soulie finite element approximation of the Stokes problem.

In recent years considerable interest has been shown in the development of computable a posteriori error estimates for the finite element method. The papers referenced in [51] provide a recent overview of the state of the art in a posteriori error estimation for nonconforming finite element approximations. However, such estimates almost always contain generic (i.e. unknown) constants and as such do not provide actual computable error bounds. In particular, for the lowest order Crouzeix–Raviart [58] finite element approximation of a second order elliptic problem, a technique was presented in [60] which allowed the derivation of two error estimators equivalent up to generic constants to the error. Subsequently, it was shown in [2] how computable upper bounds can be derived for this nonconforming element where such unknown constants are absent. Moreover, the bounds are not only quite accurate, but also easy and cheap to compute.

The second order nonconforming Fortin–Soulie finite element [71] offers a number of advantages over the first order Crouzeix–Raviart element, perhaps the most important of which being that it satisfies a discrete Korn inequality. Recently, the ideas developed that led to computable

bounds for the Crouzeix–Raviart finite element approximation in [2], were extended to the nonconforming Fortin–Soulie finite element approximation of a second order scalar elliptic problem in [14]. Since the structure of the second order nonconforming element is quite different from that of the Crouzeix–Raviart element, it is perhaps not surprising that the a posteriori error estimators for the two elements exhibit important differences.

The structure of the spaces related to the mixed formulation of the Stokes problem considered here is different from the two cases mentioned above. A reliable a posteriori error estimator was presented in [10] for a nonconforming Crouzeix–Raviart finite element approximation of the Stokes flow. The purpose of the present chapter is to extend the techniques used in [14] and [10] to the case of a Stokes flow involving the nonconforming Fortin–Soulie space.

We make use of a result from [59] to decompose the gradient of the velocity error, into what we called conforming and nonconforming parts, each of which must be bounded. The treatment of the conforming part of the error is based on a concrete expression (given in terms of the residuals in the finite element approximation and in terms of the so-called data oscillation) that delivers a fully computable bound on the conforming part of the error. The key to the construction only involves an $\underline{H}(\mathbf{div})$ lifting of the residuals similar to the ideas in [2, 13, 66, 94], in conjunction with the observation that the lifting $\underline{\sigma}_K$ is not required *per se*, only the value of its norm. The significance of this observation is that we obviate the need to solve a local problem, which leads to a much simpler and efficient implementation of the error estimator.

The estimator for the nonconforming part of the error entails the construction of an appropriate conforming approximation of the velocity. The usual approach consists of a local smoothing of the nonconforming velocity approximation. Whilst at first glance such a simple approach might lead one to suspect that the corresponding estimator might perform quite poorly, we find that the performance is, in fact, almost as good as what would be obtained using the best possible smoothing (but at a fraction of the cost).

The error estimator for the pressure error follows from the analysis of the error estimate for the velocity, but has a factor involving a lower bound for the inf-sup constant for the underlying continuous problem, for which there are available some specific values and bounds for such a constant, in the two-dimensional case (see [102] and [63]).

The results that we will present in this chapter are based on [6], but with an improvement on the estimation in the velocity and pressure errors, based on the analysis presented in [8].

3.1 The model problem.

For $\mathbf{f} \in \mathbf{L}^2(\Omega)$. We are interested in the following Stokes problem: *Find a velocity \mathbf{u} and a pressure field p such that*

$$\begin{aligned} -\Delta \mathbf{u} + \nabla p &= \mathbf{f} & \text{in } \Omega, \\ \nabla \cdot \mathbf{u} &= 0 & \text{in } \Omega, \\ \mathbf{u} &= \mathbf{0} & \text{on } \Gamma. \end{aligned} \tag{3.1}$$

The first equation is called the momentum equation and the second is the mass conservation equation.

We begin by restricting our attention to a homogeneous boundary condition, but this assumption will be relaxed in Section 3.8. To establish the weak formulation of problem (3.1), we introduce two continuous bilinear forms, $a(\cdot, \cdot) : \mathbf{H}_0^1(\Omega) \rightarrow \mathbb{R}$ and $b(\cdot, \cdot) : \mathbf{H}_0^1(\Omega) \times L_0^2(\Omega) \rightarrow \mathbb{R}$, defined by

$$a(\mathbf{u}, \mathbf{v}) := (\nabla \mathbf{u}, \nabla \mathbf{v})_\Omega \quad \text{and} \quad b(\mathbf{v}, p) := -(p, \nabla \cdot \mathbf{v})_\Omega.$$

The weak formulation of the Stokes problem then reads: *Find $(\mathbf{u}, p) \in \mathbf{H}_0^1(\Omega) \times L_0^2(\Omega)$ such that*

$$\begin{aligned} a(\mathbf{u}, \mathbf{v}) + b(\mathbf{v}, p) &= (\mathbf{f}, \mathbf{v})_\Omega \quad \forall \mathbf{v} \in \mathbf{H}_0^1(\Omega), \\ b(\mathbf{u}, q) &= 0 \quad \forall q \in L_0^2(\Omega), \end{aligned} \tag{3.2}$$

The well-posedness of problem (3.2) is a consequence of two facts: the bilinear form $(\nabla \mathbf{u}, \nabla \mathbf{v})_\Omega$ is coercive on $\mathbf{H}_0^1(\Omega)$ owing to Poincaré's inequality (see Corollary 1.2-1 in [95]), and hence is also coercive on the subspace

$$\mathbf{X} = \{\mathbf{v} \in \mathbf{H}_0^1(\Omega) : \nabla \cdot \mathbf{v} = 0\}; \tag{3.3}$$

and, there exists a constant $\beta > 0$ such that

$$\sup_{\mathbf{0} \neq \mathbf{v} \in \mathbf{H}_0^1(\Omega)} \frac{(q, \nabla \cdot \mathbf{v})_\Omega}{\|\nabla \mathbf{v}\|_{\mathbf{L}^2(\Omega)}} \geq \beta \|q\|_{L^2(\Omega)} \quad \text{for all } q \in L_0^2(\Omega). \tag{3.4}$$

The constant β is known as the inf-sup constant for the domain Ω . For more details concerning the well-posedness of problem (3.2), see Chapter 4 in [74], Chapter 4 in [69] or Chapter 12 in [40].

We are interested in a nonconforming finite element approximation of the Stokes problem. Nonconforming finite element functions are not differentiable at element boundaries, but it is possible to define an elementwise gradient ∇_h as follows

$$\nabla_h \mathbf{v}(\mathbf{x}) := \nabla \mathbf{v}(\mathbf{x}), \quad \mathbf{x} \in \text{int}(K), \quad \forall K \in \mathcal{P}.$$

In a similar way an elementwise divergence ($\nabla_h \cdot$) can also be defined. Let $\gamma \in \mathcal{E}_I$ with $\gamma = \mathcal{E}_K \cap \mathcal{E}_{K'}$ and set $\mathbf{v}|_K$ to be the restriction of $\mathbf{v} \in H^1(\mathcal{P})^2$ to the element K , then the jump in the trace of \mathbf{v} across γ is defined to be

$$[[\mathbf{v}]] := \mathbf{v}|_K - \mathbf{v}|_{K'},$$

where the elements are ordered so that the edge normal $\hat{\mathbf{n}}_\gamma$ points from K to K' .

3.2 Nonconforming finite element approximation.

To approximate the velocity field we will use the Fortin-Soulie finite element space, defined by

$$\mathbf{V}_h = \left\{ \mathbf{v} : \mathbf{v}|_K \in \mathbb{P}_2(K)^2 \text{ for all } K \in \mathcal{P}, ([[\mathbf{v}]], \mathbf{w})_\gamma = 0 \text{ for all } \mathbf{w} \in \mathbb{P}_1(\gamma)^2 \text{ with } \gamma \in \mathcal{E}_I \right\}.$$

We will also need the following subspace of \mathbf{V}_h :

$$\mathbf{V}_h^D = \left\{ \mathbf{v} \in \mathbf{V}_h : (\mathbf{v}, \mathbf{w})_\gamma = 0 \text{ for all } \mathbf{w} \in \mathbb{P}_1(\gamma)^2 \text{ for } \gamma \in \mathcal{E}_I \right\}.$$

Remark 3.2.1. *Note that this definition seems to differ from the one used in [71]. However, it is easy to see that they are equivalent [14]. For example, the condition $([[\mathbf{v}]], \mathbf{w})_\gamma = 0$, for all $\mathbf{w} \in \mathbb{P}_1(\gamma)^2$ on interior edges, is equivalent to \mathbf{v} being continuous at the two points indexed by \mathcal{G}_I (the Gauss-Legendre points) which lie on the edge γ .*

We will use the following discontinuous polynomial space to approximate the pressure field

$$P_h = \{q \in L_0^2(\Omega) : q|_K \in \mathbb{P}_1(K) \text{ for all } K \in \mathcal{P}\}.$$

The nonconforming finite element approximation of problem (3.1) then reads: *Find $(\mathbf{u}_h, p_h) \in \mathbf{V}_h^D \times P_h$ such that*

$$\begin{aligned} a_h(\mathbf{u}_h, \mathbf{v}_h) + b_h(\mathbf{v}_h, p_h) &= (\mathbf{f}, \mathbf{v}_h)_\Omega \quad \forall \mathbf{v}_h \in \mathbf{V}_h^D, \\ b_h(\mathbf{u}_h, q_h) &= 0 \quad \forall q_h \in P_h, \end{aligned} \tag{3.5}$$

where the bilinear forms $a_h(\cdot, \cdot) : \mathbf{V}_h \times \mathbf{V}_h \rightarrow \mathbb{R}$ and $b_h(\cdot, \cdot) : \mathbf{V}_h \times P_h \rightarrow \mathbb{R}$ are given by

$$a_h(\mathbf{u}, \mathbf{v}) = (\nabla_h \mathbf{u}, \nabla_h \mathbf{v})_\Omega \quad \text{and} \quad b_h(\mathbf{v}, q) = -(q, \nabla_h \cdot \mathbf{v})_\Omega.$$

These forms are continuous with respect to the broken semi-norm $\|\nabla_h \mathbf{v}\|_{L^2(\Omega)}$ and $\|q_h\|_{L^2(\Omega)}$.

Every $\mathbf{v}_h \in \mathbf{V}_h$ satisfies $\nabla_h \cdot \mathbf{v}_h \in P_h$. In fact, since $\mathbf{v}_h \in \mathbf{V}_h^D$ is continuous at the two Gauss–Legendre points on each $\gamma \in \mathcal{E}_I$ and is zero at the two Gauss–Legendre points on each $\gamma \in \mathcal{E}_\Gamma$, integration by parts yields

$$\int_{\Omega} \nabla_h \cdot \mathbf{v}_h \, dx = \sum_{K \in \mathcal{P}} \sum_{\gamma \in \mathcal{E}_K} \int_{\gamma} \mathbf{v}_h \cdot \hat{\mathbf{n}}_{\gamma}^K \, ds = \sum_{\gamma \in \mathcal{E}_I} \int_{\gamma} \frac{1}{2} [\![\mathbf{v}_h \cdot \hat{\mathbf{n}}_{\gamma}]\!]_{\gamma} \, ds + \sum_{\gamma \in \mathcal{E}_\Gamma} \int_{\gamma} \mathbf{v}_h \cdot \hat{\mathbf{n}}_{\Gamma} \, ds = 0,$$

where we have made use of the fact that $\mathbf{v}_h \cdot \hat{\mathbf{n}}_{\gamma}^K \in \mathbb{P}_2(\gamma)$, and consequently $\nabla_h \cdot \mathbf{v}_h \in L_0^2(\Omega)$.

Let \mathbf{X}_h denote the subspace of \mathbf{V}_h defined by

$$\mathbf{X}_h = \{\mathbf{v}_h \in \mathbf{V}_h : \nabla \cdot \mathbf{v}_h|_K = 0, \forall K \in \mathcal{P}\}.$$

It follows that problem (3.5) is well-posed since the bilinear form $a_h(\cdot, \cdot)$ is coercive on \mathbf{X}_h and the discrete version of the inf-sup condition (3.4) holds (for more details see [71]).

3.2.1 A Projection Operator.

In what follows it will be useful to parametrise an edge $\gamma \in \mathcal{E}_K$ by $\mathbf{x}(s_{\gamma}^K) = \mathbf{x}_l + \left(s_{\gamma}^K + \frac{|\gamma|}{2}\right) \hat{\mathbf{t}}_{\gamma}^K$ where

$$s_{\gamma}^K = \frac{|\gamma|}{2} (\lambda_r - \lambda_l) \in \left(-\frac{|\gamma|}{2}, \frac{|\gamma|}{2}\right),$$

with the tangent vector $\hat{\mathbf{t}}_{\gamma}^K$ and normal vector $\hat{\mathbf{n}}_{\gamma}^K$ to edge γ of element K oriented as shown in Figure 3.1. Then it is easy to see that for all $\mathbf{p} \in \mathbb{P}_1(\gamma)^2$ there holds,

$$\mathbf{p} - \bar{\mathbf{p}}_{\gamma} = \frac{\partial \mathbf{p}}{\partial \hat{\mathbf{t}}_{\gamma}^K} s_{\gamma}^K. \quad (3.6)$$

Let $\mathbf{\Pi}_{FS} : \mathbf{H}^1(\Omega) \rightarrow \mathbf{V}_h$ be the interpolation operator

$$\mathbf{\Pi}_{FS}(\mathbf{v}) = \sum_{K \in \mathcal{P}} \bar{\mathbf{v}}_K \theta_K + \sum_{\gamma \in \mathcal{E}} \bar{\mathbf{v}}_{\gamma} \theta_{\gamma}, \quad (3.7)$$

where for any $K \in \mathcal{P}$, the functions θ_K and θ_{γ} are given by

$$\theta_K = \begin{cases} 4 - 6 \sum_{n \in \mathcal{V}_K} \lambda_n^2 & \text{on } K, \\ 0 & \text{elsewhere,} \end{cases}$$

and for $\gamma \in \mathcal{E}_K$,

$$\theta_{\gamma} = \begin{cases} 1 - 6 \left(1 - \sum_{n \in \mathcal{V}_{\gamma}} \lambda_n\right) \sum_{n \in \mathcal{V}_{\gamma}} \lambda_n & \text{on } K, \\ 0 & \text{elsewhere.} \end{cases}$$

The scalar functions θ_K and θ_{γ} belong to the scalar version of the spaces \mathbf{V}_h^D and \mathbf{V}_h , respectively.

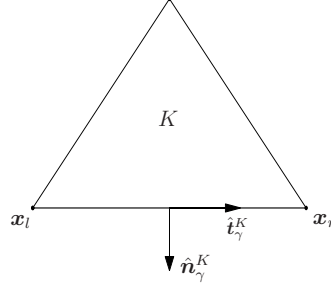


Figure 3.1: Location of the endpoints and orientation of the unit tangent and unit normal vectors on an edge γ of element K .

Remark 3.2.2. Notice that the operator $\mathbf{\Pi}_{FS}$ maps functions from $\mathbf{H}_0^1(\Omega)$ into \mathbf{V}_h^D .

The following result is a generalization to the vector-valued case of Lemma 2.1 from [14]. The operator $\mathbf{\Pi}_{FS}$ has the following properties:

Lemma 3.2.3. For all $\mathbf{v} \in \mathbf{H}^1(\Omega)$, $K \in \mathcal{P}$ and $\gamma \in \mathcal{E}_K$, the operator $\mathbf{\Pi}_{FS}$ satisfies

$$\int_K (\mathbf{v} - \mathbf{\Pi}_{FS}(\mathbf{v})) d\mathbf{x} = \mathbf{0}, \quad (3.8)$$

$$(\mathbf{v} - \mathbf{\Pi}_{FS}(\mathbf{v}), \mathbf{p})_\gamma = (\mathbf{v}, \mathbf{p} - \bar{\mathbf{p}}_\gamma)_\gamma \quad \forall \mathbf{p} \in \mathbb{P}_1(\gamma)^2, \quad (3.9)$$

$$\|\mathbf{v} - \mathbf{\Pi}_{FS}(\mathbf{v})\|_{L^2(K)} \leq C_K \|\nabla \mathbf{v}\|_{\underline{\underline{L}}^2(K)}, \quad (3.10)$$

$$\|\nabla(\mathbf{v} - \mathbf{\Pi}_{FS}(\mathbf{v}))\|_{\underline{\underline{L}}^2(K)} \leq \tilde{C}_K \|\nabla \mathbf{v}\|_{\underline{\underline{L}}^2(K)}, \quad (3.11)$$

$$\|\mathbf{v} - \mathbf{\Pi}_{FS}(\mathbf{v})\|_{L^2(\gamma)} \leq C_\gamma^K \|\nabla \mathbf{v}\|_{\underline{\underline{L}}^2(K)}, \quad (3.12)$$

where for γ, γ' being distinct edges in \mathcal{E}_K ,

$$C_K = \frac{h_K}{\pi} + \sum_{\gamma \in \mathcal{E}_K} \left(\frac{h_K}{5\pi} \left(\frac{h_K}{\pi} + \max_{\gamma' \in \mathcal{E}_K} |\gamma'| \right) \right)^{1/2}, \quad (3.13)$$

$$\tilde{C}_K = 1 + \sqrt{3} \sum_{\gamma \in \mathcal{E}_K} \frac{|\gamma|}{|K|} \left(\frac{h_K}{\pi} \left(\frac{h_K}{\pi} + \max_{\gamma' \in \mathcal{E}_K} |\gamma'| \right) \right)^{1/2}, \quad (3.14)$$

and for γ', γ'' being distinct edges in \mathcal{E}_K ,

$$C_\gamma^K = \frac{|\gamma|^{1/2}}{|K|^{1/2}} \sum_{\gamma' \in \mathcal{E}_K} \left(\left(2\delta_{\gamma\gamma'} + \frac{1}{5} \frac{|\gamma|}{|\gamma'|} (1 - \delta_{\gamma\gamma'}) \right) \frac{h_K}{\pi} \left(\frac{h_K}{\pi} + \max_{\gamma'' \in \mathcal{E}_K} |\gamma''| \right) \right)^{1/2}. \quad (3.15)$$

Proof. From the definition of the operator $\mathbf{\Pi}_{FS}$ and noticing that $(\theta_K, 1)_K = 1$ and $(\theta_\gamma, 1)_K = 0$, it follows that for $\mathbf{v} = [v_1, v_2]$

$$\int_K \mathbf{v} - \mathbf{\Pi}_{FS}(\mathbf{v}) d\mathbf{x} = \left[\int_K v_1 - \bar{v}_{1K} \theta_K dx, \int_K v_2 - \bar{v}_{2K} \theta_K dx \right] = [0, 0]$$

then (3.8) follows. Likewise, noticing that $(\theta_K, p)_{\gamma'} = 0$ and $(\theta_\gamma, p)_{\gamma'} = |\gamma| \bar{p}_\gamma \delta_{\gamma\gamma'}$ for any $p \in \mathbb{P}_1(\gamma)$ and all $\gamma, \gamma' \in \mathcal{E}$, then (3.9) follows by using the definition of the operator $\mathbf{\Pi}_{FS}$.

Using property (3.8) it follows that

$$\|\mathbf{v} - \mathbf{\Pi}_{FS}(\mathbf{v})\|_{\mathbf{L}^2(K)} = \|\mathbf{v} - \bar{\mathbf{v}}_K - \mathbf{\Pi}_{FS}(\mathbf{v} - \bar{\mathbf{v}}_K)\|_{\mathbf{L}^2(K)} \leq \|\mathbf{v} - \bar{\mathbf{v}}_K\|_{\mathbf{L}^2(K)} + \|\mathbf{\Pi}_{FS}(\mathbf{v} - \bar{\mathbf{v}}_K)\|_{\mathbf{L}^2(K)},$$

and

$$\|\nabla(\mathbf{v} - \mathbf{\Pi}_{FS}(\mathbf{v}))\|_{\mathbf{L}^2(K)} \leq \|\nabla \mathbf{v}\|_{\mathbf{L}^2(K)} + \|\nabla(\mathbf{\Pi}_{FS}(\mathbf{v} - \bar{\mathbf{v}}_K))\|_{\mathbf{L}^2(K)}.$$

From the definition of the operator $\mathbf{\Pi}_{FS}$ we obtain

$$\mathbf{\Pi}_{FS}(\mathbf{v} - \bar{\mathbf{v}}_K) = \sum_{\gamma \in \mathcal{E}_K} \overline{(\mathbf{v} - \bar{\mathbf{v}}_K)_\gamma} \theta_\gamma \leq \sum_{\gamma \in \mathcal{E}_K} \frac{1}{|\gamma|^{1/2}} \|\mathbf{v} - \bar{\mathbf{v}}_K\|_{\mathbf{L}^2(\gamma)} \theta_\gamma,$$

hence

$$\begin{aligned} \|\mathbf{\Pi}_{FS}(\mathbf{v} - \bar{\mathbf{v}}_K)\|_{\mathbf{L}^2(K)} &\leq \sum_{\gamma \in \mathcal{E}_K} \frac{1}{|\gamma|^{1/2}} \|\mathbf{v} - \bar{\mathbf{v}}_K\|_{\mathbf{L}^2(\gamma)} \|\theta_\gamma\|_{\mathbf{L}^2(K)}, \\ \|\nabla(\mathbf{\Pi}_{FS}(\mathbf{v} - \bar{\mathbf{v}}_K))\|_{\mathbf{L}^2(K)} &\leq \sum_{\gamma \in \mathcal{E}_K} \frac{1}{|\gamma|^{1/2}} \|\mathbf{v} - \bar{\mathbf{v}}_K\|_{\mathbf{L}^2(\gamma)} \|\nabla \theta_\gamma\|_{\mathbf{L}^2(K)}, \end{aligned}$$

Now (3.10) and (3.11) follows upon applying the following estimate (see [4]),

$$\|\mathbf{v} - \bar{\mathbf{v}}_K\|_{\mathbf{L}^2(\gamma)} \leq \left(\frac{|\gamma|}{|K|} \frac{h_K}{\pi} \left(\frac{h_K}{\pi} + \max_{\gamma' \in \mathcal{E}_K} |\gamma'| \right) \right)^{1/2} \|\nabla \mathbf{v}\|_{\mathbf{L}^2(K)}, \quad (3.16)$$

Lemma 2.1.1 and evaluating $\|\theta_\gamma\|_{\mathbf{L}^2(K)}$ and $\|\nabla \theta_\gamma\|_{\mathbf{L}^2(K)}$. Finally (3.12) follows applying similar arguments. \square

3.3 The error equation.

We let $e_V = \mathbf{u} - \mathbf{u}_h \in \mathbf{X} + \mathbf{X}_h$ and $e_P = p - p_h \in L_0^2(\Omega)$ denote the errors in the velocity and pressure, respectively. From (3.5) and (3.2), integration by parts, the fact that $\mathbf{v} = \mathbf{0}$ on Γ , allows us to conclude that the errors satisfy the identity

$$\begin{aligned} a_h(e_V, \mathbf{v}) + b(\mathbf{v}, e_P) &= \sum_{K \in \mathcal{P}} \left((\mathbf{f}, \mathbf{v})_K - (\nabla \mathbf{u}_h, \nabla \mathbf{v})_K + (p_h, \nabla \cdot \mathbf{v})_K \right) \\ &= \sum_{K \in \mathcal{P}} \left((\mathbf{\Pi}_K(\mathbf{f}) + \Delta \mathbf{u}_h - \nabla p_h, \mathbf{v})_K + (\mathbf{f} - \mathbf{\Pi}_K(\mathbf{f}), \mathbf{v})_K \right) - \sum_{\gamma \in \mathcal{E}_I} \left(\llbracket \nabla_h \mathbf{u}_h \cdot \hat{\mathbf{n}}_\gamma - p_h \hat{\mathbf{n}}_\gamma \rrbracket, \mathbf{v} \right)_\gamma, \end{aligned} \quad (3.17)$$

where

$$\llbracket \nabla_h \mathbf{u}_h \cdot \hat{\mathbf{n}}_\gamma - p_h \hat{\mathbf{n}}_\gamma \rrbracket = \begin{cases} (\nabla \mathbf{u}_{h|K} - p_{h|K}) \hat{\mathbf{n}}_\gamma^K + (\nabla \mathbf{u}_{h|K'} - p_{h|K'}) \hat{\mathbf{n}}_\gamma^{K'} & \text{if } \gamma = \mathcal{E}_K \cap \mathcal{E}_{K'}, \\ (\nabla \mathbf{u}_{h|K} - p_{h|K}) \hat{\mathbf{n}}_\gamma & \text{if } \gamma \in \mathcal{E}_\Gamma. \end{cases}$$

Noting that $\mathbf{\Pi}_{FS}(\mathbf{v}) \in \mathbf{V}_h^D$ for $\mathbf{v} \in \mathbf{H}_0^1(\Omega)$, where $\mathbf{\Pi}_{FS}$ is the operator defined in (3.7), then

$$0 = (\mathbf{f}, \mathbf{\Pi}_{FS}(\mathbf{v}))_\Omega - (\nabla_h \mathbf{u}_h, \nabla_h(\mathbf{\Pi}_{FS}(\mathbf{v})))_\Omega + (p_h, \nabla_h \cdot (\mathbf{\Pi}_{FS}(\mathbf{v})))_\Omega.$$

Inserting the previous equality in (3.17), then integrating by parts in conjunction with (3.9) yields

$$\begin{aligned} & a_h(\mathbf{e}_V, \mathbf{v}) + b(\mathbf{v}, \mathbf{e}_P) \\ &= \sum_{K \in \mathcal{P}} (\mathbf{\Pi}_K(\mathbf{f}) + \Delta \mathbf{u}_h - \nabla p_h, \mathbf{v} - \mathbf{\Pi}_{FS}(\mathbf{v}))_K + (\mathbf{f} - \mathbf{\Pi}_K(\mathbf{f}), \mathbf{v} - \mathbf{\Pi}_{FS}(\mathbf{v}))_K \\ &\quad - \sum_{\gamma \in \mathcal{E}_I} (\llbracket \nabla_h \mathbf{u}_h \cdot \hat{\mathbf{n}}_\gamma - p_h \hat{\mathbf{n}}_\gamma \rrbracket, \mathbf{v} - \mathbf{\Pi}_{FS}(\mathbf{v}))_\gamma \\ &= \sum_{K \in \mathcal{P}} (\mathbf{\Pi}_K(\mathbf{f}) + \Delta \mathbf{u}_h - \nabla p_h, \mathbf{v} - \mathbf{\Pi}_{FS}(\mathbf{v}))_K + (\mathbf{f} - \mathbf{\Pi}_K(\mathbf{f}), \mathbf{v} - \mathbf{\Pi}_{FS}(\mathbf{v}))_K \\ &\quad - \sum_{\gamma \in \mathcal{E}_I} \left(\llbracket \nabla_h \mathbf{u}_h \cdot \hat{\mathbf{n}}_\gamma - p_h \hat{\mathbf{n}}_\gamma \rrbracket - \overline{(\llbracket \nabla_h \mathbf{u}_h \cdot \hat{\mathbf{n}}_\gamma - p_h \hat{\mathbf{n}}_\gamma \rrbracket)_\gamma}, \mathbf{v} \right)_\gamma. \end{aligned} \quad (3.18)$$

Using the fact that $\Delta \mathbf{u}_h - \nabla p_h \in \mathbb{R}^2$ and a Taylor expansion of the projection of the datum \mathbf{f} , (3.8) leads to

$$(\mathbf{\Pi}_K(\mathbf{f}) + \Delta \mathbf{u}_h - \nabla p_h, \mathbf{v} - \mathbf{\Pi}_{FS}(\mathbf{v}))_K = (\nabla(\mathbf{\Pi}_K(\mathbf{f}))(x - \mathbf{x}_K), \mathbf{v} - \mathbf{\Pi}_{FS}(\mathbf{v}))_K, \quad (3.19)$$

where \mathbf{x}_K denotes the centroid of the element K .

Now, we use (3.6) to rewrite the boundary terms on each element K as

$$\begin{aligned} & \sum_{\gamma \in \mathcal{E}_I} \left(\llbracket \nabla_h \mathbf{u}_h \cdot \hat{\mathbf{n}}_\gamma - p_h \hat{\mathbf{n}}_\gamma \rrbracket - \overline{(\llbracket \nabla_h \mathbf{u}_h \cdot \hat{\mathbf{n}}_\gamma - p_h \hat{\mathbf{n}}_\gamma \rrbracket)_\gamma}, \mathbf{v} \right)_\gamma \\ &= \sum_{K \in \mathcal{P}} \sum_{\gamma \in \mathcal{E}_K} \alpha_\gamma \left(\llbracket \nabla_h \mathbf{u}_h \cdot \hat{\mathbf{n}}_\gamma - p_h \hat{\mathbf{n}}_\gamma \rrbracket_\gamma - \overline{(\llbracket \nabla_h \mathbf{u}_h \cdot \hat{\mathbf{n}}_\gamma - p_h \hat{\mathbf{n}}_\gamma \rrbracket)_\gamma}, \mathbf{v} \right)_\gamma \\ &= \sum_{K \in \mathcal{P}} \sum_{\gamma \in \mathcal{E}_K} \left(\alpha_\gamma \frac{\partial}{\partial t_\gamma^K} \llbracket \nabla_h \mathbf{u}_h \cdot \hat{\mathbf{n}}_\gamma - p_h \hat{\mathbf{n}}_\gamma \rrbracket_{s_\gamma^K}, \mathbf{v} \right)_\gamma, \end{aligned} \quad (3.20)$$

where the parameter α_γ is defined by

$$\alpha_\gamma = \begin{cases} 1/2 & \text{if } \gamma \in \mathcal{E}_I, \\ 0 & \text{if } \gamma \in \mathcal{E}_\Gamma. \end{cases} \quad (3.21)$$

Hence, using (3.19) and (3.20) we can rewrite (3.18) as

$$\begin{aligned} & a_h(\mathbf{e}_V, \mathbf{v}) + b(\mathbf{v}, e_P) \\ &= \sum_{K \in \mathcal{P}} \left((\nabla(\mathbf{\Pi}_K(\mathbf{f})))(\mathbf{x} - \mathbf{x}_K), \mathbf{v} - \mathbf{\Pi}_{FS}(\mathbf{v}))_K + (\mathbf{f} - \mathbf{\Pi}_K(\mathbf{f}), \mathbf{v} - \mathbf{\Pi}_{FS}(\mathbf{v}))_K \right. \\ & \quad \left. - \sum_{\gamma \in \mathcal{E}_K} \left(\alpha_\gamma \frac{\partial}{\partial \hat{\mathbf{t}}_\gamma^K} [\nabla_h \mathbf{u}_h \cdot \hat{\mathbf{n}}_\gamma - p_h \hat{\mathbf{n}}_\gamma] s_\gamma^K, \mathbf{v} \right)_\gamma \right). \end{aligned}$$

The following result will be used to deal with the first term in the previous equality.

Lemma 3.3.1. *Let $K \in \mathcal{P}$ and $\mathcal{V}_K = \{1, 2, 3\}$. Then,*

$$(\nabla(\mathbf{\Pi}_K(\mathbf{f})))(\mathbf{x} - \mathbf{x}_K), \mathbf{\Pi}_{FS}(\mathbf{v}))_K = \sum_{i=1}^3 \left(-\frac{|K|}{10|\gamma_i|} \nabla(\mathbf{\Pi}_K(\mathbf{f}))(\mathbf{x}_i - \mathbf{x}_K), \mathbf{v} \right)_{\gamma_i}$$

Proof. First notice that for any $i \in \mathcal{V}_K = \{1, 2, 3\}$, from the definition of θ_K we see that

$$(\lambda_i, \theta_K)_K = \frac{1}{3} \left(\sum_{j=1}^3 \lambda_j, \theta_K \right)_K = \frac{1}{3} (1, \theta_K)_K = \frac{|K|}{3}$$

hence $(\lambda_i - \frac{1}{3}, \theta_K)_K = 0$. Now, for $\gamma_i \in \mathcal{E}_K$ and the definition of θ_γ a simple calculation gives

$$(\lambda_i - \frac{1}{3}, \theta_{\gamma_i})_K = -\frac{|K|}{15} \text{ and } (\lambda_i - \frac{1}{3}, \theta_{\gamma_j})_K = \frac{|K|}{30} \text{ if } i \neq j, \text{ and hence}$$

$$\begin{aligned} & (\nabla(\mathbf{\Pi}_K(\mathbf{f})))(\mathbf{x} - \mathbf{x}_K), \mathbf{\Pi}_{FS}(\mathbf{v}))_K \\ &= \left(\nabla(\mathbf{\Pi}_K(\mathbf{f}))(\mathbf{x} - \mathbf{x}_K), \bar{\mathbf{v}}_K \theta_K + \sum_{j=1}^3 \bar{\mathbf{v}}_{\gamma_j} \theta_{\gamma_j} \right)_K \\ &= \left(\nabla(\mathbf{\Pi}_K(\mathbf{f})) \sum_{i=1}^3 \mathbf{x}_i \left(\lambda_i - \frac{1}{3} \right), \bar{\mathbf{v}}_K \theta_K + \sum_{j=1}^3 \bar{\mathbf{v}}_{\gamma_j} \theta_{\gamma_j} \right)_K \\ &= \left(\nabla(\mathbf{\Pi}_K(\mathbf{f})) \sum_{i=1}^3 \mathbf{x}_i \left(\lambda_i - \frac{1}{3} \right), \sum_{j=1}^3 \bar{\mathbf{v}}_{\gamma_j} \theta_{\gamma_j} \right)_K \\ &= -\frac{|K|}{10} \sum_{i=1}^3 \nabla(\mathbf{\Pi}_K(\mathbf{f}))(\mathbf{x}_i - \mathbf{x}_K) \bar{\mathbf{v}}_{\gamma_i} \\ &= \sum_{i=1}^3 \left(-\frac{|K|}{10|\gamma_i|} \nabla(\mathbf{\Pi}_K(\mathbf{f}))(\mathbf{x}_i - \mathbf{x}_K), \mathbf{v} \right)_{\gamma_i}, \end{aligned}$$

which proves the result. \square

Using the previous Lemma, we can rewrite the error equation as

$$\begin{aligned} & a_h(\mathbf{e}_V, \mathbf{v}) + b(\mathbf{v}, e_P) \\ &= \sum_{K \in \mathcal{P}} \left((\mathcal{R}_K, \mathbf{v})_K + \sum_{\gamma \in \mathcal{E}_K} (\mathcal{R}_{\gamma, K}, \mathbf{v})_\gamma + (\mathbf{f} - \mathbf{\Pi}_K(\mathbf{f}), \mathbf{v} - \mathbf{\Pi}_{FS}(\mathbf{v}))_K \right), \end{aligned} \tag{3.22}$$

where the element residual $\mathcal{R}_K \in \mathbb{P}_1(K)^2$ and the boundary residuals $\mathcal{R}_{\gamma,K} \in \mathbb{P}_1(\gamma)^2$ are defined by

$$\mathcal{R}_K := \nabla(\mathbf{\Pi}_K(\mathbf{f}))(\mathbf{x} - \mathbf{x}_K), \quad (3.23)$$

and

$$\mathcal{R}_{\gamma,K} := \frac{|K|}{10|\gamma|} \nabla(\mathbf{\Pi}_K(\mathbf{f}))(\mathbf{x}_\gamma - \mathbf{x}_K) - \alpha_\gamma \frac{\partial}{\partial \hat{\mathbf{t}}_\gamma^K} \llbracket \nabla_h \mathbf{u}_h \cdot \hat{\mathbf{n}}_\gamma - p_h \hat{\mathbf{n}}_\gamma \rrbracket_{s_\gamma^K}, \quad (3.24)$$

where \mathbf{x}_γ denotes the vertex opposite to the edge γ , respectively.

Now, the right hand side of (3.22) can be represented in a more convenient way in terms of a solution $\underline{\boldsymbol{\sigma}}_K \in \underline{\mathbf{H}}(\mathbf{div}, K)$ of a local *Neumann* problem with residuals as data:

$$(\underline{\boldsymbol{\sigma}}_K, \nabla \mathbf{v})_K = (\mathcal{R}_K, \mathbf{v})_K + \sum_{\gamma \in \mathcal{E}_K} (\mathcal{R}_{\gamma,K}, \mathbf{v})_\gamma \quad \text{for all } \mathbf{v} \in \mathbf{H}^1(\Omega), \quad (3.25)$$

This problem will have a solution if and only if the element and edge residuals satisfy the following compatibility condition

$$(\mathcal{R}_K, \mathbf{c})_K + \sum_{\gamma \in \mathcal{E}_K} (\mathcal{R}_{\gamma,K}, \mathbf{c})_\gamma = 0 \quad \text{for all } \mathbf{c} \in \mathbb{R}^2. \quad (3.26)$$

To see that this condition does hold, from (3.23), (3.24), Lemma 3.3.1, (3.19), (3.9) and (3.6), it follows that for all $\mathbf{v} \in \mathbf{H}^1(K)$,

$$\begin{aligned} & (\mathcal{R}_K, \mathbf{v})_K + \sum_{\gamma \in \mathcal{E}_K} (\mathcal{R}_{\gamma,K}, \mathbf{v})_\gamma \quad (3.27) \\ &= (\nabla(\mathbf{\Pi}_K(\mathbf{f}))(\mathbf{x} - \mathbf{x}_K), \mathbf{v})_K \\ &+ \sum_{\gamma \in \mathcal{E}_K} \left(\frac{|K|}{10|\gamma|} \nabla(\mathbf{\Pi}_K(\mathbf{f}))(\mathbf{x}_\gamma - \mathbf{x}_K) - \alpha_\gamma \frac{\partial}{\partial \hat{\mathbf{t}}_\gamma^K} \llbracket \nabla_h \mathbf{u}_h \cdot \hat{\mathbf{n}}_\gamma - p_h \hat{\mathbf{n}}_\gamma \rrbracket_{s_\gamma^K}, \mathbf{v} \right)_\gamma \\ &= (\nabla(\mathbf{\Pi}_K(\mathbf{f}))(\mathbf{x} - \mathbf{x}_K), \mathbf{v} - \mathbf{\Pi}_{FS}(\mathbf{v}))_K \\ &- \sum_{\gamma \in \mathcal{E}_K} \alpha_\gamma \left(\llbracket \nabla_h \mathbf{u}_h \cdot \hat{\mathbf{n}}_\gamma - p_h \hat{\mathbf{n}}_\gamma \rrbracket - \overline{\llbracket \nabla_h \mathbf{u}_h \cdot \hat{\mathbf{n}}_\gamma - p_h \hat{\mathbf{n}}_\gamma \rrbracket}_\gamma, \mathbf{v} \right)_\gamma \\ &= (\mathbf{\Pi}_K(\mathbf{f}) + \Delta \mathbf{u}_h - \nabla p_h, \mathbf{v} - \mathbf{\Pi}_{FS}(\mathbf{v}))_K - \sum_{\gamma \in \mathcal{E}_K} (\alpha_\gamma \llbracket \nabla \mathbf{u}_h \cdot \hat{\mathbf{n}}_\gamma - p_h \hat{\mathbf{n}}_\gamma \rrbracket, \mathbf{v} - \mathbf{\Pi}_{FS}(\mathbf{v}))_\gamma, \end{aligned}$$

then (3.26) follows since $\mathbf{\Pi}_{FS}(\mathbf{c}) = \mathbf{c}$ for all $\mathbf{c} \in \mathbb{R}^2$.

Finally, using (3.25) we can rewrite the error equation as follows

$$a_h(e_V, \mathbf{v}) + b(\mathbf{v}, e_P) = \sum_{K \in \mathcal{P}} \left((\underline{\boldsymbol{\sigma}}_K, \nabla \mathbf{v})_K + (\mathbf{f} - \mathbf{\Pi}_K(\mathbf{f}), \mathbf{v} - \mathbf{\Pi}_{FS}(\mathbf{v}))_K \right), \quad (3.28)$$

from which we will obtain an upper bound for velocity and pressure errors.

3.4 Solution of the Neumann problem.

Suppose that we have a matrix field $\underline{\underline{\sigma}}_K$ satisfying

$$-\mathbf{div} \underline{\underline{\sigma}}_K = \mathcal{R}_K \quad \text{in } K, \quad (3.29)$$

$$\underline{\underline{\sigma}}_K \hat{\mathbf{n}}_\gamma^K = \mathcal{R}_{\gamma,K} \quad \text{on each } \gamma \in \mathcal{E}_K, \quad (3.30)$$

then clearly $\underline{\underline{\sigma}}_K$ will satisfy (3.25).

The following result provides a solution to (3.29)-(3.30), which is a simple extension to the matrix-valued case of Theorem 2.1.5 and is based on the orientation of the edges, vertices, tangents and normal vectors in Figure 2.1.

Lemma 3.4.1. *The following matrix-valued function is a solution to (3.29)-(3.30),*

$$\underline{\underline{\sigma}}_K = \begin{bmatrix} \sigma_K^1 \\ \sigma_K^2 \end{bmatrix}, \quad (3.31)$$

where for $l = 1, 2$ and $i \in \mathcal{V}_K = \{1, 2, 3\}$, letting $\mathcal{R}_K = [\mathcal{R}_K^1, \mathcal{R}_K^2]$ and $\mathcal{R}_{\gamma,K} = [\mathcal{R}_{\gamma,K}^1, \mathcal{R}_{\gamma,K}^2]$, each component is given by

$$\sigma_K^l = \sum_{i=1}^3 \left((\mathcal{R}_{\gamma_i,K}^l, \lambda_{i+1})_{\gamma_i} \tilde{\psi}_{\lambda_{i+1}}^{(\gamma_i)} + (\mathcal{R}_{\gamma_i,K}^l, \lambda_{i+2})_{\gamma_i} \tilde{\psi}_{\lambda_{i+2}}^{(\gamma_i)} + (|K| \nabla(\mathcal{R}_K^l) \cdot (\mathbf{x}_i - \bar{\mathbf{x}}_K)) \psi_K^{(i)} \right), \quad (3.32)$$

where the functions $\tilde{\psi}_\lambda^{(\cdot)}$ and $\psi_K^{(\cdot)}$ are given in (2.12) and (2.13), respectively, and there exist a constant C independent of any size of the element K such that

$$\|\underline{\underline{\sigma}}_K\|_{\underline{\underline{L}}^2(K)} \leq C \left(h_K \|\mathcal{R}_K\|_{L^2(K)} + \sum_{\gamma \in \mathcal{E}_K} h_K^{1/2} \|\mathcal{R}_{\gamma,K}\|_{L^2(\gamma)} \right). \quad (3.33)$$

Proof. Since the element residual \mathcal{R}_K and the edge residuals $\mathcal{R}_{\gamma,K}$ satisfy (3.26), i.e. a condition like (2.16), then taking $p_K = \mathcal{R}_K^l$ and $p_{\gamma,K} = \mathcal{R}_{\gamma,K}^l$ in (2.18) and (2.19) in Theorem 2.1.5, the result easily follows. \square

Remark 3.4.2. *Notice that*

$$\underline{\underline{\sigma}}_K - \mathbf{curl}(\beta_K)$$

also satisfy (3.25), where β_K belongs to $\mathbf{H}_0^1(K)$, since $\mathbf{curl}(\beta_K) \hat{\mathbf{n}}_\gamma^K = \mathbf{0}$ for any $\gamma \in \mathcal{E}_K$ and $\mathbf{div}(\mathbf{curl}(\beta_K)) = \mathbf{0}$.

From [85] we know that if we take $\mathbf{v} \in \mathbf{X}$ in (3.25), then

$$\underline{\underline{\sigma}}_K - (\vartheta_K \underline{\underline{I}} + \mathbf{curl}(\beta_K))$$

will also satisfy (3.25), for any $\vartheta_K \in L^2(K)$ since $(\vartheta_K \underline{\mathbf{I}}, \nabla \mathbf{v})_K = (\vartheta_K, \nabla \cdot \mathbf{v})_K = 0$. Hence, from now on we denote

$$\underline{\boldsymbol{\sigma}}_K^*(\vartheta_K, \boldsymbol{\beta}_K) := \underline{\boldsymbol{\sigma}}_K - (\vartheta_K \underline{\mathbf{I}} + \mathbf{curl}(\boldsymbol{\beta}_K)).$$

3.5 An orthogonal decomposition of the error.

Following an idea of [60], we have the following orthogonal Helmholtz-type decomposition to the gradient of the velocity error.

Theorem 3.5.1. *For $e_V = \mathbf{u} - \mathbf{u}_h$, we can decompose its gradient as*

$$\nabla_h e_V = \nabla e_c + \underline{\boldsymbol{\varepsilon}}_{nc}, \quad (3.34)$$

where $e_c \in \mathbf{X}$ is uniquely defined by

$$(\nabla e_c, \nabla \mathbf{v}_c)_\Omega = (\nabla_h e_V, \nabla \mathbf{v}_c)_\Omega \quad \forall \mathbf{v}_c \in \mathbf{X}, \quad (3.35)$$

whilst the remainder part $\underline{\boldsymbol{\varepsilon}}_{nc}$ belongs to the closed subspace

$$\underline{\mathbf{Y}} = \left\{ \underline{\boldsymbol{w}}_{nc} \in \underline{\mathbf{L}}^2(\Omega) : (\underline{\boldsymbol{w}}_{nc}, \nabla \mathbf{v}_c)_\Omega = 0 \text{ for all } \mathbf{v}_c \in \mathbf{X} \right\} \quad (3.36)$$

of $\underline{\mathbf{L}}^2(\Omega)$ and is given by

$$\underline{\boldsymbol{\varepsilon}}_{nc} = -q \underline{\mathbf{I}} + \mathbf{curl} \mathbf{s}$$

with $q \in L_0^2(\Omega)$ and $\mathbf{s} \in \mathbf{H}^1(\Omega)$.

Proof. This decomposition can be obtained as follows. Let $(e_c, q) \in \mathbf{H}_0^1(\Omega) \times L_0^2(\Omega)$ be the solution of the following Stokes problem, with right hand side $-\mathbf{div}(\nabla_h e_V) \in \mathbf{H}^{-1}(\Omega)$, i.e.,

$$\begin{aligned} -\Delta e_c + \nabla q &= -\underline{\mathbf{div}}(\nabla_h e_V) \quad \text{in } \Omega, \\ -\mathbf{div} e_c &= 0 \quad \text{in } \Omega, \end{aligned}$$

Notice that the first equation can be rewritten as

$$\underline{\mathbf{div}}(-\nabla e_c + q \underline{\mathbf{I}} + \nabla_h e_V) = 0. \quad (3.37)$$

From (3.37), it follows that $\int_\Gamma (-\nabla e_c + q \underline{\mathbf{I}} + \nabla_h e_V) \hat{\mathbf{n}}_\Gamma = 0$, then from Theorem 3.1 in [74] there exists a function $\mathbf{s} \in \mathbf{H}^1(\Omega)$ such that

$$\nabla e_c - q \underline{\mathbf{I}} + \mathbf{curl} \mathbf{s} = \nabla_h e_V. \quad (3.38)$$

From the previous equality, it follows that

$$(\nabla \mathbf{e}_c, \nabla \mathbf{v}_c)_\Omega = (\nabla \mathbf{e}_c - q \underline{\underline{\mathbf{I}}} + \mathbf{curl} \mathbf{s}, \nabla \mathbf{v}_c)_\Omega = (\nabla_h \mathbf{e}_V, \nabla \mathbf{v}_c)_\Omega \quad \forall \mathbf{v}_c \in \mathbf{X},$$

since

$$(q \underline{\underline{\mathbf{I}}}, \nabla \mathbf{v}_c)_\Omega = (q, \nabla \cdot \mathbf{v}_c)_\Omega = 0$$

and

$$(\mathbf{curl} \mathbf{s}, \nabla \mathbf{v}_c)_\Omega = -(\mathbf{div}(\mathbf{curl} \mathbf{s}), \mathbf{v}_c)_\Omega + (\mathbf{curl} \mathbf{s} \cdot \hat{\mathbf{n}}_\Gamma, \mathbf{v}_c)_\Gamma = 0,$$

upon using the fact that $\mathbf{v}_c \in \mathbf{X}$. Now taking

$$\underline{\underline{\mathbf{e}}}_{nc} = -q \underline{\underline{\mathbf{I}}} + \mathbf{curl} \mathbf{s}, \quad (3.39)$$

the result follows. \square

The following result is a key ingredient to obtain an upper bound for the nonconforming part of the velocity error.

Lemma 3.5.2. *For $\underline{\underline{\mathbf{e}}}_{nc} \in \underline{\underline{\mathbf{Y}}}$, given in the previous theorem, there exist a function $w \in L_0^2(\Omega)$, such that*

$$(\underline{\underline{\mathbf{e}}}_{nc}, \nabla \mathbf{v})_\Omega = (w, \nabla \cdot \mathbf{v})_\Omega \quad \forall \mathbf{v} \in \mathbf{H}_0^1(\Omega), \quad (3.40)$$

i.e., $\nabla \cdot \underline{\underline{\mathbf{e}}}_{nc} = \nabla w$, which satisfies the estimate

$$\|w\|_{L^2(\Omega)} \leq \frac{1}{\beta} \|\underline{\underline{\mathbf{e}}}_{nc}\|_{L^2(\Omega)},$$

where the constant β is the inf-sup constant from (3.4).

Proof. From (3.37), (3.38) and (3.39) we know that for $\underline{\underline{\mathbf{e}}}_{nc} \in \underline{\underline{\mathbf{Y}}}$, given in the previous theorem, there exist $w \in L_0^2(\Omega)$ such that $\nabla \cdot \underline{\underline{\mathbf{e}}}_{nc} = \nabla w$. Denoting by $\mathcal{D}(\Omega)$ the space of infinitely differentiable functions with compact support in Ω , then taking $\mathbf{v} \in \mathcal{D}(\Omega)^2$, it follows that

$$(\underline{\underline{\mathbf{e}}}_{nc}, \nabla \mathbf{v})_\Omega = \langle \nabla \cdot \underline{\underline{\mathbf{e}}}_{nc}, \mathbf{v} \rangle_{\mathcal{D}', \mathcal{D}} = \langle \nabla w, \mathbf{v} \rangle_{\mathcal{D}', \mathcal{D}} = (w, \nabla \cdot \mathbf{v})_\Omega,$$

where $\langle \cdot, \cdot \rangle_{\mathcal{D}', \mathcal{D}}$ denotes a duality pairing, then equation (3.40) follows by the density of $\mathcal{D}(\Omega)^2$ in $\mathbf{H}_0^1(\Omega)$ (cf. Section 9.4 in [41]). The validity of the inf-sup condition means that we may pick $\mathbf{v} \in \mathbf{H}_0^1(\Omega)$ such that $\nabla \cdot \mathbf{v} = w$ (see Lemma 12.2.12 and Lemma 11.2.3 from [40]), and

$$\|\nabla \mathbf{v}\|_{L^2(\Omega)} \leq \frac{1}{\beta} \|w\|_{L^2(\Omega)},$$

hence

$$\beta \|w\|_{L^2(\Omega)} = \beta \frac{(w, \nabla \cdot \mathbf{v})_\Omega}{\|w\|_{L^2(\Omega)}} \leq \frac{(w, \nabla \cdot \mathbf{v})_\Omega}{\|\nabla \mathbf{v}\|_{\underline{\underline{L}}^2(\Omega)}} = \frac{(\underline{\underline{e}}_{nc}, \nabla \mathbf{v})_\Omega}{\|\nabla \mathbf{v}\|_{\underline{\underline{L}}^2(\Omega)}} \leq \|\underline{\underline{e}}_{nc}\|_{\underline{\underline{L}}^2(\Omega)},$$

upon applying the Cauchy–Schwarz inequality, which completes the proof of the assertion. \square

3.6 A guaranteed upper bound for the error.

We will derive a computable upper bound for the velocity error. Notice that an immediate consequence of Theorem 3.5.1 is the following orthogonal decomposition

$$\|\nabla_h \mathbf{e}_V\|_{\underline{\underline{L}}^2(\Omega)}^2 = \|\nabla \mathbf{e}_c\|_{\underline{\underline{L}}^2(\Omega)}^2 + \|\underline{\underline{e}}_{nc}\|_{\underline{\underline{L}}^2(\Omega)}^2. \quad (3.41)$$

Now, we will first find an upper bound on the norm of the gradient of the conforming part of the error \mathbf{e}_c , and then an upper bound for the norm of the nonconforming error $\underline{\underline{e}}_{nc}$ defined in equations (3.35) and (3.36), respectively.

To obtain an upper bound for the conforming part of the error, we will use equation (3.28) satisfied by the total errors \mathbf{e}_V and e_P , and then apply the definition of the conforming error \mathbf{e}_c .

Using (3.28), the definition of the conforming error (3.35), the fact that $b(\mathbf{v}, e_P) = 0$ for all $\mathbf{v} \in \mathbf{X}$ and with the aid of Remark 3.4.2, we can write the equation for the conforming error in the velocity field as

$$a(\mathbf{e}_c, \mathbf{v}) = \sum_{K \in \mathcal{P}} (\underline{\underline{\sigma}}_K^*(\vartheta_K, \boldsymbol{\beta}_K), \nabla \mathbf{v})_K + (\mathbf{f} - \mathbf{\Pi}_K(\mathbf{f}), \mathbf{v} - \mathbf{\Pi}_{FS}(\mathbf{v}))_K \quad \text{for all } \mathbf{v} \in \mathbf{X}. \quad (3.42)$$

Next, applying the Cauchy–Schwarz inequality and (3.10) then yields

$$a(\mathbf{e}_c, \mathbf{v}) \leq \left(\sum_{K \in \mathcal{P}} \left(\|\underline{\underline{\sigma}}_K^*(\vartheta_K, \boldsymbol{\beta}_K)\|_{\underline{\underline{L}}^2(K)} + C_K \|\mathbf{f} - \mathbf{\Pi}_K(\mathbf{f})\|_{L^2(K)} \right)^2 \right)^{1/2} \|\nabla \mathbf{v}\|_{\underline{\underline{L}}^2(\Omega)}.$$

Now letting $\mathbf{v} = \mathbf{e}_c$ in the above expression and dividing through by $\|\nabla \mathbf{e}_c\|_{L^2(\Omega)}$ we obtain an upper a posteriori error bound for the conforming part of the velocity error, namely

$$\|\nabla \mathbf{e}_c\|_{\underline{\underline{L}}^2(\Omega)}^2 \leq \sum_{K \in \mathcal{P}} \left(\|\underline{\underline{\sigma}}_K^*(\vartheta_K, \boldsymbol{\beta}_K)\|_{\underline{\underline{L}}^2(K)} + C_K \|\mathbf{f} - \mathbf{\Pi}_K(\mathbf{f})\|_{L^2(K)} \right)^2. \quad (3.43)$$

To obtain an upper bound for the nonconforming part of the error $\underline{\underline{e}}_{nc}$, by using the definition of the nonconforming error (3.36), choosing an arbitrary function $\mathbf{u}^* \in \mathbf{H}_0^1(\Omega)$ and applying

(3.40), it follows that

$$\begin{aligned}
\|\underline{\underline{\boldsymbol{\varepsilon}}}_{nc}\|_{\underline{\underline{\mathbf{L}}^2(\Omega)}}^2 &= (\nabla_h(e_V - e_c), \underline{\underline{\boldsymbol{\varepsilon}}}_{nc})_\Omega = -(\nabla_h \mathbf{u}_h, \underline{\underline{\boldsymbol{\varepsilon}}}_{nc})_\Omega \\
&= (\nabla_h(\mathbf{u}^* - \mathbf{u}_h), \underline{\underline{\boldsymbol{\varepsilon}}}_{nc})_\Omega - (\nabla \mathbf{u}^*, \underline{\underline{\boldsymbol{\varepsilon}}}_{nc})_\Omega \\
&= (\nabla_h(\mathbf{u}^* - \mathbf{u}_h), \underline{\underline{\boldsymbol{\varepsilon}}}_{nc})_\Omega - (w, \nabla \cdot \mathbf{u}^*)_\Omega.
\end{aligned} \tag{3.44}$$

Using the the Cauchy–Schwarz inequality and the bound for w in Lemma 3.5.2, in the last equation, yields

$$\|\underline{\underline{\boldsymbol{\varepsilon}}}_{nc}\|_{\underline{\underline{\mathbf{L}}^2(\Omega)}} \leq \|\nabla_h(\mathbf{u}^* - \mathbf{u}_h)\|_{\underline{\underline{\mathbf{L}}^2(\Omega)}} + \frac{1}{\beta} \|\nabla \cdot \mathbf{u}^*\|_{L^2(\Omega)}. \tag{3.45}$$

The quality of the estimator for the nonconforming part of the velocity error (3.45) depends on making a good choice for \mathbf{u}^* , which will make the local error indicator for the adaptive algorithm more or less efficient. One possibility was given in [2], where \mathbf{u}^* is constructed by post-processing the finite element approximation \mathbf{u}_h . Considering this result, we begin taking \mathbf{u}^* to be the continuous piecewise quadratic interpolant of \mathbf{u}_h on \mathcal{P} whose values at the nodes are given by

$$\mathbf{S}(\mathbf{u}_h)(\mathbf{x}_m) = \begin{cases} \sum_{K' \in \Omega_m} \frac{1}{\text{card}(\Omega_m)} \mathbf{u}_h|_{K'}(\mathbf{x}_m) & \text{for } m \notin \mathcal{N}_\Gamma, \\ \mathbf{0} & \text{for } m \in \mathcal{N}_\Gamma, \end{cases} \tag{3.46}$$

where $\text{card}(\Omega_m)$ denotes the cardinality of the set Ω_m .

Alternatively with the aim of minimising Φ_{nc} , \mathbf{u}^* could be taken equal to \mathbf{u}_{min}^* , where \mathbf{u}_{min}^* minimises

$$\int_\Omega |\nabla_h(\mathbf{u}_{min}^* - \mathbf{u}_h)|^2 + \frac{1}{\beta^2} |\nabla_h \cdot (\mathbf{u}_{min}^* - \mathbf{u}_h)|^2 d\mathbf{x}, \tag{3.47}$$

over $\mathbb{P}_2(\mathcal{P})^2$, where $\mathbb{P}_2(\mathcal{P})^2$ is the set of piecewise continuous quadratic polynomial functions constructed over the partition \mathcal{P} . Of course, determining the minimiser of (3.47) involves the assembly and solution of a global system of equations, and as such far exceeds the cost of the simple scheme given in (3.46). In the numerical results, we solved this problem in each iteration in order to compare the efficiency of the local indicator for the adaptive algorithm using both choices $\mathbf{S}(\mathbf{u}_h)$ and \mathbf{u}_{min}^* for \mathbf{u}^* . The results obtained show that the choice of the piecewise quadratic interpolant $\mathbf{S}(\mathbf{u}_h)$ is sufficient to achieve good performance of the estimator, and is in fact almost as good as the optimal choice \mathbf{u}_{min}^* .

It remains to give the upper a posteriori error bound for e_P . Splitting the gradient of the test function $\nabla \mathbf{v} = \nabla \mathbf{v}_c + \underline{\underline{\mathbf{v}}}_{nc}$ as in (3.34) in the error equation (3.28), remembering that $\nabla \cdot \mathbf{v} = \text{tr}(\nabla \mathbf{v}_c + \underline{\underline{\mathbf{v}}}_{nc}) = \text{tr}(\underline{\underline{\mathbf{v}}}_{nc})$ (since $\mathbf{v}_c \in \mathbf{X}$), where tr denotes the trace of a matrix and in conjunction with Remark 3.4.2, we obtain

$$\begin{aligned} & \left((\nabla \mathbf{e}_c, \nabla \mathbf{v}_c)_\Omega + (\underline{\underline{\mathbf{e}}}_{nc}, \underline{\underline{\mathbf{v}}}_{nc})_\Omega \right) - (e_P, \text{tr}(\underline{\underline{\mathbf{v}}}_{nc}))_\Omega = \\ & \sum_{K \in \mathcal{P}} \left((\underline{\underline{\boldsymbol{\sigma}}}_K^*(\vartheta_K, \boldsymbol{\beta}_K), \nabla \mathbf{v}_c)_K + (\underline{\underline{\boldsymbol{\sigma}}}_K^*(0, \boldsymbol{\beta}_K), \underline{\underline{\mathbf{v}}}_{nc})_K + (\mathbf{f} - \mathbf{\Pi}_K(\mathbf{f}), \mathbf{v} - \mathbf{\Pi}_{FS}(\mathbf{v}))_K \right). \end{aligned} \quad (3.48)$$

Now, let $\phi_K \in \mathbf{V}_K$ be a solution of the local problem

$$(\nabla \phi_K, \nabla \mathbf{v})_K = (\mathbf{f} - \mathbf{\Pi}_K(\mathbf{f}), \mathbf{v} - \mathbf{\Pi}_{FS}(\mathbf{v}))_K \quad \forall \mathbf{v} \in \mathbf{V}_K, \quad (3.49)$$

where $\mathbf{V}_K = \{\mathbf{v} \in \mathbf{H}^1(K) : \mathbf{v} = \mathbf{0} \text{ on } \mathcal{E}_\Gamma \cap \mathcal{E}_K\}$. Notice that from (3.49) and the properties of the projection operator $\mathbf{\Pi}$ it easily follows that

$$\|\nabla \phi_K\|_{\underline{\underline{\mathbf{L}}}^2(K)} \leq C_K \|\mathbf{f} - \mathbf{\Pi}_K(\mathbf{f})\|_{\mathbf{L}^2(K)}. \quad (3.50)$$

Since (3.49) is also valid for any $\mathbf{v}_c \in \mathbf{X}$, applying the orthogonal decomposition (3.34) to \mathbf{v} in (3.49) allows us to rewrite the right hand side of (3.48) at the element level as

$$\begin{aligned} & (\underline{\underline{\boldsymbol{\sigma}}}_K^*(\vartheta_K, \boldsymbol{\beta}_K), \nabla \mathbf{v}_c)_K + (\mathbf{f} - \mathbf{\Pi}_K(\mathbf{f}), \mathbf{v}_c - \mathbf{\Pi}_{FS}(\mathbf{v}_c))_K \\ & + (\underline{\underline{\boldsymbol{\sigma}}}_K^*(0, \boldsymbol{\beta}_K), \underline{\underline{\mathbf{v}}}_{nc})_K + (\nabla \phi_K, \underline{\underline{\mathbf{v}}}_{nc})_K. \end{aligned} \quad (3.51)$$

Inserting (3.51) into (3.48), and then using (3.42) yields

$$\begin{aligned} & - (e_P, \text{tr}(\underline{\underline{\mathbf{v}}}_{nc}))_\Omega \\ & = - (\underline{\underline{\mathbf{e}}}_{nc}, \underline{\underline{\mathbf{v}}}_{nc})_\Omega + \sum_{K \in \mathcal{P}} \left((\underline{\underline{\boldsymbol{\sigma}}}_K^*(0, \boldsymbol{\beta}_K), \underline{\underline{\mathbf{v}}}_{nc})_K + (\nabla \phi_K, \underline{\underline{\mathbf{v}}}_{nc})_K \right) \\ & \leq \left(\|\underline{\underline{\mathbf{e}}}_{nc}\|_{\underline{\underline{\mathbf{L}}}^2(\Omega)} + \left(\sum_{K \in \mathcal{P}} \left(\|\underline{\underline{\boldsymbol{\sigma}}}_K^*(0, \boldsymbol{\beta}_K)\|_{\underline{\underline{\mathbf{L}}}^2(K)} + C_K \|\mathbf{f} - \mathbf{\Pi}_K(\mathbf{f})\|_{\mathbf{L}^2(K)} \right)^2 \right)^{1/2} \right) \\ & \quad \times \|\underline{\underline{\mathbf{v}}}_{nc}\|_{\underline{\underline{\mathbf{L}}}^2(\Omega)}, \end{aligned} \quad (3.52)$$

upon applying the Cauchy–Schwarz inequality and (3.50).

Finally, thanks to the inf-sup condition, we have

$$\beta \|e_P\|_{\mathbf{L}^2(\Omega)} \leq \sup_{\mathbf{0} \neq \mathbf{v} \in \mathbf{H}_0^1(\Omega)} \frac{-(e_P, \nabla \cdot \mathbf{v})_\Omega}{\|\nabla \mathbf{v}\|_{\underline{\underline{\mathbf{L}}}^2(\Omega)}} \leq \sup_{\mathbf{0} \neq \underline{\underline{\mathbf{v}}}_{nc} \in \underline{\underline{\mathbf{Y}}}} \frac{-(e_P, \text{tr}(\underline{\underline{\mathbf{v}}}_{nc}))_\Omega}{\|\underline{\underline{\mathbf{v}}}_{nc}\|_{\underline{\underline{\mathbf{L}}}^2(\Omega)}}. \quad (3.53)$$

Hence, from (3.53) and (3.52), the orthogonal decomposition of the gradient of the velocity error in conjunction with the bounds for the conforming and nonconforming parts of the velocity error we obtain the following result.

Theorem 3.6.1. *Define the following natural norm*

$$\|(\mathbf{e}_V, e_P)\|_\Omega^2 = \|\nabla \mathbf{e}_V\|_{\underline{\mathbb{L}}^2(\Omega)}^2 + \beta^2 \|e_P\|_{L^2(\Omega)}^2.$$

Then, the velocity and pressure errors can be bounded above as

$$\|(\mathbf{e}_V, e_P)\|_\Omega^2 \leq \eta^2, \quad (3.54)$$

where the error estimator η is given by

$$\eta^2 = \Phi_c(\vartheta_K, \boldsymbol{\beta}_K)^2 + \Phi_{nc}(\mathbf{u}^*)^2 + (\Phi_c(0, \boldsymbol{\beta}_K) + \Phi_{nc}(\mathbf{u}^*))^2, \quad (3.55)$$

with the conforming estimator Φ_c given by

$$\Phi_c(\vartheta_K, \boldsymbol{\beta}_K)^2 = \sum_{K \in \mathcal{P}} (\Phi_{c,K}(\vartheta_K, \boldsymbol{\beta}_K))^2, \quad (3.56)$$

where

$$\Phi_{c,K}(\vartheta_K, \boldsymbol{\beta}_K) = \|\underline{\boldsymbol{\sigma}}_K^*(\vartheta_K, \boldsymbol{\beta}_K)\|_{\underline{\mathbb{L}}^2(K)} + C_K \|\mathbf{f} - \mathbf{\Pi}_K(\mathbf{f})\|_{L^2(K)} \quad (3.57)$$

and $\underline{\boldsymbol{\sigma}}_K^(\vartheta_K, \boldsymbol{\beta}_K) = \underline{\boldsymbol{\sigma}}_K - (\vartheta_K \underline{\mathbf{I}} - \mathbf{curl}(\boldsymbol{\beta}_K))$, being $\underline{\boldsymbol{\sigma}}_K$ the solution of (3.29)-(3.30) given in Lemma 3.4.1, $\vartheta_K \in L^2(\Omega)$ and $\boldsymbol{\beta}_K \in \mathbf{H}_0^1(K)$ are chosen to minimize $\|\underline{\boldsymbol{\sigma}}_K^*(\vartheta_K, \boldsymbol{\beta}_K)\|_{\underline{\mathbb{L}}^2(K)}$ and the constant C_K is given by (3.13). The nonconforming estimator Φ_{nc} is given by*

$$\Phi_{nc}(\mathbf{u}^*) = \|\nabla_h(\mathbf{u}^* - \mathbf{u}_h)\|_{\underline{\mathbb{L}}^2(\Omega)} + \frac{1}{\beta} \|\nabla \cdot \mathbf{u}^*\|_{L^2(\Omega)}, \quad (3.58)$$

where the function \mathbf{u}^ is given by*

$$\mathbf{u}^* = \begin{cases} \mathbf{S}(\mathbf{u}_h) & \text{given by (3.46),} \\ \text{or} \\ \mathbf{u}_{min}^* & \text{given by (3.47).} \end{cases}$$

Remark 3.6.2. *Notice that in order to obtain a guaranteed upper bound, any choice for ϑ_K and $\boldsymbol{\beta}_K$ are valid in (3.57), but to obtain an efficient error estimator we need to choose the ones that are zero or the ones that minimize $\|\underline{\boldsymbol{\sigma}}_K^*(\vartheta_K, \boldsymbol{\beta}_K)\|_{\underline{\mathbb{L}}^2(K)}$.*

3.7 Efficiency of the estimator.

Since the error estimator η is written in terms of the conforming estimator Φ_c and the nonconforming estimator Φ_{nc} , we first focus on bounding the conforming estimator.

In order to obtain the efficiency of the conforming estimator, the following results will be useful, which are based on bubble function arguments, used in [11, 103].

Lemma 3.7.1. *The element and edge residuals satisfy for all $K \in \mathcal{P}$*

$$h_K \|\mathcal{R}_K\|_{\mathbf{L}^2(K)} \leq C \left(h_K \|\mathbf{\Pi}_K(\mathbf{f}) + \Delta \mathbf{u}_h - \nabla p_h\|_{\mathbf{L}^2(K)} + \sum_{\gamma \in \mathcal{E}_K} \alpha_\gamma h_K^{1/2} \|\llbracket \nabla_h \mathbf{u}_h \cdot \hat{\mathbf{n}}_\gamma - p_h \hat{\mathbf{n}}_\gamma \rrbracket\|_{\mathbf{L}^2(\gamma)} \right),$$

and for $\gamma \in \mathcal{E}_K$,

$$h_K^{1/2} \|\mathcal{R}_{\gamma,K}\|_{\mathbf{L}^2(\gamma)} \leq C \left(h_K \|\mathbf{\Pi}_K(\mathbf{f}) + \Delta \mathbf{u}_h - \nabla p_h\|_{\mathbf{L}^2(K)} + \sum_{\gamma' \in \mathcal{E}_K} \alpha_{\gamma'} h_K^{1/2} \|\llbracket \nabla_h \mathbf{u}_h \cdot \hat{\mathbf{n}}_{\gamma'} - p_h \hat{\mathbf{n}}_{\gamma'} \rrbracket\|_{\mathbf{L}^2(\gamma')} \right).$$

Proof. First of all, we recall equation (3.27), which states that for all $\mathbf{v} \in \mathbf{H}^1(K)$,

$$\begin{aligned} & (\mathcal{R}_K, \mathbf{v})_K + \sum_{\gamma \in \mathcal{E}_K} (\mathcal{R}_{\gamma,K}, \mathbf{v})_\gamma \\ &= (\mathbf{\Pi}_K(\mathbf{f}) + \Delta \mathbf{u}_h - \nabla p_h, \mathbf{v} - \mathbf{\Pi}_{FS}(\mathbf{v}))_K - \sum_{\gamma \in \mathcal{E}_K} (\alpha_\gamma \llbracket \nabla_h \mathbf{u}_h \cdot \hat{\mathbf{n}}_\gamma - p_h \hat{\mathbf{n}}_\gamma \rrbracket, \mathbf{v} - \mathbf{\Pi}_{FS}(\mathbf{v}))_\gamma. \end{aligned} \quad (3.59)$$

Let $\beta_K = \prod_{n \in \mathcal{V}_K} \lambda_n \in H_0^1(K)$. Taking $\mathbf{v} = \beta_K \mathcal{R}_K$ in (3.59), we obtain

$$\begin{aligned} \|\beta_K^{1/2} \mathcal{R}_K\|_{\mathbf{L}^2(K)}^2 &= (\mathbf{\Pi}_K(\mathbf{f}) + \Delta \mathbf{u}_h - \nabla p_h, \beta_K \mathcal{R}_K - \mathbf{\Pi}_{FS}(\beta_K \mathcal{R}_K))_K \\ &\quad - \sum_{\gamma \in \mathcal{E}_K} (\alpha_\gamma \llbracket \nabla_h \mathbf{u}_h \cdot \hat{\mathbf{n}}_\gamma - p_h \hat{\mathbf{n}}_\gamma \rrbracket, \beta_K \mathcal{R}_K - \mathbf{\Pi}_{FS}(\beta_K \mathcal{R}_K))_\gamma \\ &\leq \|\mathbf{\Pi}_K(\mathbf{f}) + \Delta \mathbf{u}_h - \nabla p_h\|_{\mathbf{L}^2(K)} \left(\|\beta_K \mathcal{R}_K - \mathbf{\Pi}_{FS}(\beta_K \mathcal{R}_K)\|_{\mathbf{L}^2(K)} \right) \\ &\quad + \sum_{\gamma \in \mathcal{E}_K} \alpha_\gamma \|\llbracket \nabla_h \mathbf{u}_h \cdot \hat{\mathbf{n}}_\gamma - p_h \hat{\mathbf{n}}_\gamma \rrbracket\|_{\mathbf{L}^2(\gamma)} \|\beta_K \mathcal{R}_K - \mathbf{\Pi}_{FS}(\beta_K \mathcal{R}_K)\|_{\mathbf{L}^2(\gamma)}, \end{aligned}$$

upon applying the Cauchy–Schwarz inequality. Now, using Lemma 3.2.3, with the fact that $C_K \leq Ch_K$ and $C_\gamma^K \leq Ch_K^{1/2}$, the mesh regularity and Theorem 2.1.2, it follows that

$$\begin{aligned} \|\beta_K \mathcal{R}_K - \mathbf{\Pi}_{FS}(\beta_K \mathcal{R}_K)\|_{\mathbf{L}^2(K)} &\leq C_K \|\nabla(\beta_K \mathcal{R}_K)\|_{\mathbf{L}^2(K)} \lesssim C \|\beta_K^{1/2} \mathcal{R}_K\|_{\mathbf{L}^2(K)}, \\ \|\beta_K \mathcal{R}_K - \mathbf{\Pi}_{FS}(\beta_K \mathcal{R}_K)\|_{\mathbf{L}^2(\gamma)} &\leq C_\gamma^K \|\nabla(\beta_K \mathcal{R}_K)\|_{\mathbf{L}^2(K)} \lesssim Ch_K^{-1/2} \|\beta_K^{1/2} \mathcal{R}_K\|_{\mathbf{L}^2(K)}. \end{aligned}$$

Hence,

$$\begin{aligned} \|\beta_K^{1/2} \mathcal{R}_K\|_{\mathbf{L}^2(K)} &\leq C \left(\|\mathbf{\Pi}_K(\mathbf{f}) + \Delta \mathbf{u}_h - \nabla p_h\|_{\mathbf{L}^2(K)} \right. \\ &\quad \left. + h_K^{-1/2} \sum_{\gamma \in \mathcal{E}_K} \alpha_\gamma \|\llbracket \nabla_h \mathbf{u}_h \cdot \hat{\mathbf{n}}_\gamma - p_h \hat{\mathbf{n}}_\gamma \rrbracket\|_{\mathbf{L}^2(\gamma)} \right) \end{aligned}$$

and the first inequality follows by using the fact that $\|\mathcal{R}_K\|_{L^2(K)} \leq C \left\| \beta_K^{1/2} \mathcal{R}_K \right\|_{L^2(K)}$ (again using Theorem 2.1.2).

Now, for $\gamma \in \mathcal{E}_K$ let $\beta_\gamma = \prod_{n \in \mathcal{V}_\gamma} \lambda_n \in H^1(K)$. Taking $\mathbf{v} = \beta_\gamma \mathcal{R}_{\gamma,K}$ in (3.59), we obtain

$$\begin{aligned} & \left\| \beta_\gamma^{1/2} \mathcal{R}_{\gamma,K} \right\|_{L^2(\gamma)}^2 \\ &= (\mathbf{\Pi}_K(\mathbf{f}) + \Delta \mathbf{u}_h - \nabla p_h, \beta_\gamma \mathcal{R}_{\gamma,K} - \mathbf{\Pi}_{FS}(\beta_\gamma \mathcal{R}_{\gamma,K}))_K - (\mathcal{R}_K, \beta_\gamma \mathcal{R}_{\gamma,K})_K \\ & \quad - \sum_{\gamma' \in \mathcal{E}_K} (\alpha_{\gamma'} \llbracket \nabla \mathbf{u}_h \cdot \hat{\mathbf{n}}_{\gamma'} - p_h \hat{\mathbf{n}}_{\gamma'} \rrbracket, \beta_\gamma \mathcal{R}_{\gamma,K} - \mathbf{\Pi}_{FS}(\beta_\gamma \mathcal{R}_{\gamma,K}))_{\gamma'} \\ &\leq \|\mathbf{\Pi}_K(\mathbf{f}) + \Delta \mathbf{u}_h - \nabla p_h\|_{L^2(K)} \|\beta_\gamma \mathcal{R}_{\gamma,K} - \mathbf{\Pi}_{FS}(\beta_\gamma \mathcal{R}_{\gamma,K})\|_{L^2(K)} + \|\mathcal{R}_K\|_{L^2(K)} \|\beta_\gamma \mathcal{R}_{\gamma,K}\|_{L^2(K)} \\ & \quad + \sum_{\gamma' \in \mathcal{E}_K} \alpha_{\gamma'} \|\llbracket \nabla \mathbf{u}_h \cdot \hat{\mathbf{n}}_{\gamma'} - p_h \hat{\mathbf{n}}_{\gamma'} \rrbracket\|_{L^2(\gamma')} \|\beta_\gamma \mathcal{R}_{\gamma,K} - \mathbf{\Pi}_{FS}(\beta_\gamma \mathcal{R}_{\gamma,K})\|_{L^2(\gamma')}, \end{aligned}$$

upon applying the Cauchy–Schwarz inequality. Now, using Lemma 3.2.3, with the fact that $C_K \leq Ch_K$ and $C_{\gamma'}^K \leq Ch_K^{1/2}$, the mesh regularity and Theorem 2.1.3, it follows that

$$\begin{aligned} \|\beta_\gamma \mathcal{R}_{\gamma,K} - \mathbf{\Pi}_{FS}(\beta_\gamma \mathcal{R}_{\gamma,K})\|_{L^2(K)} &\leq C_K \|\nabla(\beta_\gamma \mathcal{R}_{\gamma,K})\|_{\underline{\underline{L}}^2(K)} \leq Ch_K^{1/2} \left\| \beta_\gamma^{1/2} \mathcal{R}_{\gamma,K} \right\|_{L^2(\gamma)}, \\ \|\beta_\gamma \mathcal{R}_{\gamma,K} - \mathbf{\Pi}_{FS}(\beta_\gamma \mathcal{R}_{\gamma,K})\|_{L^2(\gamma')} &\leq C_{\gamma'}^K \|\nabla(\beta_\gamma \mathcal{R}_{\gamma,K})\|_{\underline{\underline{L}}^2(K)} \leq C \left\| \beta_\gamma^{1/2} \mathcal{R}_{\gamma,K} \right\|_{L^2(\gamma)}. \end{aligned}$$

Using the fact that $\|\mathcal{R}_{\gamma,K}\|_{L^2(\gamma)} \leq C \left\| \beta_\gamma^{1/2} \mathcal{R}_{\gamma,K} \right\|_{L^2(\gamma)}$ (again using Theorem (2.1.3)), we obtain

$$\begin{aligned} \|\mathcal{R}_{\gamma,K}\|_{L^2(\gamma)} &\leq C \left(h_K^{1/2} \|\mathbf{\Pi}_K(\mathbf{f}) + \Delta \mathbf{u}_h - \nabla p_h\|_{L^2(K)} \right. \\ & \quad \left. + \sum_{\gamma' \in \mathcal{E}_K} \alpha_{\gamma'} \|\llbracket \nabla \mathbf{u}_h \cdot \hat{\mathbf{n}}_{\gamma'} - p_h \hat{\mathbf{n}}_{\gamma'} \rrbracket\|_{L^2(\gamma')} \right), \end{aligned}$$

and the second inequality follows. \square

Now, we can state the lower bound for the conforming estimator.

Lemma 3.7.2. *There exists a positive constant c , independent of the size of the elements in the mesh, such that*

$$c \Phi_{c,K}(\vartheta_K, \beta_K) \leq \sum_{K' \in \Omega_K} \left(\|\nabla_h e_V\|_{\underline{\underline{L}}^2(K')} + \beta \|e_P\|_{L^2(K')} + h_{K'} \|\mathbf{f} - \mathbf{\Pi}_{K'}(\mathbf{f})\|_{L^2(K')} \right).$$

Proof. Applying the estimate $C_K \leq Ch_K$, due to the mesh regularity, to the expression for $\Phi_{c,K}$ given in (3.57) leads to

$$\Phi_{c,K}(\vartheta_K, \beta_K) \leq C \left(\|\underline{\underline{\sigma}}_K\|_{\underline{\underline{L}}^2(K)} + h_K \|\mathbf{f} - \mathbf{\Pi}_K(\mathbf{f})\|_{L^2(K)} \right).$$

Now, (3.33) state that

$$\|\underline{\boldsymbol{g}}_K\|_{\underline{\mathbb{L}}^2(K)} \leq C \left(h_K \|\mathcal{R}_K\|_{\mathbb{L}^2(K)} + \sum_{\gamma \in \mathcal{E}_K} h_K^{1/2} \|\mathcal{R}_{\gamma,K}\|_{\mathbb{L}^2(\gamma)} \right).$$

Applying similar bubble arguments as the ones used in the previous Lemma, but now to (3.17), we obtain for all $K \in \mathcal{P}$,

$$\begin{aligned} h_K \|\mathbf{\Pi}_K(\mathbf{f}) + \Delta \mathbf{u}_h - \nabla p_h\|_{\mathbb{L}^2(K)} \\ \leq C \left(\|\nabla_h \mathbf{e}_V\|_{\underline{\mathbb{L}}^2(K)} + \beta \|e_P\|_{\mathbb{L}^2(K)} + h_K \|\mathbf{f} - \mathbf{\Pi}_K(\mathbf{f})\|_{\mathbb{L}^2(K)} \right), \end{aligned}$$

and for $\gamma \in \mathcal{E}_I$,

$$\begin{aligned} |\gamma|^{1/2} \|\nabla_h \mathbf{u}_h \hat{\mathbf{n}}_\gamma - p_h \hat{\mathbf{n}}_\gamma\|_{\mathbb{L}^2(\gamma)} \\ \leq C \sum_{K \in \Omega_\gamma} \left(\|\nabla_h \mathbf{e}_V\|_{\underline{\mathbb{L}}^2(K)} + \beta \|e_P\|_{\mathbb{L}^2(K)} + h_K \|\mathbf{f} - \mathbf{\Pi}_K(\mathbf{f})\|_{\mathbb{L}^2(K)} \right). \end{aligned}$$

Combining the above inequalities, the definition of α_γ and Lemma 3.7.1, gives the claimed result. \square

In order to obtain a lower bound for the nonconforming part of the error, we take $\mathbf{u}^* = \mathbf{S}(\mathbf{u}_h)$, and first observe that since $\mathbf{u}_h \in \mathbf{X}_h$,

$$\begin{aligned} \Phi_{nc}(\mathbf{S}(\mathbf{u}_h)) &= \|\nabla_h(\mathbf{S}(\mathbf{u}_h) - \mathbf{u}_h)\|_{\underline{\mathbb{L}}^2(\Omega)} + \frac{1}{\beta} \|\nabla \cdot \mathbf{S}(\mathbf{u}_h)\|_{\mathbb{L}^2(\Omega)} \tag{3.60} \\ &= \left(\sum_{K \in \mathcal{P}} \|\nabla(\mathbf{S}(\mathbf{u}_h) - \mathbf{u}_h)\|_{\underline{\mathbb{L}}^2(K)}^2 \right)^{1/2} + \left(\sum_{K \in \mathcal{P}} \frac{1}{\beta^2} \|\nabla \cdot \mathbf{S}(\mathbf{u}_h)\|_{\mathbb{L}^2(K)}^2 \right)^{1/2} \\ &\leq \sqrt{2} \left(\sum_{K \in \mathcal{P}} \|\nabla(\mathbf{S}(\mathbf{u}_h) - \mathbf{u}_h)\|_{\underline{\mathbb{L}}^2(K)}^2 + \frac{1}{\beta^2} \|\nabla \cdot (\mathbf{S}(\mathbf{u}_h) - \mathbf{u}_h)\|_{\mathbb{L}^2(K)}^2 \right)^{1/2} \\ &\leq C \left(\sum_{K \in \mathcal{P}} \|\nabla(\mathbf{S}(\mathbf{u}_h) - \mathbf{u}_h)\|_{\underline{\mathbb{L}}^2(K)}^2 \right)^{1/2}. \end{aligned}$$

The definition of \mathcal{N}_K and the fact that $\mathbf{S}(\mathbf{u}_h)$ and \mathbf{u}_h are polynomials of degree two on each element give

$$\mathbf{S}(\mathbf{u}_h)_K - \mathbf{u}_h|_K = \sum_{m \in \mathcal{N}_K} (\mathbf{S}(\mathbf{u}_h)(\mathbf{x}_m) - \mathbf{u}_h|_K(\mathbf{x}_m)) \varphi_m,$$

where $\{\varphi_m\}$ with $m \in \mathcal{N}_K$, is the usual nodal basis for $\mathbb{P}_2(K)$ which satisfies $\|\nabla \varphi_m\|_{\mathbb{L}^2(K)} \leq C$.

Hence,

$$\|\nabla(\mathbf{S}(\mathbf{u}_h) - \mathbf{u}_h)\|_{\underline{\mathbb{L}}^2(K)}^2 \leq C \sum_{m \in \mathcal{N}_K} |\mathbf{S}(\mathbf{u}_h)(\mathbf{x}_m) - \mathbf{u}_h|_K(\mathbf{x}_m)|^2. \tag{3.61}$$

To obtain the lower bound we need the following result to bound the terms appearing on the right hand side of the above inequality.

Lemma 3.7.3. *Let $m \in \mathcal{N}_K$. There exists a positive constant C , independent of the size of the elements in the mesh, such that*

$$|\mathbf{S}(\mathbf{u}_h)(\mathbf{x}_m) - \mathbf{u}_{h|K}(\mathbf{x}_m)| \leq C \|\underline{\mathbf{e}}_{nc}\|_{\underline{\mathbf{L}}^2(\Omega_m)},$$

where $\Omega_m = \{K \in \mathcal{P} : \mathbf{x}_m \in \overline{K} \text{ for a fixed } m \in \mathcal{N}_K\}$.

We defer the proof of this result temporarily. From the above inequality we can obtain a local lower bound on the nonconforming part of the error.

Lemma 3.7.4. *There exists a positive constant c , independent of the nonconforming error and the size of the elements in the mesh, such that*

$$c \Phi_{nc}(\mathbf{S}(\mathbf{u}_h))|_K \leq \sum_{K' \in \tilde{\Omega}_K} \|\underline{\mathbf{e}}_{nc}\|_{\underline{\mathbf{L}}^2(K')}.$$

Proof. The result follows from (3.60), (3.61) and Lemma 3.7.3. \square

In order to prove Lemma 3.7.3, the following result will be useful.

Lemma 3.7.5. *Let $K \in \mathcal{P}$ and $\gamma \in \mathcal{E}_K$. Define $\beta_\gamma^K = 60\lambda_l\lambda_r(\lambda_r - \lambda_l)$ where $\mathcal{V}(\gamma) = \{l, r\}$ and edge γ is oriented as in Figure 3.1. Then for any vector $\mathbf{c} \in \mathbb{R}^2$ and $\mathbf{p} \in \mathbb{P}_1(\gamma)^2$,*

$$(\mathbf{p}, \beta_\gamma^K \mathbf{c})_\gamma = |\gamma|^2 \frac{\partial \mathbf{p}}{\partial \hat{\mathbf{t}}_\gamma^K} \cdot \mathbf{c}.$$

Proof. The result is a simple consequence of Lemma 3.7 in [14]. \square

Proof of Lemma 3.7.3. Let $K, K' \in \mathcal{P}$ be distinct elements sharing a common edge $\gamma = \mathcal{E}_K \cap \mathcal{E}_{K'} \in \mathcal{E}_I$. Let $\mathbf{y} \in \mathbf{H}_0^1(\Omega_\gamma)$, then integration by parts allows us to say

$$(\underline{\mathbf{e}}_{nc}, \mathbf{curl}(\mathbf{y}))_\Omega = -(\nabla_h \mathbf{u}_h, \mathbf{curl}(\mathbf{y}))_{K \cup K'} = (\llbracket \nabla_h \mathbf{u}_h \cdot \hat{\mathbf{t}}_\gamma \rrbracket, \mathbf{y})_\gamma, \quad (3.62)$$

where

$$\llbracket \nabla_h \mathbf{u}_h \cdot \hat{\mathbf{t}}_\gamma \rrbracket = \nabla \mathbf{u}_{h|K} \cdot \hat{\mathbf{t}}_\gamma^K + \nabla \mathbf{u}_{h|K'} \cdot \hat{\mathbf{t}}_\gamma^{K'}.$$

Note that $\mathbf{curl}(\mathbf{y}) \in \underline{\mathbf{Y}}$ since integration by parts yields

$$(\mathbf{curl}(\mathbf{y}), \nabla \mathbf{v})_\Omega = (\underline{\mathbf{div}}(\mathbf{curl}(\mathbf{y})), \mathbf{v})_\Omega = 0 \quad \text{for all } \mathbf{v} \in \mathbf{X}.$$

In order to relate (3.62) with the quantity $\mathbf{S}(\mathbf{u}_h) - \mathbf{u}_{h|K}$ let us first consider the case when $\mathbf{x}_m \notin \Gamma$. From the definition of $\mathbf{S}(\mathbf{u}_h)$ in (3.46) and since $\sum_{K \in \Omega_m} \frac{1}{\text{card}(\Omega_m)} = 1$, there holds

$$\begin{aligned} |\mathbf{S}(\mathbf{u}_h)(\mathbf{x}_m) - \mathbf{u}_{h|K}(\mathbf{x}_m)| &= \left| \frac{1}{\text{card}(\Omega_m)} \sum_{K' \in \Omega_m \setminus K} (\mathbf{u}_{h|K}(\mathbf{x}_m) - \mathbf{u}_{h|K'}(\mathbf{x}_m)) \right| \\ &\leq C \sum_{K' \in \Omega_m \setminus K} |\mathbf{u}_{h|K}(\mathbf{x}_m) - \mathbf{u}_{h|K'}(\mathbf{x}_m)|. \end{aligned} \quad (3.63)$$

For an edge $\gamma = \mathcal{E}_K \cap \mathcal{E}_{K'}$, $\mathbf{u}_{h|K} - \mathbf{u}_{h|K'}$ vanishes at the two Gauss–Legendre points, then using the arc length parameter s_γ^K , it follows that $\mathbf{u}_{h|K} - \mathbf{u}_{h|K'} = \mathbf{r}_1 \left((s_\gamma^K)^2 - \frac{1}{12} |\gamma|^2 \right)$ with $\mathbf{r}_1 \in \mathbb{R}^2$. We can then differentiate this expression twice to obtain $2\mathbf{r}_1 = \frac{\partial}{\partial \hat{\mathbf{t}}_\gamma^K} \llbracket \nabla \mathbf{u}_h \cdot \hat{\mathbf{t}}_\gamma \rrbracket$. So, letting $s_\gamma^K = \pm \frac{|\gamma|}{2}$ or $s_\gamma^K = 0$ for an endpoint or midpoint, respectively, we see that

$$\begin{aligned} |\mathbf{u}_{h|K}(\mathbf{x}_m) - \mathbf{u}_{h|K'}(\mathbf{x}_m)| &= C |\gamma|^2 \left| \frac{\partial}{\partial \hat{\mathbf{t}}_\gamma^K} \llbracket \nabla \mathbf{u}_h \cdot \hat{\mathbf{t}}_\gamma \rrbracket \right| \\ &\leq C |\gamma|^2 \left(\left| \frac{\partial}{\partial \hat{\mathbf{t}}_\gamma^K} \llbracket \nabla \mathbf{u}_h \cdot \hat{\mathbf{t}}_\gamma \rrbracket \cdot \hat{\mathbf{t}}_\gamma^K \right| + \left| \frac{\partial}{\partial \hat{\mathbf{t}}_\gamma^K} \llbracket \nabla \mathbf{u}_h \cdot \hat{\mathbf{t}}_\gamma \rrbracket \cdot \hat{\mathbf{n}}_\gamma^K \right| \right), \end{aligned} \quad (3.64)$$

if \mathbf{x}_m is an endpoint or midpoint of edge γ . Let the vector-valued function $\beta_\gamma(\hat{\mathbf{t}}_\gamma)$ take the value $\beta_\gamma^K \hat{\mathbf{t}}_\gamma^K$ on K , $-\beta_\gamma^K \hat{\mathbf{t}}_\gamma^{K'}$ on K' and zero everywhere else with the function β_γ^K having been defined in Lemma 3.7.5. Now, defining $\beta_\gamma(\hat{\mathbf{n}}_\gamma)$ in a similar way, we can take $\mathbf{y} = \beta_\gamma(\hat{\mathbf{t}}_\gamma)$ and $\mathbf{y} = \beta_\gamma(\hat{\mathbf{n}}_\gamma)$ in (3.62) and apply the Cauchy–Schwarz inequality followed by the estimates $\|\mathbf{curl} \beta_\gamma(\hat{\mathbf{t}}_\gamma)\|_{\mathbf{L}^2(K)} \leq C$ and $\|\mathbf{curl} \beta_\gamma(\hat{\mathbf{n}}_\gamma)\|_{\mathbf{L}^2(K)} \leq C$ to obtain

$$\begin{aligned} |\gamma|^2 \left| \frac{\partial}{\partial \hat{\mathbf{t}}_\gamma^K} \llbracket \nabla \mathbf{u}_h \cdot \hat{\mathbf{t}}_\gamma \rrbracket \cdot \hat{\mathbf{t}}_\gamma^K \right| &\leq C \|\underline{\underline{\mathbf{e}}}_{nc}\|_{\underline{\underline{\mathbf{L}}}^2(\Omega_\gamma)}, \\ |\gamma|^2 \left| \frac{\partial}{\partial \hat{\mathbf{t}}_\gamma^K} \llbracket \nabla \mathbf{u}_h \cdot \hat{\mathbf{t}}_\gamma \rrbracket \cdot \hat{\mathbf{n}}_\gamma^K \right| &\leq C \|\underline{\underline{\mathbf{e}}}_{nc}\|_{\underline{\underline{\mathbf{L}}}^2(\Omega_\gamma)}. \end{aligned}$$

Substituting these bounds into (3.64) then gives

$$|\mathbf{u}_{h|K}(\mathbf{x}_m) - \mathbf{u}_{h|K'}(\mathbf{x}_m)| \leq C \|\underline{\underline{\mathbf{e}}}_{nc}\|_{\underline{\underline{\mathbf{L}}}^2(\Omega_\gamma)}. \quad (3.65)$$

This relation is valid for pairs of elements sharing a common edge γ . If the closure of elements K and K' consists of only the common point \mathbf{x}_m then we can write $|\mathbf{u}_{h|K}(\mathbf{x}_m) - \mathbf{u}_{h|K'}(\mathbf{x}_m)|$ as a telescoping sum of the jumps in \mathbf{u}_h across neighbouring edges, which we can bound using (3.65) to obtain

$$|\mathbf{u}_{h|K}(\mathbf{x}_m) - \mathbf{u}_{h|K'}(\mathbf{x}_m)| \leq C \|\underline{\underline{\mathbf{e}}}_{nc}\|_{\underline{\underline{\mathbf{L}}}^2(\Omega_m)}. \quad (3.66)$$

We defer the proof of the case when a point \mathbf{x}_m is a vertex or an edge midpoint of an edge $\gamma \in \mathcal{E}_\Gamma$ until we treat the case of non-homogeneous Dirichlet data, for which the present result is a special case (see Lemma 3.8.3). \square

3.8 Nonhomogeneous boundary data.

In this section we consider the case of nonhomogeneous boundary conditions in which the Stokes problem reads: *Find a velocity $\tilde{\mathbf{u}}$ and a pressure field \tilde{p} such that*

$$\begin{aligned} -\Delta \tilde{\mathbf{u}} + \nabla \tilde{p} &= \mathbf{f} & \text{in } \Omega, \\ \nabla \cdot \tilde{\mathbf{u}} &= 0 & \text{in } \Omega, \\ \tilde{\mathbf{u}} &= \mathbf{d} & \text{on } \Gamma, \end{aligned} \tag{3.67}$$

where the Dirichlet datum $\mathbf{d} \in H^1(\Gamma)^2$ satisfies the usual compatibility condition

$$\int_{\Gamma} \mathbf{d} \cdot \mathbf{n}_\Gamma \, ds = 0.$$

The associated weak formulation of problem (3.67) then reads: *Find $(\tilde{\mathbf{u}}, \tilde{p}) \in \mathbf{H}^1(\Omega) \times L_0^2(\Omega)$ such that*

$$\begin{aligned} a(\tilde{\mathbf{u}}, \mathbf{v}) + b(\mathbf{v}, \tilde{p}) &= (\mathbf{f}, \mathbf{v})_\Omega & \forall \mathbf{v} \in \mathbf{H}_0^1(\Omega), \\ b(\tilde{\mathbf{u}}, q) &= 0 & \forall q \in L_0^2(\Omega), \end{aligned} \tag{3.68}$$

and $\tilde{\mathbf{u}} = \mathbf{d}$ on Γ .

Let $\mathcal{J}(\mathbf{d})$ be the piecewise quadratic interpolant defined as follows: for an edge $\gamma \in \mathcal{E}_\Gamma$ with endpoints \mathbf{x}_1 and \mathbf{x}_2 ,

$$\mathcal{J}(\mathbf{d})|_\gamma = \alpha_1 \lambda_1 + \alpha_2 \lambda_2 + \alpha_3 \lambda_1 \lambda_2. \tag{3.69}$$

We take $\alpha_i = \mathbf{d}(\mathbf{x}_i)$ for $i = 1, 2$ and α_3 is fixed by requiring that

$$\int_{\gamma} (\mathcal{J}(\mathbf{d}) - \mathbf{d}) \, ds = \mathbf{0}. \tag{3.70}$$

Note that from the two conditions above it follows that $\int_{\Gamma} \mathcal{J}(\mathbf{d}) \cdot \mathbf{n}_\Gamma \, ds = 0$.

The nonconforming Fortin–Soulie finite element approximation of problem (3.68) consists of finding a pair $(\tilde{\mathbf{u}}_h, \tilde{p}_h) \in \mathbf{V}_h \times P_h$ such that

$$\begin{aligned} a(\tilde{\mathbf{u}}_h, \mathbf{v}_h) + b(\mathbf{v}_h, \tilde{p}_h) &= (\mathbf{f}, \mathbf{v}_h)_\Omega & \forall \mathbf{v}_h \in \mathbf{V}_h^D, \\ b(\tilde{\mathbf{u}}_h, q_h) &= 0 & \forall q_h \in P_h, \end{aligned} \tag{3.71}$$

subject to the boundary conditions

$$\tilde{\mathbf{u}}_h(\mathbf{x}_m) = \mathcal{J}(\mathbf{d})(\mathbf{x}_m) \text{ for all } m \in \mathcal{G}_\Gamma. \quad (3.72)$$

Note that this problem is well-posed since by construction the compatibility condition

$$0 = \int_\gamma \mathcal{J}(\mathbf{d}) \cdot \mathbf{n} \, ds = \int_\gamma \tilde{\mathbf{u}}_h \cdot \mathbf{n} \, ds \quad \text{for all } \gamma \in \mathcal{E}_\Gamma,$$

holds.

Similarly to the homogeneous case we decouple the gradient of the velocity error $\tilde{\mathbf{e}}_V := \tilde{\mathbf{u}} - \tilde{\mathbf{u}}_h$ into a conforming and a nonconforming part denoted by $\tilde{\mathbf{e}}_c$ and $\tilde{\mathbf{e}}_{nc}$, respectively. We define the estimator for the velocity and pressure as

$$\tilde{\eta}_V^2 = \Phi_c(\vartheta_K, \boldsymbol{\beta}_K)^2 + \tilde{\Phi}_{nc}^2 \quad \text{and} \quad \tilde{\eta}_P^2 = \left(\Phi_c(0, \boldsymbol{\beta}_K) + \tilde{\Phi}_{nc} \right)^2, \quad (3.73)$$

where the conforming estimator $\Phi_c(\vartheta_K, \boldsymbol{\beta}_K)$ is given by (3.56) and the nonconforming estimator $\tilde{\Phi}_{nc}$ is given by

$$\tilde{\Phi}_{nc} = \left(\sum_{K \in \mathcal{P}} \tilde{\Phi}_{nc1|K}^2 \right)^{1/2} + \frac{1}{\beta} \left(\sum_{K \in \mathcal{P}} \tilde{\Phi}_{nc2|K}^2 \right)^{1/2} \quad (3.74)$$

with

$$\tilde{\Phi}_{nc1,K} = \left\| \nabla_h \left(\tilde{\mathcal{S}}(\tilde{\mathbf{u}}_h) - \tilde{\mathbf{u}}_h \right) \right\|_{\underline{\mathcal{L}}^2(K)} + \sum_{\gamma \in \mathcal{E}_K \cap \mathcal{E}_\Gamma} \left\| \nabla E_{\gamma,K}(\mathbf{d} - \mathcal{J}(\mathbf{d})) \right\|_{\underline{\mathcal{L}}^2(K)},$$

and

$$\tilde{\Phi}_{nc2,K} = \left\| \nabla \cdot \tilde{\mathcal{S}}(\tilde{\mathbf{u}}_h) \right\|_{L^2(K)} + \sum_{\gamma \in \mathcal{E}_K \cap \mathcal{E}_\Gamma} \left\| \nabla \cdot E_{\gamma,K}(\mathbf{d} - \mathcal{J}(\mathbf{d})) \right\|_{L^2(K)}.$$

The smoothing $\tilde{\mathcal{S}}(\tilde{\mathbf{u}}_h)$ is defined in (3.81) and the extension function $E_{\gamma,K}(\mathbf{d} - \mathcal{J}(\mathbf{d}))$ is defined in (3.82). In the next section we prove the following bounds for the velocity error $\tilde{\mathbf{e}}$ and the pressure error \tilde{e}_P ,

$$\|(\tilde{\mathbf{e}}_V, \tilde{e}_P)\|_\Omega^2 \leq \tilde{\eta}_V^2 + \tilde{\eta}_P^2, \quad (3.75)$$

and

$$c(\tilde{\eta}_V^2 + \tilde{\eta}_P^2) \leq \|(\tilde{\mathbf{e}}_V, \tilde{e}_P)\|_\Omega^2 + \sum_{K \in \mathcal{P}} h_K^2 \|\mathbf{f} - \boldsymbol{\Pi}_K(\mathbf{f})\|_{L^2(K)} + \sum_{K \in \mathcal{P}} \sum_{\{\gamma \in \mathcal{E}_K \cap \mathcal{E}_\Gamma\}} \text{osc}^2(\mathbf{d}, \gamma), \quad (3.76)$$

where for an edge $\gamma \in \mathcal{E}_\Gamma \cap \mathcal{E}_K$, we define the oscillation of the Dirichlet datum as

$$\text{osc}(\mathbf{d}, \gamma) = \left\| \nabla E_{\gamma,K}(\mathbf{d} - \mathcal{J}(\mathbf{d})) \right\|_{\underline{\mathcal{L}}^2(K)}. \quad (3.77)$$

3.8.1 A posteriori analysis for the nonhomogeneous problem.

Noting that the errors \tilde{e}_V and \tilde{e}_P satisfy the same equation as in (3.22), then $\tilde{e}_c = e_c$, i.e. \tilde{e}_c will provide the same computable upper bound and local lower bound obtained in the previous sections. Hence, we only need to modify the nonconforming estimator to take the nonhomogeneous Dirichlet datum into account.

Lemma 3.8.1. *The nonconforming part of the error $\tilde{\underline{\underline{e}}}_{nc}$ satisfies*

$$\left\| \tilde{\underline{\underline{e}}}_{nc} \right\|_{\underline{\underline{L}}^2(\Omega)} \leq \tilde{\Phi}_{nc},$$

with $\tilde{\Phi}_{nc}$ given by (3.74).

Proof. Let $\tilde{\mathbf{u}}^* \in \mathbf{H}^1(\Omega)$ with $\tilde{\mathbf{u}}^* = \mathbf{d}$ on Γ . For $\underline{\underline{\mathbf{w}}}_{nc} \in \underline{\underline{\mathbf{Y}}}$, it follows that

$$\begin{aligned} \left(\tilde{\underline{\underline{e}}}_{nc}, \underline{\underline{\mathbf{w}}}_{nc} \right)_{\Omega} &= \left(\nabla_h(\tilde{e}_V - \tilde{e}_c), \underline{\underline{\mathbf{w}}}_{nc} \right)_{\Omega} = \left(\nabla_h(\tilde{\mathbf{u}} - \tilde{\mathbf{u}}_h), \underline{\underline{\mathbf{w}}}_{nc} \right)_{\Omega} \\ &= \left(\nabla_h(\tilde{\mathbf{u}}^* - \tilde{\mathbf{u}}_h), \underline{\underline{\mathbf{w}}}_{nc} \right)_{\Omega} + \left(\nabla(\tilde{\mathbf{u}} - \tilde{\mathbf{u}}^*), \underline{\underline{\mathbf{w}}}_{nc} \right)_{\Omega}, \end{aligned} \quad (3.78)$$

then taking $\underline{\underline{\mathbf{w}}}_{nc} = \tilde{\underline{\underline{e}}}_{nc}$ in the previous equality and using (3.40), yields

$$\left\| \tilde{\underline{\underline{e}}}_{nc} \right\|_{\underline{\underline{L}}^2(\Omega)}^2 = \left(\nabla_h(\tilde{\mathbf{u}}^* - \tilde{\mathbf{u}}_h), \tilde{\underline{\underline{e}}}_{nc} \right)_{\Omega} - (w, \nabla \cdot \tilde{\mathbf{u}}^*)_{\Omega}. \quad (3.79)$$

We next take $\tilde{\mathbf{u}}^*$ as

$$\tilde{\mathbf{u}}^* = \tilde{\mathbf{S}}(\tilde{\mathbf{u}}_h) + \sum_{K \in \mathcal{P}} \sum_{\gamma \in \mathcal{E}_K \cap \mathcal{E}_{\Gamma}} E_{\gamma, K}(\mathbf{d} - \mathcal{J}(\mathbf{d})), \quad (3.80)$$

where the quadratic interpolant $\tilde{\mathbf{S}}(\tilde{\mathbf{u}}_h)$ is defined by

$$\tilde{\mathbf{S}}(\tilde{\mathbf{u}}_h)(\mathbf{x}_m) = \begin{cases} \sum_{K' \in \Omega_m} \frac{1}{\text{card}(\Omega_m)} \tilde{\mathbf{u}}_h|_{K'}(\mathbf{x}_m) & \text{for } m \notin \mathcal{N}_{\Gamma}, \\ \mathcal{J}(\mathbf{d})(\mathbf{x}_m) & \text{for } m \in \mathcal{N}_{\Gamma}, \end{cases} \quad (3.81)$$

for $m \in \mathcal{N}$ and $E_{\gamma, K}(\mathbf{d} - \mathcal{J}(\mathbf{d})) \in \mathbf{H}^1(K)^2$ is any function satisfying

$$E_{\gamma, K}(\mathbf{d} - \mathcal{J}(\mathbf{d})) = \begin{cases} \mathbf{d} - \mathcal{J}(\mathbf{d}) & \text{on } \gamma, \\ \mathbf{0} & \text{on } \mathcal{E}_K \setminus \gamma, \end{cases} \quad (3.82)$$

Inserting (3.80) into (3.79) the result follows on applying Lemma 3.5.2 and the Cauchy-Schwarz inequality. \square

Remark 3.8.2. *In practical computations we use the extension operator $E_{\gamma, K}$ from [88], given by*

$$E_{\tilde{\gamma}, \hat{K}}(v) = \left(1 - x - \frac{y}{\sqrt{3}}\right) \left(1 + x - \frac{y}{\sqrt{3}}\right) \frac{\sqrt{3}}{2y} \int_{x-y/\sqrt{3}}^{x+y/\sqrt{3}} \frac{v(s)}{1-s^2} ds, \quad (3.83)$$

where the element \hat{K} has vertices at $(0, \sqrt{3})$, $(-1, 0)$ and $(1, 0)$ and edge $\hat{\gamma}$ lies on the x -axis, and satisfies

$$\|\nabla E_{\gamma,K}(\mathbf{d} - \mathcal{J}(\mathbf{d}))\|_{\underline{\underline{L}}^2(K)} \leq C|\gamma|^{1/2} \left\| \frac{\partial}{\partial s_\gamma}(\mathbf{d} - \mathcal{J}(\mathbf{d})) \right\|_{\mathbf{L}^2(\gamma)}, \quad (3.84)$$

with s_γ being the arc length parameter on edge γ and C denoting a positive constant which is independent of the size of the elements in the mesh.

Now, in order to prove the lower bound, we first observe that from the definition of the nonconforming estimator it follows that

$$\tilde{\Phi}_{nc}^2 \leq C \sum_{K \in \mathcal{P}} \left(\tilde{\Phi}_{nc1,K} + \tilde{\Phi}_{nc2,K} \right)^2.$$

Using the same argument as in the homogeneous case then yields

$$\tilde{\Phi}_{nc1,K} + \tilde{\Phi}_{nc2,K} \leq C \|\nabla_h(\tilde{\mathbf{S}}(\tilde{\mathbf{u}}_h) - \tilde{\mathbf{u}}_h)\|_{\underline{\underline{L}}^2(K)}^2 + \sum_{\gamma \in \mathcal{E}_K \cap \mathcal{E}_\Gamma} \|\nabla E_{\gamma,K}(\mathbf{d} - \mathcal{J}(\mathbf{d}))\|_{\underline{\underline{L}}^2(K)}^2.$$

This inequality allows us to prove the following result which confirms the local efficiency of the nonconforming estimator.

Lemma 3.8.3. *There exists a positive constant c , independent of the nonconforming error and the size of the elements in the mesh, such that*

$$c \left(\tilde{\Phi}_{nc1,K} + \tilde{\Phi}_{nc2,K} \right)^2 \leq \sum_{K' \in \tilde{\Omega}_K} \|\tilde{\mathbf{e}}_{nc}\|_{\underline{\underline{L}}^2(K')}^2 + \sum_{\gamma \in \tilde{\mathcal{E}}(K) \cap \mathcal{E}_\Gamma} \text{osc}^2(\mathbf{d}, \gamma),$$

where $\tilde{\mathcal{E}}(K)$ is the set of edges which have an endpoint lying on a vertex of element K .

Proof. As in the proof of the homogeneous case we have to bound $\left| \tilde{\mathbf{u}}_{h|K}(\mathbf{x}_m) - \tilde{\mathbf{S}}(\tilde{\mathbf{u}}_h)(\mathbf{x}_m) \right|$, for $m \in \mathcal{N}_K$. The same arguments used in the proof of the homogeneous case hold if \mathbf{x}_m does not lie on the boundary Γ . Therefore, it only remains to study the case when the point \mathbf{x}_m is a vertex or an edge midpoint of an edge $\gamma \in \mathcal{E}_\Gamma$, i.e. we take $\mathbf{x}_m \in \Gamma$. In such a case, it is easy to see that

$$\left| \tilde{\mathbf{u}}_{h|K}(\mathbf{x}_m) - \tilde{\mathbf{S}}(\tilde{\mathbf{u}}_h)(\mathbf{x}_m) \right| \leq \sum_{\{\gamma \in \mathcal{E}_\Gamma: \mathbf{x}_m \in \bar{\gamma}\}} \left| \tilde{\mathbf{u}}_{h|K}(\mathbf{x}_m) - \tilde{\mathbf{S}}(\tilde{\mathbf{u}}_h)(\mathbf{x}_m) \right|,$$

where $\mathbf{S}(\tilde{\mathbf{u}}_h)$ is given by (3.81). Now the right hand side can be bounded as

$$\begin{aligned} & \sum_{\{\gamma \in \mathcal{E}_\Gamma: \mathbf{x}_m \in \bar{\gamma}\}} \sum_{\{K' \in \Omega_\gamma\}} \left| \tilde{\mathbf{u}}_{h|K}(\mathbf{x}_m) - \tilde{\mathbf{S}}(\tilde{\mathbf{u}}_h)(\mathbf{x}_m) \right| \\ & \leq \sum_{\{\gamma \in \mathcal{E}_\Gamma: \mathbf{x}_m \in \bar{\gamma}\}} \sum_{\{K' \in \Omega_\gamma\}} \left(\left| \tilde{\mathbf{u}}_{h|K'}(\mathbf{x}_m) - \mathcal{J}(\mathbf{d})(\mathbf{x}_m) \right| + \left| \tilde{\mathbf{u}}_{h|K}(\mathbf{x}_m) - \tilde{\mathbf{u}}_{h|K'}(\mathbf{x}_m) \right| \right). \end{aligned}$$

The last term in the preceding inequality can be bounded using (3.66). Now we will bound the first term.

From (3.72) it follows that if $\gamma \in \mathcal{E}_\Gamma$ then $\tilde{\mathbf{u}}_h - \mathcal{J}(\mathbf{d})$ vanishes at the two mapped Gauss–Legendre points on the edge γ . Reasoning as in (3.64), we can conclude that

$$\begin{aligned} & |\tilde{\mathbf{u}}_{h|K'}(\mathbf{x}_m) - \mathcal{J}(\mathbf{d})(\mathbf{x}_m)| \\ &= C|\gamma|^2 \left| \frac{\partial}{\partial s_\gamma} \left(\frac{\partial \tilde{\mathbf{u}}_{h|K'}}{\partial s_\gamma} - \frac{\partial \mathcal{J}(\mathbf{d})}{\partial s_\gamma} \right) \right| \\ &\leq C|\gamma|^2 \left(\left| \frac{\partial}{\partial s_\gamma} \left(\frac{\partial \tilde{\mathbf{u}}_{h|K'}}{\partial s_\gamma} - \frac{\partial \mathcal{J}(\mathbf{d})}{\partial s_\gamma} \right) \cdot \hat{\mathbf{t}}_\gamma^{K'} \right| + \left| \frac{\partial}{\partial s_\gamma} \left(\frac{\partial \tilde{\mathbf{u}}_h}{\partial s_\gamma} - \frac{\partial \mathcal{J}(\mathbf{d})}{\partial s_\gamma} \right) \cdot \hat{\mathbf{n}}_\gamma^{K'} \right| \right). \end{aligned}$$

Let the vector-valued function $\beta_\gamma(\hat{\mathbf{t}}_\gamma)$ take the value $\beta_\gamma^{K'} \hat{\mathbf{t}}_\gamma^{K'}$ on K' and zero everywhere else with the function $\beta_\gamma^{K'}$ having been defined in Lemma 3.7.5. Now, defining $\beta_\gamma(\hat{\mathbf{n}}_\gamma)$ in a similar way, then taking $\underline{\underline{\mathbf{e}}}_{nc} = \mathbf{curl}(\beta_\gamma(\hat{\mathbf{t}}_\gamma))$ and $\underline{\underline{\mathbf{w}}}_{nc} = \mathbf{curl}(\beta_\gamma(\hat{\mathbf{n}}_\gamma))$ in (3.78) and integrating by parts yields

$$\left(\underline{\underline{\mathbf{e}}}_{nc}, \mathbf{curl}(\beta_\gamma(\hat{\mathbf{t}}_\gamma)) \right)_{K'} = - \left(\frac{\partial}{\partial s_\gamma}(\mathbf{d} - \mathcal{J}(\mathbf{d})) + \frac{\partial}{\partial s_\gamma}(\mathcal{J}(\mathbf{d}) - \tilde{\mathbf{u}}_{h|K'}), \beta_\gamma(\hat{\mathbf{t}}_\gamma) \right)_\gamma, \quad (3.85)$$

and

$$\left(\underline{\underline{\mathbf{e}}}_{nc}, \mathbf{curl}(\beta_\gamma(\hat{\mathbf{n}}_\gamma)) \right)_{K'} = - \left(\frac{\partial}{\partial s_\gamma}(\mathbf{d} - \mathcal{J}(\mathbf{d})) + \frac{\partial}{\partial s_\gamma}(\mathcal{J}(\mathbf{d}) - \tilde{\mathbf{u}}_{h|K'}), \beta_\gamma(\hat{\mathbf{n}}_\gamma) \right)_\gamma. \quad (3.86)$$

From the properties of the functions $\beta_\gamma(\hat{\mathbf{t}}_\gamma)$ and $\beta_\gamma(\hat{\mathbf{n}}_\gamma)$ it follows that

$$\left(\frac{\partial}{\partial s_\gamma}(\mathcal{J}(\mathbf{d}) - \tilde{\mathbf{u}}_{h|K'}), \beta_\gamma(\hat{\mathbf{t}}_\gamma) \right)_\gamma = |\gamma|^2 \left(\frac{\partial}{\partial s_\gamma} \left(\frac{\partial \mathcal{J}(\mathbf{d})}{\partial s_\gamma} - \frac{\partial \tilde{\mathbf{u}}_{h|K'}}{\partial s_\gamma} \right) \cdot \hat{\mathbf{t}}_\gamma^{K'} \right), \quad (3.87)$$

and

$$\left(\frac{\partial}{\partial s_\gamma}(\mathcal{J}(\mathbf{d}) - \tilde{\mathbf{u}}_{h|K'}), \beta_\gamma(\hat{\mathbf{n}}_\gamma) \right)_\gamma = |\gamma|^2 \left(\frac{\partial}{\partial s_\gamma} \left(\frac{\partial \mathcal{J}(\mathbf{d})}{\partial s_\gamma} - \frac{\partial \tilde{\mathbf{u}}_{h|K'}}{\partial s_\gamma} \right) \cdot \hat{\mathbf{n}}_\gamma^{K'} \right). \quad (3.88)$$

By using (3.16), (3.84), the Cauchy–Schwarz inequality and integration by parts, it follows that

$$\begin{aligned} \left(\frac{\partial}{\partial s_\gamma}(\mathbf{d} - \mathcal{J}(\mathbf{d})), \beta_\gamma(\hat{\mathbf{t}}_\gamma) \right)_\gamma &= - \left(E_{\gamma, K'}(\mathbf{d} - \mathcal{J}(\mathbf{d})) - \mathbf{c}, \frac{\partial}{\partial s_\gamma} \beta_\gamma(\hat{\mathbf{t}}_\gamma) \right)_\gamma \\ &\leq Ch_{K'}^{1/2} \|\nabla E_{\gamma, K'}(\mathbf{d} - \mathcal{J}(\mathbf{d}))\|_{\underline{\underline{L}}^2(K')} \left\| \frac{\partial}{\partial s_\gamma} \beta_\gamma(\hat{\mathbf{t}}_\gamma) \right\|_{\mathbf{L}^2(\gamma)} \\ &\leq C \|\nabla E_{\gamma, K'}(\mathbf{d} - \mathcal{J}(\mathbf{d}))\|_{\underline{\underline{L}}^2(K')}, \end{aligned} \quad (3.89)$$

where $\mathbf{c} \in \mathbb{R}^2$ is chosen so that $\|E_{\gamma, K'}(\mathbf{d} - \mathcal{J}(\mathbf{d})) - \mathbf{c}\|_{\mathbf{L}^2(\gamma)} \leq Ch_{K'}^{1/2} \|\nabla E_{\gamma, K'}(\mathbf{d} - \mathcal{J}(\mathbf{d}))\|_{\underline{\underline{L}}^2(K')}$ and we used the estimate $\left\| \frac{\partial}{\partial s_\gamma} \beta_\gamma(\hat{\mathbf{t}}_\gamma) \right\|_{\mathbf{L}^2(\gamma)} \leq Ch_{K'}^{-1/2}$. In a similar way we obtain

$$\left(\frac{\partial}{\partial s_\gamma}(\mathbf{d} - \mathcal{J}(\mathbf{d})), \beta_\gamma(\hat{\mathbf{n}}_\gamma) \right)_\gamma \leq C \|\nabla E_{\gamma, K'}(\mathbf{d} - \mathcal{J}(\mathbf{d}))\|_{\underline{\underline{L}}^2(K')}. \quad (3.90)$$

Now inserting (3.87) and (3.89) into (3.85) and (3.88) and (3.90) into (3.86) it follows that

$$\begin{aligned} |\gamma|^2 \left| \frac{\partial}{\partial s_\gamma} \left(\frac{\partial \mathcal{J}(\mathbf{d})}{\partial s_\gamma} - \frac{\partial \tilde{\mathbf{u}}_{h|\gamma}}{\partial s_\gamma} \right) \cdot \hat{\mathbf{t}}_\gamma^{K'} \right| &\leq C \left(\left\| \tilde{\mathbf{e}}_{nc} \right\|_{\underline{\underline{\mathbf{L}}^2(K')}} + \left\| \nabla E_{\gamma, K'}(\mathbf{d} - \mathcal{J}(\mathbf{d})) \right\|_{\underline{\underline{\mathbf{L}}^2(K')}} \right), \\ |\gamma|^2 \left| \frac{\partial}{\partial s_\gamma} \left(\frac{\partial \mathcal{J}(\mathbf{d})}{\partial s_\gamma} - \frac{\partial \tilde{\mathbf{u}}_{h|\gamma}}{\partial s_\gamma} \right) \cdot \hat{\mathbf{n}}_\gamma^{K'} \right| &\leq C \left(\left\| \tilde{\mathbf{e}}_{nc} \right\|_{\underline{\underline{\mathbf{L}}^2(K')}} + \left\| \nabla E_{\gamma, K'}(\mathbf{d} - \mathcal{J}(\mathbf{d})) \right\|_{\underline{\underline{\mathbf{L}}^2(K')}} \right). \end{aligned}$$

Upon combining Lemma 3.7.3, the above inequalities and the definition of the Dirichlet oscillation (3.77), the result follows. \square

Finally (3.75) follows replacing the bound for the new nonconforming error given in Lemma 3.8.1 in Section 3.6. The efficiency of the estimator in (3.76) follows using Lemma 3.7.2 and Lemma 3.8.3.

3.8.2 The extension operator $E(\mathbf{d} - \mathcal{J}(\mathbf{d}))$ is an oscillation.

We finally remark that the extra term coming from the non-homogeneous boundary datum might be seen as an oscillation term. To this end, we first give the following result:

Lemma 3.8.4. *For all $\mathbf{d} \in \mathbf{H}^2(\Gamma)$ and all $\gamma \in \mathcal{E}_\Gamma$,*

$$\left\| \frac{\partial}{\partial s_\gamma}(\mathbf{d} - \mathcal{J}(\mathbf{d})) \right\|_{\mathbf{L}^2(\gamma)} \leq |\gamma| \left\| \frac{\partial^2}{\partial s_\gamma^2}(\mathbf{d} - \mathcal{J}(\mathbf{d})) \right\|_{\mathbf{L}^2(\gamma)},$$

and there exists a positive constant C such that

$$\left\| \frac{\partial^2}{\partial s_\gamma^2}(\mathbf{d} - \mathcal{J}(\mathbf{d})) \right\|_{\mathbf{L}^2(\gamma)} \leq C \inf_{\mathbf{c} \in \mathbb{R}^2} \left\| \frac{\partial^2 \mathbf{d}}{\partial s_\gamma^2} - \mathbf{c} \right\|_{\mathbf{L}^2(\gamma)}.$$

Proof. Noting that $\mathbf{v} - \mathcal{J}(\mathbf{v}) \in \mathbf{H}_0^1(\gamma)$, then integrating by parts and applying a Poincaré inequality we obtain

$$\left\| \frac{\partial}{\partial s_\gamma}(\mathbf{v} - \mathcal{J}(\mathbf{v})) \right\|_{\mathbf{L}^2(\gamma)} \leq |\gamma| \left\| \frac{\partial^2}{\partial s_\gamma^2}(\mathbf{v} - \mathcal{J}(\mathbf{v})) \right\|_{\mathbf{L}^2(\gamma)},$$

and the first claim follows. In order to prove the second inequality, we work on the reference element $(-1, 1)$, where the interpolant $\mathcal{J} : H^1(-1, 1)^2 \rightarrow \mathbb{P}_2(-1, 1)^2$ is defined by

$$\mathcal{J}(\mathbf{d})(\pm 1) = \mathbf{d}(\pm 1) \quad \text{and} \quad \int_{-1}^1 \mathcal{J}(\mathbf{d}) ds = \int_{-1}^1 \mathbf{d} ds.$$

Then $\mathcal{J}(\mathbf{d})(s) = \frac{1}{2}(1-s)\mathbf{d}(-1) + \frac{1}{2}(1+s)\mathbf{d}(1) + \boldsymbol{\alpha}(1-s^2)$ with $\boldsymbol{\alpha}$ given by

$$\boldsymbol{\alpha} = \frac{3}{4} \left(\int_{-1}^1 \mathbf{d} ds - (\mathbf{d}(-1) + \mathbf{d}(1)) \right).$$

Since $\frac{\partial^2 \mathcal{J}(\mathbf{d})}{\partial s^2} = -2\boldsymbol{\alpha}$, the Peano Kernel theorem (cf. [61]) leads to

$$\left| \frac{\partial^2 \mathcal{J}(\mathbf{d})}{\partial s^2} \right| = \frac{3}{2} \left| \int_{-1}^1 K(s) \frac{\partial^2 \mathbf{d}}{\partial s^2} ds \right|,$$

where $K(s) = (s^2 - 1)/2$. Applying the Cauchy–Schwarz inequality, yields

$$\left\| \frac{\partial^2 \mathcal{J}(\mathbf{d})}{\partial s^2} \right\|_{\mathbf{L}^2(-1,1)} \leq \sqrt{\frac{3}{5}} \left\| \frac{\partial^2 \mathbf{d}}{\partial s^2} \right\|_{\mathbf{L}^2(-1,1)}.$$

Now, let $\mathbf{c} \in \mathbb{R}^2$ be given and define $\mathbf{q} = \frac{1}{2}\mathbf{c}(s^2 - 1)$ so $\mathcal{J}(\mathbf{q}) = \mathbf{q}$. Hence

$$\begin{aligned} \left\| \frac{\partial^2 \mathbf{d}}{\partial s^2} - \frac{\partial^2 \mathcal{J}(\mathbf{d})}{\partial s^2} \right\|_{\mathbf{L}^2(-1,1)} &= \left\| \frac{\partial^2}{\partial s^2}(\mathbf{d} - \mathbf{q}) - \frac{\partial^2}{\partial s^2} \mathcal{J}(\mathbf{d} - \mathbf{q}) \right\|_{\mathbf{L}^2(-1,1)} \\ &\leq \left(1 + \sqrt{\frac{3}{5}} \right) \left\| \frac{\partial^2}{\partial s^2}(\mathbf{d} - \mathbf{q}) \right\|_{\mathbf{L}^2(-1,1)} \\ &= \left(1 + \sqrt{\frac{3}{5}} \right) \left\| \frac{\partial^2 \mathbf{d}}{\partial s^2} - \mathbf{c} \right\|_{\mathbf{L}^2(-1,1)}, \end{aligned}$$

and the claim follows using standard scaling arguments. \square

Combining the previous result with (3.84), it follows that if $\mathbf{d} \in \mathbf{H}^2(\Gamma)$ then

$$\|\nabla E_{\gamma,K}(\mathbf{d} - \mathcal{J}(\mathbf{d}))\|_{\mathbf{L}^2(K)} \leq C|\gamma|^{3/2} \left\| \frac{\partial^2}{\partial s_\gamma^2}(\mathbf{d} - \mathcal{J}(\mathbf{d})) \right\|_{\mathbf{L}^2(\gamma)},$$

which is a higher order term.

3.9 An explicit formula to compute the norm of the solution of the Neumann problem.

In terms of practical applications, the following result will be useful.

Lemma 3.9.1. *Denote by tr the trace of a matrix. Then*

$$\inf_{\vartheta_K \in \mathbf{L}^2(K)} \left\| \boldsymbol{\sigma}_K - \vartheta_K \mathbf{I} \right\|_{\mathbf{L}^2(K)} = \left\| \boldsymbol{\sigma}_K - \frac{1}{2} \text{tr}(\boldsymbol{\sigma}_K) \mathbf{I} \right\|_{\mathbf{L}^2(K)}. \quad (3.91)$$

Proof. We only need to prove that $\frac{1}{2}\text{tr}(\boldsymbol{\sigma}_K)$ is the orthogonal projection of $\boldsymbol{\sigma}_K$ over the space of functions of the form $p\mathbf{I}$ for any $p \in \mathbf{L}^2(K)$. In fact, if $\boldsymbol{\sigma}_K = [\sigma_{i,j}]_{2 \times 2}$ then for any $p \in \mathbf{L}^2(K)$ it follows that

$$\begin{aligned} 0 &= (\boldsymbol{\sigma}_K - \vartheta_K \mathbf{I}, p\mathbf{I})_K \\ &= \int_K \begin{bmatrix} \sigma_{11} - \vartheta_K & \sigma_{12} \\ \sigma_{21} & \sigma_{22} - \vartheta_K \end{bmatrix} : p \begin{bmatrix} 1 & 0 \\ 0 & 1 \end{bmatrix} dx = (\sigma_{11} + \sigma_{22} - 2\vartheta_K, p)_K, \end{aligned}$$

which implies that $\vartheta_K = \frac{1}{2}(\sigma_{11} + \sigma_{22})$, and the result follows. \square

Now, to compute the error estimator η given in Theorem 3.6.1, we replace the conforming estimator $\Phi_c(\vartheta_K, \beta_K)$ by

$$\Phi_c \left(\frac{1}{2} \text{tr}(\underline{\sigma}_K), \beta_K \right)^2 = \sum_{K \in \mathcal{P}} \Phi_{c,K} \left(\frac{1}{2} \text{tr}(\underline{\sigma}_K), \beta_K \right)^2, \quad (3.92)$$

where the local conforming estimator is given by

$$\Phi_{c,K} \left(\frac{1}{2} \text{tr}(\underline{\sigma}_K), \beta_K \right) = \left\| \underline{\sigma}_K^* \left(\frac{1}{2} \text{tr}(\underline{\sigma}_K), \beta_K \right) \right\|_{\underline{\mathcal{L}}^2(K)} + C_K \|\mathbf{f} - \mathbf{\Pi}_K(\mathbf{f})\|_{L^2(K)}, \quad (3.93)$$

where in this case we take the solution of (3.29)-(3.30) to be

$$\underline{\sigma}_K^* \left(\frac{1}{2} \text{tr}(\underline{\sigma}_K), \beta_K \right) = \underline{\sigma}_K - \frac{1}{2} \text{tr}(\underline{\sigma}_K) \underline{\mathbf{I}} - \left(\mathbf{curl}(\beta_K) + \frac{1}{2} \text{tr}(\mathbf{curl}(\beta_K)) \underline{\mathbf{I}} \right), \quad (3.94)$$

and $\beta_K \in [H_0^1(K) \cap \mathbb{P}_3(K)]^2$ is chosen to minimize $\left\| \underline{\sigma}_K^* \left(\frac{1}{2} \text{tr}(\underline{\sigma}_K), \beta_K \right) \right\|_{\underline{\mathcal{L}}^2(K)}$.

In the case where $\vartheta_K = 0$, we take the conforming estimator as

$$\Phi_c(0, \beta_K)^2 = \sum_{K \in \mathcal{P}} \Phi_{c,K}(0, \beta_K)^2, \quad (3.95)$$

where the local conforming estimator is given by

$$\Phi_{c,K}(0, \beta_K) = \left\| \underline{\sigma}_K^*(0, \beta_K) \right\|_{\underline{\mathcal{L}}^2(K)} + C_K \|\mathbf{f} - \mathbf{\Pi}_K(\mathbf{f})\|_{L^2(K)}, \quad (3.96)$$

and in this case the solution of (3.29)-(3.30) is $\underline{\sigma}_K^*(0, \beta_K) = \underline{\sigma}_K - \mathbf{curl}(\beta_K)$ and $\beta_K \in [H_0^1(K) \cap \mathbb{P}_3(K)]^2$ is chosen to minimize $\left\| \underline{\sigma}_K^*(0, \beta_K) \right\|_{\underline{\mathcal{L}}^2(K)}$.

To evaluate the effect in all the minimization processes, we define

$$\Phi_c(0, 0)^2 = \sum_{K \in \mathcal{P}} \Phi_{c,K}(0, 0)^2, \quad (3.97)$$

where the local conforming estimator is given by

$$\Phi_{c,K}(0, 0) = \left\| \underline{\sigma}_K \right\|_{\underline{\mathcal{L}}^2(K)} + C_K \|\mathbf{f} - \mathbf{\Pi}_K(\mathbf{f})\|_{L^2(K)}. \quad (3.98)$$

In all the previous cases, $\underline{\sigma}_K$ is given in Lemma 3.4.1.

To compute the norm of $\underline{\sigma}_K^*(\vartheta_K, \beta_K)$ for all the different minimization processes, for $i \in \mathcal{V}_K = \{1, 2, 3\}$ define

$$\underline{\tau}_i^{(1)} = \begin{bmatrix} \mathbf{t}_i \\ \mathbf{0} \end{bmatrix} - \frac{\varrho}{2} \text{tr} \left(\begin{bmatrix} \mathbf{t}_i \\ \mathbf{0} \end{bmatrix} \right) \underline{\mathbf{I}} \quad \text{and} \quad \underline{\tau}_i^{(2)} = \begin{bmatrix} \mathbf{0} \\ \mathbf{t}_i \end{bmatrix} - \frac{\varrho}{2} \text{tr} \left(\begin{bmatrix} \mathbf{0} \\ \mathbf{t}_i \end{bmatrix} \right) \underline{\mathbf{I}}, \quad (3.99)$$

with $\varrho = 0$ for $\boldsymbol{\sigma}_K(0, \boldsymbol{\beta}_K)$ and $\varrho = 1$ for $\boldsymbol{\sigma}_K(\xi_K, \boldsymbol{\beta}_K)$. Now, let

$$\left(\boldsymbol{\sigma}_{\gamma_i, K}^{(l)}, \boldsymbol{\sigma}_{\gamma_i, K}^{(m)}\right)_K = \frac{1}{6480|K|} \left(\mathbf{S}_i^{(l)}\right)^T \mathbf{M}_{ii}^{(l,m)} \mathbf{S}_i^{(m)}$$

and

$$\left(\boldsymbol{\sigma}_{\gamma_i, K}^{(l)}, \boldsymbol{\sigma}_{\gamma_j, K}^{(m)}\right)_K = \frac{1}{6480|K|} \left(\mathbf{S}_i^{(l)}\right)^T \mathbf{M}_{ij}^{(l,m)} \mathbf{S}_j^{(m)}$$

where

$$\mathbf{S}_1^{(l)} = \begin{pmatrix} \left(\mathcal{R}_{\gamma_1, K}, \boldsymbol{\lambda}_2^{(l)}\right)_{\gamma_1} \\ \left(\mathcal{R}_{\gamma_1, K}, \boldsymbol{\lambda}_3^{(l)}\right)_{\gamma_1} \\ |K| \nabla(\mathcal{R}_K^l) \cdot (\mathbf{x}_1 - \bar{\mathbf{x}}_K) \end{pmatrix}$$

with $\mathbf{S}_2^{(l)}$ and $\mathbf{S}_3^{(l)}$ being defined by permuting the indices and

$$\begin{aligned} \mathbf{M}_{11}^{(l,m)} = & \begin{bmatrix} 1242 & -2322 & 54 \\ -2322 & 4482 & -126 \\ 54 & -126 & 8 \end{bmatrix} \left(\boldsymbol{\tau}_2^{(l)} : \boldsymbol{\tau}_2^{(m)}\right) + \begin{bmatrix} 1647 & -945 & -36 \\ -2889 & 1647 & 72 \\ 72 & -36 & -4 \end{bmatrix} \left(\boldsymbol{\tau}_2^{(l)} : \boldsymbol{\tau}_3^{(m)}\right) \\ & + \begin{bmatrix} 1647 & -2889 & 72 \\ -945 & 1647 & -36 \\ -36 & 72 & -4 \end{bmatrix} \left(\boldsymbol{\tau}_3^{(l)} : \boldsymbol{\tau}_2^{(m)}\right) + \begin{bmatrix} 4482 & -2322 & -126 \\ -2322 & 1242 & 54 \\ -126 & 54 & 8 \end{bmatrix} \left(\boldsymbol{\tau}_3^{(l)} : \boldsymbol{\tau}_3^{(m)}\right) \end{aligned}$$

with $\mathbf{M}_{22}^{(l,m)}$ and $\mathbf{M}_{33}^{(l,m)}$ being defined by permuting the indices and

$$\begin{aligned} \mathbf{M}_{12}^{(l,m)} = & \begin{bmatrix} 459 & -837 & 36 \\ -1161 & 2079 & -72 \\ 90 & -162 & 4 \end{bmatrix} \left(\boldsymbol{\tau}_2^{(l)} : \boldsymbol{\tau}_3^{(m)}\right) + \begin{bmatrix} 1998 & -918 & -90 \\ -4158 & 1998 & 162 \\ 162 & -90 & -4 \end{bmatrix} \left(\boldsymbol{\tau}_2^{(l)} : \boldsymbol{\tau}_1^{(m)}\right) \\ & + \begin{bmatrix} 675 & -1593 & 126 \\ -297 & 675 & -54 \\ -54 & 126 & -8 \end{bmatrix} \left(\boldsymbol{\tau}_3^{(l)} : \boldsymbol{\tau}_3^{(m)}\right) + \begin{bmatrix} 2079 & -837 & -162 \\ -1161 & 459 & 90 \\ -72 & 36 & 4 \end{bmatrix} \left(\boldsymbol{\tau}_3^{(l)} : \boldsymbol{\tau}_1^{(m)}\right) \end{aligned}$$

with $\mathbf{M}_{23}^{(l,m)}$ and $\mathbf{M}_{31}^{(l,m)}$ being defined by permuting the indices. Also, let

$$\begin{aligned} \left(\boldsymbol{\sigma}_{0, K}^{(l)}, \boldsymbol{\sigma}_{0, K}^{(m)}\right)_K = & \frac{1}{6480|K|} \left(1152 \left(\boldsymbol{\tau}_2^{(l)} : \boldsymbol{\tau}_2^{(m)}\right) + 576 \left(\boldsymbol{\tau}_2^{(l)} : \boldsymbol{\tau}_3^{(m)}\right) \right. \\ & \left. + 576 \left(\boldsymbol{\tau}_3^{(l)} : \boldsymbol{\tau}_2^{(m)}\right) + 1152 \left(\boldsymbol{\tau}_3^{(l)} : \boldsymbol{\tau}_3^{(m)}\right) \right) \end{aligned}$$

and

$$\left(\boldsymbol{\sigma}_{\gamma_i, K}^{(l)}, \boldsymbol{\sigma}_{0, K}^{(m)}\right)_K = \frac{1}{6480 |K|} \left(S_i^{(l)}\right)^T \mathbf{M}_{i0}^{(l, m)}$$

where

$$\begin{aligned} \mathbf{M}_{10}^{(l, m)} &= \begin{bmatrix} 432 \\ -432 \\ -48 \end{bmatrix} \left(\boldsymbol{\tau}_2^{(l)} : \boldsymbol{\tau}_2^{(m)}\right) + \begin{bmatrix} 648 \\ -1080 \\ 0 \end{bmatrix} \left(\boldsymbol{\tau}_2^{(l)} : \boldsymbol{\tau}_3^{(m)}\right) \\ &+ \begin{bmatrix} 1080 \\ -648 \\ 0 \end{bmatrix} \left(\boldsymbol{\tau}_3^{(l)} : \boldsymbol{\tau}_2^{(m)}\right) + \begin{bmatrix} 432 \\ -432 \\ 48 \end{bmatrix} \left(\boldsymbol{\tau}_3^{(l)} : \boldsymbol{\tau}_3^{(m)}\right) \end{aligned}$$

with $\mathbf{M}_{20}^{(l, m)}$ and $\mathbf{M}_{30}^{(l, m)}$ being defined by permuting the indices. Also, define

$$\mathbf{A} \approx = \begin{bmatrix} \left(\boldsymbol{\sigma}_{0, K}^{(1)}, \boldsymbol{\sigma}_{0, K}^{(1)}\right)_K & \left(\boldsymbol{\sigma}_{0, K}^{(1)}, \boldsymbol{\sigma}_{0, K}^{(2)}\right)_K \\ \left(\boldsymbol{\sigma}_{0, K}^{(2)}, \boldsymbol{\sigma}_{0, K}^{(1)}\right)_K & \left(\boldsymbol{\sigma}_{0, K}^{(2)}, \boldsymbol{\sigma}_{0, K}^{(2)}\right)_K \end{bmatrix}$$

and

$$\mathbf{B} = \begin{pmatrix} \sum_{l=1}^2 \sum_{i=1}^3 \left(\boldsymbol{\sigma}_{\gamma_i, K}^{(l)}, \boldsymbol{\sigma}_{0, K}^{(1)}\right)_K \\ \sum_{l=1}^2 \sum_{i=1}^3 \left(\boldsymbol{\sigma}_{\gamma_i, K}^{(l)}, \boldsymbol{\sigma}_{0, K}^{(2)}\right)_K \end{pmatrix}.$$

The following result provides a simple formula to compute the norm of the solution of the Neumann problem, which includes all the minimization procedures.

Theorem 3.9.2. *Let*

$$\begin{aligned} \left\| \boldsymbol{\sigma}_K^* (\vartheta_K, \boldsymbol{\beta}_K) \right\|_{\mathbb{L}^2(K)}^2 &= \sum_{l=1}^2 \sum_{m=1}^2 \left(\left(\boldsymbol{\sigma}_{\gamma_1, K}^{(l)}, \boldsymbol{\sigma}_{\gamma_1, K}^{(m)}\right)_K + \left(\boldsymbol{\sigma}_{\gamma_2, K}^{(l)}, \boldsymbol{\sigma}_{\gamma_2, K}^{(m)}\right)_K + \left(\boldsymbol{\sigma}_{\gamma_3, K}^{(l)}, \boldsymbol{\sigma}_{\gamma_3, K}^{(m)}\right)_K \right. \\ &+ 2 \left(\left(\boldsymbol{\sigma}_{\gamma_2, K}^{(l)}, \boldsymbol{\sigma}_{\gamma_3, K}^{(m)}\right)_K + \left(\boldsymbol{\sigma}_{\gamma_3, K}^{(l)}, \boldsymbol{\sigma}_{\gamma_1, K}^{(m)}\right)_K + \left(\boldsymbol{\sigma}_{\gamma_1, K}^{(l)}, \boldsymbol{\sigma}_{\gamma_2, K}^{(m)}\right)_K \right) \\ &- \mathbf{B}^T \mathbf{A}^{-1} \mathbf{B} \tilde{\varrho}. \end{aligned} \quad (3.100)$$

where $\tilde{\varrho} \in \{1, 0\}$. Then, we obtain $\left\| \boldsymbol{\sigma}_K^* \left(\frac{1}{2} \text{tr}(\boldsymbol{\sigma}_K), \boldsymbol{\beta}_K\right) \right\|_{\mathbb{L}^2(K)}$ by taking $\varrho = 1$ and $\tilde{\varrho} = 1$ and $\left\| \boldsymbol{\sigma}_K^*(0, \boldsymbol{\beta}_K) \right\|_{\mathbb{L}^2(K)}$ by taking $\varrho = 0$ and $\tilde{\varrho} = 1$, in the previous process, and they are minimized over $\boldsymbol{\beta}_K \in [H_0^1(K) \cap \mathbb{P}_3(K)]^2$ and finally we obtain $\left\| \boldsymbol{\sigma}_K^*(0, 0) \right\|_{\mathbb{L}^2(K)}$ by taking $\varrho = 0$ and $\tilde{\varrho} = 0$.

Proof. Just for simplicity, let us consider the case when $\varrho = 0$ and $\tilde{\varrho} = 1$. From Lemma 3.4.1

and (2.12), taking $l = 1, 2$ and $i \in \mathcal{V}_K = \{1, 2, 3\}$ defining

$$\begin{aligned} \sigma_{\gamma_1, K}^{(l)} &= \frac{1}{2|K|} \left(\left(\mathcal{R}_{\gamma_1, K}, \lambda_2^{(l)} \right)_{\gamma_1} \left((2\lambda_3 + 3\lambda_3(\lambda_2 - \lambda_1))\mathbf{t}_2 + (4\lambda_2 + 3\lambda_2(\lambda_3 - \lambda_1))\mathbf{t}_2 \right) \right. \\ &\quad \left. - \left(\mathcal{R}_{\gamma_1, K}, \lambda_3^{(l)} \right)_{\gamma_1} \left((4\lambda_3 + 3\lambda_3(\lambda_2 - \lambda_1))\mathbf{t}_2 + (2\lambda_2 + 3\lambda_2(\lambda_3 - \lambda_1))\mathbf{t}_2 \right) \right) \\ &\quad + \frac{1}{3} \left(\nabla(\mathcal{R}_K^l) \cdot (\mathbf{x}_1 - \bar{\mathbf{x}}_K) \right) \lambda_1(\lambda_3\mathbf{t}_2 - \lambda_2\mathbf{t}_3), \end{aligned}$$

with $\sigma_{\gamma_2, K}^{(l)}$ and $\sigma_{\gamma_3, K}^{(l)}$ being defined by permuting the indices and also defining

$$\begin{aligned} \sigma_{0, K}^{(l)} &= -\text{curl}(\lambda_1\lambda_2\lambda_3) \\ &= \frac{1}{2|K|} \left((\lambda_2\lambda_3 - \lambda_3\lambda_1)\mathbf{t}_2 + (\lambda_2\lambda_3 - \lambda_1\lambda_2)\mathbf{t}_3 \right) \\ &= \frac{1}{2|K|} \left((\lambda_3\lambda_1 - \lambda_1\lambda_2)\mathbf{t}_3 + (\lambda_3\lambda_1 - \lambda_2\lambda_3)\mathbf{t}_1 \right) \\ &= \frac{1}{2|K|} \left((\lambda_1\lambda_2 - \lambda_2\lambda_3)\mathbf{t}_1 + (\lambda_1\lambda_2 - \lambda_3\lambda_1)\mathbf{t}_2 \right). \end{aligned}$$

it is relatively straightforward to show that

$$\begin{aligned} \sigma_{\gamma_k, K}^{(l)} \cdot \hat{\mathbf{n}}_{\gamma_j}^K &= \mathcal{R}_{\gamma_j, K}^l \delta_{jk} \quad \text{on } \gamma_j \text{ for all } j, k = 1, 2, 3; \\ \sigma_{0, K} \cdot \hat{\mathbf{n}}_{\gamma_j}^K &= 0 \quad \text{on } \gamma_j \text{ for all } j = 1, 2, 3; \end{aligned}$$

and

$$-\text{div} \left(\sum_{i=1}^3 \sigma_{\gamma_i, K}^{(l)} \right) = \mathcal{R}_K^l \quad \text{and} \quad -\text{div}(\sigma_{0, K}) = 0 \quad \text{in } K.$$

Then it follows that

$$\underline{\sigma}_K^*(0, \beta_K) = \begin{bmatrix} \sum_{i=1}^3 \sigma_{\gamma_i, K}^{(1)} - \frac{1}{(\sigma_{0, K}^{(1)}, \sigma_{0, K}^{(1)})_K} \sum_{i=1}^3 (\sigma_{\gamma_i, K}^{(1)}, \sigma_{0, K}^{(1)})_K \sigma_{0, K}^{(1)} \\ \sum_{i=1}^3 \sigma_{\gamma_i, K}^{(2)} - \frac{1}{(\sigma_{0, K}^{(2)}, \sigma_{0, K}^{(2)})_K} \sum_{i=1}^3 (\sigma_{\gamma_i, K}^{(2)}, \sigma_{0, K}^{(2)})_K \sigma_{0, K}^{(2)} \end{bmatrix},$$

satisfies (3.29)-(3.30). We can then obtain an expression for $\|\underline{\sigma}_K^*(0, \beta_K)\|_{\underline{\mathcal{L}}^2(K)}$ which can be manipulated into the above form, where the value of $\mathbf{B}^T \mathbf{A}^{-1} \mathbf{B} \tilde{\varrho}$ has been chosen so that $\|\underline{\sigma}_K^*(0, \beta_K)\|_{\underline{\mathcal{L}}^2(K)}$ is minimised over the space of cubic bubbles. The minimization process when we take $\varrho = 1$ and $\tilde{\varrho} = 1$ follows by using similar arguments and (3.94). \square

3.10 Numerical Results.

In this section we illustrate the performance of the error estimator with two representative problems.

In the numerical experiments we calculate the exact and the estimated error in the natural norm $\|(\cdot, \cdot)\|_\Omega$ on a sequence of uniformly and adaptively refined grids, respectively. For each marked triangle a longest edge bisection step [103] was performed. As a local error indicator for the adaptive algorithm we used

$$\eta_K^2 = \begin{cases} \Phi_{c,K}^2(\vartheta_K, \boldsymbol{\beta}_K) + \Phi_{nc,K}(\mathbf{u}^*)^2 + (\Phi_{c,K}(0, \boldsymbol{\beta}_K) + \Phi_{nc,K}(\mathbf{u}^*))^2 & \text{for homogeneous} \\ & \text{Dirichlet data,} \\ \Phi_{c,K}^2(\vartheta_K, \boldsymbol{\beta}_K) + \tilde{\Phi}_{nc,K}^2 + (\Phi_{c,K}(0, \boldsymbol{\beta}_K) + \tilde{\Phi}_{nc,K})^2 & \text{for nonhomogeneous} \\ & \text{Dirichlet data,} \end{cases} \quad (3.101)$$

where $\Phi_{c,K}$ is given by (3.93), (3.96) or (3.98), depending on the minimization process, $\Phi_{nc,K}(\mathbf{u}^*)$ is given by (3.58) and $\tilde{\Phi}_{nc,K}$ is given by (3.74), and triangles are marked using the maximum strategy (mark K if $\eta_K \geq \eta_{\max}/2$). We summarize the adaptive algorithm in Table 3.1.

Adaptive mesh refinement algorithm [AMRA-S-FS].

- 1:** Set $i = 0$ and construct a mesh $\mathcal{P}_{(i)}$.
 - 2:** For each element K in $\mathcal{P}_{(i)}$, compute:
 - $\|\underline{\boldsymbol{\sigma}}_K^*(\vartheta_K, \boldsymbol{\beta}_K)\|_{\underline{\mathbf{L}}^2(K)}$ using formula (3.100).
 - $\|\mathbf{f} - \mathbf{\Pi}_K(\mathbf{f})\|_{\mathbf{L}^2(K)}$ using an appropriate quadrature formula.
 - $\Phi_{c,K}(\vartheta_K, \boldsymbol{\beta}_K)$ using (3.93), (3.96) or (3.98), depending on the minimization process.
 - $\Phi_{nc,K}(\mathbf{u}^*)$ using (3.58) for homogeneous Dirichlet data or $\tilde{\Phi}_{nc,K}$ using (3.74) in conjunction with the extension operator $E_{\gamma,K}$ given by (3.83) for nonhomogeneous Dirichlet data.
 - η_K using the previous two steps and (3.101).
 - 3:** Triangle K is marked for refinement if

$$\eta_K \geq \frac{1}{2} \max_{K \in \mathcal{P}_{(i)}} \{\eta_K\}.$$
 - 4:** From step **3** deduce a new mesh using longest edge bisection refinement.
 - 5:** Set $i \leftarrow i + 1$ and return to step **2**.
-

Table 3.1: Adaptive mesh refinement algorithm for the Stokes problem using the Fortin–Soulie finite element.

The global error estimate is, according to (3.92), (3.95) or (3.97), depending on the mini-

mization process, (3.58), (3.73) and (3.75), is given by

$$\eta^2 = \begin{cases} \Phi_c^2(\vartheta_K, \boldsymbol{\beta}_K) + \Phi_{nc}(\mathbf{u}^*)^2 + (\Phi_c(0, \boldsymbol{\beta}_K) + \Phi_{nc}(\mathbf{u}^*))^2 & \text{for homogeneous} \\ & \text{Dirichlet data,} \\ \Phi_c^2(\vartheta_K, \boldsymbol{\beta}_K) + \tilde{\Phi}_{nc}^2 + (\Phi_c(0, \boldsymbol{\beta}_K) + \tilde{\Phi}_{nc})^2 & \text{for nonhomogeneous} \\ & \text{Dirichlet data,} \end{cases}$$

When reporting numerical results, we denote by Ndofs the number of degrees of freedom and we denote by $\Theta = \frac{\eta}{\|(\mathbf{e}_V, e_P)\|_\Omega}$ the effectivity index.

Notice that in the error indicators and as well in the error estimator we have present the inf-sup constant β related to the well-posedness of the continuous problem (see (3.4)), but what is really present is the inverse of this constant, i.e. $1/\beta$, then in terms of real applications we only need a lower bound for β , which for some polyhedral domains, accurate bounds are given in [102] and a procedure to estimate it is given in [63].

Example 1: The exact velocity and pressure fields for (3.1) are given by

$$\begin{aligned} \mathbf{u} &= [x^2(x-1)^2y(y-1)(2y-1), -y^2(y-1)^2x(x-1)(2x-1)], \\ p &= xy(1-x)(1-y) - \frac{1}{36}, \end{aligned}$$

where $\Omega = (0, 1)^2$ is the unit square. A lower bound of 0.38 for the value of the inf-sup constant β was obtained in [102].

Example 2: We consider the Stokes flow over a T-shaped domain, where a quadratic inflow and outflow are imposed on $x = \pm 1.5$ and no-slip conditions are imposed elsewhere on the boundary Γ , as shown in Figure 5.1. A lower bound of 0.1 for the inf-sup constant β was also obtained in [102].

The initial meshes $\mathcal{S}_{(0)}$ and $\mathcal{T}_{(0)}$, for example 1 and 2, respectively, are shown in Figure 3.3 for the regular or adaptive refinement.

First of all, we will see the effect on the different minimization processes on the conforming and nonconforming estimator. In Table 3.2 we present three different minimizations on the conforming estimator, which are, minimize with respect to $\vartheta_K \in \mathbb{P}_2(K)$ and $\boldsymbol{\beta}_K \in [H_0^1(K) \cap \mathbb{P}_3(K)]^2$, just bubble minimization which is taking $\vartheta_K = 0$ and $\boldsymbol{\beta}_K \in [H_0^1(K) \cap \mathbb{P}_3(K)]^2$ and no minimization at all which is $\vartheta_K = 0$ and $\boldsymbol{\beta}_K = \mathbf{0}$. We also present the two different alternatives that we have for the nonconforming estimator, which are taking $\mathbf{u}^* = \mathbf{S}(\mathbf{u}_h)$ and $\mathbf{u}^* = \mathbf{u}_{min}^*$.

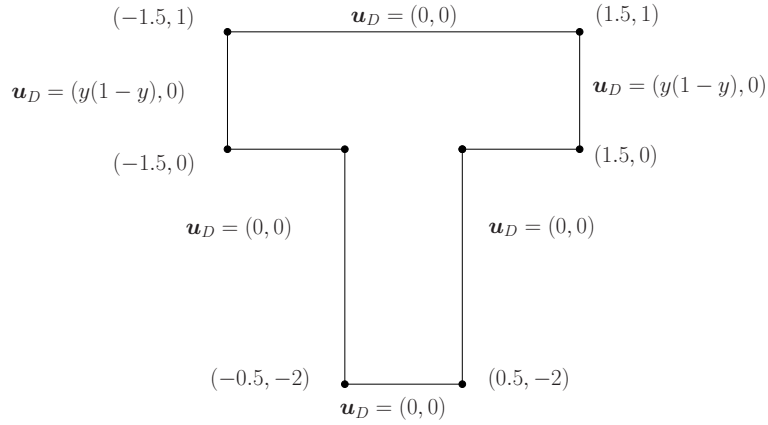


Figure 3.2: Domain and boundary conditions for Example 2.

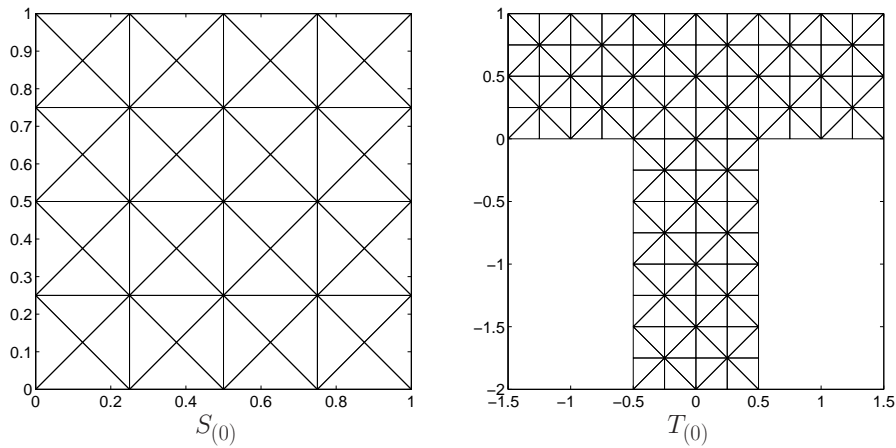


Figure 3.3: Initial mesh $S_{(0)}$ and $T_{(0)}$ for Examples 1 and 2, respectively.

From Table 3.2, we can see that for a smooth solution, the $\mathbf{L}^2(K)$ and $[H_0^1(K) \cap \mathbb{P}_3]^2$ minimization procedures do not have much impact in the accuracy of the conforming estimator, and in the case of the nonconforming estimator, also the best possible choice, which is $\mathbf{u}^* = \mathbf{u}_{min}^*$, does not have much impact in the accuracy.

From Figure 3.4 and 3.5, we can see that the actual error estimator is very accurate and from Figure 3.6 and 3.7 we can see that most of the refinement is taking place in the two reentrant corners, where the pressure presents a singular behaviour and the error estimator converges with

Ndofs	$\Phi_c(\frac{1}{2}\text{tr}(\underline{\underline{\sigma}}_K), \underline{\beta}_K)$	$\Phi_c(0, \underline{\beta}_K)$	$\Phi_c(0, 0)$	$\Phi_{nc}(\underline{u}_{min}^*)$	$\Phi_{nc}(\mathbf{S}(\underline{u}_h))$
608	0.0055848	0.0060239	0.0061888	0.0026317	0.0037594
2368	0.0011475	0.0012821	0.0013429	0.0008174	0.0010502
9344	0.0002525	0.0002900	0.0003074	0.0002344	0.0002730
37120	0.0000584	0.0000682	0.0000728	0.0000630	0.0000686
147968	0.000014	0.0000165	0.0000177	0.0000164	0.0000171

Table 3.2: The different minimization processes on the conforming and nonconforming estimator based on regular refinement using mesh $S_{(0)}$ from Figure 3.3, for Example 1.

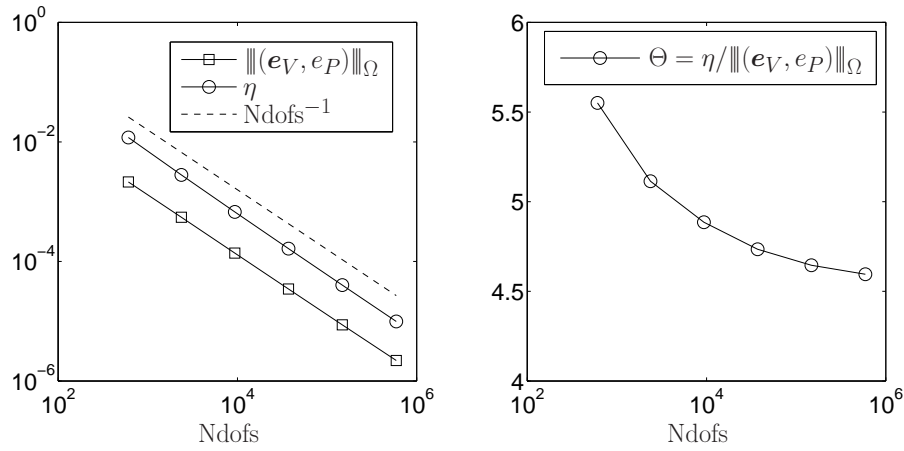


Figure 3.4: Accuracy (left) and effectivity index (right) for Example 1, using regular refinement over the mesh $S_{(0)}$ from Figure 3.3.

optimal order.

3.11 Conclusions

In this chapter we present a computable a posteriori error estimator, providing two-sided bounds on the true error measure in a natural norm. More remarkable is the fact that the error estimator actually provides a guaranteed upper bound. The analysis to obtain the guaranteed upper bound was carried out by an orthogonal decomposition of the gradient of the velocity error and was also based on the inf-sup condition related to the continuous problem, and more importantly by the properties of the nonconforming space in which we approximate the velocity field, which

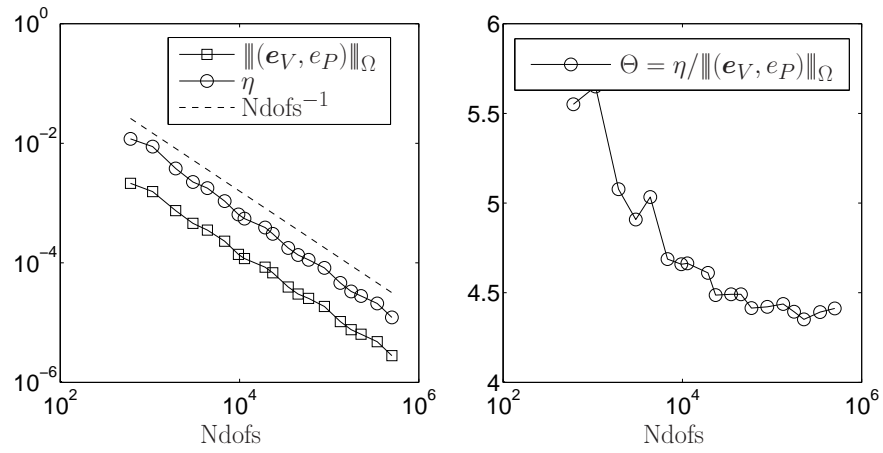


Figure 3.5: Accuracy (left) and effectivity index (right) for Example 1, using the AMRA-S-FS algorithm (Table 3.1) over the mesh $\mathcal{S}_{(0)}$ from Figure 3.3.

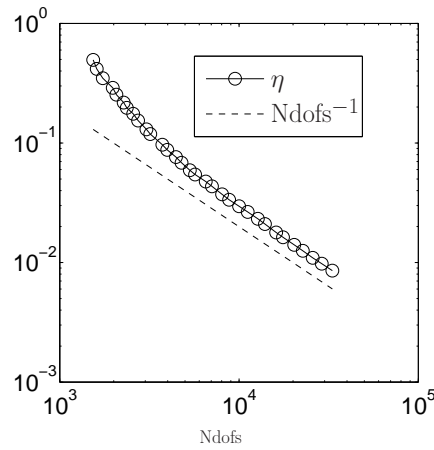


Figure 3.6: Accuracy using adaptive refinement over the mesh $\mathcal{T}_{(0)}$ from Figure 3.3, based on the AMRA-S algorithm in Table 3.1, for Example 2.

allowed the construction of an appropriate projection operator enabling to express the typical residual functional, related to the error equation, as a Neumann problem for which we have an explicit solution.

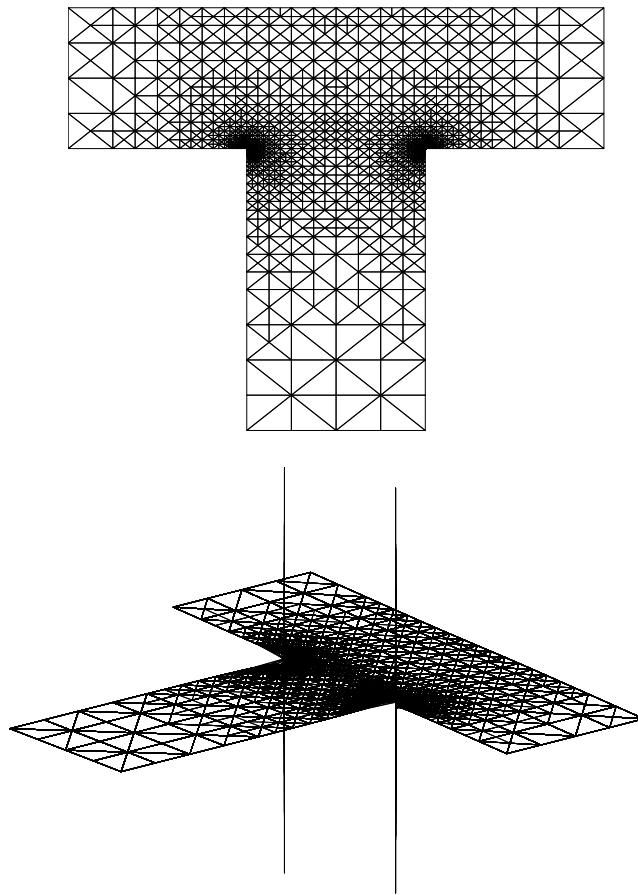


Figure 3.7: Piecewise continuous smoothing of the pressure, for Example 2.

Chapter 4

A review of the equilibrated residual method applied to a simple Poisson problem.

The previous chapter was mainly concerned with the approximation of the solution of a Stokes problem using a nonconforming finite element space, where a vital step was the construction of an appropriate projection operator. Now, if we approximate its solution by using conforming finite element spaces we do not have at hand a projection operator satisfying similar properties. Then, a completely different approach has to be considered in order to achieve the same goal. In order to illustrate the basic idea we will devote this chapter to the introduction of an equilibrated residual method applied to a simple Poisson problem, proposed by Ainsworth and Oden (cf. Chapter 6 in [11]), in which the construction of a special set of functions call the boundary fluxes and a $\mathbf{H}(\mathbf{div})$ lifting, related to the solution of a local Neumann problem, makes it possible to obtain a two-sided bounds on the error by approximating the solution using conforming finite elements. More remarkable is the fact that we can obtain the desired guaranteed upper bound which follows after the construction of a fully computable error estimator. This chapter presents a more detailed version of the analysis given in [3,5,12], restricted to the homogeneous Dirichlet case.

Our model problem is a simple Poisson problem with homogeneous Dirichlet boundary con-

dition on a domain $\Omega \subset \mathbb{R}^2$ with Lipschitz boundary Γ , i.e.: *Find u such that*

$$-\Delta u = f \quad \text{on } \Omega \quad \text{and} \quad u = 0 \quad \text{in } \Gamma. \quad (4.1)$$

4.1 The error equation.

The weak formulation associated with problem (4.1) is: *Find $u \in H_0^1(\Omega)$ such that*

$$\mathcal{B}(u, v) = \mathcal{L}(v) \quad \forall v \in H_0^1(\Omega), \quad (4.2)$$

where the bilinear form is given by $\mathcal{B}(u, v) = (\nabla u, \nabla v)_\Omega$ and the linear functional is given by $\mathcal{L}(v) = (f, v)_\Omega$. This Problem is well-posed due to the Lax–Milgram Theorem (see Chapter 2 in [40]).

Now, suppose that $V_h \subset H_0^1(\Omega)$ is a finite element subspace constructed on a regular partition \mathcal{P} of the domain Ω into triangular elements by using piecewise continuous polynomials of degree one. The finite element approximation of this problem is: *Find $u_h \in V_h$ such that*

$$\mathcal{B}(u_h, v_h) = \mathcal{L}(v_h) \quad \forall v_h \in V_h. \quad (4.3)$$

Now, let $e = u - u_h \in H_0^1(\Omega)$ be the error in the finite element approximation, then from (4.2) and (4.3) the error satisfies

$$\mathcal{B}(e, v) = \mathcal{B}(u, v) - \mathcal{B}(u_h, v) = \mathcal{L}(v) - \mathcal{B}(u_h, v) \quad \forall v \in H_0^1(\Omega). \quad (4.4)$$

The next step is to decompose the residual functional appearing in the right hand side of the previous equation, which we call the *error equation*, into contributions from the individual elements.

Let $\{g_{\gamma, K} : \gamma \in \mathcal{E}_K \text{ for all } K \in \mathcal{P}\}$ be a set of *boundary fluxes* on the elements that notionally approximate the actual flux of the true solution on the element boundaries

$$g_{\gamma, K} \approx \nabla u_h|_K \cdot \hat{\mathbf{n}}_\gamma^K.$$

Since the trace of the true fluxes are continuous on the interelement boundaries,

$$\nabla u|_K \cdot \hat{\mathbf{n}}_\gamma^K + \nabla u|_{K'} \cdot \hat{\mathbf{n}}_\gamma^K = 0 \quad \text{on } \gamma \in \mathcal{E}_K \cap \mathcal{E}_{K'},$$

and so, by analogy, the approximated fluxes are required to satisfy the condition

$$g_{\gamma, K} + g_{\gamma, K'} = 0 \quad \text{on } \gamma \in \mathcal{E}_K \cap \mathcal{E}_{K'}. \quad (4.5)$$

This condition expresses the requirement that flux should not be generated on the actual interface.

Clearly, the previous condition implies that

$$\sum_{K \in \mathcal{P}} \sum_{\gamma \in \mathcal{E}_K} (g_{\gamma,K}, v)_\gamma = 0 \quad \text{for all } v \in H_0^1(\Omega). \quad (4.6)$$

Using (4.6), we can now decompose the right hand side of the error equation into contributions from the individual elements

$$\mathcal{B}(e, v) = \mathcal{L}(v) - \mathcal{B}(u_h, v) = \sum_{K \in \mathcal{P}} \left((f, v)_K - \mathcal{B}_K(u_h, v) + \sum_{\gamma \in \mathcal{E}_K} (g_{\gamma,K}, v)_\gamma \right)$$

where $\mathcal{B}_K(u_h, v) = (\nabla u_h, \nabla v)_K$.

Integration by parts allows us to rewrite the right hand side of the error equation as

$$\begin{aligned} \mathcal{B}(e, v) &= \sum_{K \in \mathcal{P}} \left((f + \Delta u_h, v)_K + \sum_{\gamma \in \mathcal{E}_K} (g_{\gamma,K} - \nabla u_h|_K \cdot \hat{\mathbf{n}}_\gamma^K, v)_\gamma \right) \\ &= \sum_{K \in \mathcal{P}} \left((\mathcal{R}_K, v)_K + \sum_{\gamma \in \mathcal{E}_K} (\mathcal{R}_{\gamma,K}, v)_\gamma + (f - \Pi_K(f), v)_K \right), \end{aligned} \quad (4.7)$$

where the element residual \mathcal{R}_K and the edge residual $\mathcal{R}_{\gamma,K}$ are given by

$$\mathcal{R}_K = \Pi_K(f) + \Delta u_h \quad \text{and} \quad \mathcal{R}_{\gamma,K} = g_{\gamma,K} - \nabla u_h|_K \cdot \hat{\mathbf{n}}_\gamma^K, \quad (4.8)$$

respectively, and Π_K is defined in (2.1).

Let us assume for the moment that there exists a vector field $\boldsymbol{\sigma}_K \in \mathbf{H}(\mathbf{div}, K)$ satisfying the following *Neumann* problem

$$(\boldsymbol{\sigma}_K, \nabla v)_K = (\mathcal{R}_K, v)_K + \sum_{\gamma \in \mathcal{E}_K} (\mathcal{R}_{\gamma,K}, v)_\gamma, \quad (4.9)$$

for all $v \in H^1(\Omega)$. Then we can rewrite the right hand side of the error equation as

$$\mathcal{B}(e, v) = \sum_{K \in \mathcal{P}} ((\boldsymbol{\sigma}_K, \nabla v)_K + (f - \Pi_K(f), v)_K). \quad (4.10)$$

Notice that in order to be able to write the error equation in the form of (4.10), the main two hypotheses were the existence of the set of boundary fluxes $\{g_{\gamma,K}\}$ and the $\mathbf{H}(\mathbf{div}, K)$ lifting $\boldsymbol{\sigma}_K$. Now, in order to construct such boundary fluxes, it seems that the only requirement is to satisfy (4.5), a condition that we call a *consistency condition*, but in order to be able to construct the lifting $\boldsymbol{\sigma}_K$, we need to solve a Neumann problem on each element K , like in (4.9), for which a compatibility condition needs to be satisfied. In fact, taking $1 = v$ in (4.9), the Neumann problem will have a solution if and only if the interior residuals satisfy the equilibration condition

$$(\mathcal{R}_K, 1)_K + \sum_{\gamma \in \mathcal{E}_K} (\mathcal{R}_{\gamma,K}, 1)_\gamma = 0, \quad (4.11)$$

a condition that we call *zero-order equilibration condition* with respect to the boundary fluxes.

In the next two sections we detail the procedure to obtain a set of boundary fluxes satisfying the consistency and the zero-order equilibration conditions and also we will give an explicit solution to the Neumann problem.

4.2 Equilibrated fluxes on regular partitions.

This section is devoted to summarising the procedure for constructing sets of boundary fluxes satisfying the zeroth-order equilibration condition (4.11) and the consistency condition (4.5), extracted from [11], Chapter 6.

We recall that $\{\lambda_n : n \in \mathcal{V}\}$ is the Lagrange basis for the space V_h , then it follows that the Lagrange basis functions on the element K satisfy

$$\sum_{n \in \mathcal{V}_K} \lambda_n = 1 \quad \text{in } K \quad \text{and} \quad \sum_{n \in \mathcal{V}_\gamma} \lambda_n|_\gamma = 1 \quad \text{on } \gamma. \quad (4.12)$$

The procedure that will be presented produces sets of fluxes $\{g_{\gamma,K}\}$ satisfying the following two conditions:

Consistency:

$$g_{\gamma,K} + g_{\gamma,K'} = 0 \quad \text{on } \gamma \in \mathcal{E}_K \cap \mathcal{E}_{K'}. \quad (4.13)$$

Full first-order equilibration:

$$(\Pi_K(f), \lambda_n)_K - \mathcal{B}_K(u_h, \lambda_n) + \sum_{\gamma \in \mathcal{E}_K} (g_{\gamma,K}, \lambda_n)_\gamma = 0 \quad \text{for all } n \in \mathcal{V}_K, \quad (4.14)$$

which in terms of the element and edge residuals (4.8), can be rewritten as

$$(\mathcal{R}_K, \lambda_n)_K + \sum_{\gamma \in \mathcal{E}_K} (\mathcal{R}_{\gamma,K}, \lambda_n)_\gamma = 0 \quad \text{for all } n \in \mathcal{V}_K. \quad (4.15)$$

This condition actually imposes stricter requirements on the fluxes than the *zero-order* equilibration condition, but (4.11) is a direct consequence of (4.14) by using (4.12).

The fluxes $g_{\gamma,K}$ are selected to be linear functions such that they belong to the $\text{span}\{\lambda_n : n \in \mathcal{V}_\gamma\}$ for all $\gamma \in \mathcal{E}$ and a key decision is to choose the two degrees of freedom as the moments of the fluxes weighted against the basis functions on the edge γ , this is

$$\mu_{K,n}^\gamma = (g_{\gamma,K}, \lambda_n)_\gamma, \quad n \in \mathcal{V}_\gamma. \quad (4.16)$$

Now we can rewrite the consistency and the first-order conditions in terms of the moments as follows:

$$\begin{cases} \sum_{\gamma \in \mathcal{E}_K} \mu_{K,n}^\gamma = \Delta_K(\lambda_n) & \text{for all } n \in \mathcal{V}_K, \\ \mu_{K,n}^\gamma + \mu_{K',n}^\gamma = 0 & \text{for all } n \in \mathcal{V}_\gamma, \gamma = \mathcal{E}_K \cap \mathcal{E}_{K'}, \end{cases} \quad (4.17)$$

where

$$\Delta_K(\lambda_n) = \mathcal{B}_K(u_h, \lambda_n) - (f, \lambda_n)_K.$$

The condition (4.17) takes one of two distinct structures depending on the location of the node \mathbf{x}_n .

1. *Interior Vertex:* The elements and edges are labelled as shown in Figure 4.1. The moment equilibration conditions (4.17) for the element $K \in \Omega_n$ assume the form

$$\begin{cases} \mu_{1,n}^{\gamma_1} + \mu_{1,n}^{\gamma_2} = \Delta_1(\lambda_n) \\ \vdots \\ \mu_{N,n}^{\gamma_N} + \mu_{N,n}^{\gamma_1} = \Delta_N(\lambda_n), \end{cases} \quad \text{with constraints} \quad \begin{cases} \mu_{1,n}^{\gamma_1} + \mu_{N,n}^{\gamma_1} = 0 \\ \vdots \\ \mu_{N,n}^{\gamma_N} + \mu_{N-1,n}^{\gamma_N} = 0. \end{cases}$$

Inserting the constraints into the system we obtain

$$\begin{bmatrix} 1 & -1 & 0 & \cdots & 0 \\ 0 & 1 & -1 & & \vdots \\ \vdots & & \ddots & \ddots & 0 \\ 0 & & & 1 & -1 \\ -1 & 0 & \cdots & 0 & 1 \end{bmatrix} \begin{bmatrix} \mu_{1,n}^{\gamma_1} \\ \mu_{2,n}^{\gamma_2} \\ \vdots \\ \mu_{N-1,n}^{\gamma_{N-1}} \\ \mu_{N,n}^{\gamma_N} \end{bmatrix} = \begin{bmatrix} \Delta_1(\lambda_n) \\ \Delta_2(\lambda_n) \\ \vdots \\ \Delta_{N-1}(\lambda_n) \\ \Delta_N(\lambda_n) \end{bmatrix}. \quad (4.18)$$

Since the rank of the matrix associated to the linear system is $N - 1$, the solutions are not unique.

2. *Boundary Vertex:* The elements and edges are labelled as in Figure 4.2. The moment equilibration conditions (4.17) become

$$\begin{cases} \mu_{1,n}^{\gamma_1} + \mu_{1,n}^{\gamma_2} = \Delta_1(\lambda_n) \\ \vdots \\ \mu_{N,n}^{\gamma_N} + \mu_{N,n}^{\gamma_{N+1}} = \Delta_N(\lambda_n), \end{cases} \quad \text{with constraints} \quad \begin{cases} \mu_{2,n}^{\gamma_2} + \mu_{1,n}^{\gamma_2} = 0 \\ \vdots \\ \mu_{N,n}^{\gamma_N} + \mu_{N-1,n}^{\gamma_N} = 0, \end{cases}$$

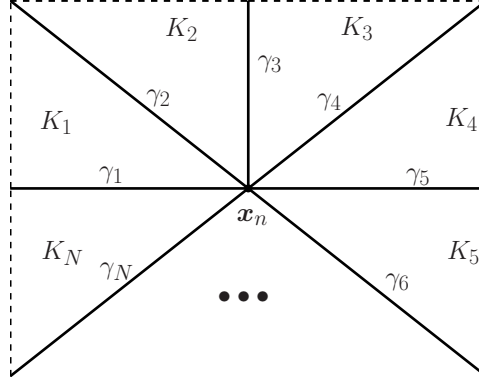


Figure 4.1: The patches Ω_n and \mathcal{E}_n of elements and edges influenced by the basis functions λ_n associated with an interior vertex at \mathbf{x}_n .

and on exterior edges γ_1 and γ_{N+1} , where a Dirichlet condition is applied, then there are no constraints on the fluxes moment, i.e.

$$\mu_{1,n}^{\gamma_1} = \text{unconstrained} \quad \text{and} \quad \mu_{N,n}^{\gamma_{N+1}} = \text{unconstrained}.$$

Arguing as before, in this case we can obtain the following linear system

$$\begin{bmatrix} 1 & -1 & 0 & \cdots & 0 \\ 0 & 1 & -1 & & \vdots \\ \vdots & & \ddots & \ddots & 0 \\ & & & 1 & -1 \\ 0 & \cdots & 0 & 1 & \end{bmatrix} \begin{bmatrix} \mu_{1,n}^{\gamma_1} \\ \mu_{2,n}^{\gamma_2} \\ \vdots \\ \mu_{N-1,n}^{\gamma_{N-1}} \\ \mu_{N,n}^{\gamma_N} \end{bmatrix} = \begin{bmatrix} \Delta_1(\lambda_n) \\ \Delta_2(\lambda_n) \\ \vdots \\ \Delta_{N-1}(\lambda_n) \\ \Delta_N(\lambda_n) \end{bmatrix}.$$

and now since the rank of the associated matrix to the linear system is N , we obtain a unique solution.

4.2.1 Procedure for the resolution of the boundary fluxes.

Due to the nonuniqueness of the patch system (4.18), the flux moments are selected so that

$$\mu_{K,n}^{\gamma} \approx \tilde{\mu}_{K,n}^{\gamma} = (\nabla u_h|_K \cdot \hat{\mathbf{n}}_{\gamma}^K, \lambda_n)_{\gamma}. \quad (4.19)$$

The role of these conditions is to remove any possible nonuniqueness by seeking flux moments that minimize the objective

$$\frac{1}{2} \sum_{K \in \Omega_n} \sum_{\gamma \in \mathcal{E}_K \cap \mathcal{E}_n} \left(\mu_{K,n}^{\gamma} - \tilde{\mu}_{K,n}^{\gamma} \right)^2 \quad (4.20)$$

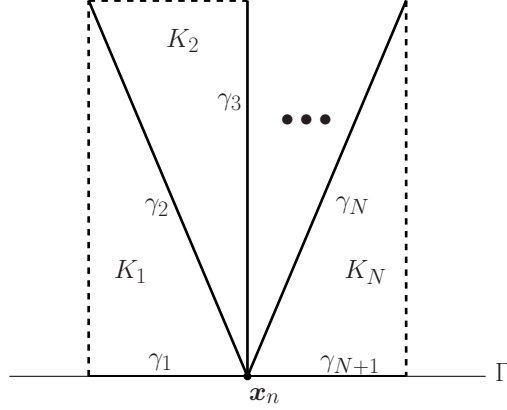


Figure 4.2: The patches Ω_n and \mathcal{E}_n of elements and edges influenced by the basis functions λ_n associated with a vertex \mathbf{x}_n located on the boundary of the domain.

To obtain the optimal solution, Lagrange multipliers can be introduced associated with the constraints (4.17). The Lagrangian is given by

$$\begin{aligned}
 L(\{\mu_{K,n}^\gamma\}, \{\lambda_\gamma\}, \{\xi_K\}) = & \\
 & \frac{1}{2} \sum_{K \in \Omega_n} \sum_{\gamma \in \mathcal{E}_K \cap \mathcal{E}_n} (\mu_{K,n}^\gamma - \tilde{\mu}_{K,n}^\gamma)^2 + \sum_{K \in \Omega_n} \xi_{K,n} \left(\Delta_K(\lambda_n) - \sum_{\gamma \in \mathcal{E}_K \cap \mathcal{E}_n} \mu_{K,n}^\gamma \right) \\
 & + \sum_{\gamma \in \mathcal{E}_K \cap \mathcal{E}_{K'} \cap \mathcal{E}_n} \lambda_{\gamma,n} (\mu_{K,n}^\gamma + \mu_{K',n}^\gamma).
 \end{aligned}$$

Since the flux moments are unconstrained on the boundary of the domain, due to the Dirichlet condition, the value of the Lagrange multiplier is set to zero. With this convention, the Euler conditions for a stationary point are then given by (4.17) supplemented with the additional conditions

$$\mu_{K,n}^\gamma - \tilde{\mu}_{K,n}^\gamma - \xi_{K,n} + \lambda_{\gamma,n} = 0 \quad (4.21)$$

and

$$\lambda_{\gamma,n} = 0 \quad \text{on } \gamma \in \Gamma. \quad (4.22)$$

These conditions may be used in conjunction with the second part of (4.17) to obtain the following formula for the edge multipliers:

$$\lambda_{\gamma,n} = \begin{cases} \frac{1}{2} (\xi_{K,n} + \xi_{K',n} + \tilde{\mu}_{K,n}^\gamma + \tilde{\mu}_{K',n}^\gamma) & \gamma \in \mathcal{E}_K \cap \mathcal{E}_{K'} \cap \mathcal{E}_n, \\ 0 & \gamma \in \mathcal{E}_K \cap \mathcal{E}_\Gamma. \end{cases}$$

If this expression is substituted back into (4.21), then one arrives at the following expression for the flux moments:

$$\mu_{K,n}^\gamma = \begin{cases} \frac{1}{2} \left(\xi_{K,n} - \xi_{K',n} + \tilde{\mu}_{K,n}^\gamma - \tilde{\mu}_{K',n}^\gamma \right) & \gamma \in \mathcal{E}_K \cap \mathcal{E}_{K'} \cap \mathcal{E}_n, \\ \xi_{K,n} + \tilde{\mu}_{K,n}^\gamma & \gamma \in \mathcal{E}_K \cap \mathcal{E}_\Gamma. \end{cases} \quad (4.23)$$

Finally, inserting this information into the first equation in (4.17) leads to the following set of conditions for the Lagrange multipliers $\{\xi_{K,n} : K \in \Omega_n\}$:

$$\frac{1}{2} \sum_{K' \in \Omega_K \cap \Omega_n} (\xi_{K,n} - \xi_{K',n}) + \sum_{\gamma \in \mathcal{E}_K \cap \mathcal{E}_n \cap \mathcal{E}_\Gamma} \xi_{K,n} = \tilde{\Delta}_K(\lambda_n) \quad \forall K \in \Omega_n, \quad (4.24)$$

where

$$\tilde{\Delta}_K(\lambda_n) = \mathcal{B}_K(u_h, \lambda_n) - (f, \lambda_n)_K - \sum_{\gamma \in \mathcal{E}_K} (\langle \nabla u_h \cdot \hat{\mathbf{n}}_\gamma^K \rangle, \lambda_n)_\gamma \quad (4.25)$$

and

$$\langle \nabla u_h \cdot \hat{\mathbf{n}}_\gamma^K \rangle = \begin{cases} \frac{1}{2} \hat{\mathbf{n}}_\gamma^K \cdot (\nabla u_{h|K} + \nabla u_{h|K'}) & \text{on } \mathcal{E}_K \cap \mathcal{E}_{K'}, \\ \nabla u_{h|K} \cdot \hat{\mathbf{n}}_\gamma^K & \text{on } \mathcal{E}_K \cap \mathcal{E}_\Gamma. \end{cases} \quad (4.26)$$

The above system consists of $\sharp \Omega_n$ equations for $\sharp \Omega_n$ unknowns, where \sharp denotes the cardinality of Ω_n . The specific form of the systems identified earlier is given below.

1. *Interior Vertex*: The equations for the interior patch in Figure 4.1 are given by

$$\frac{1}{2} \begin{bmatrix} 2 & -1 & \cdots & -1 \\ -1 & 2 & -1 & \cdots & 0 \\ \vdots & & & & \\ 0 & \cdots & -1 & 2 & -1 \\ -1 & \cdots & -1 & 2 \end{bmatrix} \begin{bmatrix} \xi_{1,n} \\ \xi_{2,n} \\ \vdots \\ \xi_{N-1,n} \\ \xi_{N,n} \end{bmatrix} = \begin{bmatrix} \tilde{\Delta}_1(\lambda_n) \\ \tilde{\Delta}_2(\lambda_n) \\ \vdots \\ \tilde{\Delta}_{N-1}(\lambda_n) \\ \tilde{\Delta}_N(\lambda_n) \end{bmatrix} \quad (4.27)$$

Although, the linear system (4.27) is singular with a null space given by a vector of ones $[1, 1, \dots, 1]$, then a solution will exist if and only if the sum of the component on right hand side data vanish, i.e.,

$$\sum_{K \in \Omega_n} \tilde{\Delta}_K(\lambda_n) = 0 \quad \text{for all } n \in \mathcal{V} \text{ and } \mathbf{x}_n \notin \Gamma, \quad (4.28)$$

but this condition follows at once on using (4.25) and taking $v = \lambda_n$ in (4.3). Now, choosing always the least square solution, we have as a consequence that this solution will depend continuously on the data

$$\sum_{K \in \Omega_n} \xi_{K,n}^2 \leq C \sum_{K \in \Omega_n} \tilde{\Delta}_K(\lambda_n)^2. \quad (4.29)$$

1. *Boundary Vertex:* The equations for the exterior patch in Figure 4.2 are given by

$$\frac{1}{2} \begin{bmatrix} 3 & -1 & \cdots & 0 \\ -1 & 2 & -1 & \cdots & 0 \\ \vdots & & & & \\ 0 & \cdots & -1 & 2 & -1 \\ 0 & \cdots & & -1 & 3 \end{bmatrix} \begin{bmatrix} \xi_{1,n} \\ \xi_{2,n} \\ \vdots \\ \xi_{N-1,n} \\ \xi_{N,n} \end{bmatrix} = \begin{bmatrix} \tilde{\Delta}_1(\lambda_n) \\ \tilde{\Delta}_2(\lambda_n) \\ \vdots \\ \tilde{\Delta}_{N-1}(\lambda_n) \\ \tilde{\Delta}_N(\lambda_n) \end{bmatrix} \quad (4.30)$$

and in this case we have a unique solution and clearly the continuous dependency (4.29).

4.3 Solution of the Neumann problem.

The full first order equilibration condition implies (4.11), hence there exists a $\boldsymbol{\sigma}_K \in \mathbf{H}(\mathbf{div}, K)$ satisfying (4.9). Suppose that we have a vector field $\boldsymbol{\sigma}_K$ satisfying

$$\begin{aligned} -\mathbf{div} \boldsymbol{\sigma}_K &= \mathcal{R}_K \quad \text{on } K, \\ \boldsymbol{\sigma}_K \cdot \hat{\mathbf{n}}_\gamma^K &= \mathcal{R}_{\gamma,K} \quad \text{in each } \gamma \in \mathcal{E}_K. \end{aligned} \quad (4.31)$$

then this $\boldsymbol{\sigma}_K$ will satisfy (4.9).

The following result provides a solution to (4.31), based on the orientation of the edges, vertices, tangents and normal vectors in Figure 2.1.

Lemma 4.3.1. *The following function is a solution to (4.31),*

$$\boldsymbol{\sigma}_K = \sum_{i=1}^3 \left((\mathcal{R}_{\gamma_i, K}, \lambda_{i+1})_{\gamma_i} \boldsymbol{\psi}_{\lambda_{i+1}}^{(\gamma_i)} + (\mathcal{R}_{\gamma_i, K}, \lambda_{i+2})_{\gamma_i} \boldsymbol{\psi}_{\lambda_{i+2}}^{(\gamma_i)} \right), \quad (4.32)$$

where $i \in \mathcal{V}_K = \{1, 2, 3\}$ and the functions $\boldsymbol{\psi}_\lambda^{(\cdot)}$ are given in (2.12). Moreover, exists a constant C independent of any size of the element K such that

$$\|\boldsymbol{\sigma}_K\|_{\mathbf{L}^2(K)} \leq C \left(h_K \|\mathcal{R}_K\|_{L^2(K)} + \sum_{\gamma \in \mathcal{E}_K} h_K^{1/2} \|\mathcal{R}_{\gamma, K}\|_{L^2(\gamma)} \right). \quad (4.33)$$

Proof. Since the element residual \mathcal{R}_K and the edge residuals $\mathcal{R}_{\gamma, K}$ satisfy (4.15), i.e. a condition like (2.17), then taking $p_K = \mathcal{R}_K$ and $p_{\gamma, K} = \mathcal{R}_{\gamma, K}$ in (2.18) and (2.19) from Theorem 2.1.5, the result easily follows. \square

Remark 4.3.2. *Notice that from (4.32) there is no need to reconstruct the real boundary flux $g_{\gamma, K}$ since the construction of $\boldsymbol{\sigma}_K$ involves only the moments of the fluxes weighted against the*

basis functions on the edge γ , i.e. we only need $\mu_{K,n}^\gamma$, given by (4.16), since

$$(\mathcal{R}_{\gamma,K}, \lambda_n)_\gamma = (g_{\gamma,K} - \nabla u_{h|K} \cdot \hat{\mathbf{n}}_\gamma^K, \lambda_n)_\gamma = \mu_{K,n}^\gamma - (\nabla u_{h|K} \cdot \hat{\mathbf{n}}_\gamma^K, \lambda_n)_\gamma.$$

Remark 4.3.3. Let us finally note that

$$\boldsymbol{\sigma}_K - \text{curl}(b_K),$$

where $b_K \in H_0^1(K)$, is also a solution of (4.31), since $\mathbf{div}(\text{curl}(b_K)) = 0$ and $\text{curl}(b_K)\hat{\mathbf{n}}_\gamma^K = 0$ for any $\gamma \in \mathcal{E}_K$. Hence, from now on we denote by

$$\boldsymbol{\sigma}_K^*(b_K) = \boldsymbol{\sigma}_K - \text{curl}(b_K).$$

4.4 A guaranteed upper bound for the error.

From the properties of the orthogonal projection (2.1) and with the aid of the Poincaré inequality (Theorem 2.2), we get

$$\begin{aligned} (f - \Pi_K(f), v)_K &= (f - \Pi_K(f), v - \bar{v}_K)_K \\ &\leq \frac{h_K}{\pi} \|f - \Pi_K(f)\|_{L^2(K)} \|\nabla v\|_{L^2(K)}. \end{aligned} \quad (4.34)$$

Since we constructed an explicit solution to the Neumann problem, applying the Cauchy–Schwarz inequality and (4.34) in the error equation (4.10) in conjunction with Remark 4.3.3, we obtain

$$\mathcal{B}(e, v) \leq \left(\sum_{K \in \mathcal{P}} \left(\|\boldsymbol{\sigma}_K^*(b_K)\|_{L^2(K)} + \frac{h_K}{\pi} \|f - \Pi_K(f)\|_{L^2(K)} \right)^2 \right)^{1/2} \|\nabla v\|_{L^2(\Omega)}.$$

One immediate consequence of this result is a guaranteed upper bound on the true error, in fact

$$\begin{aligned} \|\nabla e\|_{L^2(\Omega)} &= \sup_{0 \neq v \in H_0^1(\Omega)} \frac{\mathcal{B}(e, v)}{\|\nabla v\|_{L^2(\Omega)}} \\ &\leq \left(\sum_{K \in \mathcal{P}} \left(\|\boldsymbol{\sigma}_K^*(b_K)\|_{L^2(K)} + \frac{h_K}{\pi} \|f - \Pi_K(f)\|_{L^2(K)} \right)^2 \right)^{1/2}. \end{aligned}$$

Summarizing all the previous findings, we have the following upper bound for the error.

Theorem 4.4.1. *The error can be bounded above as*

$$\|\nabla e\|_{L^2(\Omega)}^2 \leq \eta^2, \quad (4.35)$$

where the error estimator is given by $\eta^2 := \sum_{K \in \mathcal{P}} \eta_K^2$, and the error indicators η_K are

$$\eta_K = \|\boldsymbol{\sigma}_K^*(b_K)\|_{L^2(K)} + \frac{h_K}{\pi} \|f - \Pi_K(f)\|_{L^2(K)} \quad (4.36)$$

where $\boldsymbol{\sigma}_K(b_K) = \boldsymbol{\sigma}_K - \text{curl}(b_K)$, $\boldsymbol{\sigma}_K$ is given by (4.32) and $b_K \in H_0^1(K)$ is chosen to minimize $\|\boldsymbol{\sigma}_K^*(b_K)\|_{L^2(K)}$.

4.5 Efficiency of the estimator.

Theorem (4.4.1) shows that the error estimator η obtained by solving the Neumann local problem (4.31) with the introduction of a set of equilibrated boundary fluxes $\{g_{\gamma,K}\}$ provides a guaranteed upper bound on the error. The purpose of this section is to show that the procedure presented in the previous section, actually leads to an estimator that provides a two-sided bounds on the error.

We first state the following stability result for the procedure described in Section 4.2.

Theorem 4.5.1. *Let $\{g_{\gamma,K}\}$ be the set of equilibrated boundary fluxes satisfying the consistency and the full-first order equilibration conditions, described in Section 4.2. Then, for each element K ,*

$$\begin{aligned} & \sum_{\gamma \in \mathcal{E}_K} h_K \|g_{\gamma,K} - \langle \nabla u_h \cdot \hat{\mathbf{n}}_\gamma^K \rangle\|_{L^2(\gamma)} \\ & \leq C \left(\sum_{n \in \mathcal{V}_\gamma} \sum_{K' \in \Omega_n} \left(h_{K'} \|\mathcal{R}_{K'}\|_{L^2(K')} + h_{K'}^{1/2} \sum_{\gamma \in \mathcal{E}_{K'} \cap \mathcal{E}_n} \|\nabla u_h \cdot \hat{\mathbf{n}}_\gamma\|_{L^2(\gamma)} \right) \right), \end{aligned} \quad (4.37)$$

where

$$\langle \nabla u_h \cdot \hat{\mathbf{n}}_\gamma \rangle = \begin{cases} \frac{1}{2} \hat{\mathbf{n}}_\gamma^K \cdot (\nabla u_{h|K} - \nabla u_{h|K'}) & \text{if } \gamma \in \mathcal{E}_K \cap \mathcal{E}_{K'} \\ 0 & \text{if } \gamma \in \mathcal{E}_K \cap \mathcal{E}_\Gamma. \end{cases} \quad (4.38)$$

Proof. For an edge γ with $\mathcal{V}_\gamma = \{l, r\}$, let

$$\hat{\mu}_{K,n}^\gamma = (g_{\gamma,K} - \langle \nabla u_h \cdot \hat{\mathbf{n}}_\gamma^K \rangle, \lambda_n)_\gamma, \quad (4.39)$$

since $g_{\gamma,K} - \langle \nabla u_h \cdot \hat{\mathbf{n}}_\gamma^K \rangle \in \mathbb{P}_1(\gamma)$, using Lemma 2.1.4 it follows that

$$g_{\gamma,K} - \langle \nabla u_h \cdot \hat{\mathbf{n}}_\gamma^K \rangle = \hat{\mu}_{K,l}^\gamma \frac{2}{|\gamma|} (2\lambda_l - \lambda_r) + \hat{\mu}_{K,r}^\gamma \frac{2}{|\gamma|} (2\lambda_r - \lambda_l).$$

Therefore,

$$\|g_{\gamma,K} - \langle \nabla u_h \cdot \hat{\mathbf{n}}_\gamma^K \rangle\|_{L^2(\gamma)} \leq \left| \hat{\mu}_{K,l}^\gamma \right| \left\| \frac{2}{|\gamma|} (2\lambda_l - \lambda_r) \right\|_{L^2(\gamma)} + \left| \hat{\mu}_{K,r}^\gamma \right| \left\| \frac{2}{|\gamma|} (2\lambda_r - \lambda_l) \right\|_{L^2(\gamma)}$$

and since

$$\left\| \frac{2}{|\gamma|} (2\lambda_l - \lambda_r) \right\|_{L^2(\gamma)}^2 = \left\| \frac{2}{|\gamma|} (2\lambda_r - \lambda_l) \right\|_{L^2(\gamma)}^2 \leq \frac{C}{|\gamma|},$$

it follows that

$$|\gamma| \|g_{\gamma,K} - \langle \nabla u_h \cdot \hat{\mathbf{n}}_\gamma^K \rangle\|_{L^2(\gamma)}^2 \leq C \sum_{n \in \mathcal{V}_\gamma} \left| \hat{\mu}_{K,n}^\gamma \right|^2. \quad (4.40)$$

With the aid of (4.19) and (4.26), we conclude that

$$\langle \nabla u_h \cdot \hat{\mathbf{n}}_\gamma, \lambda_n \rangle_\gamma = \begin{cases} \frac{1}{2} (\tilde{\mu}_{K,n}^\gamma - \tilde{\mu}_{K',n}^\gamma) & \text{on } \gamma \in \mathcal{E}_K \cap \mathcal{E}_{K'} \\ \tilde{\mu}_{K,n}^\gamma & \text{on } \gamma \in \mathcal{E}_K \cap \mathcal{E}_\Gamma \end{cases}$$

and hence, thanks to (4.23),

$$\hat{\mu}_{K,n}^\gamma = \begin{cases} \frac{1}{2} (\xi_{K,n} - \xi_{K',n}) & \text{on } \gamma \in \mathcal{E}_K \cap \mathcal{E}_{K'} \\ \xi_{K,n} & \text{on } \gamma \in \mathcal{E}_K \cap \mathcal{E}_\Gamma \end{cases}$$

where $\{\xi_{K,n}\}$ are determined by (4.24) and satisfy (4.29). Hence,

$$\left| \hat{\mu}_{K,n}^\gamma \right| \leq C \sum_{K' \in \Omega_n} \xi_{K',n}^2 \leq C \sum_{K' \in \Omega_n} \tilde{\Delta}_{K'}(\lambda_n)^2. \quad (4.41)$$

Integration by parts in (4.25), gives

$$\tilde{\Delta}_{K'}(\lambda_n) = -(\mathcal{R}_{K'}, \lambda_n)_{K'} - \sum_{\gamma \in \mathcal{E}_{K'}} ([\nabla u_h \cdot \hat{\mathbf{n}}_\gamma], \lambda_n)_\gamma.$$

Finally applying the Cauchy-Schwarz inequality, it follows that

$$\begin{aligned} \left| \tilde{\Delta}_{K'}(\lambda_n) \right| &\leq \|\mathcal{R}_{K'}\|_{L^2(K')} \|\lambda_n\|_{L^2(K')} + \sum_{\gamma \in \mathcal{E}_{K'}} \|\nabla u_h \cdot \hat{\mathbf{n}}_\gamma\|_{L^2(\gamma)} \|\lambda_n\|_{L^2(\gamma)} \\ &\leq C \left(h_{K'} \|\mathcal{R}_{K'}\|_{L^2(K')} + \sum_{\gamma \in \mathcal{E}_{K'} \cap \mathcal{E}_n} |\gamma|^{1/2} \|\nabla u_h \cdot \hat{\mathbf{n}}_\gamma\|_{L^2(\gamma)} \right), \end{aligned}$$

and then the result follows upon inserting the previous bound into (4.41), the resulting one into (4.40) and by the mesh regularity. \square

Integration by parts in (4.4) and using (4.8) and (4.38), allows us to rewrite the error equation as

$$\sum_{K \in \mathcal{P}} \left((\mathcal{R}_K, v)_K - \sum_{\gamma \in \mathcal{E}_K} ([\nabla u_h \cdot \hat{\mathbf{n}}_\gamma], v)_\gamma \right) = (\nabla e, \nabla v)_\Omega - \sum_{K \in \mathcal{P}} (f - \Pi_K(f), v)_K. \quad (4.42)$$

Now we will apply standard bubble arguments used in [11, 103] and Section 3.7 to the previous error equation. We include the details for completeness.

Lemma 4.5.2. *The element residual \mathcal{R}_K satisfies*

$$h_K \|\mathcal{R}_K\|_{L^2(K)} \leq C (\|\nabla e\|_{L^2(K)} + h_K \|f - \Pi_K(f)\|_{L^2(K)}), \quad (4.43)$$

Proof. Letting $\beta_K = \prod_{n \in \mathcal{V}_K} \lambda_n$ and extending by zero in the region $\Omega \setminus K$ we obtain $\beta_K \in H_0^1(\Omega)$.

Taking $v = \beta_K \mathcal{R}_K$ in (4.42), we obtain

$$\begin{aligned} & \left\| \beta_K^{1/2} \mathcal{R}_K \right\|_{L^2(K)}^2 \\ &= (\nabla e, \nabla(\beta_K \mathcal{R}_K))_K - (f - \Pi_K(f), \beta_K \mathcal{R}_K)_K \\ &\leq \|\nabla e\|_{L^2(K)} \|\nabla(\beta_K \mathcal{R}_K)\|_{L^2(K)} + \|f - \Pi_K(f)\|_{L^2(K)} \|\beta_K \mathcal{R}_K\|_{L^2(K)} \\ &\leq C \left(h_K^{-1} \|\nabla e\|_{L^2(K)} + \|f - \Pi_K(f)\|_{L^2(K)} \right) \left\| \beta_K^{1/2} \mathcal{R}_K \right\|_{L^2(K)}, \end{aligned}$$

upon using the Cauchy–Schwarz inequality and Theorem 2.1.2. Now the result follows using the fact that $\|\mathcal{R}_K\|_{L^2(K)} \leq C \left\| \beta_K^{1/2} \mathcal{R}_K \right\|_{L^2(K)}$ (again using Theorem 2.1.2). \square

Lemma 4.5.3. *The jump discontinuity in the approximation of the normal fluxes at interelement boundaries satisfies*

$$h_K^{1/2} \sum_{\gamma \in \mathcal{E}_K} \|[\nabla u_h \cdot \hat{\mathbf{n}}_\gamma]\|_{L^2(\gamma)} \leq C \left(\sum_{K' \in \Omega_K} \|\nabla e\|_{L^2(K')} + h_{K'} \|f - \Pi_{K'}(f)\|_{L^2(K')} \right), \quad (4.44)$$

Proof. For $\gamma \in \mathcal{E}_K \cap \mathcal{E}_I$, let $\beta_\gamma = \prod_{n \in \mathcal{V}_\gamma} \lambda_n$ and extending by zero in the region $\Omega \setminus \Omega_\gamma$ we obtain $\beta_\gamma \in H_0^1(\Omega)$. Taking $v = -\beta_\gamma [\nabla u_h \cdot \hat{\mathbf{n}}_\gamma]$ in (4.42), we obtain

$$\begin{aligned} & 2 \left\| \beta_\gamma^{1/2} [\nabla u_h \cdot \hat{\mathbf{n}}_\gamma] \right\|_{L^2(\gamma)}^2 \\ &= \sum_{K \in \Omega_\gamma} \left(-(\nabla e, \nabla(\beta_\gamma [\nabla u_h \cdot \hat{\mathbf{n}}_\gamma]))_K + (f - \Pi_K(f), \beta_\gamma [\nabla u_h \cdot \hat{\mathbf{n}}_\gamma])_K + (\mathcal{R}_K, \beta_\gamma [\nabla u_h \cdot \hat{\mathbf{n}}_\gamma])_K \right) \\ &\leq \sum_{K \in \Omega_\gamma} \left(\|\nabla e\|_{L^2(K)} \|\nabla(\beta_\gamma [\nabla u_h \cdot \hat{\mathbf{n}}_\gamma])\|_{L^2(K)} + \|\mathcal{R}_K\|_{L^2(K)} \|\beta_\gamma [\nabla u_h \cdot \hat{\mathbf{n}}_\gamma]\|_{L^2(K)} \right. \\ &\quad \left. + \|f - \Pi_K(f)\|_{L^2(K)} \|\beta_\gamma [\nabla u_h \cdot \hat{\mathbf{n}}_\gamma]\|_{L^2(K)} \right) \\ &\leq C \left(\sum_{K \in \Omega_\gamma} \left(h_K^{-1/2} \|\nabla e\|_{L^2(K)} + h_K^{1/2} \|f - \Pi_K(f)\|_{L^2(K)} \right) \right) \left\| \beta_\gamma^{1/2} [\nabla u_h \cdot \hat{\mathbf{n}}_\gamma] \right\|_{L^2(\gamma)}, \end{aligned}$$

upon using the Cauchy–Schwarz inequality, Theorem 2.1.3 and (4.43), with a similar bound for the remaining two edges. Now the result follows upon using the fact that $\|[\nabla u_h \cdot \hat{\mathbf{n}}_\gamma]\|_{L^2(K)} \leq C \left\| \beta_\gamma^{1/2} [\nabla u_h \cdot \hat{\mathbf{n}}_\gamma] \right\|_{L^2(K)}$ (again using Theorem 2.1.3) and summing over the remaining edges. \square

Notice that from (4.8), (4.26) and (4.38) it follows that

$$\mathcal{R}_{\gamma,K} = g_{\gamma,K} - \langle \nabla u_h \cdot \hat{\mathbf{n}}_\gamma^K \rangle - [\nabla u_h \cdot \hat{\mathbf{n}}_\gamma]. \quad (4.45)$$

Using (4.33) in Lemma 4.3.1 with Remark 4.3.3 and (4.36), we get

$$\begin{aligned} \eta_K^2 &\leq C \left(\sum_{\gamma \in \mathcal{E}_K} \left(h_K^2 \|\mathcal{R}_{\gamma,K}^2\|_{L^2(\gamma)} \right) + h_K^2 \|f - \Pi_K(f)\|_{L^2(K)}^2 \right) \\ &\leq C \left(\sum_{\gamma \in \mathcal{E}_K} \left(h_K^2 \|g_{\gamma,K} - \langle \nabla u_h \cdot \hat{\mathbf{n}}_\gamma^K \rangle\|_{L^2(\gamma)}^2 + h_K^2 \|[\nabla u_h \cdot \hat{\mathbf{n}}_\gamma]\|_{L^2(\gamma)}^2 \right) \right. \\ &\quad \left. + h_K^2 \|f - \Pi_K(f)\|_{L^2(K)}^2 \right). \end{aligned}$$

Using Theorem 4.5.1 in conjunction with (4.43) and (4.44) and the previous bound for η_K , we just proved the following result.

Theorem 4.5.4. *Let η_K be given by (4.36). Then, there exists $c > 0$, independent of any mesh size, such that*

$$c \eta_K^2 \leq \sum_{K' \in \tilde{\Omega}_K} \left(\|\nabla e\|_{L^2(K')}^2 + h_{K'}^2 \|f - \Pi_{K'}(f)\|_{L^2(K')}^2 \right).$$

4.6 An explicit formula to compute the norm of the solution of the Neumann problem.

In terms of practical applications, we will take $b_K \in H_0^1(K) \cap \mathbb{P}_3(K)$ in Theorem 4.4.1, for which it follows that

$$\left(\min_{b_K \in H_0^1(K) \cap \mathbb{P}_3(K)} \|\sigma_K^*(b_K)\|_{L^2(K)} \right)^2 = \|\sigma_K\|_{L^2(K)}^2 - \frac{(\sigma_K, \operatorname{curl}(\beta_K))_K^2}{\|\operatorname{curl}(\beta_K)\|_{L^2(K)}^2}.$$

where $\beta_K = \prod_{n \in \mathcal{V}_K} \lambda_n$. In fact, since $H_0^1(K) \cap \mathbb{P}_3(K) = \operatorname{span}(\beta_K)$ we can take $b_K = \alpha \beta_K$ for some $\alpha \in \mathbb{R}$, then

$$\|\sigma_K - \operatorname{curl}(\alpha \beta_K)\|_{L^2(K)}^2 = \|\sigma_K\|_{L^2(K)}^2 + \alpha^2 \|\operatorname{curl}(\beta_K)\|_{L^2(K)}^2 - 2\alpha (\sigma_K, \operatorname{curl}(\beta_K))_K,$$

and minimizing with respect to α we obtain

$$\alpha = \frac{(\sigma_K, \operatorname{curl}(\beta_K))_K}{\|\operatorname{curl}(\beta_K)\|_{L^2(K)}^2}.$$

Let the edges, vertices, tangent vectors and unit normal vectors of an element K be labelled as in Figure 2.1. Then, for $i \in \mathcal{V}_K = \{1, 2, 3\}$ define

$$\mathbf{M}_{11} \approx \begin{bmatrix} 13 & -21 \\ -21 & 57 \end{bmatrix} \mathbf{t}_2 \cdot \mathbf{t}_2 + \begin{bmatrix} -9 & -5 \\ -5 & -9 \end{bmatrix} \mathbf{t}_2 \cdot \mathbf{t}_3 + \begin{bmatrix} 57 & -21 \\ -21 & 13 \end{bmatrix} \mathbf{t}_3 \cdot \mathbf{t}_3,$$

with $\underline{\underline{M}}_{22}$ and $\underline{\underline{M}}_{33}$ being defined by permuting the indices and

$$\underline{\underline{M}}_{12} = \begin{bmatrix} 6 & 18 \\ -8 & 4 \end{bmatrix} \mathbf{t}_1 \cdot \mathbf{t}_1 + \begin{bmatrix} -29 & -25 \\ -55 & -29 \end{bmatrix} \mathbf{t}_1 \cdot \mathbf{t}_2 + \begin{bmatrix} -4 & 18 \\ -21 & 13 \end{bmatrix} \mathbf{t}_2 \cdot \mathbf{t}_2,$$

with $\underline{\underline{M}}_{23}$ and $\underline{\underline{M}}_{31}$ being defined by permuting the indices and

$$\mathbf{M}_{10} = \begin{bmatrix} -1 \\ -3 \end{bmatrix} \mathbf{t}_2 \cdot \mathbf{t}_2 + \begin{bmatrix} 4 \\ -4 \end{bmatrix} \mathbf{t}_2 \cdot \mathbf{t}_3 + \begin{bmatrix} 3 \\ 1 \end{bmatrix} \mathbf{t}_3 \cdot \mathbf{t}_3,$$

with \mathbf{M}_{20} and \mathbf{M}_{30} being defined by permuting the indices and

$$\mathbf{S}_1 = \begin{bmatrix} (\mathcal{R}_{\gamma_1, K}, \lambda_2)_{\gamma_1} \\ (\mathcal{R}_{\gamma_1, K}, \lambda_3)_{\gamma_1} \end{bmatrix},$$

with \mathbf{S}_2 and \mathbf{S}_3 being defined by permuting the indices. Now, let

$$\begin{aligned} (\boldsymbol{\sigma}_{\gamma_i, K}, \boldsymbol{\sigma}_{\gamma_j, K})_K &= \frac{1}{360|K|} \mathbf{S}_i^T \underline{\underline{M}}_{ij} \mathbf{S}_j, \\ (\boldsymbol{\sigma}_{\gamma_i, K}, \boldsymbol{\sigma}_{0, K})_K &= \frac{1}{360|K|} \mathbf{S}_i^T \mathbf{M}_{i0}, \\ \varrho_K &= \frac{1}{(\boldsymbol{\sigma}_{0, K}, \boldsymbol{\sigma}_{0, K})_K} \left(\sum_{i=1}^3 (\boldsymbol{\sigma}_{\gamma_i, K}, \boldsymbol{\sigma}_{0, K})_K \right)^2, \end{aligned}$$

where

$$(\boldsymbol{\sigma}_{0, K}, \boldsymbol{\sigma}_{0, K})_K = \frac{1}{360|K|} (\mathbf{t}_1 \cdot \mathbf{t}_1 + \mathbf{t}_2 \cdot \mathbf{t}_2 + \mathbf{t}_3 \cdot \mathbf{t}_3 + \mathbf{t}_2 \cdot \mathbf{t}_3 + \mathbf{t}_3 \cdot \mathbf{t}_1 + \mathbf{t}_1 \cdot \mathbf{t}_2).$$

The following result provides a simple formula to compute the norm of the solution of the Neumann problem (4.31), minimized over a cubic bubble space.

Theorem 4.6.1. *The following equality holds,*

$$\begin{aligned} \left(\min_{b_K \in H_0^1(K) \cap \mathbb{P}_3(K)} \|\boldsymbol{\sigma}_K^*(b_K)\|_{L^2(K)} \right)^2 &= (\boldsymbol{\sigma}_{\gamma_1, K}, \boldsymbol{\sigma}_{\gamma_1, K})_K + (\boldsymbol{\sigma}_{\gamma_2, K}, \boldsymbol{\sigma}_{\gamma_2, K})_K + (\boldsymbol{\sigma}_{\gamma_3, K}, \boldsymbol{\sigma}_{\gamma_2, K})_K \\ &\quad + 2 \left((\boldsymbol{\sigma}_{\gamma_2, K}, \boldsymbol{\sigma}_{\gamma_3, K})_K + (\boldsymbol{\sigma}_{\gamma_3, K}, \boldsymbol{\sigma}_{\gamma_1, K})_K + (\boldsymbol{\sigma}_{\gamma_1, K}, \boldsymbol{\sigma}_{\gamma_2, K})_K \right) \\ &\quad - \varrho_K. \end{aligned} \tag{4.46}$$

Proof. From Lemma 4.3.1 and (2.14), taking $\mathcal{V}_K = \{1, 2, 3\}$ define

$$\begin{aligned} \boldsymbol{\sigma}_{\gamma_1, K} &= \frac{1}{2|K|} \left((\mathcal{R}_{\gamma_1, K}, \lambda_2)_{\gamma_1} \left((2\lambda_3 - 3\lambda_2 - \lambda_1)\lambda_3 \mathbf{t}_2 + (4\lambda_2 - \lambda_3 - 7\lambda_1)\lambda_2 \mathbf{t}_3 \right) \right. \\ &\quad \left. - (\mathcal{R}_{\gamma_1, K}, \lambda_3)_{\gamma_1} \left((4\lambda_3 - \lambda_2 - 7\lambda_1)\lambda_3 \mathbf{t}_2 + (2\lambda_2 - 3\lambda_3 - \lambda_1)\lambda_2 \mathbf{t}_3 \right) \right), \end{aligned}$$

with $\sigma_{\gamma_2, K}$ and $\sigma_{\gamma_3, K}$ being defined by permuting the indices. Also, define

$$\begin{aligned}\sigma_{0, K} &= -\operatorname{curl}(\lambda_1 \lambda_2 \lambda_3) \\ &= \frac{1}{2|K|}((\lambda_2 \lambda_3 - \lambda_3 \lambda_1) \mathbf{t}_2 + (\lambda_2 \lambda_3 - \lambda_1 \lambda_2) \mathbf{t}_3) \\ &= \frac{1}{2|K|}((\lambda_3 \lambda_1 - \lambda_1 \lambda_2) \mathbf{t}_3 + (\lambda_3 \lambda_1 - \lambda_2 \lambda_3) \mathbf{t}_1) \\ &= \frac{1}{2|K|}((\lambda_1 \lambda_2 - \lambda_2 \lambda_3) \mathbf{t}_1 + (\lambda_1 \lambda_2 - \lambda_3 \lambda_1) \mathbf{t}_2).\end{aligned}$$

Now, it is relatively straightforward to show that

$$\begin{aligned}\sigma_{\gamma_k, K} \cdot \hat{\mathbf{n}}_{\gamma_l}^K &= \mathcal{R}_{\gamma_l, K} \delta_{lk} \quad \text{on } \gamma_l \text{ for all } l, k = 1, 2, 3; \\ \sigma_{0, K} \cdot \hat{\mathbf{n}}_{\gamma_l}^K &= 0 \quad \text{on } \gamma_l \text{ for all } l = 1, 2, 3;\end{aligned}$$

and

$$(\sigma_{\gamma_k, K}, \nabla p)_K = (\sigma_{0, K}, \nabla p)_K = 0 \quad \text{for all } p \in \mathbb{P}_1(K) \text{ for } k = 1, 2, 3.$$

Then it follows that

$$\sigma_K^*(b_K) := \sum_{i=1}^3 \sigma_{\gamma_i, K} - \frac{1}{(\sigma_{0, K}, \sigma_{0, K})_K} \sum_{i=1}^3 (\sigma_{\gamma_i, K}, \sigma_{0, K})_K \sigma_{0, K},$$

satisfies

$$\sigma_K^*(b_K) \cdot \hat{\mathbf{n}}_{\gamma_k}^K = \mathcal{R}_{\gamma, K} \quad \text{on } \gamma_k \text{ for } k = 1, 2, 3$$

and

$$(\sigma_K(b_K), \nabla p)_K = 0 \quad \text{for all } p \in \mathbb{P}_1(K),$$

which in conjunction with the full first order equilibration condition (4.14), Lemma 4.3.1 and Theorem 4.4.1 implies that this $\sigma_K^*(b_K)$ is a solution to the Neumann problem. We can then obtain an expression for $\|\sigma_K^*(b_K)\|_{\mathbf{L}^2(K)}$ which can be manipulated into the above form, where the value of ϱ_K has been chosen so that $\|\sigma_K^*(b_K)\|_{\mathbf{L}^2(K)}$ is minimised over the space of cubic bubbles. \square

4.7 A numerical result.

We illustrate the performance of the error estimators for a representative problem in this section.

In the numerical experiments we calculate the exact and the estimated error in the $H^1(\Omega)$ semi-norm on a sequence of uniformly and adaptively refined grids, respectively. For each marked

triangle a longest edge bisection step [103] was performed. As a local error indicator for the adaptive algorithm we used (cf. Section 4.4)

$$\eta_K^2 = \left(\|\boldsymbol{\sigma}_K^*(b_K)\|_{L^2(K)} + \frac{h_K}{\pi} \|f - \Pi_K(f)\|_{L^2(K)} \right)^2, \quad (4.47)$$

and triangles are marked using the maximum strategy (mark K if $\eta_K \geq \eta_{\max}/2$). To summarize, we present the adaptive refinement algorithm in Table 4.1.

Adaptive mesh refinement algorithm [AMRA-P].

- 1:** Set $i = 0$ and construct a mesh $\mathcal{P}_{(i)}$.
- 2:** For each element K in $\mathcal{P}_{(i)}$, compute:
 - $\|\boldsymbol{\sigma}_K^*(b_K)\|_{L^2(K)}$ using formula (4.46).
 - $\|f - \Pi_K(f)\|_{L^2(K)}$ using an appropriate quadrature formula.
 - η_K using the previous two steps and (4.47).

- 3:** Triangle K is marked for refinement if

$$\eta_K \geq \frac{1}{2} \max_{K \in \mathcal{P}_{(i)}} \{\eta_K\}.$$

- 4:** From step **3** deduce a new mesh using longest edge bisection refinement.
 - 5:** Set $i \leftarrow i + 1$ and return to step **2**.
-

Table 4.1: Adaptive mesh refinement algorithm for a simple Poisson problem.

The global error estimate is, according to (4.35), given by

$$\eta = \left(\sum_{K \in \mathcal{P}} \eta_K^2 \right)^{1/2}.$$

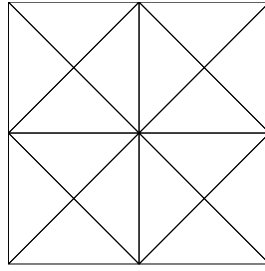
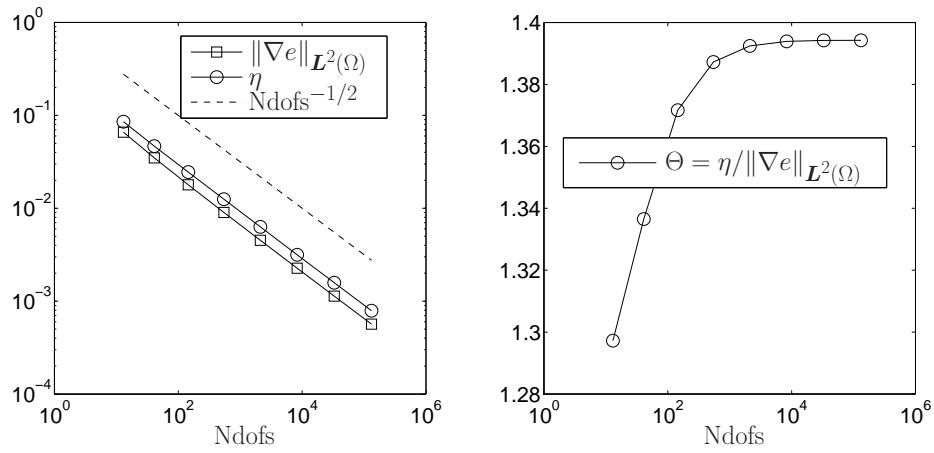
When reporting numerical results, we denote by Ndofs the number of degrees of freedom and we denote by $\Theta = \frac{\eta}{\|\nabla e\|_{L^2(\Omega)}}$ the effectivity index.

Example 1: Let $\Omega = (0, 1)^2$ denote the unit square. The exact solution for (4.1) is given by

$$u = xy(1-x)(1-y).$$

The first mesh $\mathcal{P}_{(0)}$, that we will use to perform the uniform or adaptive refinement procedures, is shown in Figure 4.3.

From Figure 4.4 and 4.5 we can see that the error estimator provides a very accurate guaranteed upper bound.

Figure 4.3: Initial mesh $\mathcal{P}_{(0)}$ for Example 1.Figure 4.4: Accuracy (left) and effectivity index (right) for Example 1, using regular refinement over the mesh $\mathcal{P}_{(0)}$ from Figure 4.3.

4.8 Conclusions

In this chapter we presented an error estimator providing two-sided bounds on the error up to higher order terms, based on the equilibrated residual method proposed in [11], where the most notorious difference is that in [11] the construction of the error estimator requires the approximation of a local residual problem, which in our case was changed into a Neumann problem in which case we provide an analytical solution, which is not needed *per se*, as we provide a simple formula for its norm.

This chapter can be seen as a different alternative to existing error estimators for conforming methods for the Poisson problem like the ones in [62, 87, 97, 107].

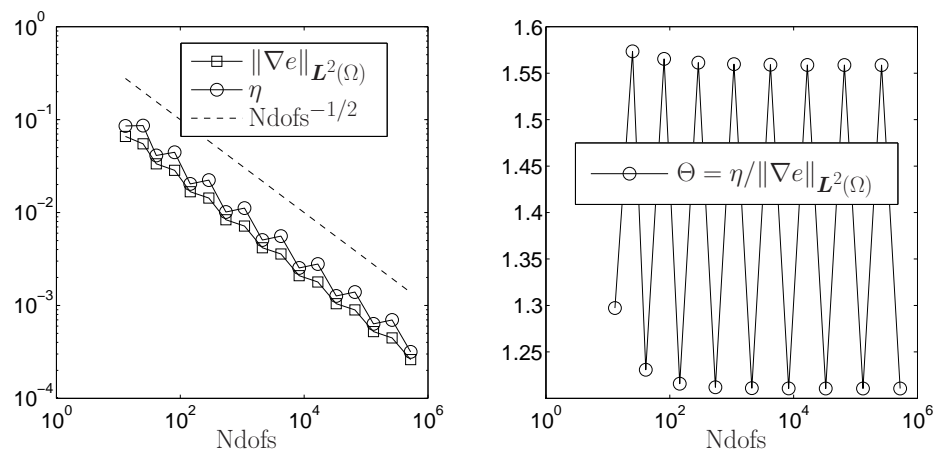


Figure 4.5: Accuracy (left) and effectivity index (right) for Example 1, using the AMRA-P algorithm (Table 4.1) over the mesh $\mathcal{P}_{(0)}$ from Figure 4.3, based on the Adaptive mesh refinement algorithm.

Chapter 5

Application of the equilibrated residual method to the Stokes problem using stabilized conforming finite element approximations.

The numerical approximation of the Stokes problem generally follows one of two complementary approaches. The first consists of using discrete velocity-pressure spaces satisfying the discrete inf-sup condition. Many such methods are available in the literature (see [38, 74] for extensive reviews). However, one perceived drawback of this approach is the fact that the discrete spaces cannot be of the same polynomial order in both variables whilst maintaining stability. The second approach, which is our main interest in this chapter, consists of adding so-called stabilizing terms to the discrete formulation using an equal (or more general non inf-sup stable) order velocity-pressure combination. These stabilizing terms can depend on residuals of the equation at the element level, or can simply be based on compensating for the inf-sup deficiency of the pressure. For extensive reviews on different alternatives for stabilized finite element methods see [32, 98].

The development of our a posteriori error estimator follows the same basic structure presented in Chapter 3, i.e., we will decompose the gradient of the velocity field into conforming and nonconforming parts, each of which must be bounded. The treatment for the conforming part, is now based on a generalization of the equilibrated residual method to the vector-valued case, which allows to rewrite the residual functional as a Neumann problem, for which we have an explicit solution. The estimator for the nonconforming part can be easily obtained by using Lemma 3.5.2, and finally the error estimation for the pressure error can be obtained using similar arguments as the ones of Section 3.6, i.e., using the inf-sup condition related to the continuous problem.

We continue the study of the Stokes problem, which is: *For given data $\mathbf{f} \in \mathbf{L}^2(\Omega)$, find a velocity \mathbf{u} and a pressure field p such that*

$$-\nu\Delta\mathbf{u} + \nabla p = \mathbf{f}, \quad \nabla \cdot \mathbf{u} = 0 \quad \text{in } \Omega \quad \text{and} \quad \mathbf{u} = \mathbf{0} \quad \text{on } \Gamma, \quad (5.1)$$

where $\nu > 0$ is the fluid viscosity.

To simplify the notation trough the chapter we rewrite the weak formulation as follows: *Find $(\mathbf{u}, p) \in \mathbf{H}_0^1(\Omega) \times L_0^2(\Omega)$ such that*

$$\mathcal{B}(\mathbf{u}, p; \mathbf{v}, q) = \mathcal{L}(\mathbf{v}, q) \quad \text{for all } (\mathbf{v}, q) \in \mathbf{H}_0^1(\Omega) \times L_0^2(\Omega), \quad (5.2)$$

where

$$\mathcal{B}(\mathbf{u}, p; \mathbf{v}, q) = \nu(\nabla\mathbf{u}, \nabla\mathbf{v})_\Omega - (p, \nabla \cdot \mathbf{v})_\Omega + (q, \nabla \cdot \mathbf{u})_\Omega \quad \text{and} \quad \mathcal{L}(\mathbf{v}, q) = (\mathbf{f}, \mathbf{v})_\Omega. \quad (5.3)$$

and as we stated in the first Chapter 3, problem (5.2) is well-posed.

The results that will be presented in this and the next chapter are based on [8], but the analysis of the a posteriori error estimation will consider a wider family of low-order stabilized methods.

5.1 Stabilized finite element methods.

Given a conforming subspace $\mathbf{V}_h \subset \mathbf{H}_0^1(\Omega)$ and $Q_h \subset L_0^2(\Omega)$, a stabilized finite element approximation of the Stokes problem reads: *Find a pair $(\mathbf{u}_h, p_h) \in \mathbf{V}_h \times Q_h$ such that,*

$$\mathcal{B}(\mathbf{u}_h, p_h; \mathbf{v}, q) + \alpha (\mathcal{S}^{mo}(\mathbf{u}_h, p_h, \mathbf{f}; \mathbf{v}) + \mathcal{S}^{ma}(\mathbf{u}_h, p_h, \mathbf{f}; q)) = \mathcal{L}(\mathbf{v}, q), \quad (5.4)$$

for all $(\mathbf{v}, q) \in \mathbf{V}_h \times Q_h$, where $\mathcal{S}^{mo}(\mathbf{u}_h, p_h, \mathbf{f}; \mathbf{v})$ and $\mathcal{S}^{ma}(\mathbf{u}_h, p_h, \mathbf{f}; q)$ are stabilization terms related to the momentum and mass conservation equations, respectively, and the parameter α is a positive constant usually referred to as the *stabilization parameter*.

Many stabilized finite element methods are available, and below we give examples of stabilized finite element methods which can be used to approximate the solution of the Stokes problem. We shall employ various combinations of discrete velocity-pressure spaces, depending on the particular choice of stabilization (see Table 5.1), constructed using standard piecewise polynomial spaces on the partition \mathcal{P}

$$X_h^l = \{v \in L^2(\Omega) : v|_K \in \mathbb{P}_l(K) \text{ for all } K \in \mathcal{P}\},$$

for a non-negative integer l .

Method	Velocity Space \mathbf{V}_h	–	Pressure Space Q_h
$\mathbb{P}_1^2 - \mathbb{P}_0$			$\mathbb{P}_0 = X_h^0 \cap L_0^2(\Omega)$
$\mathbb{P}_1^2 - \mathbb{P}_1^{cts}$	$\mathbb{P}_1^2 = \mathbf{X}_h^1 \cap \mathbf{H}_0^1(\Omega)$		$\mathbb{P}_1^{cts} = X_h^1 \cap H^1(\Omega) \cap L_0^2(\Omega)$
$\mathbb{P}_1^2 - \mathbb{P}_1^{dis}$			$\mathbb{P}_1^{dis} = X_h^1 \cap L_0^2(\Omega)$

Table 5.1: Discrete velocity-pressure space combinations used in conjunction with the stabilized formulations.

5.1.1 Pressure-Stabilization.

The following stabilized finite element methods only present stabilization related to the mass conservation equation, i.e.,

$$\mathcal{S}^{mo}(\mathbf{u}_h, p_h, \mathbf{f}; \mathbf{v}) = 0.$$

• **Galerkin Least–Squares-type (GLS) or Petrov-Galerkin Pressure stabilization** [79, 80, 84, 98]: The stabilizing term is given by:

$$\mathcal{S}^{ma}(\mathbf{u}_h, p_h, \mathbf{f}; q) = - \sum_{K \in \mathcal{P}} \frac{h_K^2}{\nu} (\mathbf{f} - \nabla p_h, \nabla q)_K + \sum_{\gamma \in \mathcal{E}_I} \frac{|\gamma|}{\nu} (\llbracket p_h \rrbracket, \llbracket q \rrbracket)_\gamma,$$

or

$$\mathcal{S}^{ma}(\mathbf{u}_h, p_h, \mathbf{f}; q) = \sum_{K \in \mathcal{P}} \frac{h_K^2}{\nu} (\nabla p_h, \nabla q)_K + \sum_{\gamma \in \mathcal{E}_I} \frac{|\gamma|}{\nu} (\llbracket p_h \rrbracket, \llbracket q \rrbracket)_\gamma,$$

and may be used in conjunction with a $\mathbb{P}_1^2 - \mathbb{P}_1^{cts}$, $\mathbb{P}_1^2 - \mathbb{P}_1^{dis}$ or $\mathbb{P}_1^2 - \mathbb{P}_0$ pair. See also [67] for a local variant.

- **Brezzi and Pitkäranta (BP)** [45]: The stabilizing term reads:

$$\mathcal{S}^{ma}(\mathbf{u}_h, p_h, \mathbf{f}; q) = \sum_{K \in \mathcal{P}} \frac{h_K^2}{\nu} (\nabla p_h, \nabla q)_K,$$

for a $\mathbb{P}_1^2 - \mathbb{P}_1^{cts}$ pair.

- **Local Projection methods (LPS)** [34]: The stabilizing term is:

$$\mathcal{S}^{ma}(\mathbf{u}_h, p_h, \mathbf{f}; q) = \sum_{\tilde{K} \in \tilde{\mathcal{P}}} \frac{h_{\tilde{K}}^2}{\nu} \left(\nabla p_h - \overline{(\nabla p_h)}_{\tilde{K}}, \nabla q \right)_{\tilde{K}},$$

where (\mathbf{u}_h, p_h) and (\mathbf{v}, q) belong to the space $\tilde{\mathbf{V}}_h \times \tilde{Q}_h$ constructed on a partition $\tilde{\mathcal{P}}$ built by subdividing each element K of \mathcal{P} into three sub-elements (for details, see [34]).

- **Polynomial pressure methods (PPS)** [37, 64]: The stabilizing term reads:

$$\mathcal{S}^{ma}(\mathbf{u}_h, p_h, \mathbf{f}; q) = \sum_{K \in \mathcal{P}} \frac{1}{\nu} ((I - \Pi)p_h, (I - \Pi)q)_K,$$

and the operator Π may be taken as $\Pi(v)|_K = \bar{v}_K$ for the $\mathbb{P}_1^2 - \mathbb{P}_1^{cts}$ pair or a Clément-like interpolator for the $\mathbb{P}_1^2 - \mathbb{P}_0$ pair (see Section 6 in [37] for more details about the operator Π). See also [31] for a consistent variation of the method.

All of the previous methods constitute stable and convergent schemes. However, alternative methods exist based on discretizing a regularization of the basic Stokes problem. Such methods, whilst stable, are inconsistent and non-convergent in general, but can nevertheless deliver useful approximations.

- **Penalty pressure-type methods (PEPS)** [50]: The stabilizing term reads:

$$\mathcal{S}^{ma}(\mathbf{u}_h, p_h, \mathbf{f}; q) = \sum_{K \in \mathcal{P}} (p_h, q)_K,$$

and may be used in conjunction with a $\mathbb{P}_1^2 - \mathbb{P}_1^{cts}$, $\mathbb{P}_1^2 - \mathbb{P}_1^{dis}$ or a $\mathbb{P}_1^2 - \mathbb{P}_0$ pair.

5.1.2 Pressure-Velocity-Stabilization.

The following stabilized finite element methods present stabilization, in both, the momentum and mass conservation equations:

- **Galerkin Least–Squares-type (GLS) or Streamline Diffusion methods (SDS)** [98]:

The stabilizing term reads:

$$\mathcal{S}^{mo}(\mathbf{u}_h, p_h, \mathbf{f}; \mathbf{v}) = \sum_{K \in \mathcal{P}} \nu (\nabla \cdot \mathbf{u}_h, \nabla \cdot \mathbf{v})_K,$$

and

$$\mathcal{S}^{ma}(\mathbf{u}_h, p_h, \mathbf{f}; q) = \sum_{K \in \mathcal{P}} \frac{h_K^2}{\nu} (\mathbf{f} - \nabla p, \nabla q)_K + \sum_{\gamma \in \mathcal{E}_I} \frac{|\gamma|}{\nu} (\llbracket p_h \rrbracket, \llbracket q \rrbracket)_\gamma,$$

and may be used in conjunction with a $\mathbb{P}_1^2 - \mathbb{P}_1^{cts}$, $\mathbb{P}_1^2 - \mathbb{P}_1^{dis}$ or a $\mathbb{P}_1^2 - \mathbb{P}_0$ pair.

- **Edge-residual methods (ABV)** [21, 22]: The stabilizing term reads:

$$\mathcal{S}^{mo}(\mathbf{u}_h, p_h, \mathbf{f}; \mathbf{v}) = \sum_{\gamma \in \mathcal{E}_I} \frac{|\gamma|}{\nu} (\llbracket \nabla \mathbf{u}_h \cdot \hat{\mathbf{n}}_\gamma - p_h \hat{\mathbf{n}}_\gamma \rrbracket, \llbracket \nabla \mathbf{v} \cdot \hat{\mathbf{n}}_\gamma \rrbracket)_\gamma$$

and

$$\begin{aligned} \mathcal{S}^{ma}(\mathbf{u}_h, p_h, \mathbf{f}; q) &= \sum_{K \in \mathcal{P}} \frac{h_K^2}{\nu} (\mathbf{f} - \nabla p, \nabla q)_K \\ &\quad + \sum_{\gamma \in \mathcal{E}_I} \frac{|\gamma|}{\nu} (\llbracket \nabla \mathbf{u}_h \cdot \hat{\mathbf{n}}_\gamma - p_h \hat{\mathbf{n}}_\gamma \rrbracket, \llbracket -q \hat{\mathbf{n}}_\gamma \rrbracket)_\gamma, \end{aligned}$$

where for $\gamma \in \mathcal{E}_K \cap \mathcal{E}_{K'} \cap \mathcal{E}_I$,

$$\llbracket \nabla \mathbf{u}_h \cdot \hat{\mathbf{n}}_\gamma - p_h \hat{\mathbf{n}}_\gamma \rrbracket = \nabla \mathbf{u}_{h|K} \cdot \hat{\mathbf{n}}_\gamma^K - p_{h|K} \hat{\mathbf{n}}_\gamma^K + \nabla \mathbf{u}_{h|K'} \cdot \hat{\mathbf{n}}_\gamma^{K'} - p_{h|K'} \hat{\mathbf{n}}_\gamma^{K'},$$

and may be used in conjunction with a $\mathbb{P}_1^2 - \mathbb{P}_1^{cts}$, $\mathbb{P}_1^2 - \mathbb{P}_1^{dis}$ or a $\mathbb{P}_1^2 - \mathbb{P}_0$ pair.

In order to be able to apply our a posteriori analysis, we will need to establish some assumptions, but only over the stabilization term related to the momentum equation. The two properties that we will assume are:

Assumption 1: Localization over elements,

$$\mathcal{S}^{mo}(\mathbf{u}_h, p_h, \mathbf{f}; \mathbf{v}) = \sum_{K \in \mathcal{P}} \mathcal{S}_K^{mo}(\mathbf{u}_h, p_h, \mathbf{f}; \mathbf{v}),$$

where

$$\begin{aligned} \mathcal{S}_K^{mo}(\mathbf{u}_h, p_h, \mathbf{f}; \mathbf{v}) &= \nu (\nabla \cdot \mathbf{u}_h, \mathcal{D}_1(\mathbf{v}))_K + \frac{h_K^2}{\nu} (\mathbf{f} + \nabla p_{h|K}, \mathcal{D}_2(\mathbf{v}))_K \\ &\quad + \sum_{\gamma \in \mathcal{E}_K} \frac{|\gamma|}{\nu} (\llbracket \nabla \mathbf{u}_h \cdot \hat{\mathbf{n}}_\gamma - p_h \hat{\mathbf{n}}_\gamma \rrbracket, \mathcal{D}_3(\mathbf{v}))_\gamma, \end{aligned} \quad (5.5)$$

where

$$\llbracket \nabla \mathbf{u}_h \cdot \hat{\mathbf{n}}_\gamma - p_h \hat{\mathbf{n}}_\gamma \rrbracket = \begin{cases} \nabla \mathbf{u}_{h|K} \cdot \hat{\mathbf{n}}_\gamma^K - p_{h|K} \hat{\mathbf{n}}_\gamma^K & \text{if } \gamma \in \mathcal{E}_K \cap \mathcal{E}_{K'} \cap \mathcal{E}_I \\ \quad + \nabla \mathbf{u}_{h|K'} \cdot \hat{\mathbf{n}}_\gamma^{K'} - p_{h|K'} \hat{\mathbf{n}}_\gamma^{K'} & \\ 0 & \text{if } \gamma \in \mathcal{E}_K \cap \mathcal{E}_{K'} \cap \mathcal{E}_\Gamma \end{cases} \quad (5.6)$$

and $\mathcal{D}_1 : \mathbb{P}_1^2(K) \rightarrow \mathbb{P}_1(K)$, $\mathcal{D}_2 : \mathbb{P}_1^2(K) \rightarrow \mathbb{P}_1^2(K)$, $\mathcal{D}_3 : \mathbb{P}_1^2(\gamma) \rightarrow \mathbb{P}_1^2(\gamma)$ are linear operators, such that

$$\begin{aligned} \mathcal{D}_1(\mathbf{c}) &= \mathbf{0} \quad \forall \mathbf{c} \in \mathbb{R}^2 \quad \text{and} \quad \|\mathcal{D}_1(\mathbf{p})\|_{L^2(K)} \leq C \quad \text{for all } \mathbf{p} \in \mathbb{P}_1^2(K), \\ \mathcal{D}_2(\mathbf{c}) &= \mathbf{0} \quad \forall \mathbf{c} \in \mathbb{R}^2 \quad \text{and} \quad \|\mathcal{D}_2(\mathbf{p})\|_{L^2(K)} \leq C \quad \text{for all } \mathbf{p} \in \mathbb{P}_1^2(K), \\ \mathcal{D}_3(\mathbf{c}) &= \mathbf{0} \quad \forall \mathbf{c} \in \mathbb{R}^2 \quad \text{and} \quad \|\mathcal{D}_3(\mathbf{p})\|_{L^2(\gamma)} \leq C \quad \text{for all } \mathbf{p} \in \mathbb{P}_1^2(K). \end{aligned} \quad (5.7)$$

Assumption 2: Restriction over the patches,

$$\mathcal{S}^{mo}(\mathbf{u}_h, p_h, \mathbf{f}; \boldsymbol{\lambda}_n^{(i)}) = \sum_{K \in \Omega_n} \mathcal{S}_K^{mo}(\mathbf{u}_h, p_h, \mathbf{f}; \boldsymbol{\lambda}_n^{(i)}) \quad \text{for all } n \in \mathcal{V}, \text{ and } i = 1, 2.$$

Remark 5.1.1. Notice that all the previous stabilized methods satisfy our assumptions, but only when they are decomposed in an appropriate way. For example, in the **ABV** method, if we take

$$\mathcal{S}_K^{mo}(\mathbf{u}_h, p_h, \mathbf{f}; \mathbf{v}) = \sum_{\gamma \in \mathcal{E}_K \cap \mathcal{E}_I} \frac{|\gamma|}{2\nu} (\llbracket \nabla \mathbf{u}_h \cdot \hat{\mathbf{n}}_\gamma - p_h \hat{\mathbf{n}}_\gamma \rrbracket, \llbracket \nabla \mathbf{v} \cdot \hat{\mathbf{n}}_\gamma \rrbracket)_\gamma$$

then we will be violating Assumption 1 and 2, but taking

$$\mathcal{S}_K^{mo}(\mathbf{u}_h, p_h, \mathbf{f}; \mathbf{v}) = \sum_{\gamma \in \mathcal{E}_K \cap \mathcal{E}_I} \frac{|\gamma|}{\nu} (\llbracket \nabla \mathbf{u}_h \cdot \hat{\mathbf{n}}_\gamma - p_h \hat{\mathbf{n}}_\gamma \rrbracket, \nabla \mathbf{v}|_K \cdot \hat{\mathbf{n}}_\gamma^K)_\gamma,$$

then both assumptions will be satisfied.

Finally, we note that all of the results remain valid in the case of non-homogeneous Dirichlet data $\mathbf{u} = \mathbf{u}_D$ on Γ in (5.1), for given $\mathbf{u}_D \in \mathbf{V}_h$. From now on c or C will denote positive constants which are independent of any mesh size, the viscosity ν and the stabilization parameter α .

5.2 The error equation.

If (\mathbf{u}, p) is the solution of (5.2) and (\mathbf{u}_h, p_h) is the solution of (5.4), we denote by $\mathbf{e}_V = \mathbf{u} - \mathbf{u}_h \in \mathbf{H}_0^1(\Omega)$ and $e_P = p - p_h \in L_0^2(\Omega)$ the errors in velocity and pressure, respectively. Thanks to (5.2) and (5.3), the errors satisfy for all $\mathbf{v} \in \mathbf{H}_0^1(\Omega)$ and $q \in L_0^2(\Omega)$,

$$\mathcal{B}(\mathbf{e}_V, e_P; \mathbf{v}, q) = \sum_{K \in \mathcal{P}} \left((\mathbf{f}, \mathbf{v})_K - \nu (\nabla \mathbf{u}_h, \nabla \mathbf{v})_K + (p_h, \nabla \cdot \mathbf{v})_K - (q, \nabla \cdot \mathbf{u}_h)_K \right),$$

which, as usual, we call the *error equation*.

Following the same ideas of Chapter 4, to propose an a posteriori error estimator we start by defining a set of equilibrated boundary fluxes $\{\mathbf{g}_{\gamma, K}\}$ that notionally approximate the normal fluxes over the element boundaries,

$$\mathbf{g}_{\gamma, K} \approx \nu \nabla \mathbf{u} \cdot \hat{\mathbf{n}}_\gamma^K - p \hat{\mathbf{n}}_\gamma^K.$$

Since the traces of the true fluxes are continuous on the interior edges, we will require that the flux functions $\mathbf{g}_{\gamma,K}$ satisfy the following condition

$$\mathbf{g}_{\gamma,K} + \mathbf{g}_{\gamma,K'} = \mathbf{0} \quad \text{if } \gamma = \mathcal{E}_K \cap \mathcal{E}_{K'} \quad \text{for } K, K' \in \mathcal{P}. \quad (5.8)$$

Using the fact that $\mathbf{v} \in \mathbf{H}_0^1(\Omega)$, we can incorporate the boundary fluxes into the error equation and integrate by parts to yield

$$\mathcal{B}(\mathbf{e}_V, e_P; \mathbf{v}, q) = \sum_{K \in \mathcal{P}} \left((\mathcal{R}_K, \mathbf{v})_K + \sum_{\gamma \in \mathcal{E}_K} (\mathcal{R}_{\gamma,K}, \mathbf{v})_\gamma + (\mathbf{f} - \Pi_K(\mathbf{f}), \mathbf{v})_K - (q, \nabla \cdot \mathbf{u}_h)_K \right), \quad (5.9)$$

where the element residual \mathcal{R}_K is given by

$$\mathcal{R}_K = \Pi_K(\mathbf{f}) - \nabla p_h \quad \text{in } K, \quad (5.10)$$

and the boundary residuals $\mathcal{R}_{\gamma,K}$ are given by

$$\mathcal{R}_{\gamma,K} = \mathbf{g}_{\gamma,K} - \nu \nabla \mathbf{u}_h|_K \cdot \hat{\mathbf{n}}_\gamma^K + p_h|_K \hat{\mathbf{n}}_\gamma^K \quad \text{on each } \gamma \in \mathcal{E}_K. \quad (5.11)$$

The right hand side of (5.9) can be represented in a more convenient way in terms of a solution $\underline{\underline{\sigma}}_K \in \underline{\underline{\mathbf{H}}}(\mathbf{div}; K)$ of a local Neumann problem with the residuals as data:

$$(\underline{\underline{\sigma}}_K, \nabla \mathbf{v})_K = (\mathcal{R}_K, \mathbf{v})_K + \sum_{\gamma \in \mathcal{E}_K} (\mathcal{R}_{\gamma,K}, \mathbf{v})_\gamma \quad \forall \mathbf{v} \in \mathbf{H}^1(\Omega), \quad (5.12)$$

We already stated in previous chapters that this problem will have a solution if and only if the interior and boundary residuals satisfy the compatibility condition

$$(\mathcal{R}_K, \mathbf{c})_K + \sum_{\gamma \in \mathcal{E}_K} (\mathcal{R}_{\gamma,K}, \mathbf{c})_\gamma = 0 \quad \forall \mathbf{c} \in \mathbb{R}^2, \quad (5.13)$$

which is called a *zeroth-order equilibration condition* in terms of the fluxes.

By taking into account the previous remark and also using the properties of the orthogonal projection we can rewrite (5.9) as

$$\mathcal{B}(\mathbf{e}_V, e_P; \mathbf{v}, q) = \sum_{K \in \mathcal{P}} \left((\underline{\underline{\sigma}}_K, \nabla \mathbf{v})_K + (\mathbf{f} - \Pi_K(\mathbf{f}), \mathbf{v} - \bar{\mathbf{v}}_K)_K - (q, \nabla \cdot \mathbf{u}_h)_K \right). \quad (5.14)$$

5.3 Construction of the equilibrated boundary fluxes.

We now describe the procedure to develop a set of boundary fluxes $\{\mathbf{g}_{\gamma,K}\}$ satisfying (5.8) and (5.13), which is the extension of the procedure described in Section 4.2 to the vector-valued case. From (5.10) we have that $\mathcal{R}_K \in \mathbb{P}_1(K)^2$ and we choose $\mathbf{g}_{\gamma,K} \in \mathbb{P}_1(\gamma)^2$, leading to $\mathcal{R}_{\gamma,K} \in \mathbb{P}_1(\gamma)^2$.

We want to define $\mathbf{g}_{\gamma,K} \in \mathbb{P}_1(\gamma)^2$ with $\gamma \in \mathcal{E}_K$ to satisfy the conditions:

- **Consistency:**

$$\mathbf{g}_{\gamma,K} + \mathbf{g}_{\gamma,K'} = \mathbf{0} \quad \text{if } \gamma = \mathcal{E}_K \cap \mathcal{E}_{K'} \quad \text{for } K, K' \in \mathcal{P}. \quad (5.15)$$

- **Full first order equilibration:**

$$\begin{aligned} 0 &= (\mathbf{\Pi}_K(\mathbf{f}) - \nabla p_h, \boldsymbol{\theta})_K + \sum_{\gamma \in \mathcal{E}_K} (\mathbf{g}_{\gamma,K} - \nu \nabla \mathbf{u}_{h|K} \cdot \hat{\mathbf{n}}_\gamma^K + p_{h|K} \hat{\mathbf{n}}_\gamma^K, \boldsymbol{\theta})_\gamma \\ &\quad - \alpha \mathcal{S}_K^{mo}(\mathbf{u}_h, p_h, \mathbf{f}; \boldsymbol{\theta}) \\ &= (\mathcal{R}_K, \boldsymbol{\theta})_K + \sum_{\gamma \in \mathcal{E}_K} (\mathcal{R}_{\gamma,K}, \boldsymbol{\theta})_\gamma - \alpha \mathcal{S}_K^{mo}(\mathbf{u}_h, p_h, \mathbf{f}; \boldsymbol{\theta}), \end{aligned} \quad (5.16)$$

for all $\boldsymbol{\theta} \in \mathbb{P}_1(K)^2$ and all $K \in \mathcal{P}$.

Since the flux $\mathbf{g}_{\gamma,K}$ is a linear function on each edge, it is uniquely determined by the moments

$$\mu_{K,n}^{\gamma,i} = \left(\mathbf{g}_{\gamma,K}, \boldsymbol{\lambda}_n^{(i)} \right)_\gamma \quad \text{with } n \in \mathcal{V}_\gamma. \quad (5.17)$$

We briefly outline the main steps to obtain all the moments $\mu_{K,n}^{\gamma,i}$, which appear as a slight variation of the method presented in Section 4.2.

Let

$$\langle \mathbf{J} \rangle_{\gamma,K} = \begin{cases} \frac{1}{2} (\mathbf{J}_{\gamma,K} - \mathbf{J}_{\gamma,K'}) & \text{if } \gamma \in \mathcal{E}_K \cap \mathcal{E}_{K'}, \\ \mathbf{J}_{\gamma,K} & \text{if } \gamma \in \mathcal{E}_K \cap \mathcal{E}_\Gamma, \end{cases} \quad (5.18)$$

with

$$\mathbf{J}_{\gamma,K} = \nu \nabla \mathbf{u}_{h|K} \cdot \hat{\mathbf{n}}_\gamma^K - p_{h|K} \hat{\mathbf{n}}_\gamma^K \quad \text{for } \gamma \in \mathcal{E}_K. \quad (5.19)$$

We look for the moments $\mu_{K,n}^{\gamma,i}$ of $\mathbf{g}_{\gamma,K}$ in the form

$$\mu_{K,n}^{\gamma,i} = \begin{cases} \frac{1}{2} \left(\xi_{K,n}^{(i)} - \xi_{K',n}^{(i)} \right) + \left(\langle \mathbf{J} \rangle_{\gamma,K}, \boldsymbol{\lambda}_n^{(i)} \right)_\gamma & \text{if } \gamma \in \mathcal{E}_K \cap \mathcal{E}_{K'}, \\ \xi_{K,n}^{(i)} + \left(\mathbf{J}_{\gamma,K}, \boldsymbol{\lambda}_n^{(i)} \right)_\gamma & \text{if } \gamma \in \mathcal{E}_K \cap \mathcal{E}_\Gamma, \end{cases} \quad (5.20)$$

where the parameters $\xi_{K,n}^{(i)}$ are obtained by solving a system of equations analogous to (4.24):

$$\frac{1}{2} \sum_{K' \in \Omega_n \cap \Omega_K} \left(\xi_{K,n}^{(i)} - \xi_{K',n}^{(i)} \right) + \sum_{\gamma \in \mathcal{E}_K \cap \mathcal{E}_\Gamma \cap \mathcal{E}_n} \xi_{K,n}^{(i)} = \Delta_K \left(\boldsymbol{\lambda}_n^{(i)} \right) \quad \forall K \in \Omega_n, \quad (5.21)$$

with

$$\begin{aligned} \Delta_K \left(\boldsymbol{\lambda}_n^{(i)} \right) &= \nu \left(\nabla \mathbf{u}_h, \nabla \boldsymbol{\lambda}_n^{(i)} \right)_K - \left(p_h, \nabla \cdot \boldsymbol{\lambda}_n^{(i)} \right)_K - \left(\mathbf{f}, \boldsymbol{\lambda}_n^{(i)} \right)_K - \sum_{\gamma \in \mathcal{E}_K} \left(\langle \mathbf{J} \rangle_{\gamma,K}, \boldsymbol{\lambda}_n^{(i)} \right)_\gamma \\ &\quad + \alpha \mathcal{S}_K^{mo} \left(\mathbf{u}_h, p_h, \mathbf{f}; \boldsymbol{\lambda}_n^{(i)} \right), \end{aligned} \quad (5.22)$$

where α is the stabilization parameter and S_K^{mo} is a stabilization term related to the momentum equation, satisfying **Assumptions 1** and **2**.

The above system consists of $\#\Omega_n$ equations for $\#\Omega_n$ unknowns, where $\#\Omega_n$ denotes the cardinality of Ω_n . As was stated in the previous chapter, the linear system (5.21) fails to have a unique solution, but a solution which depends continuously on the data $\left\{ \Delta_K \left(\boldsymbol{\lambda}_n^{(i)} \right), K \in \Omega_n \right\}$ can always be found provided that the following compatibility condition holds:

$$\sum_{K \in \Omega_n} \Delta_K \left(\boldsymbol{\lambda}_n^{(i)} \right) = 0 \quad \text{for all } n \in \mathcal{V} \text{ and } \boldsymbol{x}_n \notin \Gamma, \quad (5.23)$$

which follows at once on using the definition (5.22), taking $\boldsymbol{v} = \boldsymbol{\lambda}_n^{(i)}$ and $q = 0$ in (5.4) and by **Assumption 2**.

5.4 Solution of the Neumann problem.

The solution of (5.12), will be carried out by solving the following problem

$$-\operatorname{div} \underline{\underline{\boldsymbol{\sigma}}}_K = \mathcal{R}_K \quad \text{in } K, \quad (5.24)$$

$$\underline{\underline{\boldsymbol{\sigma}}}_K \hat{\boldsymbol{n}}_\gamma^K = \mathcal{R}_{\gamma,K} \quad \text{on each } \gamma \in \mathcal{E}_K, \quad (5.25)$$

which clearly implies (5.12). The following result provides a solution to (5.24)-(5.25), which is a simple extension to the matrix-valued case of Theorem 2.1.5 and is based on the orientation of the edges, vertices, tangents and normal vectors in Figure 2.1.

Lemma 5.4.1. *The following matrix valued function is a solution to the Neumann-type problem (5.24)-(5.25),*

$$\underline{\underline{\boldsymbol{\sigma}}}_K = \begin{bmatrix} \boldsymbol{\sigma}_K^1 \\ \boldsymbol{\sigma}_K^2 \end{bmatrix},$$

where for $l = 1, 2$, $i \in \mathcal{V}_K = \{1, 2, 3\}$, letting $\mathcal{R}_K = [\mathcal{R}_K^1, \mathcal{R}_K^2]$ and $\mathcal{R}_{\gamma,K} = [\mathcal{R}_{\gamma,K}^1, \mathcal{R}_{\gamma,K}^2]$, each component is given by

$$\boldsymbol{\sigma}_K^l = \sum_{i=1}^3 \left((\mathcal{R}_{\gamma_i,K}^l, \lambda_{i+1})_{\gamma_i} \tilde{\boldsymbol{\psi}}_{\lambda_{i+1}}^{(\gamma_i)} + (\mathcal{R}_{\gamma_i,K}^l, \lambda_{i+2})_{\gamma_i} \tilde{\boldsymbol{\psi}}_{\lambda_{i+2}}^{(\gamma_i)} + (|K| \nabla(\mathcal{R}_K^l) \cdot (\boldsymbol{x}_i - \bar{\boldsymbol{x}}_K)) \boldsymbol{\psi}_K^{(i)} \right), \quad (5.26)$$

when a **Pressure-Velocity-Stabilization** method is applied. In the presence of only **Pressure-Stabilization**, each component is given by

$$\boldsymbol{\sigma}_K^l = \sum_{i=1}^3 \left((\mathcal{R}_{\gamma_i,K}^l, \lambda_{i+1})_{\gamma_i} \boldsymbol{\psi}_{\lambda_{i+1}}^{(\gamma_i)} + (\mathcal{R}_{\gamma_i,K}^l, \lambda_{i+2})_{\gamma_i} \boldsymbol{\psi}_{\lambda_{i+2}}^{(\gamma_i)} \right), \quad (5.27)$$

where the functions $\tilde{\psi}_\lambda^{(\cdot)}$, $\psi_\lambda^{(\cdot)}$ and $\psi_K^{(\cdot)}$ are given in (2.12) and (2.13). Also, for both stabilization methods, there exist a positive constant C independent of any mesh size, such that

$$\|\underline{\sigma}_K\|_{\underline{\mathbb{L}}^2(K)} \leq C \left(h_K \|\mathcal{R}_K\|_{L^2(K)} + \sum_{\gamma \in \mathcal{E}_K} h_K^{1/2} \|\mathcal{R}_{\gamma,K}\|_{L^2(\gamma)} \right). \quad (5.28)$$

Proof. First notice that when a Pressure-Velocity-Stabilization is applied, then (5.16) and **Assumption 2** imply that the element residual \mathcal{R}_K and the edge residuals $\mathcal{R}_{\gamma,K}$ satisfy only a compatibility condition like in (2.16). Then, taking $p_K = \mathcal{R}_K^l$ and $p_{\gamma,K} = \mathcal{R}_{\gamma,K}^l$ in (2.18) and (2.19) in Theorem 2.1.5, the result easily follows. Now, when a Pressure-Stabilization method is applied, since there is no stabilization terms in (5.16), we have that the element and edge residuals satisfies a condition like (2.17), hence taking $p_K = \mathcal{R}_K^l$ and $p_{\gamma,K} = \mathcal{R}_{\gamma,K}^l$ in (2.20) and (2.21) in Theorem 2.1.5, the result easily follows. \square

Remark 5.4.2. To conclude the discussion of the Neumann problem, based on Remark (3.4.2), we have that $\underline{\sigma}_K - \mathbf{curl}(\beta_K)$ also satisfy (5.12), where β_K belongs to $\mathbf{H}_0^1(K)$, since $\mathbf{curl}(\beta_K) \hat{\mathbf{n}}_\gamma^K = \mathbf{0}$ for any $\gamma \in \mathcal{E}_K$ and $\mathbf{div}(\mathbf{curl}(\beta_K)) = \mathbf{0}$. And, we also know that if we take $\mathbf{v} \in \mathbf{X}$ in (5.12) then $\underline{\sigma}_K - (\vartheta_K \underline{\mathbf{I}} + \mathbf{curl}(\beta_K))$ will also satisfy (5.12) for any $\vartheta_K \in L^2(K)$ since $(\vartheta_K \underline{\mathbf{I}}, \nabla \mathbf{v})_K = (\vartheta_K, \nabla \cdot \mathbf{v})_K = 0$, where $\underline{\mathbf{I}}$ denotes the two by two identity matrix. Hence, from now on we denote

$$\underline{\sigma}_K^*(\vartheta_K, \beta_K) = \underline{\sigma}_K - (\vartheta_K \underline{\mathbf{I}} + \mathbf{curl}(\beta_K)).$$

5.5 A guaranteed upper bound for the errors.

In order to obtain an upper bound for the velocity error, we make use of the orthogonal decomposition presented in Section 3.5, i.e., for $\mathbf{e}_V = \mathbf{u} - \mathbf{u}_h$, we can decompose its gradient as

$$\nabla \mathbf{e}_V = \nabla \mathbf{e}_c + \underline{\mathbf{e}}_{nc}, \quad (5.29)$$

where $\mathbf{e}_c \in \mathbf{X}$ is uniquely defined by

$$(\nabla \mathbf{e}_c, \nabla \mathbf{v}_c)_\Omega = (\nabla \mathbf{e}_V, \nabla \mathbf{v}_c)_\Omega \quad \forall \mathbf{v}_c \in \mathbf{X}, \quad (5.30)$$

whilst the remainder part $\underline{\mathbf{e}}_{nc}$ belongs to the closed subspace

$$\underline{\mathbf{Y}} = \left\{ \underline{\mathbf{w}}_{nc} \in \underline{\mathbb{L}}^2(\Omega) : (\underline{\mathbf{w}}_{nc}, \nabla \mathbf{v}_c)_\Omega = 0 \text{ for all } \mathbf{v}_c \in \mathbf{X} \right\} \quad (5.31)$$

of $\underline{\underline{L}}^2(\Omega)$, hence we obtained

$$\|\nabla e_V\|_{\underline{\underline{L}}^2(\Omega)}^2 = \|\nabla e_c\|_{\underline{\underline{L}}^2(\Omega)}^2 + \|\underline{\underline{e}}_{nc}\|_{\underline{\underline{L}}^2(\Omega)}^2. \quad (5.32)$$

Remark 5.5.1. *Even though we are just dealing with conforming approximation to the solution of the Stokes problem, the fact that we are decomposing the error still using a nonconforming part, is to take into account how well the incompressibility condition is being approximated.*

From the definition of e_c in (5.30), taking $q = 0$ in (5.14) and Remark 5.4.2, it follows that, for all $\mathbf{v} \in \mathbf{X}$,

$$\nu(\nabla e_c, \nabla \mathbf{v})_\Omega = \sum_{K \in \mathcal{P}} \left((\underline{\underline{\sigma}}_K^*(\vartheta_K, \beta_K), \nabla \mathbf{v})_K + (\mathbf{f} - \mathbf{\Pi}_K(\mathbf{f}), \mathbf{v} - \bar{\mathbf{v}}_K)_K \right). \quad (5.33)$$

Hence,

$$\nu^2 \|\nabla e_c\|_{\underline{\underline{L}}^2(\Omega)}^2 \leq \sum_{K \in \mathcal{P}} \left(\|\underline{\underline{\sigma}}_K^*(\vartheta_K, \beta_K)\|_{\underline{\underline{L}}^2(K)} + \frac{h_K}{\pi} \|\mathbf{f} - \mathbf{\Pi}_K(\mathbf{f})\|_{\mathbf{L}^2(K)} \right)^2, \quad (5.34)$$

upon applying the Cauchy–Schwarz inequality and the optimal Poincaré inequality (see Lemma 2.1.1).

In order to obtain an upper bound for the nonconforming part of the error, from Lemma 3.5.2, we obtain

$$\begin{aligned} \|\underline{\underline{e}}_{nc}\|_{\underline{\underline{L}}^2(\Omega)}^2 &= (\nabla(e_V - e_c), \underline{\underline{e}}_{nc})_\Omega = -(\nabla \mathbf{u}_h, \underline{\underline{e}}_{nc})_\Omega = -(w, \nabla \cdot \mathbf{u}_h)_\Omega \\ &\leq \frac{1}{\beta} \|\nabla \cdot \mathbf{u}_h\|_{L^2(\Omega)} \|\underline{\underline{e}}_{nc}\|_{\underline{\underline{L}}^2(\Omega)}, \end{aligned}$$

and then we arrive at the following upper bound for the nonconforming error

$$\|\underline{\underline{e}}_{nc}\|_{\underline{\underline{L}}^2(\Omega)} \leq \frac{1}{\beta} \|\nabla \cdot \mathbf{u}_h\|_{L^2(\Omega)}. \quad (5.35)$$

Hence, from (5.32), (5.34) and (5.35) we can bound the velocity error as follows

$$\begin{aligned} &\nu^2 \|\nabla e_V\|_{\underline{\underline{L}}^2(\Omega)}^2 \\ &\leq \sum_{K \in \mathcal{P}} \left(\|\underline{\underline{\sigma}}_K^*(\vartheta_K, \beta_K)\|_{\underline{\underline{L}}^2(K)} + \frac{h_K}{\pi} \|\mathbf{f} - \mathbf{\Pi}_K(\mathbf{f})\|_{\mathbf{L}^2(K)} \right)^2 + \frac{\nu^2}{\beta^2} \|\nabla \cdot \mathbf{u}_h\|_{L^2(\Omega)}^2. \end{aligned}$$

It remains to give the upper a posteriori error bound for e_P . Splitting the gradient of the test function $\nabla \mathbf{v} = \nabla \mathbf{v}_c + \underline{\underline{\mathbf{v}}}_{nc}$ as in (5.29), noticing that $\nabla \cdot \mathbf{v} = \text{tr}(\nabla \mathbf{v}_c + \underline{\underline{\mathbf{v}}}_{nc}) = \text{tr}(\underline{\underline{\mathbf{v}}}_{nc})$ (since $\mathbf{v}_c \in \mathbf{X}$), where tr denotes the trace of a matrix and taking $q = 0$ in the error equation (5.14),

we obtain

$$\begin{aligned} & \nu \left((\nabla e_c, \nabla \mathbf{v}_c)_\Omega + (\underline{\boldsymbol{\varepsilon}}_{nc}, \underline{\mathbf{v}}_{nc})_\Omega \right) - (e_P, \text{tr}(\underline{\mathbf{v}}_{nc}))_\Omega = \\ & \sum_{K \in \mathcal{P}} \left((\underline{\boldsymbol{\sigma}}_K^*(\vartheta_K, \boldsymbol{\beta}_K), \nabla \mathbf{v}_c)_K + (\underline{\boldsymbol{\sigma}}_K^*(0, \boldsymbol{\beta}_K), \underline{\mathbf{v}}_{nc})_K + (\mathbf{f} - \boldsymbol{\Pi}_K(\mathbf{f}), \mathbf{v} - \bar{\mathbf{v}}_K)_K \right). \end{aligned} \quad (5.36)$$

Now, let $\phi_K \in \mathbf{V}_K$ be a solution of the local problem

$$(\nabla \phi_K, \nabla \mathbf{v})_K = (\mathbf{f} - \boldsymbol{\Pi}_K(\mathbf{f}), \mathbf{v} - \bar{\mathbf{v}}_K)_K \quad \forall \mathbf{v} \in \mathbf{V}_K, \quad (5.37)$$

where $\mathbf{V}_K = \{\mathbf{v} \in \mathbf{H}^1(K) : \mathbf{v} = \mathbf{0} \text{ on } \mathcal{E}_\Gamma \cap \mathcal{E}_K\}$. Notice that from (5.37) and Theorem 2.1.1 it easily follows that

$$\|\nabla \phi_K\|_{\underline{\mathbf{L}}^2(K)} \leq \frac{h_K}{\pi} \|\mathbf{f} - \boldsymbol{\Pi}_K(\mathbf{f})\|_{\mathbf{L}^2(K)}. \quad (5.38)$$

Since (5.37) is also valid for any $\mathbf{v}_c \in \mathbf{X}$, applying the orthogonal decomposition (5.29) to \mathbf{v} in (5.37) allows us to rewrite the right hand side of (5.36) at the element level as

$$\begin{aligned} & (\underline{\boldsymbol{\sigma}}_K^*(\vartheta_K, \boldsymbol{\beta}_K), \nabla \mathbf{v}_c)_K + (\mathbf{f} - \boldsymbol{\Pi}_K(\mathbf{f}), \mathbf{v}_c - \overline{(\mathbf{v}_c)}_K)_K \\ & + (\underline{\boldsymbol{\sigma}}_K^*(0, \boldsymbol{\beta}_K), \underline{\mathbf{v}}_{nc})_K + (\nabla \phi_K, \underline{\mathbf{v}}_{nc})_K. \end{aligned} \quad (5.39)$$

Inserting (5.39) into (5.36), and then using (5.33) yields

$$\begin{aligned} & - (e_P, \text{tr}(\underline{\mathbf{v}}_{nc}))_\Omega \\ & = -\nu (\underline{\boldsymbol{\varepsilon}}_{nc}, \underline{\mathbf{v}}_{nc})_\Omega + \sum_{K \in \mathcal{E}} \left((\underline{\boldsymbol{\sigma}}_K^*(0, \boldsymbol{\beta}_K), \underline{\mathbf{v}}_{nc})_K + (\nabla \phi_K, \underline{\mathbf{v}}_{nc})_K \right) \\ & \leq \left(\|\underline{\boldsymbol{\varepsilon}}_{nc}\|_{\underline{\mathbf{L}}^2(\Omega)} + \left(\sum_{K \in \mathcal{P}} \left(\|\underline{\boldsymbol{\sigma}}_K^*(0, \boldsymbol{\beta}_K)\|_{\underline{\mathbf{L}}^2(K)} + \frac{h_K}{\pi} \|\mathbf{f} - \boldsymbol{\Pi}_K(\mathbf{f})\|_{\mathbf{L}^2(K)} \right)^2 \right)^{1/2} \right) \\ & \quad \times \|\underline{\mathbf{v}}_{nc}\|_{\underline{\mathbf{L}}^2(\Omega)}, \end{aligned} \quad (5.40)$$

upon applying the Cauchy–Schwarz inequality, (5.38) and the definition of the conforming and nonconforming estimators.

Finally, thanks to the inf-sup condition, we have

$$\beta \|e_P\|_{\mathbf{L}^2(\Omega)} \leq \sup_{\mathbf{0} \neq \mathbf{v} \in \mathbf{H}_0^1(\Omega)} \frac{-(e_P, \nabla \cdot \mathbf{v})_\Omega}{\|\nabla \mathbf{v}\|_{\underline{\mathbf{L}}^2(\Omega)}} \leq \sup_{\underline{\mathbf{0}} \neq \underline{\mathbf{v}}_{nc} \in \underline{\mathbf{Y}}} \frac{-(e_P, \text{tr}(\underline{\mathbf{v}}_{nc}))_\Omega}{\|\underline{\mathbf{v}}_{nc}\|_{\underline{\mathbf{L}}^2(\Omega)}}. \quad (5.41)$$

Hence, from (5.41) and (5.40), the orthogonal decomposition of the gradient of the velocity error in conjunction with the bounds for the conforming and nonconforming parts of the velocity error we obtain the following result.

Theorem 5.5.2. *Define the following natural norm*

$$\|(\mathbf{e}_V, e_P)\|_{\Omega}^2 = \nu^2 \|\nabla \mathbf{e}_V\|_{\underline{\mathbf{L}}^2(\Omega)}^2 + \beta^2 \|e_P\|_{L^2(\Omega)}^2.$$

Then, the velocity and the pressure errors can be bounded above as

$$\|(\mathbf{e}_V, e_P)\|_{\Omega}^2 \leq \eta^2, \quad (5.42)$$

where the error estimator η is given by

$$\eta^2 = \Phi_c(\vartheta_K, \boldsymbol{\beta}_K)^2 + \Phi_{nc}^2 + (\Phi_c(0, \boldsymbol{\beta}_K) + \Phi_{nc})^2, \quad (5.43)$$

with the conforming estimator Φ_c given by

$$\Phi_c(\vartheta_K, \boldsymbol{\beta}_K)^2 = \sum_{K \in \mathcal{P}} \Phi_{c,K}(\vartheta_K, \boldsymbol{\beta}_K)^2, \quad (5.44)$$

where

$$\Phi_{c,K}(\vartheta_K, \boldsymbol{\beta}_K) = \|\underline{\boldsymbol{\sigma}}_K^*(\vartheta_K, \boldsymbol{\beta}_K)\|_{\underline{\mathbf{L}}^2(K)} + \frac{h_K}{\pi} \|\mathbf{f} - \mathbf{\Pi}_K(\mathbf{f})\|_{L^2(K)} \quad (5.45)$$

and $\underline{\boldsymbol{\sigma}}_K^(\vartheta_K, \boldsymbol{\beta}_K) = \underline{\boldsymbol{\sigma}}_K - (\vartheta_K \underline{\mathbf{I}} - \mathbf{curl}(\boldsymbol{\beta}_K))$, being $\underline{\boldsymbol{\sigma}}_K$ the solution of (5.24)-(5.25) given in Lemma 5.4.1 and $\vartheta_K \in L^2(\Omega)$ and $\boldsymbol{\beta}_K \in \mathbf{H}_0^1(K)$ are chosen to minimize $\|\underline{\boldsymbol{\sigma}}_K^*(\vartheta_K, \boldsymbol{\beta}_K)\|_{\underline{\mathbf{L}}^2(K)}$.*

The nonconforming estimator Φ_{nc} is given by

$$\Phi_{nc} = \frac{\nu}{\beta} \|\nabla \cdot \mathbf{u}_h\|_{L^2(\Omega)}. \quad (5.46)$$

Remark 5.5.3. *Notice that the error estimator η and the velocity and pressure errors (\mathbf{e}_V, e_P) actually depend on the selection of the stabilization parameter, so to be more precise we should write $\eta = \eta(\alpha)$ and $(\mathbf{e}_V, e_P) = (\mathbf{e}_V, e_P)(\alpha)$, but for the moment we will skip this notation for simplicity.*

5.6 Efficiency of the estimator.

Since the error estimator η is written in terms of the conforming estimator Φ_c and the nonconforming estimator Φ_{nc} , we first focus on bounding the conforming estimator.

Defining

$$[\mathbf{J}]_{\gamma} = \begin{cases} \frac{1}{2} (\mathbf{J}_{\gamma,K} + \mathbf{J}_{\gamma,K'}) & \text{if } \gamma \in \mathcal{E}_K \cap \mathcal{E}_{K'}, \\ \mathbf{0} & \text{if } \gamma \in \mathcal{E}_K \cap \mathcal{E}_{\Gamma}, \end{cases}$$

from (5.18) it follows that $\mathcal{R}_{\gamma,K} = \mathbf{g}_{\gamma,K} - \langle \mathbf{J} \rangle_{\gamma,K} - [\mathbf{J}]_{\gamma}$. From Theorem 5.5.2 and Lemma 5.4.1 it follows that

$$\begin{aligned} \Phi_{c,K}(\vartheta_K, \beta_K)^2 &\leq C \left(h_K^2 \|\mathcal{R}_K\|_{\mathbf{L}^2(K)}^2 + h_K \sum_{\gamma \in \mathcal{E}_K} \|\mathcal{R}_{\gamma,K}\|_{\mathbf{L}^2(\gamma)}^2 + h_K^2 \|\mathbf{f} - \mathbf{\Pi}_K(\mathbf{f})\|_{\mathbf{L}^2(K)}^2 \right) \\ &\leq C \left(h_K^2 \|\mathcal{R}_K\|_{\mathbf{L}^2(K)}^2 + h_K \sum_{\gamma \in \mathcal{E}_K} \left(\|\mathbf{g}_{\gamma,K} - \langle \mathbf{J} \rangle_{\gamma,K}\|_{\mathbf{L}^2(\gamma)}^2 + \|[\mathbf{J}]_{\gamma}\|_{\mathbf{L}^2(\gamma)}^2 \right) \right. \\ &\quad \left. + h_K^2 \|\mathbf{f} - \mathbf{\Pi}_K(\mathbf{f})\|_{\mathbf{L}^2(K)}^2 \right). \end{aligned} \quad (5.47)$$

To obtain a lower bound, each term on the right hand side of (5.47) should be bounded by the errors. In fact, first notice that we can write the error equation (5.2) for any $\mathbf{v} \in \mathbf{H}_0^1(\Omega)$, as follows

$$\begin{aligned} \sum_{K \in \mathcal{P}} \left((\mathcal{R}_K, \mathbf{v})_K - \sum_{\gamma \in \mathcal{E}_K} ([\mathbf{J}]_{\gamma}, \mathbf{v})_{\gamma} \right) & \quad (5.48) \\ &= \nu (\nabla \mathbf{e}, \nabla \mathbf{v})_{\Omega} + (e_P, \nabla \cdot \mathbf{v})_{\Omega} - \sum_{K \in \mathcal{P}} (\mathbf{f} - \mathbf{\Pi}_K(\mathbf{f}), \mathbf{v})_K. \end{aligned}$$

Now applying similar bubble arguments, to the ones presented in Sections 3.7 and 4.5, using the error equation (5.48), it can be proved that, for all $K \in \mathcal{P}$,

$$h_K \|\mathcal{R}_K\|_{\mathbf{L}^2(K)} \leq C \left(\nu \|\nabla \mathbf{e}_V\|_{\mathbf{L}^2(K)} + \beta \|e_P\|_{\mathbf{L}^2(K)} + h_K \|\mathbf{f} - \mathbf{\Pi}_K(\mathbf{f})\|_{\mathbf{L}^2(K)} \right), \quad (5.49)$$

and

$$\begin{aligned} \sum_{\gamma \in \mathcal{E}_K} h_K^{1/2} \|[\mathbf{J}]_{\gamma}\|_{\mathbf{L}^2(\gamma)} & \quad (5.50) \\ &\leq C \left(\sum_{K' \in \Omega_K} \nu \|\nabla \mathbf{e}_V\|_{\mathbf{L}^2(K')} + \beta \|e_P\|_{\mathbf{L}^2(K')} + h_{K'} \|\mathbf{f} - \mathbf{\Pi}_{K'}(\mathbf{f})\|_{\mathbf{L}^2(K')} \right). \end{aligned}$$

Following the same arguments as in Theorem 4.5.1, we deduce that

$$h_K^{1/2} \|\mathbf{g}_{\gamma,K} - \langle \mathbf{J} \rangle_{\gamma}\|_{\mathbf{L}^2(\gamma)} \leq C \sum_{n \in \mathcal{V}_{\gamma}} \sum_{K \in \Omega_n} \left| \Delta_K(\boldsymbol{\lambda}_n^{(i)}) \right|, \quad (5.51)$$

with $\Delta_K(\boldsymbol{\lambda}_n^{(i)})$ given by (5.22). Integration by parts in (5.22), using the definition of the stabilized term (5.5) and the fact that $\nu \nabla \mathbf{u}_{h|K} \hat{\mathbf{n}}_{\gamma}^K - p_h \hat{\mathbf{n}}_{\gamma}^K = \langle \mathbf{J} \rangle_{\gamma,K} + [\mathbf{J}]_{\gamma}$, yields

$$\begin{aligned} \left| \Delta_K(\boldsymbol{\lambda}_n^{(i)}) \right| &= \left| - \left(\mathcal{R}_K, \boldsymbol{\lambda}_n^{(i)} \right)_K + \sum_{\gamma \in \mathcal{E}_K} \left([\mathbf{J}]_{\gamma}, \boldsymbol{\lambda}_n^{(i)} \right)_{\gamma} + \alpha \nu \left(\nabla \cdot \mathbf{u}_{h|K}, \mathcal{D}_1(\boldsymbol{\lambda}_n^{(i)}) \right)_K \right. \\ &\quad \left. + \frac{\alpha h_K^2}{\nu} \left(\left(\mathcal{R}_K, \mathcal{D}_2(\boldsymbol{\lambda}_n^{(i)}) \right)_K + \left(\mathbf{f} - \mathbf{\Pi}_K(\mathbf{f}), \mathcal{D}_2(\boldsymbol{\lambda}_n^{(i)}) \right)_K \right) \right. \\ &\quad \left. + \sum_{\gamma \in \mathcal{E}_K} \frac{2\alpha |\gamma|}{\nu} \left([\mathbf{J}]_{\gamma}, \mathcal{D}_3(\boldsymbol{\lambda}_n^{(i)}) \right)_{\gamma} \right|. \end{aligned}$$

Now each term of the previous equality can be bounded as follows

$$\begin{aligned}
\left(\mathcal{R}_K, \boldsymbol{\lambda}_n^{(i)}\right)_K &\leq Ch_K \|\mathcal{R}_K\|_{L^2(K)}, \\
\sum_{\gamma \in \mathcal{E}_K} \left([\mathbf{J}]_\gamma, \boldsymbol{\lambda}_n^{(i)}\right)_\gamma &\leq C \sum_{\gamma \in \mathcal{E}_K} h_K^{1/2} \left\| [\mathbf{J}]_\gamma \right\|_{L^2(\gamma)}, \\
\alpha \nu \left(\nabla \cdot \mathbf{u}_{h|K}, \mathcal{D}_1 \left(\boldsymbol{\lambda}_n^{(i)}\right)\right)_K &= \alpha \nu \left(\nabla \cdot \mathbf{u}_{h|K} - \nabla \cdot \mathbf{u}, \mathcal{D}_1 \left(\boldsymbol{\lambda}_n^{(i)}\right)\right)_K \\
&\leq C \alpha \nu \|\nabla \cdot (\mathbf{u}_{h|K} - \mathbf{u})\|_{L^2(K)} \\
&\leq C \alpha \nu \|\nabla \mathbf{e}_V\|_{\underline{\mathbb{L}}^2(K)}, \\
\frac{\alpha h_K^2}{\nu} \left(\mathcal{R}_K, \mathcal{D}_2 \left(\boldsymbol{\lambda}_n^{(i)}\right)\right)_K &\leq C \frac{\alpha h_K}{\nu} h_K \|\mathcal{R}_K\|_{L^2(K)}, \\
\frac{\alpha h_K^2}{\nu} \left(\mathbf{f} - \boldsymbol{\Pi}_K(\mathbf{f}), \mathcal{D}_2 \left(\boldsymbol{\lambda}_n^{(i)}\right)\right)_K &\leq C \frac{\alpha h_K}{\nu} h_K \|\mathbf{f} - \boldsymbol{\Pi}_K(\mathbf{f})\|_{L^2(K)}, \\
\sum_{\gamma \in \mathcal{E}_K} \frac{\alpha |\gamma|}{\nu} \left([\mathbf{J}]_\gamma, \mathcal{D}_3 \left(\boldsymbol{\lambda}_n^{(i)}\right)\right)_\gamma &\leq C \sum_{\gamma \in \mathcal{E}_K} \frac{\alpha h_K^{1/2}}{\nu} h_K^{1/2} \left\| [\mathbf{J}]_\gamma \right\|_{L^2(\gamma)},
\end{aligned}$$

upon applying the Cauchy–Schwarz inequality, the fact that $\left\| \boldsymbol{\lambda}_n^{(i)} \right\|_{L^2(K)} \leq Ch_K$, $\left\| \boldsymbol{\lambda}_n^{(i)} \right\|_{L^2(\gamma)} \leq Ch_K^{1/2}$, (5.7), the fact that the true solution $\mathbf{u} \in \mathbf{X}$ and the definition of the velocity error. From all the previous bounds it follows that

$$\begin{aligned}
\left| \Delta_K \left(\boldsymbol{\lambda}_n^{(i)}\right) \right| &\leq C \left(\left(1 + \frac{\alpha h_K}{\nu}\right) h_K \|\mathcal{R}_K\|_{L^2(K)} + \left(1 + \frac{\alpha h_K^{1/2}}{\nu}\right) \sum_{\gamma \in \mathcal{E}_K} h_K^{1/2} \left\| [\mathbf{J}]_\gamma \right\|_{L^2(\gamma)} \right. \\
&\quad \left. + \alpha \nu \|\nabla \mathbf{e}_V\|_{\underline{\mathbb{L}}^2(K)} + \frac{\alpha h_K}{\nu} h_K \|\mathbf{f} - \boldsymbol{\Pi}_K(\mathbf{f})\|_{L^2(K)} \right). \tag{5.52}
\end{aligned}$$

Inserting the previous bound into (5.51) to then use (5.49) and (5.50) and (5.47) and also noticing that for Pressure-Stabilization methods all the terms related to stabilization in the momentum equation disappear on the previous analysis, yields to the following result.

Theorem 5.6.1. *Let $\Phi_{c,K}(\vartheta_K, \boldsymbol{\beta}_K)$ be given by (5.44). Then, there exists $c > 0$, independent of any mesh size, the viscosity ν and the parameter α , such that*

$$c \Phi_{c,K}(\vartheta_K, \boldsymbol{\beta}_K)^2 \leq \sum_{K' \in \hat{\Omega}_K} \mathcal{M}_{K',S}^2 \left(\left\| (\mathbf{e}_V, \mathbf{e}_P) \right\|_{K'}^2 + h_{K'}^2 \|\mathbf{f} - \boldsymbol{\Pi}_{K'}(\mathbf{f})\|_{L^2(K')}^2 \right),$$

where

$$\mathcal{M}_{K,S} = \begin{cases} \max \left\{ 1 + \frac{\alpha h_K^{1/2}}{\nu}, 1 + \alpha \right\} & \text{for Pressure-Velocity-Stabilization,} \\ 1 & \text{for Pressure-Stabilization.} \end{cases} \tag{5.53}$$

The lower bound for the nonconforming estimator easily follows upon noting that, since the solution \mathbf{u} of (5.2) belongs to the space \mathbf{X} , then

$$\Phi_{nc,K} = \frac{1}{\beta} \|\nabla \cdot \mathbf{u}_{h|K}\|_{L^2(K)} = \frac{1}{\beta} \|\nabla \cdot (\mathbf{u}_{h|K} - \mathbf{u})\|_{L^2(K)} \leq \frac{\sqrt{2}}{\beta} \|\nabla e_V\|_{\underline{\underline{L}}^2(K)}. \quad (5.54)$$

From Theorem 5.6.1 and (5.54), we have the following result.

Theorem 5.6.2. *Define the local error indicator η_K as*

$$\eta_K^2 = \Phi_{c,K}^2(\vartheta_K, \boldsymbol{\beta}_K) + \Phi_{nc,K}^2 + (\Phi_{c,K}(0, \boldsymbol{\beta}_K) + \Phi_{nc,K})^2,$$

where $\Phi_{c,K}$ is given by (5.45) and $\Phi_{nc,K}$ given by (5.54). Then, there exists a constant c , independent of the viscosity ν and the stabilization parameter α , such that

$$c \eta_K^2 \leq C \sum_{K' \in \bar{\Omega}_K} \mathcal{M}_{K',S}^2 \left(\| (e_V, e_P) \|_{K'}^2 + h_{K'}^2 \| \mathbf{f} - \boldsymbol{\Pi}_{K'}(\mathbf{f}) \|_{L^2(K')}^2 \right), \quad (5.55)$$

with $\mathcal{M}_{K',S}$ given by (5.53).

Remark 5.6.3. *Notice that for the **Pressure-Stabilization** methods the two-sided bounds on the error measured in the natural norm are completely robust with respect to the viscosity ν and the stabilization parameter α , which leaves some room to improvement, in terms that we can search for an optimal value for the stabilization parameter hopefully leading to a tighter upper bound, which will be the topic of the next chapter.*

Unfortunately for the **Pressure-Velocity-Stabilization** methods the lower bound is not robust since it depends on the viscosity ν and the stabilization parameter α , in the form

$$\max \left\{ 1 + \frac{\alpha h_K^{1/2}}{\nu}, 1 + \alpha \right\}.$$

5.7 An explicit formula to compute the norm of the solution of the Neumann problem.

In terms of practical applications, following similar argument to the ones presented in Sections 3.9 and 4.6, letting the edges, vertices, tangent vectors and unit normal vectors of an element K be labelled as in Figure 2.1, then:

Formula for Pressure-Stabilization methods: To compute and minimize the norm of $\underline{\underline{\sigma}}_K^*(\vartheta_K, \boldsymbol{\beta}_K)$, for $i \in \mathcal{V}_K = \{1, 2, 3\}$ define

$$\underline{\underline{\tau}}_i^{(1)} = \begin{bmatrix} \mathbf{t}_i \\ \mathbf{0} \end{bmatrix} - \frac{\rho}{2} \text{tr} \left(\begin{bmatrix} \mathbf{t}_i \\ \mathbf{0} \end{bmatrix} \right) \underline{\underline{\mathbf{I}}} \quad \text{and} \quad \underline{\underline{\tau}}_i^{(2)} = \begin{bmatrix} \mathbf{0} \\ \mathbf{t}_i \end{bmatrix} - \frac{\rho}{2} \text{tr} \left(\begin{bmatrix} \mathbf{0} \\ \mathbf{t}_i \end{bmatrix} \right) \underline{\underline{\mathbf{I}}}, \quad (5.56)$$

with $\varrho = 0$ for $\boldsymbol{\sigma}_{\approx K}^*(0, \boldsymbol{\beta}_K)$ and $\varrho = 1$ for $\boldsymbol{\sigma}_{\approx K}^*(\vartheta_K, \boldsymbol{\beta}_K)$. Now, let

$$\left(\boldsymbol{\sigma}_{K,\gamma_i}^{(l)}, \boldsymbol{\sigma}_{K,\gamma_i}^{(m)}\right)_K = \frac{1}{720|K|} \left(\mathbf{S}_i^{(l)}\right)^T \mathbf{M}_{\approx ii}^{(l,m)} \mathbf{S}_i^{(m)}$$

and

$$\left(\boldsymbol{\sigma}_{K,\gamma_i}^{(l)}, \boldsymbol{\sigma}_{K,\gamma_j}^{(m)}\right)_K = \frac{1}{720|K|} \left(\mathbf{S}_i^{(l)}\right)^T \mathbf{M}_{\approx ij}^{(l,m)} \mathbf{S}_j^{(m)}$$

where

$$\mathbf{S}_1^{(l)} = \begin{pmatrix} \left(\mathcal{R}_{\gamma_1,K}, \boldsymbol{\lambda}_2^{(l)}\right)_{\gamma_1} \\ \left(\mathcal{R}_{\gamma_1,K}, \boldsymbol{\lambda}_3^{(l)}\right)_{\gamma_1} \end{pmatrix}$$

with $\mathbf{S}_2^{(l)}$ and $\mathbf{S}_3^{(l)}$ being defined by permuting the indices and

$$\begin{aligned} \mathbf{M}_{\approx 11}^{(l,m)} &= \begin{bmatrix} 26 & -42 \\ -42 & 114 \end{bmatrix} \left(\boldsymbol{\tau}_2^{(l)} : \boldsymbol{\tau}_2^{(m)}\right) + \begin{bmatrix} -9 & 7 \\ -17 & -9 \end{bmatrix} \left(\boldsymbol{\tau}_2^{(l)} : \boldsymbol{\tau}_3^{(m)}\right) \\ &+ \begin{bmatrix} -9 & -17 \\ 7 & -9 \end{bmatrix} \left(\boldsymbol{\tau}_3^{(l)} : \boldsymbol{\tau}_2^{(m)}\right) + \begin{bmatrix} 114 & -42 \\ -42 & 26 \end{bmatrix} \left(\boldsymbol{\tau}_3^{(l)} : \boldsymbol{\tau}_3^{(m)}\right) \end{aligned}$$

with $\mathbf{M}_{\approx 22}^{(l,m)}$ and $\mathbf{M}_{\approx 33}^{(l,m)}$ being defined by permuting the indices and

$$\begin{aligned} \mathbf{M}_{\approx 12}^{(l,m)} &= \begin{bmatrix} -5 & -5 \\ 15 & -25 \end{bmatrix} \left(\boldsymbol{\tau}_2^{(l)} : \boldsymbol{\tau}_3^{(m)}\right) + \begin{bmatrix} 54 & -22 \\ -78 & 54 \end{bmatrix} \left(\boldsymbol{\tau}_2^{(l)} : \boldsymbol{\tau}_1^{(m)}\right) \\ &+ \begin{bmatrix} -13 & 31 \\ -1 & -13 \end{bmatrix} \left(\boldsymbol{\tau}_3^{(l)} : \boldsymbol{\tau}_3^{(m)}\right) + \begin{bmatrix} -25 & -5 \\ 15 & -5 \end{bmatrix} \left(\boldsymbol{\tau}_3^{(l)} : \boldsymbol{\tau}_1^{(m)}\right) \end{aligned}$$

with $\mathbf{M}_{\approx 23}^{(l,m)}$ and $\mathbf{M}_{\approx 31}^{(l,m)}$ being defined by permuting the indices. Also, let

$$\begin{aligned} \left(\boldsymbol{\sigma}_{K,0}^{(l)}, \boldsymbol{\sigma}_{K,0}^{(m)}\right)_K &= \frac{1}{720|K|} \left(2 \left(\boldsymbol{\tau}_2^{(l)} : \boldsymbol{\tau}_2^{(m)}\right) + \left(\boldsymbol{\tau}_2^{(l)} : \boldsymbol{\tau}_3^{(m)}\right) \right. \\ &\quad \left. + \left(\boldsymbol{\tau}_3^{(l)} : \boldsymbol{\tau}_2^{(m)}\right) + 2 \left(\boldsymbol{\tau}_3^{(l)} : \boldsymbol{\tau}_3^{(m)}\right) \right) \end{aligned}$$

and

$$\left(\boldsymbol{\sigma}_{K,\gamma_i}^{(l)}, \boldsymbol{\sigma}_{K,0}^{(m)}\right)_K = \frac{1}{720|K|} \left(\mathbf{S}_i^{(l)}\right)^T \mathbf{M}_{i0}^{(l,m)}$$

where

$$\begin{aligned} \mathbf{M}_{10}^{(l,m)} &= \begin{bmatrix} -2 \\ -6 \end{bmatrix} \left(\boldsymbol{\tau}_2^{(l)} : \boldsymbol{\tau}_2^{(m)}\right) + \begin{bmatrix} 1 \\ -7 \end{bmatrix} \left(\boldsymbol{\tau}_2^{(l)} : \boldsymbol{\tau}_3^{(m)}\right) \\ &+ \begin{bmatrix} 7 \\ -1 \end{bmatrix} \left(\boldsymbol{\tau}_3^{(l)} : \boldsymbol{\tau}_2^{(m)}\right) + \begin{bmatrix} 6 \\ 2 \end{bmatrix} \left(\boldsymbol{\tau}_3^{(l)} : \boldsymbol{\tau}_3^{(m)}\right) \end{aligned}$$

with $M_{20}^{(l,m)}$ and $M_{30}^{(l,m)}$ being defined by permuting the indices. Also, define

$$\mathbf{A} \approx \begin{bmatrix} \left(\boldsymbol{\sigma}_{K,0}^{(1)}, \boldsymbol{\sigma}_{K,0}^{(1)} \right)_K & \left(\boldsymbol{\sigma}_{K,0}^{(1)}, \boldsymbol{\sigma}_{K,0}^{(2)} \right)_K \\ \left(\boldsymbol{\sigma}_{K,0}^{(2)}, \boldsymbol{\sigma}_{K,0}^{(1)} \right)_K & \left(\boldsymbol{\sigma}_{K,0}^{(2)}, \boldsymbol{\sigma}_{K,0}^{(2)} \right)_K \end{bmatrix}$$

and

$$\mathbf{B} = \begin{pmatrix} \sum_{l=1}^2 \sum_{i=1}^3 \left(\boldsymbol{\sigma}_{K,\gamma_i}^{(l)}, \boldsymbol{\sigma}_{K,0}^{(1)} \right)_K \\ \sum_{l=1}^2 \sum_{i=1}^3 \left(\boldsymbol{\sigma}_{K,\gamma_i}^{(l)}, \boldsymbol{\sigma}_{K,0}^{(2)} \right)_K \end{pmatrix}.$$

Then,

$$\begin{aligned} \left\| \boldsymbol{\sigma}_K^*(\vartheta_K, \boldsymbol{\beta}_K) \right\|_{\mathbb{L}^2(K)}^2 &= \sum_{l=1}^2 \sum_{m=1}^2 \left(\left(\boldsymbol{\sigma}_{K,\gamma_1}^{(l)}, \boldsymbol{\sigma}_{K,\gamma_1}^{(m)} \right)_K + \left(\boldsymbol{\sigma}_{K,\gamma_2}^{(l)}, \boldsymbol{\sigma}_{K,\gamma_2}^{(m)} \right)_K + \left(\boldsymbol{\sigma}_{K,\gamma_3}^{(l)}, \boldsymbol{\sigma}_{K,\gamma_3}^{(m)} \right)_K \right. \\ &\quad \left. + 2 \left(\left(\boldsymbol{\sigma}_{K,\gamma_2}^{(l)}, \boldsymbol{\sigma}_{K,\gamma_3}^{(m)} \right)_K + \left(\boldsymbol{\sigma}_{K,\gamma_3}^{(l)}, \boldsymbol{\sigma}_{K,\gamma_1}^{(m)} \right)_K + \left(\boldsymbol{\sigma}_{K,\gamma_1}^{(l)}, \boldsymbol{\sigma}_{K,\gamma_2}^{(m)} \right)_K \right) \right) \\ &\quad - \mathbf{B}^T \mathbf{A}^{-1} \mathbf{B}. \end{aligned} \quad (5.57)$$

Now, $\left\| \boldsymbol{\sigma}_K^*(\vartheta_K, \boldsymbol{\beta}_K) \right\|_{\mathbb{L}^2(K)}$ is minimized over $\vartheta_K \in \mathbb{P}_2(K)$ and $\boldsymbol{\beta}_K \in (H_0^1(K) \cap \mathbb{P}_3(K))^2$ when we take $\varrho = 1$ in the previous process, and to obtain minimization over just $\boldsymbol{\beta}_K \in (H_0^1(K) \cap \mathbb{P}_3(K))^2$, simply take $\varrho = 0$ and repeating the same procedure we obtain $\left\| \boldsymbol{\sigma}_K^*(0, \boldsymbol{\beta}_K) \right\|_{\mathbb{L}^2(K)}^2$.

Formula for Pressure-Velocity-Stabilization methods: To compute and minimize the norm of $\boldsymbol{\sigma}_K^*(\vartheta_K, \boldsymbol{\beta}_K)$, for $i \in \mathcal{V}_K = \{1, 2, 3\}$ define

$$\boldsymbol{\tau}_i^{(1)} = \begin{bmatrix} \mathbf{t}_i \\ \mathbf{0} \end{bmatrix} - \frac{\varrho}{2} \operatorname{tr} \left(\begin{bmatrix} \mathbf{t}_i \\ \mathbf{0} \end{bmatrix} \right) \mathbf{I} \quad \text{and} \quad \boldsymbol{\tau}_i^{(2)} = \begin{bmatrix} \mathbf{0} \\ \mathbf{t}_i \end{bmatrix} - \frac{\varrho}{2} \operatorname{tr} \left(\begin{bmatrix} \mathbf{0} \\ \mathbf{t}_i \end{bmatrix} \right) \mathbf{I}, \quad (5.58)$$

with $\varrho = 0$ for $\boldsymbol{\sigma}_K(0, \boldsymbol{\beta}_K)$ and $\varrho = 1$ for $\boldsymbol{\sigma}_K(\xi_K, \boldsymbol{\beta}_K)$. Now, let

$$\left(\boldsymbol{\sigma}_{K,\gamma_i}^{(l)}, \boldsymbol{\sigma}_{K,\gamma_i}^{(m)} \right)_K = \frac{1}{6480 |K|} \left(\mathbf{S}_i^{(l)} \right)^T \mathbf{M}_{ii}^{(l,m)} \mathbf{S}_i^{(m)}$$

and

$$\left(\boldsymbol{\sigma}_{K,\gamma_i}^{(l)}, \boldsymbol{\sigma}_{K,\gamma_j}^{(m)} \right)_K = \frac{1}{6480 |K|} \left(\mathbf{S}_i^{(l)} \right)^T \mathbf{M}_{ij}^{(l,m)} \mathbf{S}_j^{(m)}$$

where

$$\mathbf{S}_1^{(l)} = \begin{pmatrix} \left(\mathcal{R}_{\gamma_1,K}, \boldsymbol{\lambda}_2^{(l)} \right)_{\gamma_1} \\ \left(\mathcal{R}_{\gamma_1,K}, \boldsymbol{\lambda}_3^{(l)} \right)_{\gamma_1} \\ |K| \nabla(\mathcal{R}_K^l) \cdot (\mathbf{x}_1 - \bar{\mathbf{x}}_K) \end{pmatrix}$$

with $\mathbf{S}_2^{(l)}$ and $\mathbf{S}_3^{(l)}$ being defined by permuting the indices and

$$\begin{aligned} \mathbf{M}_{11}^{(l,m)} = & \begin{bmatrix} 1242 & -2322 & 54 \\ -2322 & 4482 & -126 \\ 54 & -126 & 8 \end{bmatrix} \begin{pmatrix} \tau_2^{(l)} : \tau_2^{(m)} \end{pmatrix} + \begin{bmatrix} 1647 & -945 & -36 \\ -2889 & 1647 & 72 \\ 72 & -36 & -4 \end{bmatrix} \begin{pmatrix} \tau_2^{(l)} : \tau_3^{(m)} \end{pmatrix} \\ & + \begin{bmatrix} 1647 & -2889 & 72 \\ -945 & 1647 & -36 \\ -36 & 72 & -4 \end{bmatrix} \begin{pmatrix} \tau_3^{(l)} : \tau_2^{(m)} \end{pmatrix} + \begin{bmatrix} 4482 & -2322 & -126 \\ -2322 & 1242 & 54 \\ -126 & 54 & 8 \end{bmatrix} \begin{pmatrix} \tau_3^{(l)} : \tau_3^{(m)} \end{pmatrix} \end{aligned}$$

with $\mathbf{M}_{22}^{(l,m)}$ and $\mathbf{M}_{33}^{(l,m)}$ being defined by permuting the indices and

$$\begin{aligned} \mathbf{M}_{12}^{(l,m)} = & \begin{bmatrix} 459 & -837 & 36 \\ -1161 & 2079 & -72 \\ 90 & -162 & 4 \end{bmatrix} \begin{pmatrix} \tau_2^{(l)} : \tau_3^{(m)} \end{pmatrix} + \begin{bmatrix} 1998 & -918 & -90 \\ -4158 & 1998 & 162 \\ 162 & -90 & -4 \end{bmatrix} \begin{pmatrix} \tau_2^{(l)} : \tau_1^{(m)} \end{pmatrix} \\ & + \begin{bmatrix} 675 & -1593 & 126 \\ -297 & 675 & -54 \\ -54 & 126 & -8 \end{bmatrix} \begin{pmatrix} \tau_3^{(l)} : \tau_3^{(m)} \end{pmatrix} + \begin{bmatrix} 2079 & -837 & -162 \\ -1161 & 459 & 90 \\ -72 & 36 & 4 \end{bmatrix} \begin{pmatrix} \tau_3^{(l)} : \tau_1^{(m)} \end{pmatrix} \end{aligned}$$

with $\mathbf{M}_{23}^{(l,m)}$ and $\mathbf{M}_{31}^{(l,m)}$ being defined by permuting the indices. Also, let

$$\begin{aligned} \left(\sigma_{K,0}^{(l)}, \sigma_{K,0}^{(m)} \right)_K = & \frac{1}{6480 |K|} \left(18 \begin{pmatrix} \tau_2^{(l)} : \tau_2^{(m)} \end{pmatrix} + 9 \begin{pmatrix} \tau_2^{(l)} : \tau_3^{(m)} \end{pmatrix} \right. \\ & \left. + 9 \begin{pmatrix} \tau_3^{(l)} : \tau_2^{(m)} \end{pmatrix} + 18 \begin{pmatrix} \tau_3^{(l)} : \tau_3^{(m)} \end{pmatrix} \right) \end{aligned}$$

and

$$\left(\sigma_{K,\gamma_i}^{(l)}, \sigma_{K,0}^{(m)} \right)_K = \frac{1}{6480 |K|} \left(\mathbf{S}_i^{(l)} \right)^T \mathbf{M}_{i0}^{(l,m)}$$

where

$$\begin{aligned} \mathbf{M}_{10}^{(l,m)} = & \begin{bmatrix} 54 \\ -54 \\ -6 \end{bmatrix} \begin{pmatrix} \tau_2^{(l)} : \tau_2^{(m)} \end{pmatrix} + \begin{bmatrix} 81 \\ -135 \\ 0 \end{bmatrix} \begin{pmatrix} \tau_2^{(l)} : \tau_3^{(m)} \end{pmatrix} \\ & + \begin{bmatrix} 135 \\ -81 \\ 0 \end{bmatrix} \begin{pmatrix} \tau_3^{(l)} : \tau_2^{(m)} \end{pmatrix} + \begin{bmatrix} 54 \\ -54 \\ 6 \end{bmatrix} \begin{pmatrix} \tau_3^{(l)} : \tau_3^{(m)} \end{pmatrix} \end{aligned}$$

with $M_{20}^{(l,m)}$ and $M_{30}^{(l,m)}$ being defined by permuting the indices. Also, define

$$\mathbf{A} = \begin{bmatrix} \left(\sigma_{K,0}^{(1)}, \sigma_{K,0}^{(1)} \right)_K & \left(\sigma_{K,0}^{(1)}, \sigma_{K,0}^{(2)} \right)_K \\ \left(\sigma_{K,0}^{(2)}, \sigma_{K,0}^{(1)} \right)_K & \left(\sigma_{K,0}^{(2)}, \sigma_{K,0}^{(2)} \right)_K \end{bmatrix}$$

and

$$\mathbf{B} = \begin{pmatrix} \sum_{l=1}^2 \sum_{i=1}^3 \left(\sigma_{K,\gamma_i}^{(l)}, \sigma_{K,0}^{(1)} \right)_K \\ \sum_{l=1}^2 \sum_{i=1}^3 \left(\sigma_{K,\gamma_i}^{(l)}, \sigma_{K,0}^{(2)} \right)_K \end{pmatrix}.$$

Then,

$$\begin{aligned} \left\| \underline{\sigma}_K(\vartheta_K, \beta_K) \right\|_{\underline{\mathbb{L}}^2(K)}^2 &= \sum_{l=1}^2 \sum_{m=1}^2 \left(\left(\sigma_{K,\gamma_1}^{(l)}, \sigma_{K,\gamma_1}^{(m)} \right)_K + \left(\sigma_{K,\gamma_2}^{(l)}, \sigma_{K,\gamma_2}^{(m)} \right)_K + \left(\sigma_{K,\gamma_3}^{(l)}, \sigma_{K,\gamma_3}^{(m)} \right)_K \right. \\ &\quad \left. + 2 \left(\left(\sigma_{K,\gamma_2}^{(l)}, \sigma_{K,\gamma_3}^{(m)} \right)_K + \left(\sigma_{K,\gamma_3}^{(l)}, \sigma_{K,\gamma_1}^{(m)} \right)_K + \left(\sigma_{K,\gamma_1}^{(l)}, \sigma_{K,\gamma_2}^{(m)} \right)_K \right) \right) \\ &\quad - \mathbf{B}^T \mathbf{A}^{-1} \mathbf{B}. \end{aligned} \quad (5.59)$$

Now, $\left\| \underline{\sigma}_K^*(\vartheta_K, \beta_K) \right\|_{\underline{\mathbb{L}}^2(K)}$ is minimized over $\vartheta_K \in \mathbb{P}_2(K)$ and $\beta_K \in (H_0^1(K) \cap \mathbb{P}_3(K))^2$ when we take $\varrho = 1$ in the previous process, and to obtain minimization over just $\beta_K \in (H_0^1(K) \cap \mathbb{P}_3(K))^2$, simply take $\varrho = 0$ and repeating the same procedure we obtain $\left\| \underline{\sigma}_K^*(0, \beta_K) \right\|_{\underline{\mathbb{L}}^2(K)}$.

5.8 Numerical results.

In this section we illustrate the performance of the error estimator with two representative problems.

In the numerical experiments we calculate the exact and the estimated error in the natural norm $\|(\cdot, \cdot)\|_{\Omega}$ on a sequence of uniformly and adaptively refined grids, respectively. For each marked triangle a longest edge bisection step [103] was performed. As a local error indicator for the adaptive algorithm we used

$$\eta_K^2 = \Phi_{c,K}^2(\vartheta_K, \beta_K) + \Phi_{nc,K}^2 + (\Phi_{c,K}(0, \beta_K) + \Phi_{nc,K})^2, \quad (5.60)$$

where $\Phi_{c,K}$ is given by (5.45) and $\Phi_{nc,K}$ is given by (5.54), and triangles are marked using the maximum strategy (mark K if $\eta_K \geq \eta_{\max}/2$). We summarize the adaptive algorithm in Table 5.2.

The global error estimate is, according to (5.43), given by

$$\eta = \left(\Phi_c^2(\vartheta_K, \beta_K) + \Phi_{nc}^2 + (\Phi_c(0, \beta_K) + \Phi_{nc})^2 \right)^{1/2}.$$

Adaptive mesh refinement algorithm [AMRA-S].

- 1:** Set $i = 0$ and construct a mesh $\mathcal{P}_{(i)}$.
 - 2:** For each element K in $\mathcal{P}_{(i)}$, compute:
 - $\|\boldsymbol{\sigma}_K^*(\boldsymbol{\vartheta}_K, \boldsymbol{\beta}_K)\|_{\underline{\mathbb{L}}^2(K)}$ using formula (5.57) when **Pressure-Stabilized** methods are used or (5.59) when **Pressure-Velocity-Stabilized** methods are used.
 - $\|\mathbf{f} - \boldsymbol{\Pi}_K(\mathbf{f})\|_{L^2(K)}$ using an appropriate quadrature formula.
 - $\Phi_{c,K}(\boldsymbol{\vartheta}_K, \boldsymbol{\beta}_K)$ using (5.45).
 - $\Phi_{nc,K}(\boldsymbol{\vartheta}_K, \boldsymbol{\beta}_K)$ using (5.54).
 - η_K using the previous two steps and (5.60).
 - 3:** Triangle K is marked for refinement if

$$\eta_K \geq \frac{1}{2} \max_{K \in \mathcal{P}_{(i)}} \{\eta_K\}.$$
 - 4:** From step **3** deduce a new mesh using longest edge bisection refinement.
 - 5:** Set $i \leftarrow i + 1$ and return to step **2**.
-

Table 5.2: Adaptive mesh refinement algorithm for the Stokes problem.

When reporting numerical results, we denote by Ndofs the number of degrees of freedom and we denote by $\Theta = \frac{\eta}{\|(e_V, e_P)\|_{\Omega}}$ the effectivity index and for the approximation of the solution of the Stokes problem we use the **ABV** method with a $\mathbb{P}_1^2 - \mathbb{P}_0$ combination.

Example 1: The exact velocity and pressure fields for (5.1) are given by

$$\begin{aligned} \mathbf{u} &= [x^2(x-1)^2y(y-1)(2y-1), -y^2(y-1)^2x(x-1)(2x-1)], \\ p &= xy(1-x)(1-y) - \frac{1}{36}, \end{aligned}$$

where $\Omega = (0,1)^2$ is the unit square. We take $\nu = 1$ and, as we stated before, we take a lower bound of 0.38 for the value of the inf-sup constant β .

Example 2: We consider the Stokes flow over a T-shaped domain, where a linear inflow and outflow are imposed on $x = \pm 1.5$ and no-slip conditions are imposed elsewhere on the boundary Γ except on the top of the boundary, where we impose a fixed velocity $\mathbf{u} = (1,0)$, as shown in Figure 5.1. We take $\nu = 1$ and, as we stated before, we take a lower bound of 0.1 for the value

of the inf-sup constant β .

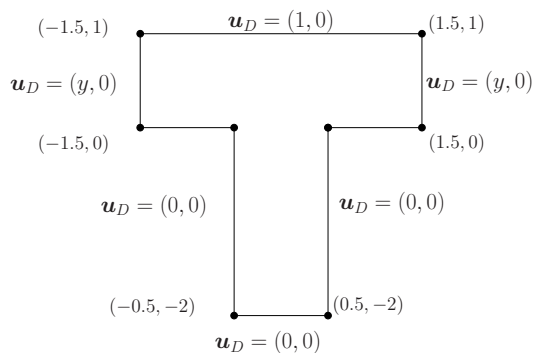


Figure 5.1: Domain and boundary conditions for Example 2.

The initial meshes $\mathcal{S}_{(0)}$ and $\mathcal{T}_{(0)}$, for example 1 and 2, respectively, are shown in Figure 5.2 for the regular or adaptive refinement.

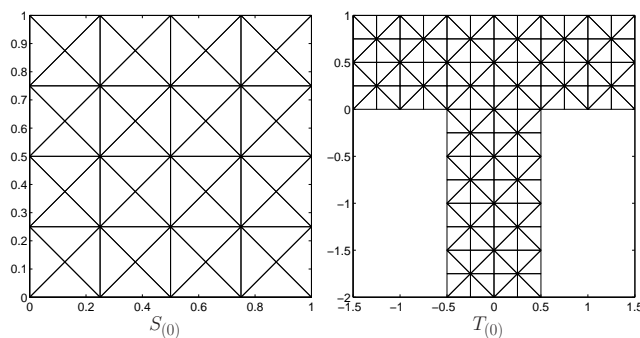


Figure 5.2: Initial mesh $\mathcal{S}_{(0)}$ and $\mathcal{T}_{(0)}$ for Examples 1 and 2, respectively.

For example 1 we depict the accuracy and effectivity indices using the **ABV** ($\mathbb{P}_1^2 - \mathbb{P}_0$) method in Figures 5.3 and 5.4. We can observe that the error estimator provide a very affective guaranteed upper bound. Now, for the second problem, we can see from Figures 5.5 and 5.6 that the error estimator decay with optimal order and also in the adaptive procedure all the refinement is taking place in the two re entrant corners, which is where the pressure present a singular behaviour.

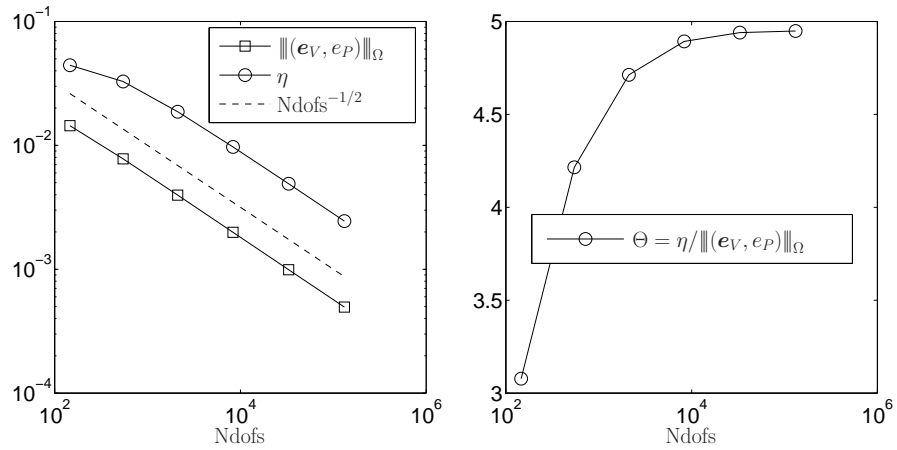


Figure 5.3: Accuracy (left) and effectivity index (right) for Example 1, using regular refinement over the mesh $\mathcal{S}_{(0)}$ from Figure 5.2, with a **ABV** ($\mathbb{P}_1^2 - \mathbb{P}_0$) method.

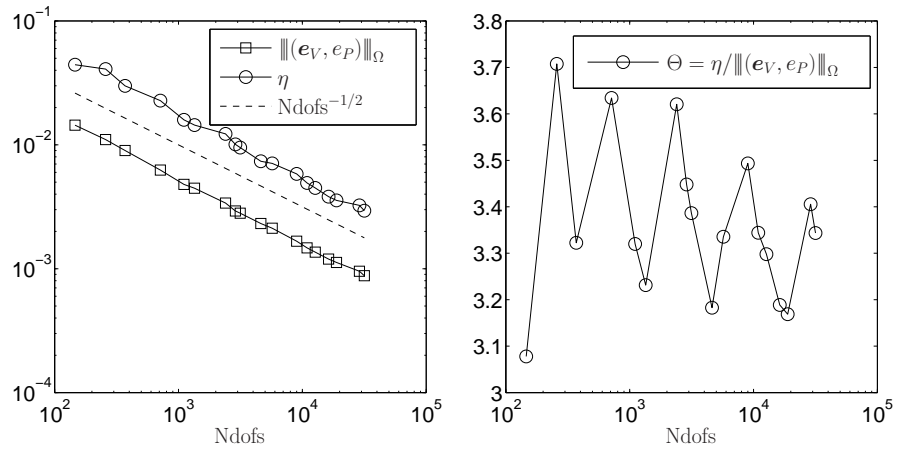


Figure 5.4: Accuracy (left) and effectivity index (right) for Example 1, using adaptive refinement over the mesh $\mathcal{S}_{(0)}$ from Figure 5.2, based on the AMRA-S algorithm in Table 5.2 with a **ABV** ($\mathbb{P}_1^2 - \mathbb{P}_0$) method.

5.9 An alternative guaranteed upper bound for the error.

The following alternative approach can be applied to the nonconforming Fortan-Soulie and the stabilized finite element approximations to the Stokes problem. For simplicity, we consider the case when $\nu = 1$ and homogeneous Dirichlet boundary conditions. From Lemma 3.1 in [75], we

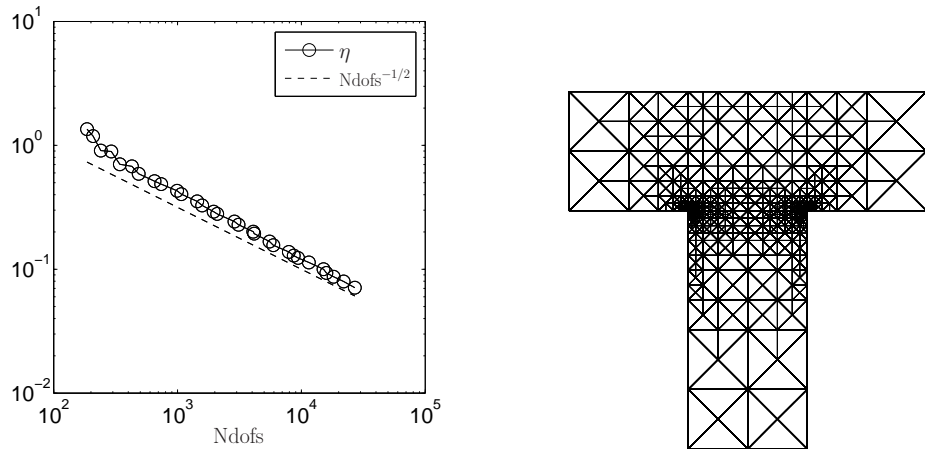


Figure 5.5: Accuracy (left) and adaptive refinement over the mesh $\mathcal{T}_{(0)}$ from Figure 5.2, based on the AMRA-S algorithm in Table 5.2 (right) with a **ABV** ($\mathbb{P}_1^2 - \mathbb{P}_0$) method, for Example 2.

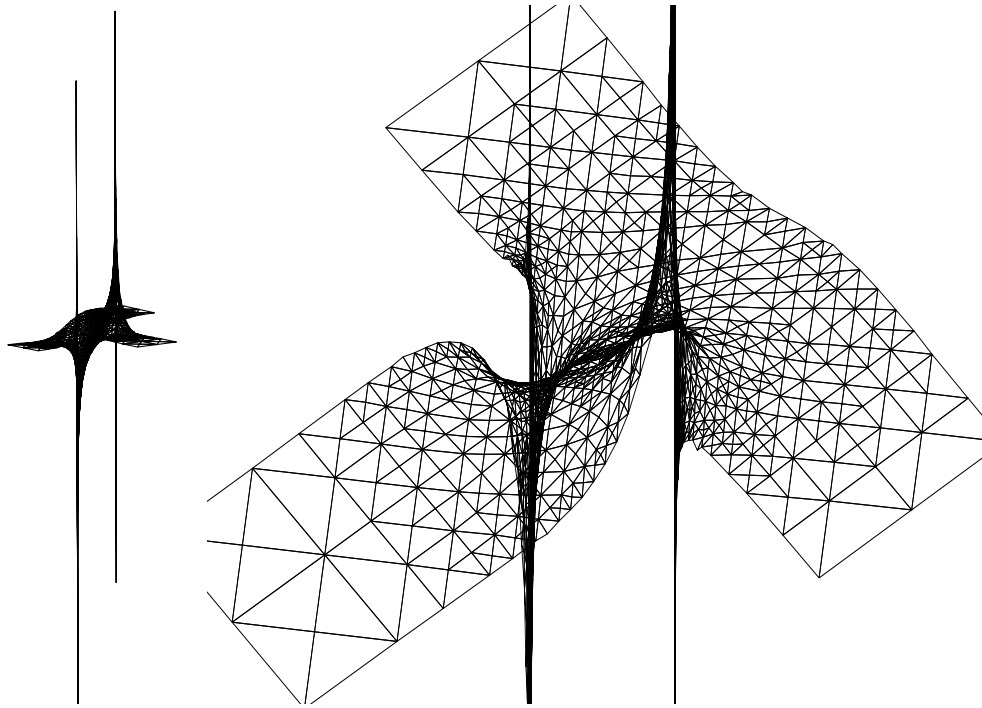


Figure 5.6: A piecewise continuous smoothing elevation of the pressure, for Example 2.

have the following computable upper bound

$$\|(e_V, e_P)\|_{\Omega} \leq \frac{\sqrt{5} + 1}{2} \sup_{(\mathbf{0}, 0) \neq (\mathbf{v}, q) \in \mathbf{H}_0^1(\Omega) \times L_0^2(\Omega)} \frac{\mathcal{B}(e_V, e_P; \mathbf{v}, q)}{\|(\mathbf{v}, q)\|_{\Omega}},$$

and then using (5.14) (or (7.17)), the Cauchy–Schwarz inequality and the definition of the conforming and nonconforming estimators given in Section 5.5 (or Section 3.6), we obtain

$$\mathcal{B}(e_V, e_P; \mathbf{v}, q) \leq (\Phi_c(0, \boldsymbol{\beta}_K)^2 + \Phi_{nc}^2)^{1/2} \|(\mathbf{v}, q)\|_\Omega.$$

As an immediate consequence we obtain the following alternative computable upper bound for the error

$$\|(e_V, e_P)\|_\Omega^2 \leq \left(\frac{\sqrt{5}+1}{2}\right)^2 (\Phi_c(0, \boldsymbol{\beta}_K)^2 + \Phi_{nc}^2). \quad (5.61)$$

Notice that if we were just interested in the estimation of the velocity field, then the estimation using the orthogonal decomposition (5.29) leads to a tighter upper bound, i.e. from Theorem 5.5.2 (or Theorem 3.6.1) we obtain

$$\|\nabla e_V\|_{\underline{\underline{L}}^2(\Omega)}^2 \leq \Phi_c(\vartheta_K, \boldsymbol{\beta}_K)^2 + \Phi_{nc}^2 < \left(\frac{\sqrt{5}+1}{2}\right)^2 (\Phi_c(0, \boldsymbol{\beta}_K)^2 + \Phi_{nc}^2).$$

Likewise, if one wishes to estimate the pressure error only, a superior upper bound again follows by using the orthogonal decomposition, i.e. from Theorem 5.5.2 (or Theorem 3.6.1) we obtain

$$\|e_P\|_{L^2(\Omega)}^2 \leq (\Phi_c(0, \boldsymbol{\beta}_K) + \Phi_{nc})^2 < \left(\frac{\sqrt{5}+1}{2}\right)^2 (\Phi_c(0, \boldsymbol{\beta}_K)^2 + \Phi_{nc}^2).$$

If one wishes to estimate the combined error, Theorem 5.5.2 (or Theorem 3.6.1) and (5.61) yield:

$$\begin{aligned} \|(e_V, e_P)\|_\Omega &\leq \eta_O^2 := \Phi_c(\vartheta_K, \boldsymbol{\beta}_K)^2 + \Phi_{nc}^2 + (\Phi_c(0, \boldsymbol{\beta}_K) + \Phi_{nc})^2, \\ \|(e_V, e_P)\|_\Omega &\leq \eta_{IS}^2 := \left(\frac{\sqrt{5}+1}{2}\right)^2 (\Phi_c(0, \boldsymbol{\beta}_K)^2 + \Phi_{nc}^2), \end{aligned}$$

which in turn gives

$$0.618 = \frac{2}{1+\sqrt{5}} \leq \frac{\theta_O}{\theta_{IS}} = \frac{\eta_O}{\eta_{IS}} \leq \frac{2\sqrt{3}}{1+\sqrt{5}} = 1.07,$$

where $\theta_O = \frac{\eta_O}{\|(e_V, e_P)\|_\Omega}$ and $\theta_{IS} = \frac{\eta_{IS}}{\|(e_V, e_P)\|_\Omega}$ are the effectivity indices. Hence,

$$1 \leq \theta_O \leq 1.07 \theta_{IS} \quad \text{and} \quad 1 \leq \theta_{IS} \leq 1.618 \theta_O,$$

leading to the conclusion that the estimator η_O is in general a sharper bound when we used the orthogonal decomposition of the gradient of the velocity field.

5.10 Conclusions

In this chapter we introduced a fully computable a posteriori error estimator for the Stokes problem using a wide family of low-order stabilized finite element methods. The analysis was

mainly based on the orthogonal decomposition for the gradient of the velocity error, the inf-sup condition related to the continuous problem and the equilibrated residual method. Now, the generalization of the equilibrated residual method to the vector-valued case allows to cover a wide family of methods and also to rewrite the residual functional as a Neumann problem. For the latter problem we provide an explicit formula to compute its norm with different minimization procedures, improving the accuracy of the error estimator with no extra cost.

Chapter 6

On the adaptive selection of the parameter in stabilized finite element approximations.

One characteristic feature of stabilized methods is the presence of a positive constant multiplying the stabilization term. Naturally, the question of the selection of the actual value of the stabilization parameter in practical computation arises which, although not affecting the rate of convergence, can have a significant impact on the absolute value of the error. Considerable effort has been expended in the quest to avoid having to make an ad hoc decision about the specific choice of the parameter. Variational multiscale methods (including RFB's and, recently, PGEM methods [29, 31, 44, 78]) may be regarded as a systematic approach to the selection of an explicit, closed form of the value of the stabilization parameter, thereby rendering the methods parameter-free.

In this chapter we continue the study of the a posteriori error analysis for the Stokes problem using low order stabilized finite element methods, since as was mentioned in Remark 5.6.3, when the stabilized method only consider stabilization in the mass conservation equation, then the developed error estimator provide a two-sided bounds on the error being completely robust with respect to viscosity ν and the stabilization parameter α . Hence, our guaranteed upper bound given in (5.42) can hopefully be improved, in the sense that choosing an appropriate value for

the stabilization parameter it may lead to a tighter upper bound, which clearly will improve the efficiency in the estimation.

In this chapter our approach is based on the premise that the best parameter is the one for which the error is minimal. Of course, the true value of the error is generally unknown. However, since we have at hand a computable quantity $\eta(\alpha)$, which depends on the value α of the stabilization parameter, which delivers a two-sided bounds on the true error $(\mathbf{e}_V, e_P)(\alpha)$, also depending on the stabilization parameter, in the natural norm $\|(\mathbf{e}_V, e_P)(\alpha)\|_\Omega$ up to higher order terms (see Theorems 5.5.2 and 5.6.2), i.e. there exists a constant $c > 0$ independent of α and ν , such that

$$c \eta(\alpha) + \text{h.o.t.} \leq \|(\mathbf{e}_V, e_P)(\alpha)\|_\Omega \leq \eta(\alpha), \quad (6.1)$$

then what is really needed is the value of α for which $\eta(\alpha)$ is a minimum to coincide with the value of α at which the true error has a minimum. Then the developed method, from the previous chapter, for defining such a computable quantity $\eta(\alpha)$, satisfying (6.1) up to higher order oscillation terms, is a key component of our approach.

The search for the optimal value of the stabilization parameter has been considered before. For example, in [35] a residual based a posteriori error estimator was also minimized in order to obtain a value for the stabilization parameter (see also [82] for convection-diffusion problems), whilst in [100] the value is chosen by minimizing the condition number of the associated Schur complement system for the pressure field, but non of them gives a fully computable error estimator.

The development of the measure $\eta(\alpha)$ is only one part of the story and we must also select an algorithm for approximating its minima. The expression for $\eta(\alpha)$ depends on the stabilized finite element approximation obtained using a particular value α for the stabilization parameter. Thus, each evaluation of $\eta(\alpha)$ entails the computation of a finite element approximation. Furthermore, one does not have ready access to derivative information. These considerations suggest the use of a derivative free optimization approach (cf. [55] for an extensive review of the DFO method), to search for the value α_{opt} for which η is minimized.

From Section 7.3, we can see that often the developers of a particular stabilized method give a recommendation, which it will denote by α_{rec} , for the value of the stabilization parameter to be used in practical computations, but in some cases no such value is identified, in which case, in the absence of further information, we select the parameter equal to one. In Table 6.1, we summarize, for each Pressure-Stabilization method the recommended value of the stabilization

parameter.

Pressure-Stabilization Methods	α_{rec}
Galerkin least-Squares-type [GLS]	$\frac{1}{24}$
Brezzi and Pitkäranta [BP]	1
Local Projection methods [LPS]	1
Polynomial pressure methods [PPS]	1
Penalty pressure-type [PEPS]	1

Table 6.1: Recommended value for the stabilization parameter for the Pressure-Stabilization Methods.

6.1 An algorithm for selecting the stabilization parameter on a given mesh.

Although the a priori rate of convergence of a stabilized method is independent of the value of the stabilization parameter (provided the discrete problem is well-posed), the absolute value of the error varies depending on the choice of the parameter. In order to illustrate this point we consider the two simple examples given in Section (5.8).

We shall present results for Examples 1 and 2 obtained by using meshes S-(a) to S-(d) and T-(a) to T-(d) shown in Figures 6.1 and 6.2, respectively.

The values of the norm of the error obtained for various stabilized schemes and various values of the stabilization parameter on fixed meshes are illustrated in Figures 6.3 and 6.4. It is clear that in some cases the choice of the parameter α can significantly affect the error. In particular, an inappropriate choice can result in a loss of a factor of two, or sometimes much more, in the accuracy compared with a more judicious choice. In terms of practical computation this means that a careful choice of α can sometimes be at least as effective as a global mesh refinement.

Occasionally, we shall omit the α dependency and write η in place of $\eta(\alpha)$ and (e_V, e_P) in place of $(e_V, e_P)(\alpha)$, but it should be borne in mind that the estimator is computed using the finite element approximation obtained using the value α as the stabilization parameter.

The values of the quantity $\eta(\alpha)$ are also shown along with the true error in Figures 6.3 to 6.5. We observe that the α -dependency of both the exact error and the estimator are in good

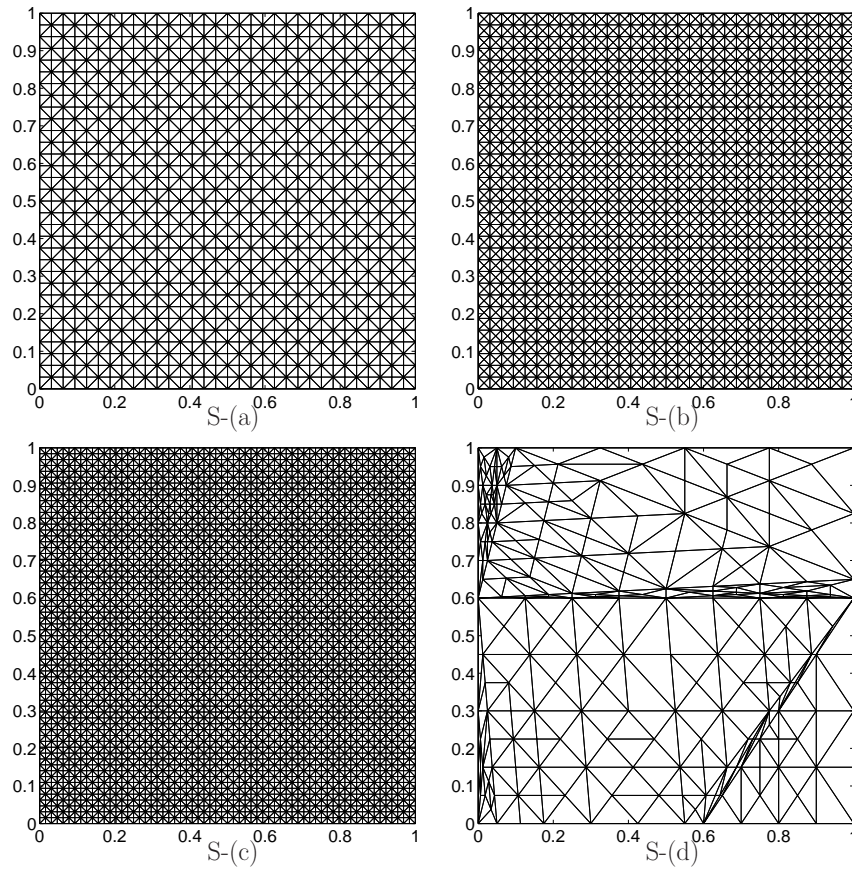


Figure 6.1: Uniform mesh S-(a) with 2048, S-(b) with 4096, S-(c) with 8192 elements and distorted mesh S-(d) with 412 elements, for Example 1.

agreement (Example 1). Significantly, both exhibit minima at roughly the same locations. This correlation suggests selecting the stabilization parameter α to minimize the upper bound $\eta(\alpha)$ for the true error. Whilst the values of the estimated and true errors may differ, the proximity of the minimizers means that the resulting choice of α will be near optimal.

It remains to select an appropriate method for obtaining the minimizer of η . We propose to use the Trust-Region Derivative Free Optimization algorithm (DFO, see [56] and references therein) to approximate the minimiser of $\eta(\alpha)$. For the readers convenience, we give a brief description of the method which is described in full detail in [57] and [54].

We begin by choosing constants $\varepsilon_{\mathcal{D}}, \Lambda, \Delta_{max} > 0$, $0 \leq \text{tol}_0 \leq \text{tol}_1 < 1$, $0 < \omega_0 < 1 < \omega_1$ and a trust-region radius $\Delta_0 \in (0, \Delta_{max}]$. Construct a fully-quadratic model (in the sense of Section 3 in [54]), by evaluating $\eta(\alpha)$ at a set of three sample points $\alpha_0 = \{\alpha_1, \alpha_2, \alpha_3\}$ to obtain

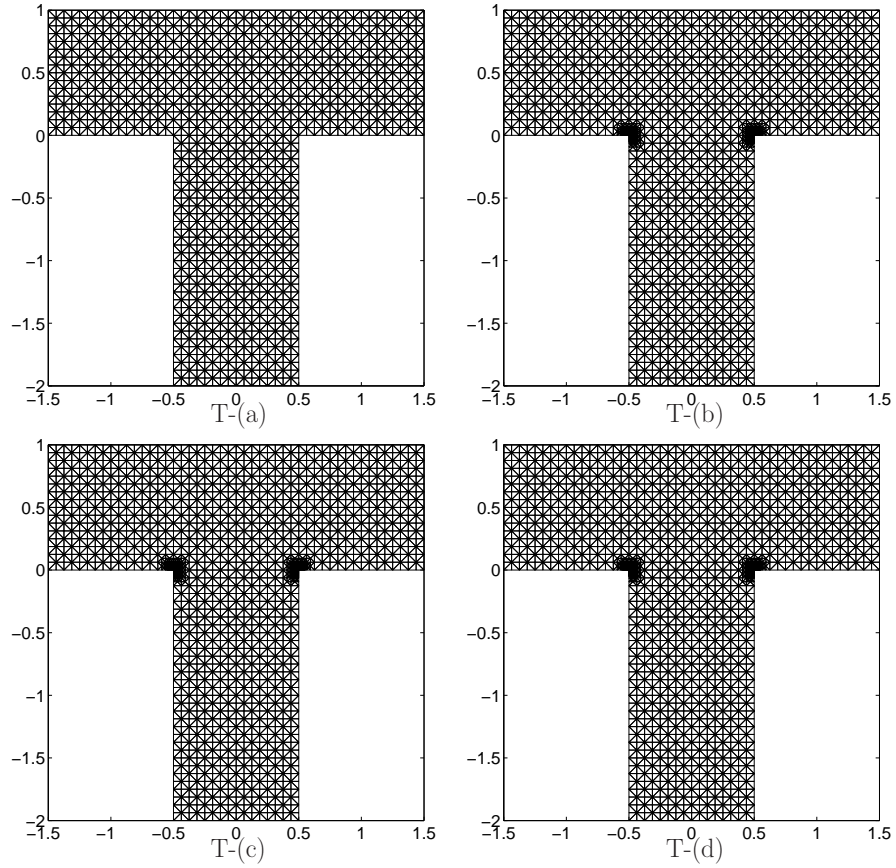


Figure 6.2: Mesh T -(a) with 2560, T -(b) with 5076, T -(c) with 7108 and T -(d) with 11006 elements, for Example 2.

a quadratic interpolant, given by

$$m_0(\alpha) = c_0 + \alpha g_0 + \alpha^2 H_0,$$

where $c_0, g_0, H_0 \in \mathbb{R}$. Denote by $\mathcal{D}_0(\alpha) = \max\{|g_0 + 2\alpha H_0|, |2H_0|\}$ and choose any initial point χ_0 from the sample points, which in our case we take the one with minimum value of $\eta(\alpha)$. If there are two such choices for χ_0 , then choose the one maximizing $\mathcal{D}_0(\chi_0)$ and if there are still two choices, either is used at random. If there are three such choices then use a model-improvement algorithm (Algorithm 6.2 from [54]), based on moving the sample points in order to obtain a fully-quadratic model. Set $k = 0$.

If $\mathcal{D}_k(\chi_k) \leq \varepsilon_{\mathcal{D}}$ call a model-improvement algorithm (Algorithm 6.2 from [54]) to obtain a new quadratic model, otherwise compute the step s_k that sufficiently reduces the model $m_k(\alpha)$

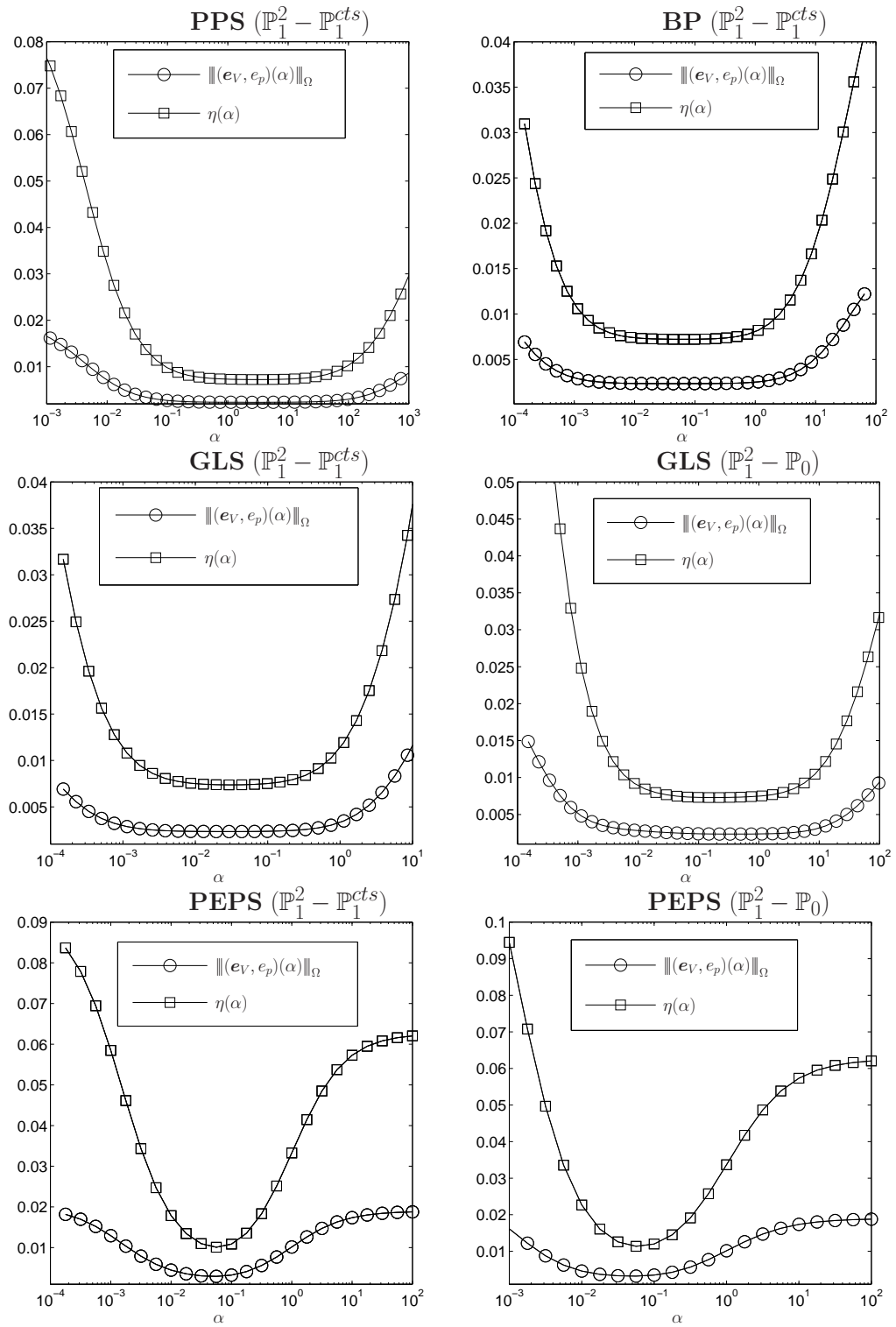


Figure 6.3: Accuracy for different values of α using mesh S-(c) from Figure 6.1, for Example 1.

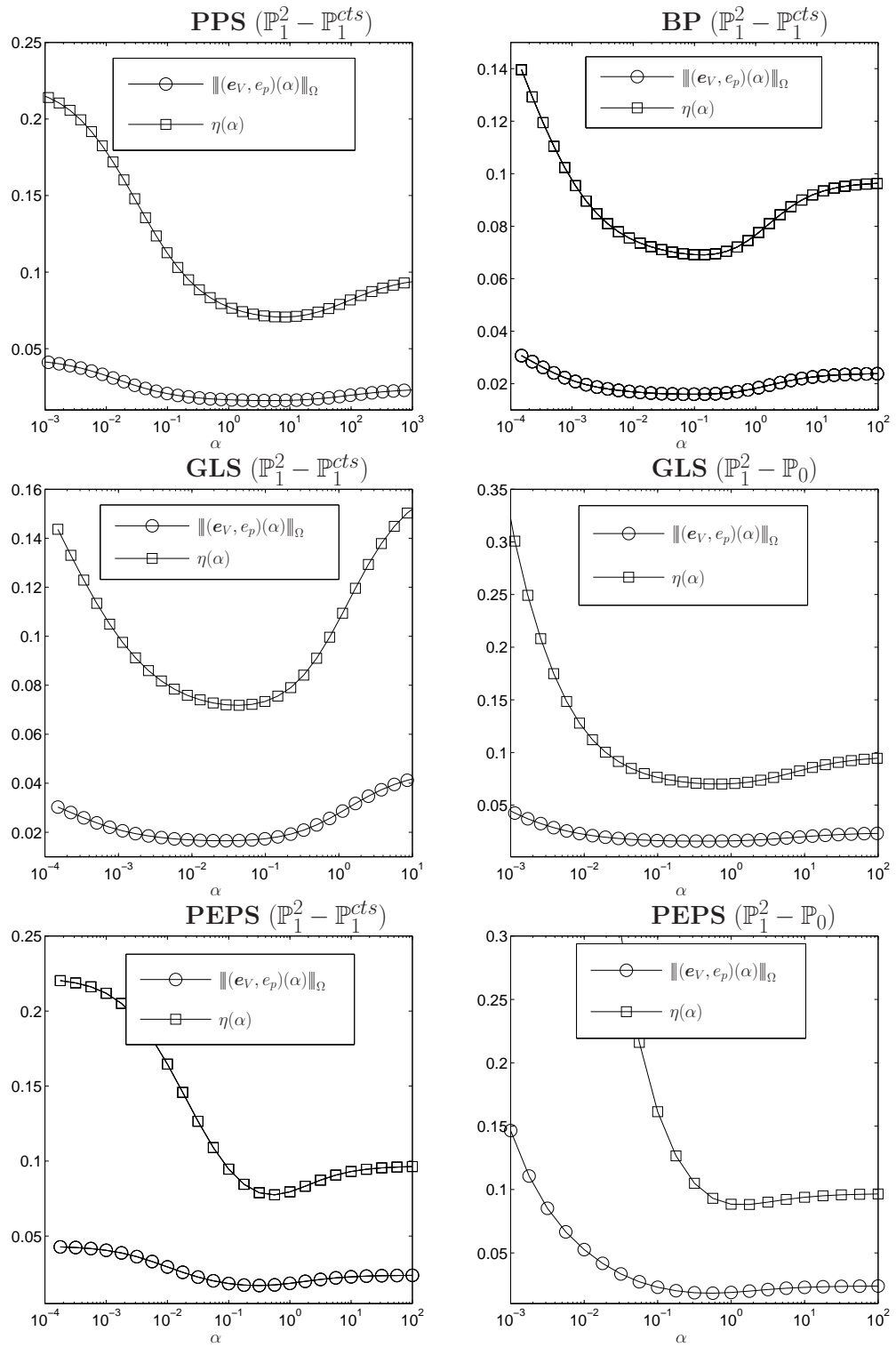


Figure 6.4: Accuracy for different values of α using mesh $S(d)$ from Figure 6.1, for Example 1.

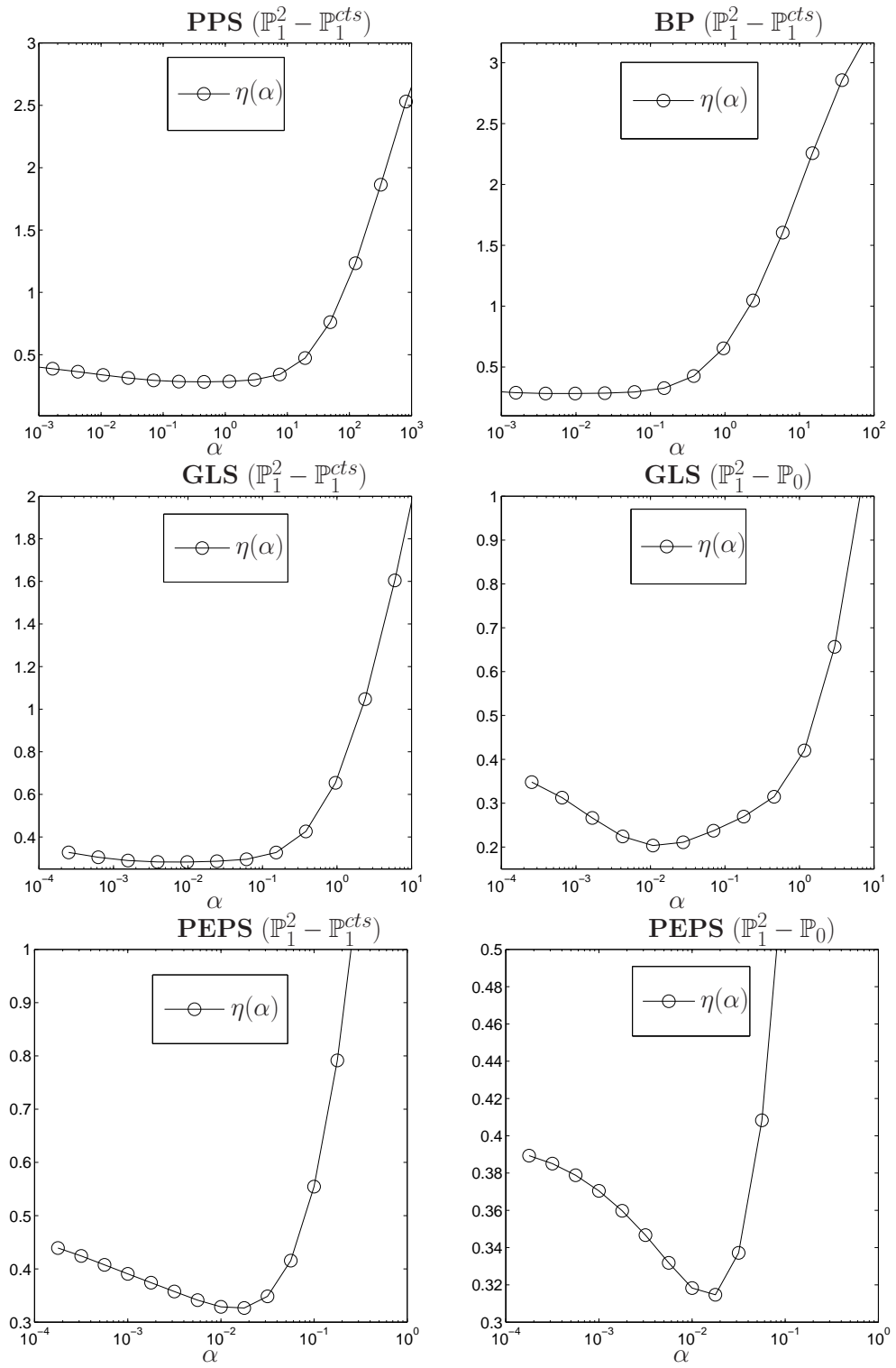


Figure 6.5: Accuracy for different values of α using mesh T-(d) from Figure 6.2, for Example 2.

by solving the trust region problem

$$\min_{s \in (-\Delta_k, \Delta_k)} m(\chi_k + s).$$

Compute $\eta(\chi_k + s_k)$ and define

$$\rho_k = \frac{\eta(\chi_k) - \eta(\chi_k + s_k)}{m(\chi_k) - m(\chi_k + s_k)}.$$

If $\rho_k \geq \text{tol}_1$ or if both $\rho_k \geq \text{tol}_0$ and the model is fully-quadratic, then the new iterate $\chi_{k+1} = \chi_k + s_k$ replaces the sample point with the largest value of η , resulting in a new sample set α_{k+1} from which we obtain a new fully-quadratic model $m_{k+1}(\alpha)$; otherwise use the model-improvement algorithm (Algorithm 6.2 from [54]) and define $m_{k+1}(\alpha)$ to be the (possibly improved) model.

Update the trust-region radius as follows. Set

$$\Delta_{k+1} \in \begin{cases} \{\min\{\omega_1 \Delta_k, \Delta_{max}\}\} & \text{if } \rho_k \geq \text{tol}_1 \text{ and } \Delta_k < \Lambda \mathcal{D}_k(\chi_k), \\ [\Delta_k, \min\{\omega_1 \Delta_k, \Delta_{max}\}] & \text{if } \rho_k \geq \text{tol}_1 \text{ and } \Delta_k \geq \Lambda \mathcal{D}_k(\chi_k), \\ \{\omega_0 \Delta_k\} & \text{if } \rho_k < \text{tol}_1 \text{ and } m_k \text{ is fully-quadratic,} \\ \{\Delta_k\} & \text{if } \rho_k < \text{tol}_1 \text{ and } m_k \text{ is not fully-quadratic.} \end{cases}$$

Take $\alpha_{opt} = \arg \min\{\eta(\alpha) : \alpha \in \alpha_{k+1}\}$, increment k and repeat the algorithm.

In Figures 6.6 and 6.7 the DFO search is presented for just the **GLS** ($\mathbb{P}_1^2 - \mathbb{P}_1^{cts}$) and **PEPS** ($\mathbb{P}_1^2 - \mathbb{P}_0$) methods, using the fixed meshes S-(c) and S-(d) from Figure 6.1 and mesh T-(d) from Figure 6.2, where for each iteration we show the upgraded sample set until it has converged to the best approximation of the optimal value of the stabilization parameter, which later will be denoted by α_{opt} .

Finally for Examples 1 and 2, we perform the DFO algorithm on meshes S-(a) to S-(d) and meshes T-(a) to T-(d) from Figure 6.2 (which we obtained by refining about the re-entrant corners), respectively. We measure the gain using the best approximation α_{opt} of the optimal value for the stabilization parameter compared with the recommended value α_{rec} , by calculating the percentage gain, i.e.

$$\mathcal{G} = 100 \frac{\eta(\alpha_{rec}) - \eta(\alpha_{opt})}{\eta(\alpha_{rec})} \%.$$

All the findings of performing the DFO search on fixed meshes are shown in Table 6.2, where we present the percentage gains \mathcal{G} and the approximations of the optimal value for the stabilization parameter α_{opt} .

Notice that the optimal value of α in general differs from the recommended a priori choice α_{rec} . Moreover we can see that the optimal value can be quite different from one problem to

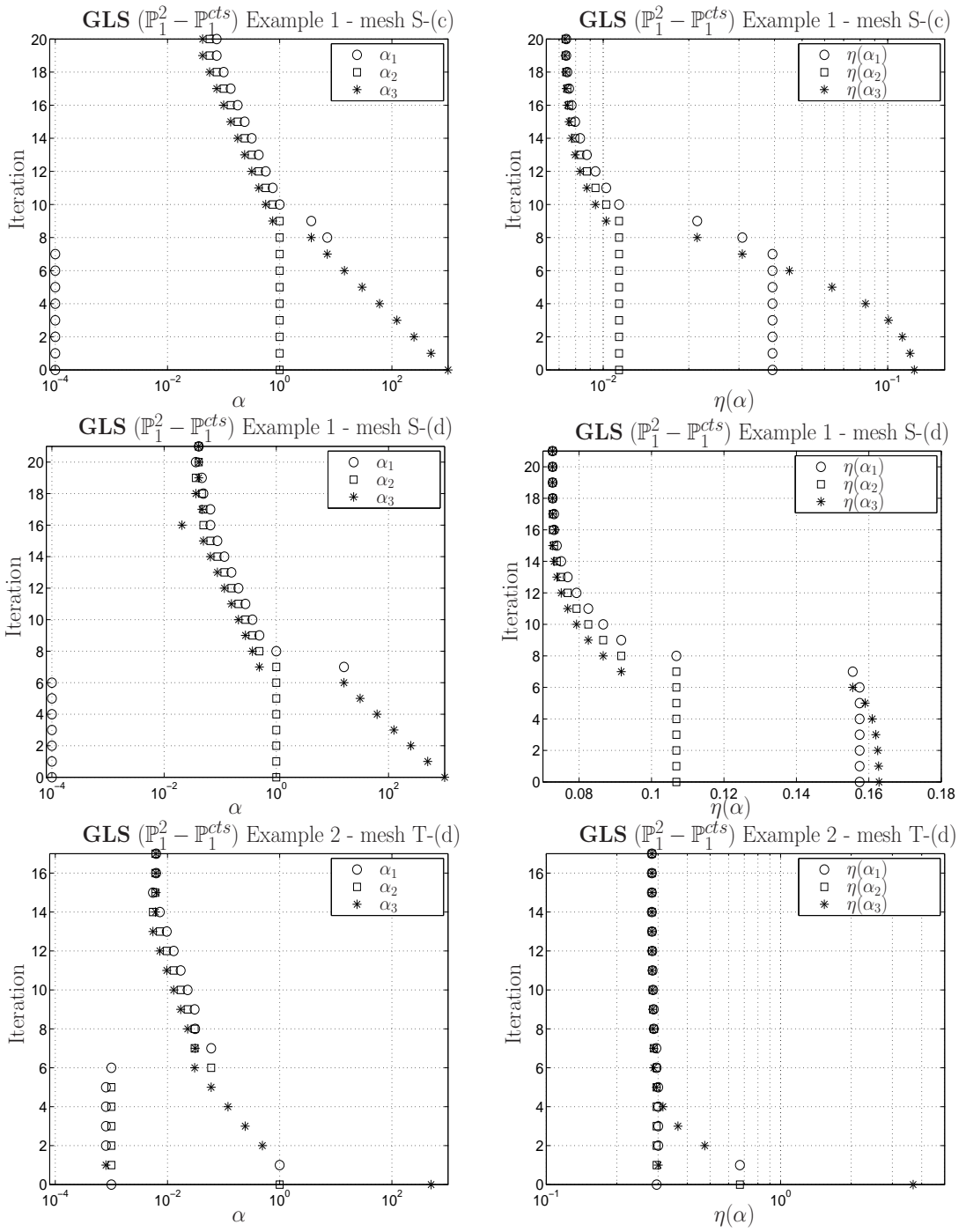


Figure 6.6: DFO search for Examples 1 and 2 using the $\mathbf{GLS}(\mathbb{P}_1^2 - \mathbb{P}_1^{cts})$ method and fixed meshes S-(c), S(d) and T(d).

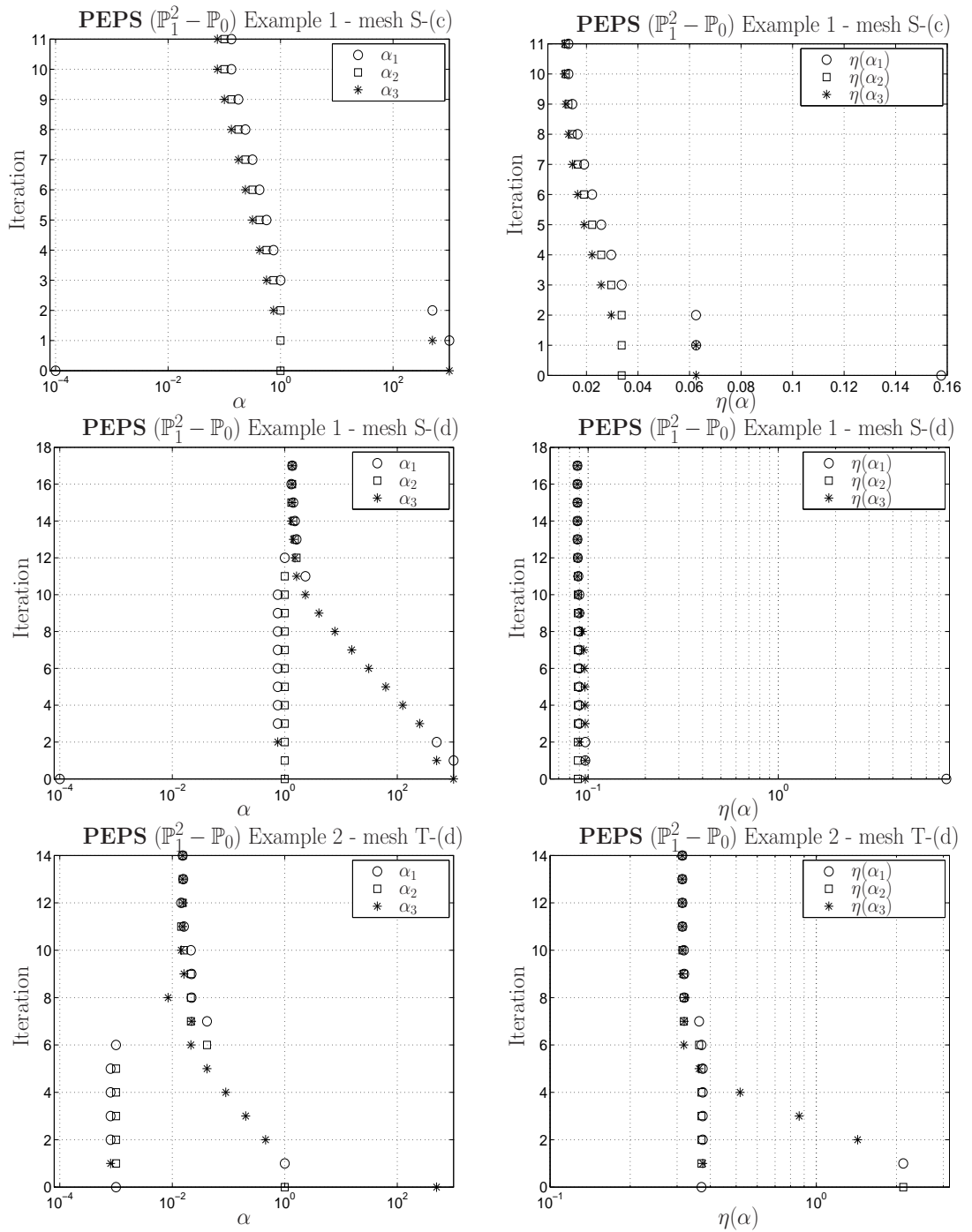


Figure 6.7: DFO search for Examples 1 and 2 using the **PEPS** ($\mathbb{P}_1^2 - \mathbb{P}_0$) method and fixed meshes S-(c), S(d) and T(d).

Mesh	PPS		BP		GLS		GLS		PEPS		PEPS	
	$(\mathbb{P}_1^2 - \mathbb{P}_1^{cts})$		$(\mathbb{P}_1^2 - \mathbb{P}_1^{cts})$		$(\mathbb{P}_1^2 - \mathbb{P}_1^{cts})$		$(\mathbb{P}_1^2 - \mathbb{P}_0)$		$(\mathbb{P}_1^2 - \mathbb{P}_1^{cts})$		$(\mathbb{P}_1^2 - \mathbb{P}_0)$	
	$\alpha_{rec} = 1$		$\alpha_{rec} = 1$		$\alpha_{rec} = 1/24$		$\alpha_{rec} = 1/24$		$\alpha_{rec} = 1$		$\alpha_{rec} = 1$	
	\mathcal{G}	α_{opt}	\mathcal{G}	α_{opt}	\mathcal{G}	α_{opt}	\mathcal{G}	α_{opt}	\mathcal{G}	α_{opt}	\mathcal{G}	α_{opt}
S-(a)	2.1	3.2176	16.4	0.0648	0.19	0.0308	5.1	0.2052	47.9	0.1336	43.4	0.1234
S-(b)	0.02	1.2938	14	0.0325	0.8	0.0176	0.1	0.061	67.3	0.036	70.6	0.0019
S-(c)	1.025	4.42	10.9	0.0636	10^{-6}	0.0423	0.83	0.1781	69.14	0.0752	65.9	0.0752
S-(d)	8.5	7.6146	9.6	0.1781	10^{-4}	0.0413	18.5	0.6649	1.9	0.7005	0.55	1.3519
T-(a)	8.3	0.1953	50.75	0.0025	15.7	0.0032	14.2	0.0089	72.9	0.0217	79.9	0.0188
T-(b)	1.5	0.3189	56.6	0.005	3.9	0.005	8.57	0.0129	84.1	0.0146	84.8	0.0149
T-(c)	0.78	0.4039	56.89	0.0074	2.32	0.0055	8.2	0.0133	84.2	0.015	85.03	0.0146
T-(d)	0.94	0.4219	57.9	0.0062	3.25	0.0062	9.5	0.0127	84.6	0.0146	85.1	0.0153

Table 6.2: Percentage gain \mathcal{G} and α_{opt} , for Examples 1 and 2 using fixed meshes S- and T-, respectively.

another and that we always gain by searching for the optimal value, particularly when the mesh is irregular or the true solution is non-smooth.

6.2 Selection of the stabilization parameter on a sequence of adaptively refined meshes.

The results in the previous section are concerned with fixed meshes. We now apply the approach in the context of an adaptive mesh refinement procedure, driven using the local error indicator

$$\eta_K^2(\alpha) = \Phi_{c,K}^2(\vartheta_K, \beta_K) + \nu^2 \Phi_{nc,K}^2 + (\Phi_{c,K}(0, \beta_K) + \nu \Phi_{nc,K})^2, \quad (6.2)$$

where $\Phi_{c,K}(\cdot, \cdot)$ is given by (5.45) and $\Phi_{nc,K}$ is given by (5.54).

Ideally, one would optimize over α on every mesh constructed throughout the adaptive refinement procedure. In practice, the cost of such a procedure would be prohibitive and, fortunately, is unnecessary. Instead we propose to optimize the choice of α *once* on the initial mesh, and then retain this value on all the subsequent adaptively refined meshes. In Figures 6.8, 6.9 and 6.10 we present the results obtained using both the *Idealised algorithm* and the proposed *Practical algorithm* from Table 6.3, to approximate the same examples considered in the previous section.

Idealised algorithm:

Adaptive mesh refinement and DFO search [IA-AMR-DFO-S].

- 1:** Construct mesh $\mathcal{P}_{(0)}$. Set $i = 0$.
 - 2:** Performing the DFO algorithm on the fixed mesh $\mathcal{P}_{(i)}$, compute $\alpha_{opt}^{(i)}$.
 - 3:** For each element K in $\mathcal{P}_{(i)}$, compute a local error indicator $\eta_K(\alpha_{opt}^{(i)})$, using the AMRA-S algorithm from Table 5.2.
 - 4:** Triangle K is marked for refinement if

$$\eta_K(\alpha_{opt}^{(i)}) \geq \frac{1}{2} \max_{K \in \mathcal{P}_{(i)}} \eta_K(\alpha_{opt}^{(i)}).$$
 - 5:** From step 4 deduce a new mesh using longest edge bisection refinement.
 - 6:** Set $i \leftarrow i + 1$ and return to step 2.
-

Practical algorithm:.

Adaptive mesh refinement and DFO search [PA-AMR-DFO-S].

- 1:** Construct mesh $\mathcal{P}_{(0)}$.
 - 2:** Performing the DFO algorithm on the fixed mesh $\mathcal{P}_{(0)}$, compute $\alpha_{opt}^{(0)}$ and set $i = 0$.
 - 3:** For each element K in $\mathcal{P}_{(i)}$, compute a local error indicator $\eta_K(\alpha_{opt}^{(0)})$, using the AMRA-S algorithm from Table 5.2.
 - 4:** Triangle K is marked for refinement if

$$\eta_K(\alpha_{opt}^{(0)}) \geq \frac{1}{2} \max_{K \in \mathcal{P}_{(i)}} \eta_K(\alpha_{opt}^{(0)}).$$
 - 5:** From step 4 deduce a new mesh using longest edge bisection refinement.
 - 6:** Set $i \leftarrow i + 1$ and return to step 3.
-

Table 6.3: Idealised and practical algorithms for adaptive mesh refinement and DFO search for the Stokes problem.

For Examples 1 and 2, we obtain the accuracy and effectivity indices, starting the algorithms using mesh $S_{(0)}$ and $T_{(0)}$ from Figure 5.2, respectively.

The results obtained show that the performance of both algorithms is virtually identical, indicating that the optimal choice of α changes little from the value obtained based on the initial coarse mesh.

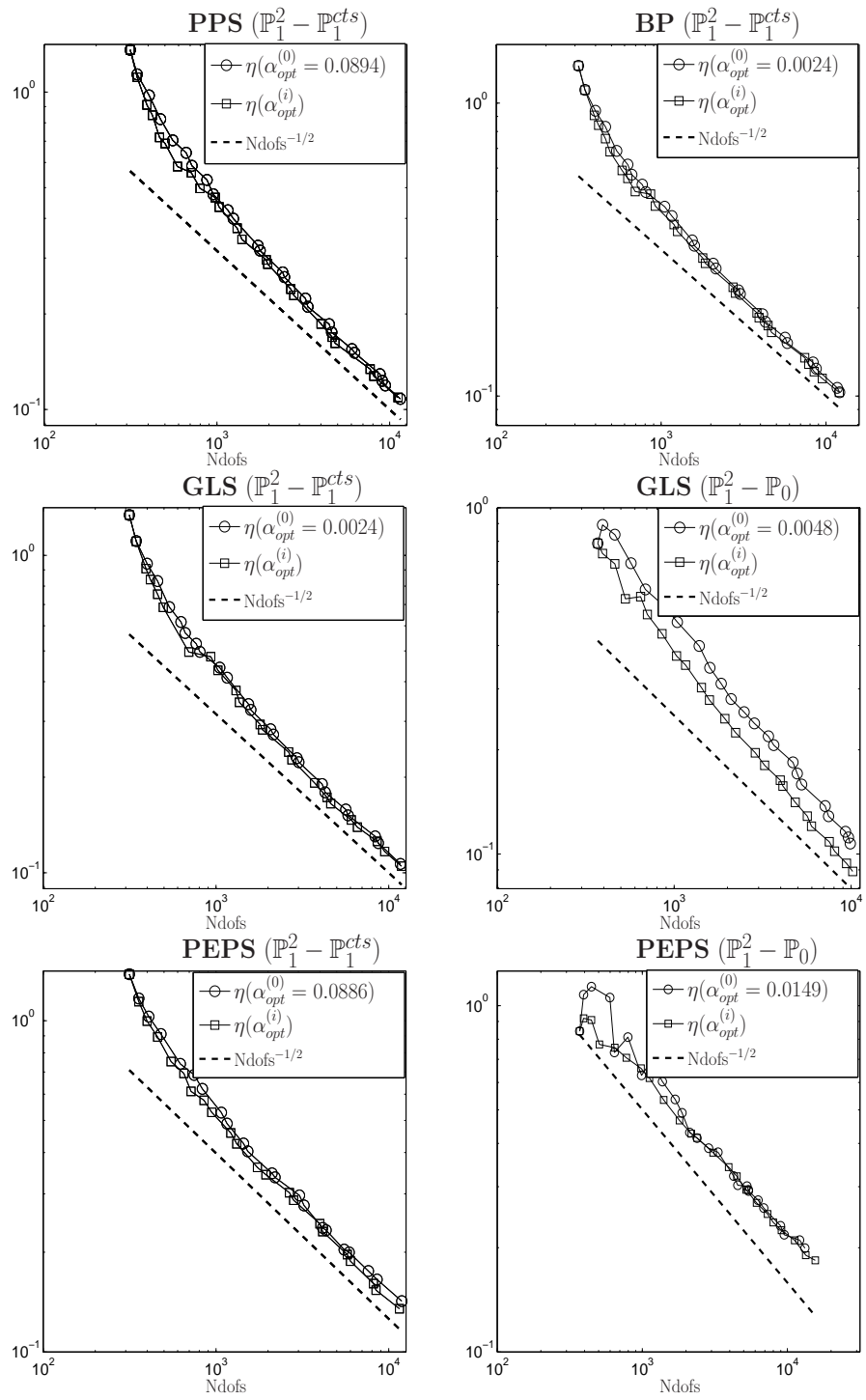


Figure 6.8: Accuracy using the IA-AMR-DFO-S and PA-AMR-DFO-S algorithms (see Table 6.3), for Example 2.

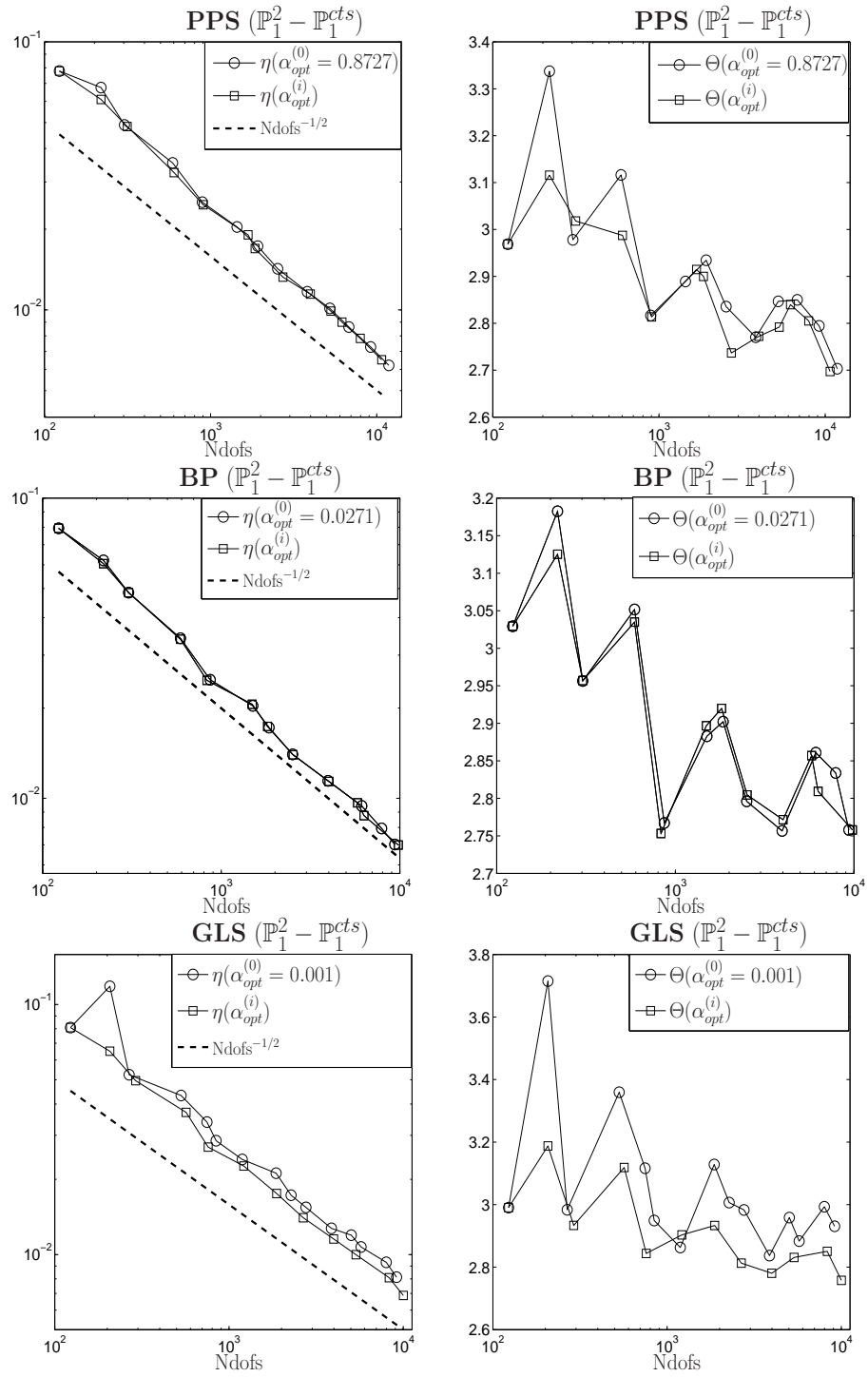


Figure 6.9: Accuracy and effectivity indices using the IA-AMR-DFO-S and PA-AMR-DFO-S algorithms (see Table 6.3), for Example 1.

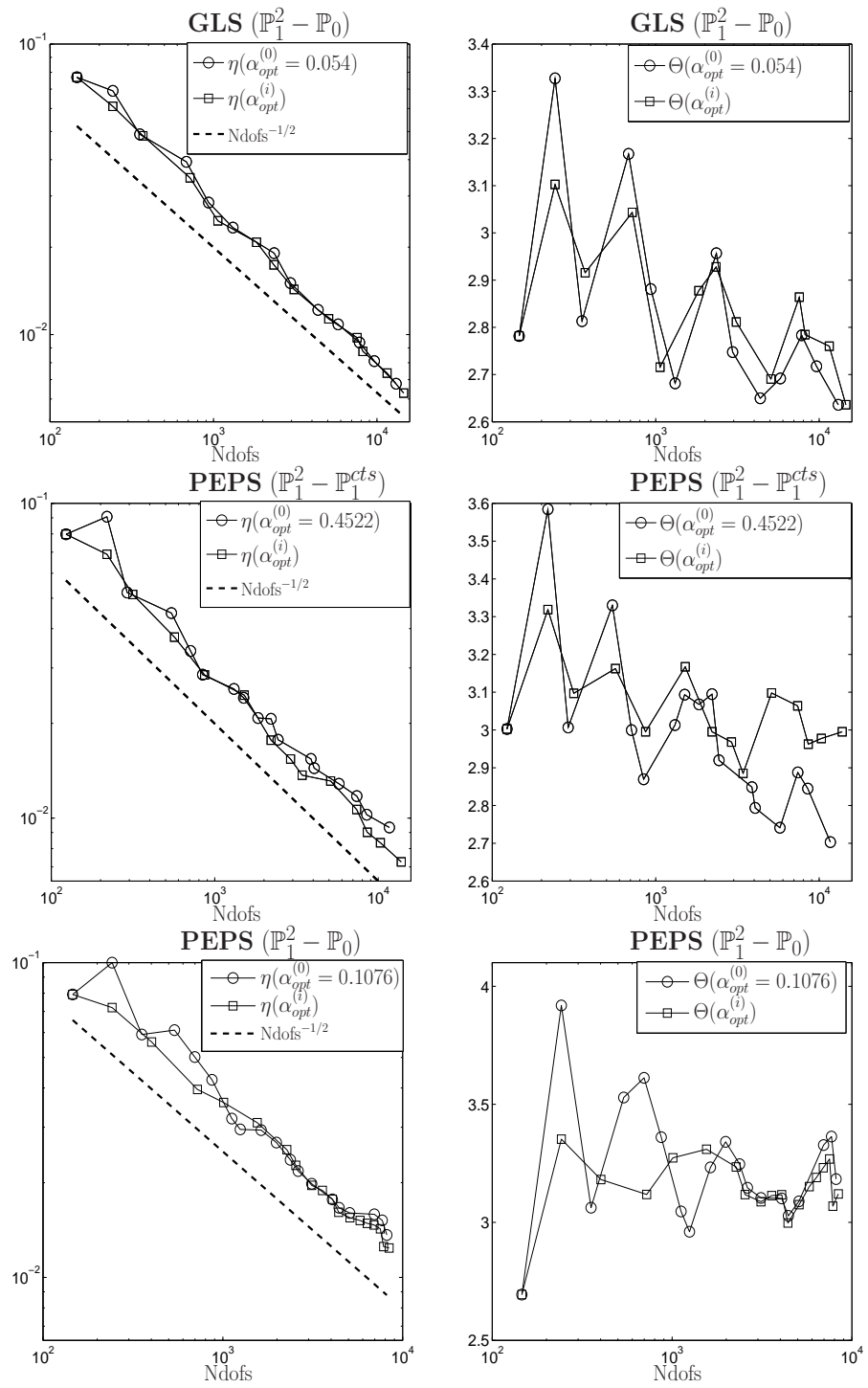


Figure 6.10: Accuracy and effectivity indices using the IA-AMR-DFO-S and PA-AMR-DFO-S algorithms (see Table 6.3), for Example 1.

6.3 Conclusions

A systematic approach was developed for the selection of the stabilization parameter for stabilized finite element approximation of the Stokes problem, whereby the parameter is chosen to minimize a computable upper bound for the error in the approximation. The approach is applied in the context of both a single, fixed, mesh and for an adaptive mesh refinement procedure. The optimization is carried out by a derivative free optimization algorithm (DFO) and is based on minimizing a new fully computable error estimator. Numerical results were presented illustrating the theory and the performance of the estimator together with the optimization algorithm.

Chapter 7

Application of the equilibrated residual method to an Advection-Reaction-Diffusion problem.

The numerical solution of an advection-reaction-diffusion equation using a standard Galerkin formulation usually yields inaccurately approximated solutions. This disappointing behaviour occurs because such methods lose stability and cannot adequately approximate solutions inside layers. For over more than two decades, a variety of finite element approaches have been proposed to overcome such situations. In general these methods add mesh-dependent terms to the weighting functions with the aim of getting an oscillation-free solution (see [18, 19, 39, 46, 48, 49, 53, 72, 73, 76, 81, 98] and the references therein). More recently, many a posteriori error estimator are being developed for different numerical schemes (see [19, 23–25, 47, 91, 99, 104]). However, the majority of these estimators obtained are not actually computable since they involve either a generic unknown constant or the solution of (local) infinite dimensional Dirichlet or Neumann problems (which cannot be solved exactly). In [36, 105] a posteriori error estimators were developed which are robust with respect to the physical parameters, but as with the previous cited references, they do not provide a guaranteed upper bound and the norm used to estimate the

error is in a norm that incorporates the standard energy norm and a dual norm of the convective derivative or depend strongly on the physical parameters of the equation, respectively. More recently, in [106] a fully computable a posteriori error estimator was derived in the framework of a nonconforming finite element approximation, where the local efficiency depends on the local Péclet number in two and three dimensions and similar results were obtained in [70] but in the framework of discontinuous Galerkin finite element approximations.

This chapter is devoted to the application of the equilibrated residual method, discussed in the previous three chapters, to an advection-reaction-diffusion problem using a conforming finite element approximation, for which our main interest is in low-order residual-based stabilized finite element approximations (cf. Section 3, Part III in [98]), in which case we will develop a fully computable a posteriori error estimator in the two and three-dimensional cases.

7.1 Preliminaries.

Let $\Omega \subset \mathbb{R}^d$, be a simple polygonal domain when $d = 2$ and a polyhedral domain when $d = 3$, with boundary Γ . Consider a family of partitions \mathcal{P} of the domain into the union of nonoverlapping, shape-regular triangular ($d = 2$) or tetrahedral ($d = 3$) elements in the sense of Ciarlet (cf. [52]).

When $d = 3$, for scalar functions $v = v(x, y, z)$, we let the gradient operator to be defined by

$$\nabla v = \left(\frac{\partial v}{\partial x}, \frac{\partial v}{\partial y}, \frac{\partial v}{\partial z} \right).$$

For vector valued functions $\mathbf{v} = [v_1(x, y, z), v_2(x, y, z), v_3(x, y, z)]$, we let the divergence and gradient operators be defined by

$$\mathbf{div} \mathbf{v} = \nabla \cdot \mathbf{v} = \frac{\partial v_1}{\partial x} + \frac{\partial v_2}{\partial y} + \frac{\partial v_3}{\partial z} \quad \text{and} \quad \nabla \mathbf{v} = \begin{bmatrix} \frac{\partial v_1}{\partial x} & \frac{\partial v_1}{\partial y} & \frac{\partial v_1}{\partial z} \\ \frac{\partial v_2}{\partial x} & \frac{\partial v_2}{\partial y} & \frac{\partial v_2}{\partial z} \\ \frac{\partial v_3}{\partial x} & \frac{\partial v_3}{\partial y} & \frac{\partial v_3}{\partial z} \end{bmatrix},$$

respectively.

Trough this chapter, in the case of a polygonal domain, we keep the notation related to the triangulation of the domain from Section 2.1.1. In the case $d = 3$, for a fixed partition, let:

- \mathcal{F} denote the set of all faces;
- $\mathcal{F}_I \subset \mathcal{F}$ denote the set of internal faces;
- $\mathcal{F}_\Gamma \subset \mathcal{F}$ denote the set of boundary faces;

- \mathcal{V} index the set $\{\mathbf{x}_n\}_{n \in \mathcal{V}}$ of all element vertices;
- $\Omega_n = \{K \in \mathcal{P} : \mathbf{x}_n \in \overline{K} \text{ for a fixed } n \in \mathcal{V}\}$ is the patch consisting of elements K for which \mathbf{x}_n is a vertex;
- \mathcal{F}_n denotes the set of faces that have \mathbf{x}_n as a vertex;
- \mathbf{n}_Γ denote the unit outer normal vector to Γ ;
- λ_n denote the function which is piecewise linear on \mathcal{P} and vanishes at all the vertices in \mathcal{P} , except \mathbf{x}_n , where it takes the value one, i.e. $\lambda_n(\mathbf{x}_m) = \delta_{nm}$ with $n, m \in \mathcal{V}$ and δ_{nm} denote the Kronecker symbol.

For a tetrahedron K , let:

- $\mathbb{P}_n(K)$ denote the space of polynomials on K of total degree at most n ;
- \mathcal{V}_K index the set $\{\mathbf{x}_n\}_{n \in \mathcal{V}_K}$ of all the vertices of the element K ;
- Ω_K denotes the set of elements that share a face with element K ;
- $\tilde{\Omega}$ denotes the set of elements that share a face or a vertex with element K ;
- \mathcal{F}_K denote the set containing the individual faces of element K ;
- $|K|$ denote the volume of the element K ;
- h_K denote the length of the longest edge of element K ;
- $\hat{\mathbf{n}}_\gamma^K$ denote the unit exterior normal vector to the face $\gamma \in \mathcal{F}_K \subset \partial K$;
- $v|_K$ denote the restriction of v to the element K ;
- $\bar{\mathbf{x}}_K = \frac{1}{4} \sum_{i \in \mathcal{V}_K} \mathbf{x}_i$.

For a face $\gamma \in \mathcal{F}$, let:

- $\mathbb{P}_n(\gamma)$ denote the space of polynomials on γ of total degree at most n ;
- \mathcal{V}_γ index the set $\{\mathbf{x}_n\}_{n \in \mathcal{V}_\gamma}$ of all the vertices of the face γ ;
- $\Omega_\gamma = \{K \in \mathcal{P} : \gamma \in \mathcal{F}_K\}$;
- $|\gamma|$ denote the area of the face γ ;

- $v|_\gamma$ denote the restriction of v to the face γ .

Remark 7.1.1. Notice that we keep a very similar notation as the one use in the two-dimensional case, and the reason to do that is just because the analysis, that will be just presented in the three-dimensional case, follows very similar arguments and constructions from all the previous chapters.

Notice that the projection operator Π_K is defined in the three-dimensional case as the one in (2.1) and Theorem 2.1.1 also holds when $d = 3$.

For $K \in \mathcal{P}$, throughout we shall make use of the following formula:

$$(\lambda_i^a \lambda_j^b \lambda_k^c \lambda_l^d, 1)_K = \frac{6(a!b!c!d!)}{(a+b+c+d+3)!} |K|, \quad (7.1)$$

for $a, b, c, d \geq 0$ and $\mathcal{V}_K = \{i, j, k, l\}$ and, with $\mathcal{V}_\gamma = \{i, j, k\}$, for $a, b, c \geq 0$,

$$(\lambda_i^a \lambda_j^b \lambda_k^c, 1)_\gamma = \frac{2(a!b!c!)}{(a+b+c+2)!} |\gamma|. \quad (7.2)$$

The following result presents a basis to polynomial functions of degree one defined on faces of the partition.

Lemma 7.1.2. Any polynomial function $p \in \mathbb{P}_1(\gamma)$ can be written as

$$p = (p, \lambda_1)_\gamma \frac{3}{|\gamma|} (3\lambda_1 - \lambda_2 - \lambda_3) + (p, \lambda_2)_\gamma \frac{3}{|\gamma|} (3\lambda_2 - \lambda_1 - \lambda_3) + (p, \lambda_3)_\gamma \frac{3}{|\gamma|} (3\lambda_3 - \lambda_1 - \lambda_2), \quad (7.3)$$

where $\mathcal{V}_\gamma = \{1, 2, 3\}$.

Proof. Let $p = \alpha_1 \lambda_1 + \alpha_2 \lambda_2 + \alpha_3 \lambda_3$, where α_1, α_2 and α_3 are constant to be determined. Now, the unknowns satisfy the conditions

$$(\lambda_1, \lambda_1)_\gamma \alpha_1 + (\lambda_2, \lambda_1)_\gamma \alpha_2 + (\lambda_3, \lambda_1)_\gamma \alpha_3 = (p, \lambda_1)_\gamma,$$

$$(\lambda_1, \lambda_2)_\gamma \alpha_1 + (\lambda_2, \lambda_2)_\gamma \alpha_2 + (\lambda_3, \lambda_2)_\gamma \alpha_3 = (p, \lambda_2)_\gamma,$$

$$(\lambda_1, \lambda_3)_\gamma \alpha_1 + (\lambda_2, \lambda_3)_\gamma \alpha_2 + (\lambda_3, \lambda_3)_\gamma \alpha_3 = (p, \lambda_3)_\gamma.$$

Equally well,

$$\mathbf{M}_\gamma \begin{bmatrix} \alpha_1 \\ \alpha_2 \\ \alpha_3 \end{bmatrix} = \begin{bmatrix} (p, \lambda_1)_\gamma \\ (p, \lambda_2)_\gamma \\ (p, \lambda_3)_\gamma \end{bmatrix},$$

where \mathbf{M}_γ is the mass matrix for the basis functions on the face γ . A simple computation using (7.2) shows that

$$\mathbf{M}_\gamma = \frac{|\gamma|}{12} \begin{bmatrix} 2 & 1 & 1 \\ 1 & 2 & 1 \\ 1 & 1 & 2 \end{bmatrix},$$

and hence

$$\begin{aligned} \alpha_1 &= \frac{3}{|\gamma|} (3(p, \lambda_1)_\gamma - (p, \lambda_2)_\gamma - (p, \lambda_3)_\gamma), \\ \alpha_2 &= \frac{3}{|\gamma|} (3(p, \lambda_2)_\gamma - (p, \lambda_1)_\gamma - (p, \lambda_3)_\gamma), \\ \alpha_3 &= \frac{3}{|\gamma|} (3(p, \lambda_3)_\gamma - (p, \lambda_1)_\gamma - (p, \lambda_2)_\gamma), \end{aligned}$$

which prove the result. \square

Also notice that for the bubble function arguments, Theorems 2.1.2 and 2.1.3 hold unchanged.

In trying to obtain a fully computable quantity being equivalent to the error (up to higher order terms) in the three-dimensional case, for each element $K \in \mathcal{P}$, a Neumann problem also need to be solved, i.e, we will need the solution of the following problem: *Find $\boldsymbol{\sigma}_K$ such that,*

$$\begin{aligned} -\operatorname{div} \boldsymbol{\sigma}_K &= p_K & \text{in } K \\ \boldsymbol{\sigma}_K \cdot \hat{\mathbf{n}}_\gamma^K &= p_{\gamma,K} & \text{on each } \gamma \in \mathcal{F}_K, \end{aligned} \tag{7.4}$$

for given $p_K \in \mathbb{P}_1(K)$ and $p_{\gamma,K} \in \mathbb{P}_1(\gamma)$. To be able to obtain such solutions, the following functions will be useful. Let the vertices, faces and unit normal vectors of an element $K \in \mathcal{P}$ be labelled as in Figure 7.1.

Let $i, j, k, l \in \mathcal{V}_K = \{1, 2, 3, 4\}$ be distinct and define

$$\mathbf{t}_{ij} = \mathbf{x}_j - \mathbf{x}_i,$$

then the normal vectors for the element K satisfy,

$$|\gamma_i| \hat{\mathbf{n}}_i \cdot \mathbf{t}_{ij} = 3|K|, \quad |\gamma_i| \hat{\mathbf{n}}_i \cdot \mathbf{t}_{ji} = -3|K| \quad \text{and} \quad \hat{\mathbf{n}}_i \cdot \mathbf{t}_{jk} = 0, \tag{7.5}$$

and the piecewise linear functions λ satisfy

$$\sum_{i \in \mathcal{V}_K} \lambda_i = 1, \quad \sum_{i \in \mathcal{V}_\gamma} \lambda_i|_\gamma = 1 \quad \text{and} \quad \nabla \lambda_i = -\frac{|\gamma_i|}{3|K|} \hat{\mathbf{n}}_i. \tag{7.6}$$

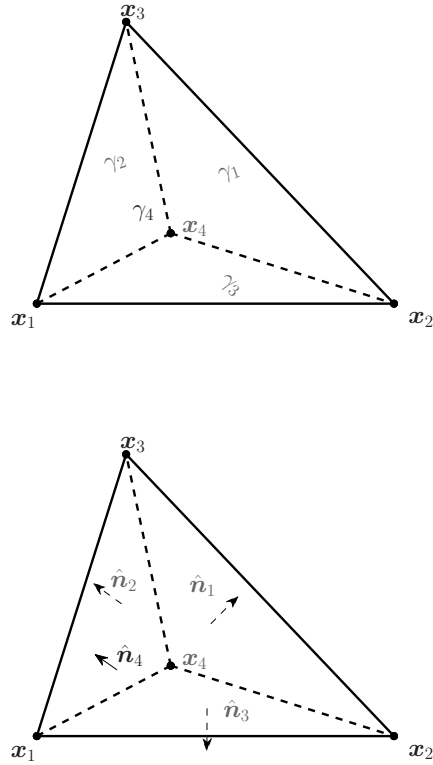


Figure 7.1: The labelling and positioning of the vertices, faces and unit normal vectors of element K . The face γ_i of a tetrahedral element K lies opposite to the vertex x_i and \hat{n}_i is the outer unit normal vector to face γ_i , for $i \in \mathcal{V}_K = \{1, 2, 3, 4\}$.

For the element K , let

$$\begin{aligned} \psi_{i,j} = \frac{1}{4|K|} & \left((12\lambda_j + 19\lambda_k + 19\lambda_l - 2\lambda_i)\lambda_j t_{ij} \right. \\ & + (3\lambda_i - 4\lambda_k - 4\lambda_l - 11\lambda_j)\lambda_k t_{ik} \\ & \left. + (3\lambda_i - 4\lambda_k - 4\lambda_l - 11\lambda_j)\lambda_l t_{il} \right), \end{aligned} \quad (7.7)$$

and

$$\psi_{K,i} = -\frac{1}{4|K|} \lambda_i (\lambda_j t_{ij} + \lambda_k t_{ik} + \lambda_l t_{il}). \quad (7.8)$$

Then, for $m, n \in \mathcal{V}_K = \{1, 2, 3, 4\}$, using (7.1), (7.2), (7.5) and (7.6), we deduce that

$$\begin{aligned} -\mathbf{div} \boldsymbol{\psi}_{i,j} &= -\frac{1}{|K|}, \\ \left(\mathbf{div} \boldsymbol{\psi}_{i,j}, \lambda_m - \frac{1}{4} \right)_K &= 0, & -\mathbf{div} \boldsymbol{\psi}_{K,i} &= \frac{1}{|K|} \left(\lambda_i - \frac{1}{4} \right), \\ \left(\boldsymbol{\psi}_{i,j} \cdot \hat{\mathbf{n}}_m, \lambda_n \right)_{|\gamma_m} &= \delta_{im} \delta_{jn}, & \left(\boldsymbol{\psi}_{K,i} \cdot \hat{\mathbf{n}}_m \right)_{|\gamma_m} &= 0, \end{aligned} \quad (7.9)$$

and

$$\|\boldsymbol{\psi}_{i,j}\|_{L^2(K)} \leq Ch_K^{-1/2}, \quad \|\boldsymbol{\psi}_{K,i}\|_{L^2(K)} \leq Ch_K^{-1/2}. \quad (7.10)$$

where the constant C does not depend on any size of the element K . With these functions we can give some explicit solutions to the Neumann problem (7.4), if the element and boundary data satisfy the following compatibility condition

$$(p_K, c)_K + \sum_{\gamma \in \mathcal{F}_K} (p_{\gamma,K}, c) = 0 \quad \text{for any } c \in \mathbb{R}. \quad (7.11)$$

The next result provides some particular solutions to (7.4) based on the functions previously presented.

Theorem 7.1.3. *Let $p_K \in \mathbb{P}_1(K)$ and $p_{\gamma,K} \in \mathbb{P}_1(\gamma)$ for each $\gamma \in \mathcal{F}_K$ be given. If p_K and $p_{\gamma,K}$ satisfy (7.11), then*

$$\begin{aligned} \boldsymbol{\sigma}_K = \sum_{i=1}^4 \left(& (p_{\gamma_i,K}, \lambda_{i+1})_{\gamma_i} \boldsymbol{\psi}_{i,i+1} + (p_{\gamma_i,K}, \lambda_{i+2})_{\gamma_i} \boldsymbol{\psi}_{i,i+2} + (p_{\gamma_i,K}, \lambda_{i+3})_{\gamma_i} \boldsymbol{\psi}_{i,i+3} \right. \\ & \left. + (|K| \nabla(p_K) \cdot (\mathbf{x}_i - \bar{\mathbf{x}}_K)) \boldsymbol{\psi}_{K,i} \right), \end{aligned} \quad (7.12)$$

is a solution to (7.4) and

$$\|\boldsymbol{\sigma}_K\|_{L^2(K)} \leq C \left(h_K \|p_K\|_{L^2(K)} + \sum_{\gamma \in \mathcal{F}_K} h_K^{1/2} \|p_{\gamma,K}\|_{L^2(\gamma)} \right). \quad (7.13)$$

where $i \in \mathcal{V}_K = \{1, 2, 3, 4\}$, the indices are to be understood module 4 and the constant C is independent of h_K , p_K and $p_{\gamma,K}$.

Proof. Let $i, m, n \in \mathcal{V}_K = \{1, 2, 3, 4\}$, then for any $\gamma_k \in \mathcal{F}_K$ let us restrict $\boldsymbol{\sigma}_K$, given by (7.12), to the face γ_m to then be multiply by $\hat{\mathbf{n}}_{\gamma_m}^K$ and then integrated against a barycentric coordinate

λ_n over the face λ_m . Then using (7.9), it follows that

$$\begin{aligned}
& (\boldsymbol{\sigma}_K \cdot \hat{\mathbf{n}}_{\gamma_m}^K, \lambda_n)_{\gamma_m} \\
&= \sum_{i=1}^4 \left((p_{\gamma_i, K}, \lambda_{i+1})_{\gamma_i} (\boldsymbol{\psi}_{i, i+1} \cdot \hat{\mathbf{n}}_{\gamma_m}^K, \lambda_n)_{\gamma_m} + (p_{\gamma_i, K}, \lambda_{i+2})_{\gamma_i} (\boldsymbol{\psi}_{i, i+2} \cdot \hat{\mathbf{n}}_{\gamma_m}^K, \lambda_n)_{\gamma_m} \right. \\
&\quad \left. + (p_{\gamma_i, K}, \lambda_{i+3})_{\gamma_i} (\boldsymbol{\psi}_{i, i+3} \cdot \hat{\mathbf{n}}_{\gamma_m}^K, \lambda_n)_{\gamma_m} + (|K| \nabla(p_K) \cdot (\mathbf{x}_i - \bar{\mathbf{x}}_K)) (\boldsymbol{\psi}_{K, i} \cdot \hat{\mathbf{n}}_{\gamma_m}^K, \lambda_n)_{\gamma_m} \right) \\
&= (p_{\gamma_m, K}, \lambda_{m+1})_{\gamma_m} \delta_{m+1, n} + (p_{\gamma_m, K}, \lambda_{m+2})_{\gamma_m} \delta_{m+2, n} + (p_{\gamma_m, K}, \lambda_{m+3})_{\gamma_m} \delta_{m+3, n},
\end{aligned}$$

hence

$$(\boldsymbol{\sigma}_K \cdot \hat{\mathbf{n}}_m^K, \lambda_n)_{\gamma_m} = (p_{\gamma_m, K}, \lambda_n)_{\gamma_m} \quad \text{for any } n \in \mathcal{V}_{\gamma_m},$$

then $\boldsymbol{\sigma}_K \cdot \hat{\mathbf{n}}_m^K = p_{\gamma_m, K}$ in γ_m . Now, regarding the divergence, again using (7.9), we obtain

$$\begin{aligned}
& -\operatorname{div} \boldsymbol{\sigma}_K \\
&= \sum_{i=1}^4 \left(\frac{1}{|K|} (p_{\gamma_i, K}, 1)_{\gamma_i} + \nabla(p_K) \cdot (\mathbf{x}_i - \bar{\mathbf{x}}_K) \left(\lambda_i - \frac{1}{4} \right) \right) \\
&= \frac{1}{|K|} (p_K, 1)_K + \nabla(p_K) \cdot (\mathbf{x} - \bar{\mathbf{x}}_K) \\
&= p_K,
\end{aligned}$$

upon using (7.11) and the fact that p_K is an affine function. Now, for the norm of $\boldsymbol{\sigma}_K$ we obtain

$$\begin{aligned}
& \|\boldsymbol{\sigma}_K\|_{L^2(K)}^2 \\
&\leq C \sum_{i=1}^4 \|p_{\gamma_i, K}\|_{L^2(\gamma_i)}^2 \left(\|\lambda_{i+1}\|_{L^2(\gamma_i)}^2 \|\boldsymbol{\psi}_{i, i+1}\|_{L^2(K)}^2 + \|\lambda_{i+2}\|_{L^2(\gamma_i)}^2 \|\boldsymbol{\psi}_{i, i+2}\|_{L^2(K)}^2 \right. \\
&\quad \left. + \|\lambda_{i+3}\|_{L^2(\gamma_i)}^2 \|\boldsymbol{\psi}_{i, i+3}\|_{L^2(K)}^2 \right) + |K| \|\nabla(p_K)\|_{L^2(K)}^2 |\mathbf{x}_i - \bar{\mathbf{x}}_K|^2 h_K^{-1} \\
&\leq C \left(h_K^2 \|p_K\|_{L^2(K)}^2 + \sum_{i=1}^4 h_K \|p_{\gamma_i, K}\|_{L^2(\gamma_i)}^2 \right),
\end{aligned}$$

upon using the Cauchy–Schwarz inequality, (7.1), (7.2) and the mesh regularity. Hence, (7.13) follows. \square

7.2 The model problem.

We are interested in the following advection-reaction-diffusion problem. For given data $f \in L^2(\Omega)$: Find u such that

$$\begin{aligned} -\nu\Delta u + \mathbf{a} \cdot \nabla u + \kappa u &= f \quad \text{in } \Omega, \\ u &= 0 \quad \text{on } \Gamma, \end{aligned} \tag{7.14}$$

where $\nu > 0$ is a constant diffusion coefficient, \mathbf{a} is a $\mathbf{L}^\infty(\Omega)$ solenoidal field and $\kappa \geq 0$ corresponds to a constant dissipation coefficient.

The weak formulation of (7.14) then reads: Find $u \in H_0^1(\Omega)$ such that

$$\mathcal{B}(u, v) = \mathcal{L}(v) \quad \text{for all } v \in H_0^1(\Omega), \tag{7.15}$$

where

$$\mathcal{B}(u, v) = \nu(\nabla u, \nabla v)_\Omega + (\mathbf{a} \cdot \nabla u, v)_\Omega + \kappa(u, v)_\Omega \quad \text{and} \quad \mathcal{L}(v) = (f, v)_\Omega. \tag{7.16}$$

We consider the energy norm

$$\|u\|_\Omega^2 = \nu\|\nabla u\|_{L^2(\Omega)}^2 + \kappa\|u\|_{L^2(\Omega)}^2,$$

defined on $H^1(\Omega)$. Noticing that $(\mathbf{a} \cdot \nabla v, v)_\Omega = 0$ for all $v \in H_0^1(\Omega)$, since \mathbf{a} is solenoidal, then

$$\mathcal{B}(v, v) = \nu\|\nabla v\|_{L^2(\Omega)}^2 + \kappa\|v\|_{L^2(\Omega)}^2 \quad \text{for all } v \in H_0^1(\Omega),$$

and it is not difficult to see that $\mathcal{B}(v, w) \leq C\|v\|_\Omega\|w\|_\Omega$ for any $v, w \in H_0^1(\Omega)$. Hence, the well-posedness of the problem follows by the Lax–Milgram Theorem (see Chapter 3 in [69]).

7.3 A Stabilized finite element method (SUPG).

To approximate the solution of this problem we will consider a stabilized finite element approximation, which reads as follows: Find $u_h \in V_h$ such that

$$\mathcal{B}(u_h, v) + \mathcal{S}(u_h, f; v) = \mathcal{L}(v) \quad \text{for all } v \in V_h, \tag{7.17}$$

where $\mathcal{B}(\cdot, \cdot)$ and $\mathcal{L}(\cdot)$ are given in (7.16), $\mathcal{S}(\cdot, \cdot; \cdot)$ is a stabilizing term and V_h is a finite element space constructed using piecewise continuous polynomials of degree one, based on \mathcal{P} .

Many stabilized finite element methods are available, but here we focus on a Streamline Upwind-Petrov Galerkin stabilized finite element method (SUPG), which was first introduced by

Hughes and Brooks [77] for the numerical solution of convection-dominated convection-diffusion problems (see also [46, 72]).

For the SUPG method the stabilizing term is given by

$$\mathcal{S}(u_h, f; v) = \sum_{K \in \mathcal{P}} S_K(u_h|_K, f; v), \quad (7.18)$$

where

$$S_K(u_h, f; v) = (-\mathcal{R}_K, \tau_K \mathbf{a} \cdot \nabla v)_K,$$

and the residual operator \mathcal{R}_K is given by

$$\mathcal{R}_K = f - \mathbf{a} \cdot \nabla u_h|_K - \kappa u_h|_K. \quad (7.19)$$

We will always assume that the stabilization parameter τ_K satisfies

$$\|\tau_K\|_{L^\infty(K)} \leq C \frac{h_K}{\|\mathbf{a}\|_{L^\infty(K)}} \quad \text{for all } K \in \mathcal{P}. \quad (7.20)$$

The choice $\tau_K = 0$ yields the standard Galerkin formulation; the choice $\tau_K > 0$ corresponds to the SUPG-discretizations (see [46, 72]).

Here and in what follows the local mesh Péclet number is defined by

$$Pe_K = \frac{\|\mathbf{a}\|_{L^\infty(K)} h_K}{2\nu}. \quad (7.21)$$

7.4 The error equation.

Let $e = u - u_h$ denote the error in the stabilized finite element approximation, then from (7.17) and (7.16) it follows that the error satisfies

$$\begin{aligned} \mathcal{B}(e, v) &= \sum_{K \in \mathcal{P}} ((f, v)_K - \nu(\nabla u_h|_K, \nabla v)_K - (\mathbf{a} \cdot \nabla u_h|_K, v)_K - \kappa(u_h|_K, v)_K) \\ &= \sum_{K \in \mathcal{P}} ((\Pi_K(\mathcal{R}_K), v)_K - \nu(\nabla u_h|_K, \nabla v)_K + (\Psi - \Pi_K(\Psi), v)_K), \end{aligned} \quad (7.22)$$

where \mathcal{R}_K is given by (7.19) and

$$\Psi = f - \mathbf{a} \cdot \nabla u_h. \quad (7.23)$$

In the following, we will introduce the equilibrated boundary fluxes, but just for the three-dimensional case following [16], since the equilibrated fluxes in two dimensions can be easily obtained from Sections 4.2 and 5.3.

Let us suppose for the moment that there exists a set of *boundary fluxes* $\{g_{\gamma,K} : \gamma \in \mathcal{F}_K\}$ on the elements $K \in \mathcal{P}$ satisfying $g_{\gamma,K} + g_{\gamma,K'} = 0$ on $\mathcal{F}_K \cap \mathcal{F}_{K'}$ for $K, K' \in \mathcal{P}$. Then, using the fact that $v \in H_0^1(\Omega)$ and integration by parts, yields

$$\mathcal{B}(e, v) = \sum_{K \in \mathcal{P}} \left((\Pi_K(\mathcal{R}_K), v)_K + \sum_{\gamma \in \mathcal{F}_K} (\mathcal{R}_{\gamma,K}, v)_\gamma + (\Psi - \Pi_K(\Psi), v)_K \right),$$

where the face residual is given by

$$\mathcal{R}_{\gamma,K} = g_{\gamma,K} - \nu \nabla u_h|_K \cdot \hat{\mathbf{n}}_\gamma^K.$$

Let us assume for the moment that there exists a vector field $\boldsymbol{\sigma}_K \in \mathbf{H}(\mathbf{div}, K)$ satisfying the following *Neumann* problem

$$(\boldsymbol{\sigma}_K, \nabla v)_K = (\Pi_K(\mathcal{R}_K), v)_K + \sum_{\gamma \in \mathcal{F}_K} (\mathcal{R}_{\gamma,K}, v)_\gamma \quad \text{for all } v \in H^1(\Omega). \quad (7.24)$$

As was mentioned before this problem will have a solution if and only if the residuals satisfy the compatibility condition

$$0 = (\Pi_K(\mathcal{R}_K), c)_K + \sum_{\gamma \in \mathcal{F}_K} (\mathcal{R}_{\gamma,K}, c)_\gamma \quad \text{for all } c \in \mathbb{R}. \quad (7.25)$$

Hence, we can finally rewrite the error equation as

$$\mathcal{B}(e, v) = \sum_{K \in \mathcal{P}} ((\boldsymbol{\sigma}_K, \nabla v)_K + (\Psi - \Pi_K(\Psi), v)_K). \quad (7.26)$$

7.5 Construction of the equilibrated boundary fluxes in 3D.

In order to obtain a guaranteed upper bound for the error, we need to construct an appropriate set of equilibrated boundary fluxes $g_{\gamma,K} \in \mathbb{P}_1(\gamma)$ which, based on [16], need to satisfy:

Consistency: If $\gamma = \mathcal{F}_K \cap \mathcal{F}_{K'}$ for $K, K' \in \mathcal{P}$, then

$$g_{\gamma,K} + g_{\gamma,K'} = 0. \quad (7.27)$$

Full first order equilibration: For all $n \in \mathcal{V}_K$,

$$0 = (\Pi_K(f), \lambda_n)_K - \mathcal{B}_K(u_h|_K, \lambda_n) - \mathcal{S}_K(u_h, f; \lambda_n) + \sum_{\gamma \in \mathcal{F}_K} (g_{\gamma,K}, \lambda_n)_\gamma, \quad (7.28)$$

where $\mathcal{B}_K(u_h|_K, \lambda_n) = \nu(\nabla u_h|_K, \nabla \lambda_n)_K + (\mathbf{a} \cdot \nabla u_h|_K, \lambda_n)_K + \kappa(u_h|_K, \lambda_n)_K$, for all $K \in \mathcal{P}$. In terms of the residual, (7.28) can be written as

$$(\Pi_K(\mathcal{R}_K), \lambda_n)_K + \sum_{\gamma \in \mathcal{F}_K} (\mathcal{R}_{\gamma,K}, \lambda_n) - \mathcal{S}_K(u_h, f; \lambda_n) = 0 \quad \text{for all } n \in \mathcal{V}_K. \quad (7.29)$$

Since the flux $g_{\gamma,K}$ is a linear function on each edge, it is uniquely determined by the moments

$$\mu_{K,n}^\gamma = (g_{\gamma,K}, \lambda_n)_\gamma, \quad n \in \mathcal{V}_\gamma. \quad (7.30)$$

We briefly outline the main steps to obtain all the moments $\mu_{K,n}^\gamma$, which is virtually identical to the one described in Section 4.2. Let

$$\langle J \rangle_{\gamma,K} = \begin{cases} \frac{1}{2} (J_{\gamma,K} - J_{\gamma,K'}) & \text{if } \gamma \in \mathcal{F}_K \cap \mathcal{F}_{K'}, \\ J_{\gamma,K} & \text{if } \gamma \in \mathcal{F}_K \cap \mathcal{F}_\Gamma, \end{cases} \quad (7.31)$$

with

$$J_{\gamma,K} = \nu \nabla u_h|_K \cdot \hat{\mathbf{n}}_\gamma^K \quad \text{for } \gamma \in \mathcal{F}_K. \quad (7.32)$$

We look for the moments $\mu_{K,n}^\gamma$ of $g_{\gamma,K}$ in the form

$$\mu_{K,n}^\gamma = \begin{cases} \frac{1}{2} (\xi_{K,n} - \xi_{K',n}) + (\langle J \rangle_{\gamma,K}, \lambda_n)_\gamma & \text{if } \gamma \in \mathcal{F}_K \cap \mathcal{F}_{K'}, \\ \xi_{K,n} + (J_{\gamma,K}, \lambda_n)_\gamma & \text{if } \gamma \in \mathcal{F}_K \cap \mathcal{F}_\Gamma, \end{cases} \quad (7.33)$$

where the parameters $\xi_{K,n}$ are obtained by solving a system of equations analogous to (4.24):

$$\frac{1}{2} \sum_{K' \in \Omega_n \cap \Omega_K} (\xi_{K,n} - \xi_{K',n}) + \sum_{\gamma \in \mathcal{F}_K \cap \mathcal{F}_\Gamma \cap \mathcal{F}_n} \xi_{K,n} = \tilde{\Delta}_K(\lambda_n) \quad \forall K \in \Omega_n, \quad (7.34)$$

where

$$\tilde{\Delta}_K(\lambda_n) = \mathcal{B}_K(u_h|_K, \lambda_n) + \mathcal{S}_K(u_h, f; \lambda_n) - (f, \lambda_n)_K - \sum_{\gamma \in \mathcal{F}_K} (\langle J \rangle_{\gamma,K}, \lambda_n)_\gamma. \quad (7.35)$$

As we stated before, (7.34) represents a system of $\#\Omega_n$ equations for $\#\Omega_n$ unknowns, but we already know that we can always find a solution which depends continuously on the data $\{\tilde{\Delta}_K(\lambda_n), K \in \Omega_n\}$ provided that the following compatibility condition holds:

$$\sum_{K \in \Omega_n} \tilde{\Delta}_K(\lambda_n) = 0 \quad \text{for all } n \in \mathcal{V} \text{ and } \mathbf{x}_n \notin \Gamma, \quad (7.36)$$

which follows at once on using the definition (7.35), (7.18) and taking $v = \lambda_n$ in (7.17).

7.6 Solution of the Neumann problem.

The Neumann problem to be solved in this case is

$$\begin{aligned} -\operatorname{div} \boldsymbol{\sigma}_K &= \Pi_K(\mathcal{R}_K) \quad \text{on } K, \\ \boldsymbol{\sigma}_K \cdot \hat{\mathbf{n}}_\gamma^K &= \mathcal{R}_{\gamma,K} \quad \text{in each } \gamma \in \mathcal{F}_K. \end{aligned} \quad (7.37)$$

The following result provides a solution to (7.37), based on the orientation of the vertices and normal vectors in Figure 7.1 in the three-dimensional case.

Lemma 7.6.1. *The following function is a solution to (7.37),*

$$\begin{aligned} \boldsymbol{\sigma}_K = \sum_{i=1}^4 \left((\mathcal{R}_{\gamma_i,K}, \lambda_{i+1})_{\gamma_i} \boldsymbol{\psi}_{i,i+1} + (\mathcal{R}_{\gamma_i,K}, \lambda_{i+2})_{\gamma_i} \boldsymbol{\psi}_{i,i+2} + (\mathcal{R}_{\gamma_i,K}, \lambda_{i+3})_{\gamma_i} \boldsymbol{\psi}_{i,i+3} \right. \\ \left. + (|K| \nabla(\Pi_K(\mathcal{R}_K)) \cdot (\mathbf{x}_i - \bar{\mathbf{x}}_K)) \boldsymbol{\psi}_{K,i} \right), \end{aligned} \quad (7.38)$$

where the functions $\boldsymbol{\psi}_{\cdot,\cdot}$ and $\boldsymbol{\psi}_{K,\cdot}$ are given in (7.7) and (7.8), respectively, $i \in \mathcal{V}_K = \{1, 2, 3, 4\}$ and the indices are to be understood module 4. Moreover, there exists a constant C independent of any size of the element K such that

$$\|\boldsymbol{\sigma}_K\|_{L^2(K)} \leq C \left(h_K \|\Pi_K(\mathcal{R}_K)\|_{L^2(K)} + \sum_{\gamma \in \mathcal{F}_K} h_K^{1/2} \|\mathcal{R}_{\gamma,K}\|_{L^2(\gamma)} \right). \quad (7.39)$$

and the constant C is independent of h_K , p_K and $p_{\gamma,K}$.

Proof. From (7.28), (7.6) and $\mathcal{S}_K(u_h, f; 1) = 0$, implies that the element residual $\Pi_K(\mathcal{R}_K)$ and the edge residuals $\mathcal{R}_{\gamma,K}$ satisfy (7.25), i.e. a condition like (7.11), then taking $p_K = \mathcal{R}_K$ and $p_{\gamma,K} = \mathcal{R}_{\gamma,K}$ (7.12) and (7.13) in Theorem 7.1.3, the result easily follows. \square

In the two-dimensional case the following result holds as a complete analogue to the previous result.

Lemma 7.6.2. *The following function is a solution to (7.37),*

$$\boldsymbol{\sigma}_K = \sum_{i=1}^3 \left((\mathcal{R}_{\gamma_i,K}, \lambda_{i+1})_{\gamma_i} \tilde{\boldsymbol{\psi}}_{\lambda_{i+1}}^{(\gamma_i)} + (\mathcal{R}_{\gamma_i,K}, \lambda_{i+2})_{\gamma_i} \tilde{\boldsymbol{\psi}}_{\lambda_{i+2}}^{(\gamma_i)} + (|K| \nabla(\Pi_K(\mathcal{R}_K)) \cdot (\mathbf{x}_i - \bar{\mathbf{x}}_K)) \boldsymbol{\psi}_K^{(i)} \right), \quad (7.40)$$

where $i \in \mathcal{V}_K = \{1, 2, 3\}$ and the functions $\tilde{\boldsymbol{\psi}}_\lambda^{(\cdot)}$ and $\boldsymbol{\psi}_K^{(\cdot)}$ are given in (2.12) and (2.13), respectively. Moreover, exists a constant C independent of any size of the element K such that

$$\|\boldsymbol{\sigma}_K\|_{L^2(K)} \leq C \left(h_K \|\Pi_K(\mathcal{R}_K)\|_{L^2(K)} + \sum_{\gamma \in \mathcal{E}_K} h_K^{1/2} \|\mathcal{R}_{\gamma,K}\|_{L^2(\gamma)} \right). \quad (7.41)$$

Proof. The result follows using exactly the same argument as in the three-dimensional case, but just restricted to the construction of the boundary fluxes and the properties of the barycentric functions in the two-dimensional case. \square

7.7 A guaranteed upper bound for the error.

In the following we present the analysis to obtain a fully computable upper bound assuming that $\kappa > 0$. From the properties of the orthogonal projection and with the aid of the Poincaré inequality (see Theorem (2.1.1)), we get

$$\begin{aligned} (\Psi - \Pi_K(\Psi), v)_K &= (\Psi - \Pi_K(\Psi), v - \bar{v}_K)_K \\ &\leq \frac{h_K}{\pi} \|\Psi - \Pi_K(\Psi)\|_{L^2(K)} \|\nabla v\|_{L^2(K)} \\ &\leq \frac{h_K}{\pi\sqrt{\nu}} \|\Psi - \Pi_K(\Psi)\|_{L^2(K)} \|v\|_K, \end{aligned}$$

and simply applying the Cauchy-Schwarz inequality we obtain

$$(\Psi - \Pi_K(\Psi), v)_K \leq \|\Psi - \Pi_K(\Psi)\|_{L^2(K)} \|v\|_{L^2(K)} \leq \frac{1}{\sqrt{\kappa}} \|\Psi - \Pi_K(\Psi)\|_{L^2(K)} \|v\|_K.$$

Hence

$$(\Psi - \Pi_K(\Psi), v)_K \leq \min \left\{ \frac{h_K}{\pi\sqrt{\nu}}, \frac{1}{\sqrt{\kappa}} \right\} \|\Psi - \Pi_K(\Psi)\|_{L^2(K)} \|v\|_K. \quad (7.42)$$

Applying the Cauchy-Schwarz inequality with (7.42) in (7.26), then we obtain

$$\begin{aligned} \mathcal{B}(e, v) &= \sum_{K \in \mathcal{P}} ((\sigma_K, \nabla v)_K + (\Psi - \Pi_K(\Psi), v)_K) \\ &\leq \sum_{K \in \mathcal{P}} \left(\left(\frac{1}{\sqrt{\nu}} \|\sigma_K\|_{L^2(K)} + \min \left\{ \frac{h_K}{\pi\sqrt{\nu}}, \frac{1}{\sqrt{\kappa}} \right\} \|\Psi - \Pi_K(\Psi)\|_{L^2(K)} \right) \|v\|_K \right) \\ &\leq \left(\sum_{K \in \mathcal{P}} \left(\frac{1}{\sqrt{\nu}} \|\sigma_K\|_{L^2(K)} + \min \left\{ \frac{h_K}{\pi\sqrt{\nu}}, \frac{1}{\sqrt{\kappa}} \right\} \|\Psi - \Pi_K(\Psi)\|_{L^2(K)} \right)^2 \right)^{1/2} \|v\|_\Omega. \end{aligned}$$

Now taking $v = e$ in the previous bound and then dividing both sides of the inequality by $\|e\|_\Omega$, we obtain the following result.

Theorem 7.7.1. *For each element $K \in \mathcal{P}$, define a local error indicator as*

$$\eta_K = \frac{1}{\sqrt{\nu}} \|\sigma_K\|_{L^2(K)} + \min \left\{ \frac{h_K}{\pi\sqrt{\nu}}, \frac{1}{\sqrt{\kappa}} \right\} \|\Psi - \Pi_K(\Psi)\|_K, \quad (7.43)$$

where σ_K given by (7.40) in the two-dimensional case and by (7.38) in the three-dimensional case. Then

$$\|e\|_{\Omega}^2 \leq \eta^2 := \sum_{K \in \mathcal{P}} \eta_K^2. \quad (7.44)$$

7.8 Efficiency of the estimator.

From Section 7.4 and using the definition of the residual operator \mathcal{R}_K , we can rewrite the error equation as

$$\begin{aligned} & \sum_{K \in \mathcal{P}} \left((\Pi_K(\mathcal{R}_K), v)_K - \sum_{\gamma \in \mathcal{F}_K} ([J]_{\gamma}, v)_{\gamma} \right) \\ &= \nu (\nabla e, \nabla v)_{\Omega} + (\mathbf{a} \cdot \nabla e, v)_{\Omega} + \kappa (e, v)_{\Omega} - \sum_{K \in \mathcal{P}} (\Psi - \Pi_K(\Psi), v)_K, \end{aligned} \quad (7.45)$$

where

$$[J]_{\gamma} = \begin{cases} \frac{1}{2}(J_{\gamma, K} + J_{\gamma, K'}) & \text{if } \gamma \in \mathcal{F}_K \cap \mathcal{F}_{K'}, \\ 0 & \text{if } \gamma \in \mathcal{F}_K \cap \mathcal{F}_{\Gamma}, \end{cases} \quad (7.46)$$

with $J_{\gamma, K}$ given by (7.32).

Now we will apply standard bubble functions arguments, used in all the previous chapters, to the previous error equation.

Lemma 7.8.1. *The orthogonal projection of the element residual \mathcal{R}_K satisfies*

$$h_K^2 \|\Pi_K(\mathcal{R}_K)\|_{L^2(K)}^2 \leq C \left(\mathcal{M}_K^2 h_K^2 \|e\|_K^2 + h_K^2 \|\Psi - \Pi_K(\Psi)\|_{L^2(K)}^2 \right), \quad (7.47)$$

where

$$\mathcal{M}_K = \max \left\{ \frac{\sqrt{\nu}}{h_K}, \frac{\|\mathbf{a}\|_{L^{\infty}(K)}}{\sqrt{\nu}}, \sqrt{\kappa} \right\}. \quad (7.48)$$

Proof. Letting $\beta_K = \prod_{n \in \mathcal{V}_K} \lambda_n$ and extending it by zero to $\Omega \setminus K$ we obtain $\beta_K \in H_0^1(\Omega)$. Taking

$v = \beta_K \Pi_K(\mathcal{R}_K)$ in (7.45), we obtain

$$\begin{aligned}
& \left\| \beta_K^{1/2} \Pi_K(\mathcal{R}_K) \right\|_{L^2(K)}^2 \\
&= \nu (\nabla e, \nabla(\beta_K \Pi_K(\mathcal{R}_K)))_K + (\mathbf{a} \cdot \nabla e, \beta_K \Pi_K(\mathcal{R}_K))_K + \kappa (e, \beta_K \Pi_K(\mathcal{R}_K))_K \\
&\quad + (\Psi - \Pi_K(\Psi), \beta_K \Pi_K(\mathcal{R}_K))_K \\
&\leq \sqrt{\nu} \|\nabla e\|_{L^2(K)} \frac{\sqrt{\nu}}{h_K} \|\beta_K \Pi_K(\mathcal{R}_K)\|_{L^2(K)} + \frac{\|\mathbf{a}\|_{L^\infty(K)}}{\sqrt{\nu}} \sqrt{\nu} \|\nabla e\|_{L^2(K)} \|\beta_K \Pi_K(\mathcal{R}_K)\|_{L^2(K)} \\
&\quad + \sqrt{\kappa} \|e\|_{L^2(K)} \sqrt{\kappa} \|\beta_K \Pi_K(\mathcal{R}_K)\|_{L^2(K)} + \|\Psi - \Pi_K(\Psi)\|_{L^2(K)} \|\beta_K \Pi_K(\mathcal{R}_K)\|_{L^2(K)} \\
&\leq C \left(\max \left\{ \frac{\sqrt{\nu}}{h_K}, \frac{\|\mathbf{a}\|_{L^\infty(K)}}{\sqrt{\nu}}, \sqrt{\kappa} \right\} \left(\sqrt{\nu} \|\nabla e\|_{L^2(K)} + \sqrt{\kappa} \|e\|_{L^2(K)} \right) \right. \\
&\quad \left. + \|\Psi - \Pi_K(\Psi)\|_{L^2(K)} \right) \left\| \beta_K^{1/2} \Pi_K(\mathcal{R}_K) \right\|_{L^2(K)} \\
&\leq C \left(\max \left\{ \frac{\sqrt{\nu}}{h_K}, \frac{\|\mathbf{a}\|_{L^\infty(K)}}{\sqrt{\nu}}, \sqrt{\kappa} \right\} \|e\|_K + \|\Psi - \Pi_K(\Psi)\|_{L^2(K)} \right) \left\| \beta_K^{1/2} \Pi_K(\mathcal{R}_K) \right\|_{L^2(K)},
\end{aligned}$$

upon using the Cauchy–Schwarz inequality and Theorem 2.1.2. Now the result follows using the fact that $\|\Pi_K(\mathcal{R}_K)\|_{L^2(K)} \leq C \left\| \beta_K^{1/2} \Pi_K(\mathcal{R}_K) \right\|_{L^2(K)}$ (again using Theorem 2.1.2). \square

Lemma 7.8.2. *The jump discontinuity in the approximation of the normal fluxes at interelement boundaries, satisfies*

$$\sum_{\gamma \in \mathcal{F}_K} h_K \|[J]_\gamma\|_{L^2(\gamma)}^2 \leq C \sum_{K' \in \Omega_K} \left(\mathcal{M}_{K'}^2 h_{K'}^2 \|e\|_{K'}^2 + h_{K'}^2 \|\Psi - \Pi_{K'}(\Psi)\|_{L^2(K')}^2 \right). \quad (7.49)$$

Proof. For $\gamma \in \mathcal{F}_K \cap \mathcal{F}_I$, let $\beta_\gamma = \prod_{n \in \mathcal{V}_\gamma} \lambda_n$ and extending by zero in the region $\Omega \setminus \Omega_\gamma$ we obtain $\beta_\gamma \in H_0^1(\Omega)$. Taking $v = -\beta_\gamma [J]_\gamma$ in (7.45), we obtain

$$\begin{aligned}
2 \left\| \beta_\gamma^{1/2} [J]_\gamma \right\|_{L^2(\gamma)}^2 &= \sum_{K \in \Omega_\gamma} \left(-\nu (\nabla e, \nabla(\beta_\gamma [J]_\gamma))_K - (\mathbf{a} \cdot \nabla e, \beta_\gamma [J]_\gamma)_K - \kappa (e, \beta_\gamma [J]_\gamma)_K \right. \\
&\quad \left. + (\Psi - \Pi_K(\Psi), \beta_\gamma [J]_\gamma)_K + (\Pi_K(\mathcal{R}_K), \beta_\gamma [J]_\gamma)_K \right) \\
&\leq C \sum_{K \in \Omega_\gamma} \left(\sqrt{\nu} \|\nabla e\|_{L^2(K)} \frac{\sqrt{\nu}}{h_K^{1/2}} \left\| \beta_\gamma^{1/2} [J]_\gamma \right\|_{L^2(\gamma)} + \frac{\|\mathbf{a}\|_{L^\infty(K)} h_K^{1/2}}{\sqrt{\nu}} \sqrt{\nu} \|\nabla e\|_{L^2(K)} \left\| \beta_\gamma^{1/2} [J]_\gamma \right\|_{L^2(\gamma)} \right. \\
&\quad \left. + \sqrt{\kappa} \|e\|_{L^2(K)} \sqrt{\kappa} h_K^{1/2} \left\| \beta_\gamma^{1/2} [J]_\gamma \right\|_{L^2(\gamma)} + h_K^{1/2} \left(\|\Pi_K(\mathcal{R}_K)\|_{L^2(K)} + \|\Psi - \Pi_K(\Psi)\|_{L^2(K)} \right) \left\| \beta_\gamma^{1/2} [J]_\gamma \right\|_{L^2(\gamma)} \right) \\
&\leq C \sum_{K \in \Omega_\gamma} \left(h_K^{1/2} \max \left\{ \frac{\sqrt{\nu}}{h_K}, \frac{\|\mathbf{a}\|_{L^\infty(K)}}{\sqrt{\nu}}, \sqrt{\kappa} \right\} \|e\|_K + h_K^{1/2} \|\Psi - \Pi_K(\Psi)\|_{L^2(K)} \right) \left\| \beta_\gamma^{1/2} [J]_\gamma \right\|_{L^2(\gamma)},
\end{aligned}$$

upon using the Cauchy–Schwarz inequality, Theorem 2.1.3 and (7.47), with a similar bound for

the remaining faces. Now the result follows using the fact that $\| [J]_\gamma \|_{L^2(K)} \leq C \left\| \beta_\gamma^{1/2} [J]_\gamma \right\|_{L^2(K)}$ (again using Theorem 2.1.3) and summing over all the faces in the element. \square

Following exactly the same steps as in the proof of Theorem 4.5.1, but now applied to the fluxes constructed in Section 7.5 in conjunction with Lemma 7.1.2, it follows that

$$h_K^2 \left\| g_{\gamma,K} - \langle J \rangle_{\gamma,K} \right\|_{L^2(\gamma)}^2 \leq C \sum_{n \in \mathcal{V}_\gamma} \sum_{K' \in \Omega_n} \left| \tilde{\Delta}_{K'}(\lambda_n) \right|^2, \quad (7.50)$$

where $\tilde{\Delta}_{K'}(\lambda_n)$ is given by (7.35). Integrating by parts in (7.35), the definition of the stabilization term, (7.46) and (7.31), yields

$$\begin{aligned} & \left| \tilde{\Delta}_{K'}(\lambda_n) \right|^2 \\ &= \left| \left(\Pi_K(\mathcal{R}_K), \lambda_n + \tau_K \mathbf{a} \cdot \nabla \lambda_n \right)_K + (\Psi - \Pi_K(\Psi), \tau_K \mathbf{a} \cdot \nabla \lambda_n)_K - \sum_{\gamma \in \mathcal{F}_K} ([J]_\gamma, \lambda_n)_\gamma \right|^2. \end{aligned} \quad (7.51)$$

Now each term on the right hand side can be bounded as follows,

$$\begin{aligned} \left(\Pi_K(\mathcal{R}_K), \lambda_n + \tau_K \mathbf{a} \cdot \nabla \lambda_n \right)_K &\leq \|\Pi_K(\mathcal{R}_K)\|_{L^2(K)} \left(\|\lambda_n\|_{L^2(K)} + \|\tau_K \mathbf{a} \cdot \nabla \lambda_n\|_{L^2(K)} \right) \\ &\leq C \|\Pi_K(\mathcal{R}_K)\|_{L^2(K)} \left(h_K^{3/2} + \|\tau_K\|_{L^\infty(K)} \|\mathbf{a}\|_{L^\infty(K)} h_K^{1/2} \right) \\ &\leq C h_K^{3/2} \|\Pi_K(\mathcal{R}_K)\|_{L^2(K)}, \end{aligned}$$

upon using the mesh regularity, the Cauchy–Schwarz inequality and assumption (7.20). Similarly the second term can be bounded as

$$\begin{aligned} (\Psi - \Pi_K(\Psi), \tau_K \mathbf{a} \cdot \nabla \lambda_n)_K &\leq C \|\Psi - \Pi_K(\Psi)\|_{L^2(K)} \|\tau_K \mathbf{a} \cdot \nabla \lambda_n\|_{L^2(K)} \\ &\leq C h_K \|\Psi - \Pi_K(\Psi)\|_{L^2(K)} \frac{\|\tau_K\|_{L^\infty(K)} \|\mathbf{a}\|_{L^\infty(K)}}{h_K^{1/2}} \\ &\leq C h_K^{3/2} \|\Psi - \Pi_K(\Psi)\|_{L^2(K)}, \end{aligned}$$

again using the mesh regularity, the Cauchy–Schwarz inequality and assumption (7.20). Finally, the third term can be bounded as

$$\sum_{\gamma \in \mathcal{F}_K} ([J]_\gamma, \lambda_n)_\gamma \leq \sum_{\gamma \in \mathcal{F}_K} h_K \| [J]_\gamma \|_{L^2(\gamma)}.$$

Inserting the previous bounds into (7.50), yields

$$\begin{aligned} & h_K \left\| g_{\gamma,K} - \langle J \rangle_{\gamma,K} \right\|_{L^2(\gamma)}^2 \\ &\leq C \sum_{n \in \mathcal{V}_\gamma} \sum_{K' \in \Omega_n} \left(h_{K'}^2 \|\Pi_{K'}(\mathcal{R}_{K'})\|_{L^2(K')}^2 + h_{K'}^2 \|\Psi - \Pi_{K'}(\Psi)\|_{L^2(K')}^2 + \sum_{\gamma \in \mathcal{F}_{K'}} h_{K'} \| [J]_\gamma \|_{L^2(\gamma)}^2 \right). \end{aligned} \quad (7.52)$$

Using the result from Lemma 7.8.1 and Lemma 7.8.2, in the previous bound we obtain the following result.

Lemma 7.8.3. *Let $\{g_{\gamma,K}\}$ be the set of equilibrated boundary satisfying the consistency and the full-first order equilibration conditions, described in Section 7.5. Then, for each element K ,*

$$h_K \sum_{\gamma \in \mathcal{F}_K} \left\| g_{\gamma,K} - \langle J \rangle_{\gamma,K} \right\|_{L^2(\gamma)}^2 \leq C \left(\sum_{K' \in \tilde{\Omega}_K} \mathcal{M}_{K'}^2 h_{K'}^2 \|e\|_{K'}^2 + h_{K'}^2 \|\Psi - \Pi_K(\Psi)\|_{L^2(K')}^2 \right). \quad (7.53)$$

Using Theorem 7.7.1 and Lemma 7.6.1, we can bound the local error indicator η_K as follows

$$\begin{aligned} \eta_K^2 &\leq C \left(\frac{1}{\nu} \|\sigma_K\|_{L^2(K)}^2 + \left(\min \left\{ \frac{h_K}{\pi\sqrt{\nu}}, \frac{1}{\sqrt{\kappa}} \right\} \right)^2 \|\Psi - \Pi_K(\Psi)\|_{L^2(K)}^2 \right) \\ &\leq C \left(\frac{1}{\nu} \left(h_K^2 \|\Pi_K(\mathcal{R}_K)\|_{L^2(K)}^2 + \sum_{\gamma \in \mathcal{F}_K} \left(h_K \|g_{\gamma,K} - \langle J \rangle_{\gamma,K}\|_{L^2(\gamma)}^2 + h_K \|[J]_{\gamma}\|_{L^2(\gamma)}^2 \right) \right) \right. \\ &\quad \left. + \left(\min \left\{ \frac{h_K}{\pi\sqrt{\nu}}, \frac{1}{\sqrt{\kappa}} \right\} \right)^2 \|\Psi - \Pi_K(\Psi)\|_{L^2(K)}^2 \right). \end{aligned} \quad (7.54)$$

Now, from Lemma 7.53, Lemma 7.8.2 and Lemma 7.47, we obtain

$$\eta_K^2 \leq C \left(\sum_{K' \in \tilde{\Omega}_K} \frac{1}{\nu} h_{K'}^2 \mathcal{M}_{K'}^2 \|e\|_{K'} + \left(\frac{h_{K'}^2}{\nu} + \left(\min \left\{ \frac{h_{K'}}{\pi\sqrt{\nu}}, \frac{1}{\sqrt{\kappa}} \right\} \right)^2 \right) \|\Psi_{K'} - \Pi_{K'}(\Psi)\|_{K'} \right).$$

The above inequality induce the definition of the following constant

$$\Phi_K^2 := \frac{1}{\nu} h_K^2 \mathcal{M}_K^2 = 4 \max \left\{ \frac{1}{4}, Pe_K^2, \frac{\kappa h_K^2}{\nu} \right\}, \quad (7.55)$$

whose limiting behaviour is given by

$$\Phi_K^2 \approx \begin{cases} 1 & \text{if } \nu \gg \|\mathbf{a}\|_{L^\infty(\Omega)} \text{ and } \nu \gg \kappa, \\ Pe_K^2 & \text{if } \|\mathbf{a}\|_{L^\infty(\Omega)} \gg \nu \text{ and } \|\mathbf{a}\|_{L^\infty(\Omega)} \gg \kappa, \\ \frac{\kappa h_K^2}{\nu} & \text{if } \kappa \gg \|\mathbf{a}\|_{L^\infty(\Omega)} \text{ and } \kappa \gg \nu. \end{cases} \quad (7.56)$$

To summarize, collecting all the results in this section we obtain.

Theorem 7.8.4. *The local error estimator η_K , given in (7.43), satisfy*

$$\eta_K^2 \leq C \sum_{K' \in \tilde{\Omega}_K} \left(\Phi_{K'}^2 \|e\|_{K'}^2 + \left(\frac{h_{K'}^2}{\nu} + \left(\min \left\{ \frac{h_{K'}}{\pi\sqrt{\nu}}, \frac{1}{\sqrt{\kappa}} \right\} \right)^2 \right) \|\Psi_{K'} - \Pi_{K'}(\Psi)\|_{L^2(K')}^2 \right),$$

where $\Phi_{K'}$ is given by (7.55).

Remark 7.8.5. *In the case when $\kappa = 0$, following exactly the same arguments it follows that*

$$\|e\|_{\Omega}^2 := \nu \|\nabla e\|_{\mathbf{L}^2(\Omega)}^2 \leq \eta^2 := \sum_{K \in \mathcal{P}} \eta_K^2.$$

where

$$\eta_K = \frac{1}{\sqrt{\nu}} \|\sigma_K\|_{\mathbf{L}^2(K)} + \frac{h_K}{\pi\sqrt{\nu}} \|\Psi - \Pi_K(\Psi)\|_{\mathbf{L}^2(K)}.$$

In the local efficiency the same result holds, but now defining the constant \mathcal{M}_K as

$$\mathcal{M}_K = \max \left\{ \frac{\sqrt{\nu}}{h_K}, \frac{\|\mathbf{a}\|_{\mathbf{L}^\infty(K)}}{\sqrt{\nu}} \right\}.$$

7.9 An explicit formula to compute the norm of the solution of the Neumann problem.

In this section we will present formulas to compute the norm of the solution of the Neumann problem in the two and three-dimensional case.

Formula in the two-dimensional case: First we present an explicit formula for the solution of the Neumann problem in the two-dimensional case. Let the edges, vertices, tangent vectors and unit normal vectors of an element K be labelled as in Figure 2.1. Then, for $i \in \mathcal{V}_K = \{1, 2, 3\}$ define

$$\begin{aligned} \tilde{\mathbf{M}}_{11} = & \begin{bmatrix} 621 & -1161 & 27 \\ -1161 & 2241 & -63 \\ 27 & -63 & 4 \end{bmatrix} \mathbf{t}_2 \cdot \mathbf{t}_2 + \begin{bmatrix} 1647 & -1917 & 18 \\ -1917 & 1647 & 18 \\ 18 & 18 & -4 \end{bmatrix} \mathbf{t}_2 \cdot \mathbf{t}_3 \\ & + \begin{bmatrix} 2241 & -1161 & -63 \\ -1161 & 621 & 27 \\ -63 & 27 & 4 \end{bmatrix} \mathbf{t}_3 \cdot \mathbf{t}_3, \end{aligned}$$

with $\tilde{\mathbf{M}}_{22}$ and $\tilde{\mathbf{M}}_{33}$ being defined by permuting the indices and

$$\begin{aligned} \tilde{\mathbf{M}}_{12} = & \begin{bmatrix} -702 & -378 & 144 \\ 432 & 108 & -72 \\ 9 & 45 & -6 \end{bmatrix} \mathbf{t}_1 \cdot \mathbf{t}_1 + \begin{bmatrix} 405 & -1215 & 144 \\ -1215 & 405 & 18 \\ 18 & 144 & -14 \end{bmatrix} \mathbf{t}_1 \cdot \mathbf{t}_2 \\ & + \begin{bmatrix} 108 & -378 & 45 \\ 432 & -702 & 9 \\ -72 & 144 & -6 \end{bmatrix} \mathbf{t}_2 \cdot \mathbf{t}_2, \end{aligned}$$

with $\underline{\underline{M}}_{23}$ and $\underline{\underline{M}}_{31}$ being defined by permuting the indices and

$$\mathbf{M}_{10} = \begin{bmatrix} 27 \\ -27 \\ -3 \end{bmatrix} \mathbf{t}_2 \cdot \mathbf{t}_2 + \begin{bmatrix} 108 \\ -108 \\ 0 \end{bmatrix} \mathbf{t}_2 \cdot \mathbf{t}_3 + \begin{bmatrix} 27 \\ -27 \\ 3 \end{bmatrix} \mathbf{t}_3 \cdot \mathbf{t}_3,$$

with \mathbf{M}_{20} and \mathbf{M}_{30} being defined by permuting the indices and

$$\mathbf{S}_1 = \begin{bmatrix} (\mathcal{R}_{\gamma_1, K}, \lambda_2)_{\gamma_1} \\ (\mathcal{R}_{\gamma_1, K}, \lambda_3)_{\gamma_1} \\ |K| \nabla(\Pi_K(\mathcal{R}_K)) \cdot \mathbf{x}_1 \end{bmatrix},$$

with \mathbf{S}_2 and \mathbf{S}_3 being defined by permuting the indices. Now, let

$$\begin{aligned} (\boldsymbol{\sigma}_{\gamma_i, K}, \boldsymbol{\sigma}_{\gamma_j, K})_K &= \frac{1}{3240|K|} \mathbf{S}_i^T \underline{\underline{M}}_{ij} \mathbf{S}_j, \\ (\boldsymbol{\sigma}_{\gamma_i, K}, \boldsymbol{\sigma}_{0, K})_K &= \frac{1}{3240|K|} \mathbf{S}_i^T \mathbf{M}_{i0}, \\ \varrho_K &= \frac{1}{(\boldsymbol{\sigma}_{0, K}, \boldsymbol{\sigma}_{0, K})_K} \left(\sum_{i=1}^3 (\boldsymbol{\sigma}_{\gamma_i, K}, \boldsymbol{\sigma}_{0, K})_K \right)^2, \end{aligned}$$

where

$$(\boldsymbol{\sigma}_{0, K}, \boldsymbol{\sigma}_{0, K})_K = \frac{9}{3240|K|} (\mathbf{t}_1 \cdot \mathbf{t}_1 + \mathbf{t}_2 \cdot \mathbf{t}_2 + \mathbf{t}_3 \cdot \mathbf{t}_3 + \mathbf{t}_2 \cdot \mathbf{t}_3 + \mathbf{t}_3 \cdot \mathbf{t}_1 + \mathbf{t}_1 \cdot \mathbf{t}_2).$$

Now, following very similar arguments as the ones given in proof of Theorem 4.6.1, we have that the following formula gives the norm of the solution of the Neumann problem (7.37), minimized over a cubic bubble space.

$$\begin{aligned} \left(\min_{b_K \in H_0^1(K) \cap \mathbb{P}_3(K)} \|\boldsymbol{\sigma}_K - b_K\|_{L^2(K)} \right)^2 &= (\boldsymbol{\sigma}_{\gamma_1, K}, \boldsymbol{\sigma}_{\gamma_1, K})_K + (\boldsymbol{\sigma}_{\gamma_2, K}, \boldsymbol{\sigma}_{\gamma_2, K})_K + (\boldsymbol{\sigma}_{\gamma_3, K}, \boldsymbol{\sigma}_{\gamma_2, K})_K \\ &\quad + 2((\boldsymbol{\sigma}_{\gamma_2, K}, \boldsymbol{\sigma}_{\gamma_3, K})_K + (\boldsymbol{\sigma}_{\gamma_3, K}, \boldsymbol{\sigma}_{\gamma_1, K})_K + (\boldsymbol{\sigma}_{\gamma_1, K}, \boldsymbol{\sigma}_{\gamma_2, K})_K) \\ &\quad - \varrho_K. \end{aligned} \tag{7.57}$$

Formula in the three-dimensional case: Now we present an explicit formula for the solution of the Neumann problem in three-dimensional case. Let the vertices and unit normal vectors of an element K be labelled as in Figure 7.1. Then, for $i, j, k, l \in \mathcal{V}_K = \{1, 2, 3, 4\}$ being

distinct define

$$\begin{aligned}
 \mathbf{M}_{\approx j,k,l}^{\gamma_i, \gamma_i} = & \\
 & \begin{bmatrix} 12684 & -4326 & -4326 & -140 \\ -4326 & 1540 & 1442 & 42 \\ -4326 & 1442 & 1540 & 42 \\ -140 & 42 & 42 & 4 \end{bmatrix} \mathbf{t}_{ij} \cdot \mathbf{t}_{ij} + \begin{bmatrix} -5894 & 8680 & -1442 & -49 \\ 8680 & -5894 & -1442 & -49 \\ -1442 & -1442 & 1540 & 42 \\ -49 & -49 & 42 & 4 \end{bmatrix} \mathbf{t}_{ij} \cdot \mathbf{t}_{ik} + \\
 & \begin{bmatrix} -5894 & -1442 & 8680 & -49 \\ -1442 & 1540 & -1442 & 42 \\ 8680 & -1442 & -5894 & -49 \\ -49 & 42 & -49 & 4 \end{bmatrix} \mathbf{t}_{ij} \cdot \mathbf{t}_{il} + \begin{bmatrix} 1540 & -4326 & 1442 & 42 \\ -4326 & 12684 & -4326 & -140 \\ 1442 & -4326 & 1540 & 42 \\ 42 & -140 & 42 & 4 \end{bmatrix} \mathbf{t}_{ik} \cdot \mathbf{t}_{ik} + \\
 & \begin{bmatrix} 1540 & -1442 & -1442 & 42 \\ -1442 & -5894 & 8680 & -49 \\ -1442 & 8680 & -5894 & -49 \\ 42 & -49 & -49 & 4 \end{bmatrix} \mathbf{t}_{ik} \cdot \mathbf{t}_{il} + \begin{bmatrix} 1540 & 1442 & -4326 & 42 \\ 1442 & 1540 & -4326 & 42 \\ -4326 & -4326 & 12684 & -140 \\ 42 & 42 & -140 & 4 \end{bmatrix} \mathbf{t}_{il} \cdot \mathbf{t}_{il},
 \end{aligned}$$

and

$$\begin{aligned}
 \mathbf{N}_{\approx k,l}^{\gamma_i, \gamma_j} = & \\
 & \begin{bmatrix} -2506 & -2506 & -1036 & 504 \\ 1162 & 672 & 182 & -168 \\ 672 & 1162 & 182 & -168 \\ 14 & 14 & 84 & -8 \end{bmatrix} \mathbf{t}_{ij} \cdot \mathbf{t}_{ij} + \begin{bmatrix} 7658 & -1232 & -1722 & -315 \\ -9002 & -798 & 1064 & 427 \\ 672 & 1358 & -14 & -56 \\ 0 & 7 & 105 & -3 \end{bmatrix} \mathbf{t}_{ij} \cdot \mathbf{t}_{ik} + \\
 & \begin{bmatrix} -1232 & 7658 & -1722 & -315 \\ 1358 & 672 & -14 & -56 \\ -798 & -9002 & 1064 & 427 \\ 7 & 0 & 105 & -3 \end{bmatrix} \mathbf{t}_{ij} \cdot \mathbf{t}_{il} + \begin{bmatrix} -3738 & 1246 & 1148 & 70 \\ 11802 & -4032 & -3738 & -182 \\ -4032 & 1442 & 1246 & 56 \\ -182 & 56 & 70 & 2 \end{bmatrix} \mathbf{t}_{ik} \cdot \mathbf{t}_{ik} + \\
 & \begin{bmatrix} -1246 & -1246 & 1148 & 70 \\ -5600 & 8190 & -1246 & -63 \\ 8190 & -5600 & -1246 & -63 \\ -63 & -63 & 70 & 2 \end{bmatrix} \mathbf{t}_{ik} \cdot \mathbf{t}_{il} + \begin{bmatrix} 1246 & -3738 & 1148 & 70 \\ 1442 & -4032 & 1246 & 56 \\ -4032 & 11802 & -3738 & -182 \\ 56 & -182 & 70 & 2 \end{bmatrix} \mathbf{t}_{il} \cdot \mathbf{t}_{il},
 \end{aligned}$$

where

$$\mathbf{t}_{ij} = \mathbf{x}_j - \mathbf{x}_i.$$

Now, define

$$\mathbf{S}_{j,k,l}^{\gamma_i} = \begin{bmatrix} (\mathcal{R}_{\gamma_i,K}, \lambda_j)_{\gamma_i} \\ (\mathcal{R}_{\gamma_i,K}, \lambda_k)_{\gamma_i} \\ (\mathcal{R}_{\gamma_i,K}, \lambda_l)_{\gamma_i} \\ |K|\nabla(\Pi_K(\mathcal{R}_K)) \cdot (\mathbf{x}_i - \bar{\mathbf{x}}_K) \end{bmatrix} \quad \text{and} \quad \mathbf{S}_{k,l,i}^{\gamma_j} = \begin{bmatrix} (\mathcal{R}_{\gamma_j,K}, \lambda_k)_{\gamma_j} \\ (\mathcal{R}_{\gamma_j,K}, \lambda_l)_{\gamma_j} \\ (\mathcal{R}_{\gamma_j,K}, \lambda_i)_{\gamma_j} \\ |K|\nabla(\Pi_K(\mathcal{R}_K)) \cdot (\mathbf{x}_j - \bar{\mathbf{x}}_K) \end{bmatrix}.$$

and also let

$$\begin{aligned} (\boldsymbol{\sigma}_{\gamma_i,K}, \boldsymbol{\sigma}_{\gamma_i,K})_K &= \frac{1}{13440|K|} (\mathbf{S}_{j,k,l}^{\gamma_i})^T \mathbf{M}_{j,k,l}^{\gamma_i,\gamma_i} \mathbf{S}_{j,k,l}^{\gamma_i}, \\ (\boldsymbol{\sigma}_{\gamma_i,K}, \boldsymbol{\sigma}_{\gamma_j,K})_K &= \frac{1}{13440|K|} (\mathbf{S}_{j,k,l}^{\gamma_i})^T \mathbf{N}_{k,l}^{\gamma_i,\gamma_j} \mathbf{S}_{k,l,i}^{\gamma_j}. \end{aligned}$$

Following very similar arguments as the ones given in proof of Theorem 4.6.1, we have that the following formula gives the norm of the solution of the Neumann problem (7.37)

$$\begin{aligned} \|\boldsymbol{\sigma}_K\|_{L^2(K)}^2 &= \tag{7.58} \\ &(\boldsymbol{\sigma}_{\gamma_1,K}, \boldsymbol{\sigma}_{\gamma_1,K})_K + (\boldsymbol{\sigma}_{\gamma_2,K}, \boldsymbol{\sigma}_{\gamma_2,K})_K + (\boldsymbol{\sigma}_{\gamma_3,K}, \boldsymbol{\sigma}_{\gamma_3,K})_K + (\boldsymbol{\sigma}_{\gamma_4,K}, \boldsymbol{\sigma}_{\gamma_4,K})_K \\ &+ 2 \left((\boldsymbol{\sigma}_{\gamma_1,K}, \boldsymbol{\sigma}_{\gamma_2,K})_K + (\boldsymbol{\sigma}_{\gamma_2,K}, \boldsymbol{\sigma}_{\gamma_3,K})_K + (\boldsymbol{\sigma}_{\gamma_3,K}, \boldsymbol{\sigma}_{\gamma_4,K})_K + (\boldsymbol{\sigma}_{\gamma_4,K}, \boldsymbol{\sigma}_{\gamma_1,K})_K \right. \\ &\left. + (\boldsymbol{\sigma}_{\gamma_1,K}, \boldsymbol{\sigma}_{\gamma_3,K})_K + (\boldsymbol{\sigma}_{\gamma_2,K}, \boldsymbol{\sigma}_{\gamma_4,K})_K \right). \end{aligned}$$

By setting i, j, k and l to the appropriate values all ten terms on the right hand side of (7.58) can be calculated:

$$\begin{aligned} i = 1, \quad j = 2, \quad k = 3, \quad l = 4 & \text{ yields } (\boldsymbol{\sigma}_{\gamma_1,K}, \boldsymbol{\sigma}_{\gamma_1,K})_K \quad \text{and} \quad (\boldsymbol{\sigma}_{\gamma_1,K}, \boldsymbol{\sigma}_{\gamma_2,K})_K; \\ i = 2, \quad j = 3, \quad k = 4, \quad l = 1 & \text{ yields } (\boldsymbol{\sigma}_{\gamma_2,K}, \boldsymbol{\sigma}_{\gamma_2,K})_K \quad \text{and} \quad (\boldsymbol{\sigma}_{\gamma_2,K}, \boldsymbol{\sigma}_{\gamma_3,K})_K; \\ i = 3, \quad j = 4, \quad k = 1, \quad l = 2 & \text{ yields } (\boldsymbol{\sigma}_{\gamma_3,K}, \boldsymbol{\sigma}_{\gamma_3,K})_K \quad \text{and} \quad (\boldsymbol{\sigma}_{\gamma_3,K}, \boldsymbol{\sigma}_{\gamma_4,K})_K; \\ i = 4, \quad j = 1, \quad k = 2, \quad l = 3 & \text{ yields } (\boldsymbol{\sigma}_{\gamma_4,K}, \boldsymbol{\sigma}_{\gamma_4,K})_K \quad \text{and} \quad (\boldsymbol{\sigma}_{\gamma_4,K}, \boldsymbol{\sigma}_{\gamma_1,K})_K; \\ i = 1, \quad j = 3, \quad k = 2, \quad l = 4 & \text{ yields } (\boldsymbol{\sigma}_{\gamma_1,K}, \boldsymbol{\sigma}_{\gamma_3,K})_K; \\ i = 2, \quad j = 4, \quad k = 3, \quad l = 1 & \text{ yields } (\boldsymbol{\sigma}_{\gamma_2,K}, \boldsymbol{\sigma}_{\gamma_4,K})_K. \end{aligned} \tag{7.59}$$

7.10 Numerical results.

In this section we present two series of numerical examples to illustrate the performance of the error estimator.

In the extensive literature for stabilized finite element methods for problem (7.4), there exist many different designs for the stabilization parameter τ_K . In terms of practical applications and

following [72] (see Remark 8), we tune the stabilization parameter as follows:

$$\tau_K = \begin{cases} \frac{h_K}{2|\mathbf{a}(\mathbf{x})|} & \text{if } Pe_K > 1, \\ 0 & \text{if } Pe_K \leq 1, \end{cases} \quad (7.60)$$

where the local mesh Péclet number is given in (7.21).

In the experiments we calculate the exact and the estimated error in the energy norm $\|\cdot\|_\Omega$ on a sequence of uniformly and adaptively refined grids, respectively. As a local error indicator for the adaptive algorithm we use (see Section 7.7)

$$\eta_K = \begin{cases} \frac{1}{\sqrt{\nu}} \|\boldsymbol{\sigma}_K\|_{L^2(K)} + \min \left\{ \frac{h_K}{\pi\sqrt{\nu}}, \frac{1}{\sqrt{\kappa}} \right\} \|\Psi - \Pi_K(\Psi)\|_K & \text{if } \kappa > 0, \\ \frac{1}{\sqrt{\nu}} \|\boldsymbol{\sigma}_K\|_{L^2(K)} + \frac{h_K}{\pi\sqrt{\nu}} \|\Psi - \Pi_K(\Psi)\|_K & \text{if } \kappa = 0. \end{cases} \quad (7.61)$$

where the minimized norm of $\boldsymbol{\sigma}_K$ is given by (7.57) in the two-dimensional case, by (7.58) in the three-dimensional case and Ψ is given by (7.23). The triangles are marked using the maximum strategy (mark K if $\eta_K \geq \eta_{\max}/2$). We summarize the adaptive algorithm in Table 7.1.

Adaptive mesh refinement algorithm [AMRA-CDR].

- 1:** Set $i = 0$ and construct a mesh $\mathcal{P}_{(i)}$.
 - 2:** For each element K in $\mathcal{P}_{(i)}$, compute:
 - $\|\boldsymbol{\sigma}_K\|_{L^2(K)}$ using (7.57) when $d = 2$ or (7.58) when $d = 3$.
 - $\|\Psi - \Pi_K(\Psi)\|_{L^2(K)}$ using an appropriate quadrature formula, where Ψ is given by (7.23).
 - η_K using the previous two steps and (7.61).
 - 3:** Triangle K is marked for refinement if

$$\eta_K \geq \frac{1}{2} \max_{K \in \mathcal{P}_{(i)}} \{\eta_K\}.$$
 - 4:** From step **3** deduce a new mesh.
 - 5:** Set $i \leftarrow i + 1$ and return to step **2**.
-

Table 7.1: Adaptive mesh refinement algorithm for an advection-reaction-diffusion problem.

The global error estimate is, according to (7.44), given by

$$\eta = \left(\sum_{K \in \mathcal{P}} \eta_K^2 \right)^{1/2}.$$

As before, we denote by N_{dofs} the number of degrees of freedom and we denote by $\Theta = \frac{\eta}{\|\epsilon\|_\Omega}$ the effectivity index.

First we illustrate the performance of the error estimator in the two-dimensional case with two representative examples, where we let the domain $\Omega = (0, 1)^2$ be a unit square and the first mesh $\mathcal{P}_{(0)}$ to perform the adaptive algorithm is given in Figure 7.2.

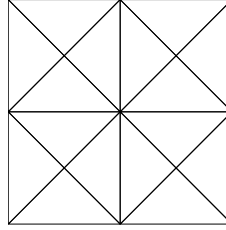


Figure 7.2: Initial mesh $\mathcal{P}_{(0)}$ for Examples 1 and 2.

Example 1: For this example we choose $\nu = \kappa = 1$ and $\mathbf{a} = [1, 1]$ and the exact solution for (7.14) is given by

$$u = xy(1-x)(1-y).$$

Example 2: For this example we let the exact solution for (7.14) be given by

$$u = y(1-y) \left(x - \frac{e^{-(1-x)/\nu} - e^{-1/\nu}}{1 - e^{-1/\nu}} \right),$$

where $\nu > 0$, $\kappa \geq 0$ and we take $\mathbf{a} = [1, 0]$.

Ndofs	13	39	116	393	1348	2868	6970	13302	33809
Θ	24.13	14.5	9.43	6.43	4.49	3.23	2.43	1.96	1.51

Table 7.2: Effectivity indices from Figure 7.4 (top).

Ndofs	13	40	119	331	883	2059	6247	12303	30873
Θ	26.36	14.33	9.11	6.25	4.43	3.2	2.41	1.95	1.5

Table 7.3: Effectivity indices from Figure 7.4 (bottom).

In Figures 7.3 and 7.4 we present the accuracy and effectivity indices for Examples 1 and 2. For Example 1 in Figure 7.3 we can see that when all the physical parameters are of order one and the solution is smooth the error estimator is very accurate. For Example 2 in Figures

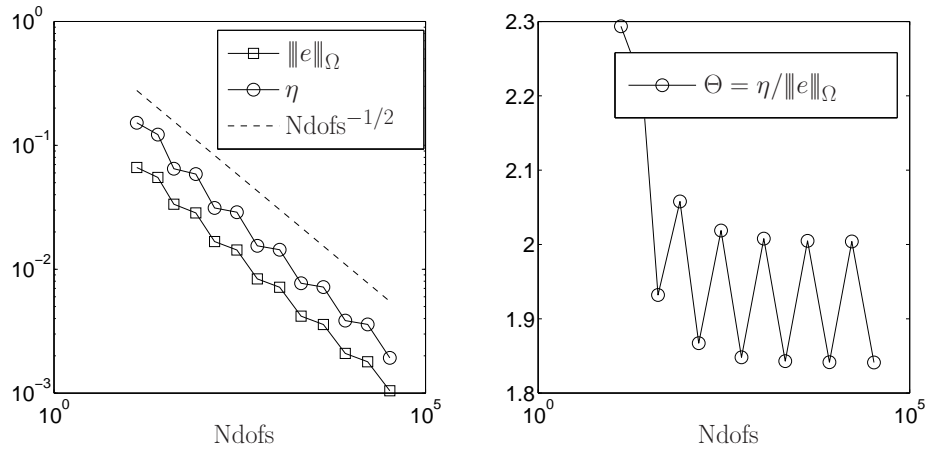


Figure 7.3: Accuracy (left) and effectivity index (right) for Example 1, using adaptive refinement over the mesh $\mathcal{P}_{(0)}$ from Figure 7.2, based on the AMRA-CDR algorithm (see Table 7.1).

7.5 and 7.6 we can see that most of the refinement is taking place in the boundary layer at $x = 1$ and when the layer is resolved we can see from Figure 7.4 and Tables 7.2 and 7.3 that the error estimator is very accurate. In Figures 7.7 and 7.8 we present the local contribution to the error indicators of the norm of the solution of the Neumann problem and the oscillation term for Example 2, where we can see that the oscillation term is negligible compared with the norm of the solution of the Neumann problem as expected.

Next, we illustrate the performance of the error estimator in the three-dimensional case, with two representative examples where we let the domain $\Omega = (0, 1)^3$ to be a unit cube and the first mesh $\mathcal{P}_{(0)}$ to perform the adaptive algorithm is given in Figure 7.9.

Example 4: We choose $\nu = \kappa = 1$ and $\mathbf{a} = [1, 1, 1]$ and the exact solution for (7.14) is given by

$$u = xyz(1-x)(1-y)(1-z).$$

Example 5: The exact solution for (7.14) is given by

$$u = yz(1-y)(1-z) \left(x - \frac{e^{-(1-x)/\nu} - e^{-1/\nu}}{1 - e^{-1/\nu}} \right),$$

where $\nu = 10^{-3}$ and we take $\kappa = 1$ and $\mathbf{a} = [1, 1, 1]$.

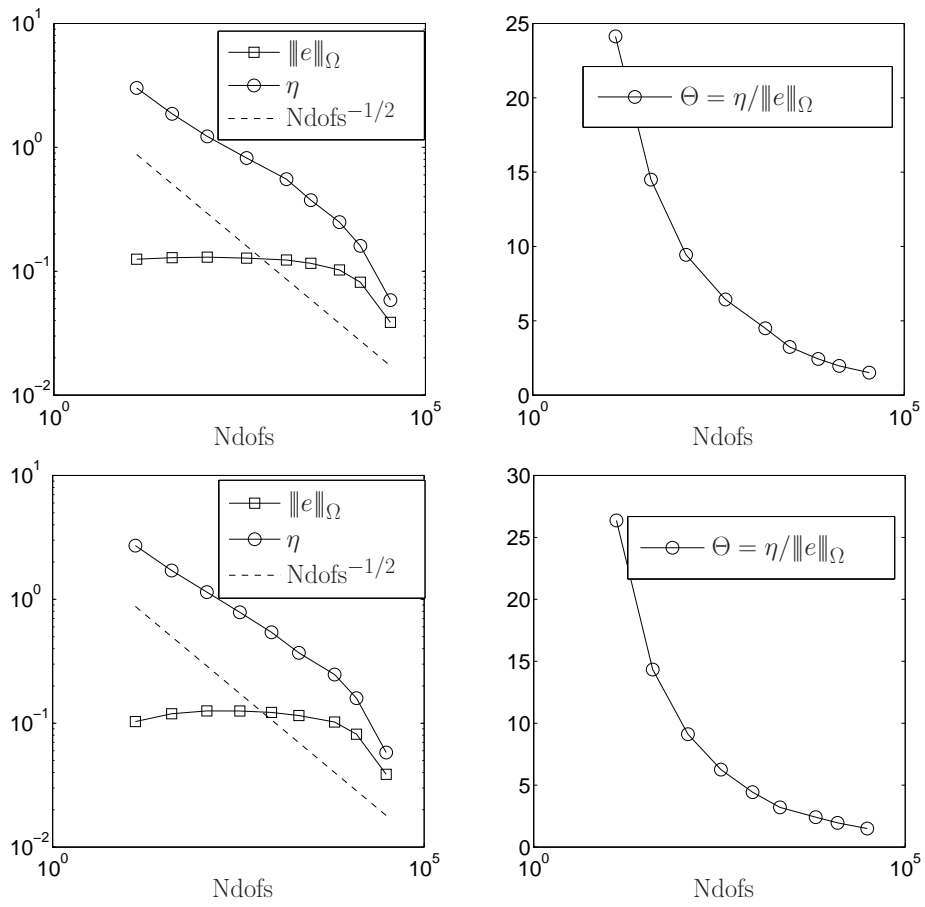


Figure 7.4: Accuracy (left) and effectivity index (right) for Example 2 taking $\nu = 10^{-3}$ and $\kappa = 1$ (top) and $\kappa = 0$ bottom, using adaptive refinement over the mesh $\mathcal{P}_{(0)}$ from Figure 7.2, based on the AMRA-CDR algorithm (see Table 7.1).

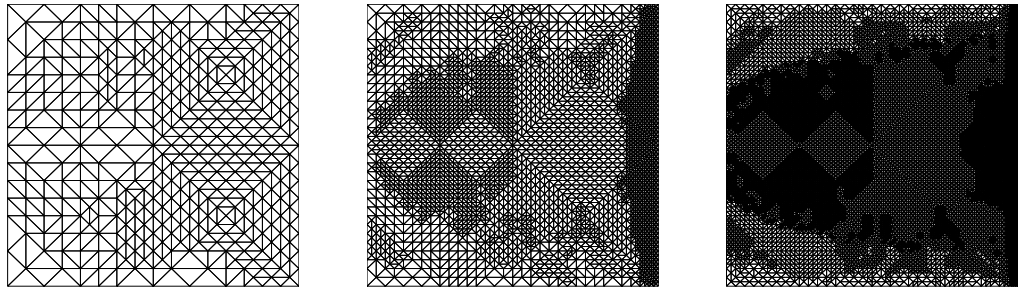


Figure 7.5: A series of adaptive refinements for Example 2 taking $\nu = 10^{-3}$ and $\kappa = 1$.

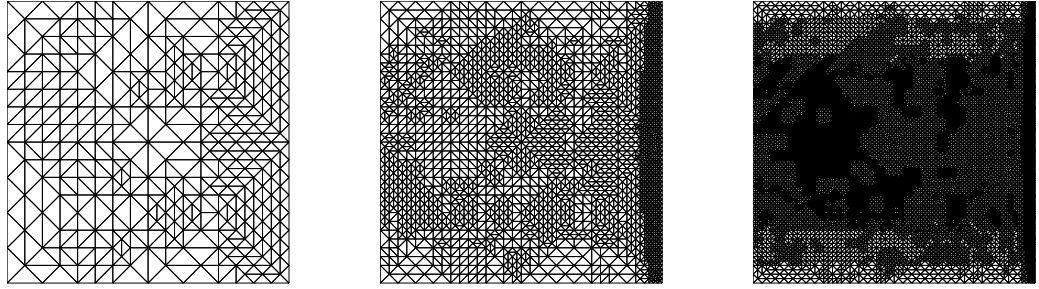


Figure 7.6: A series of adaptive refinements for Example 2 taking $\nu = 10^{-3}$ and $\kappa = 0$.

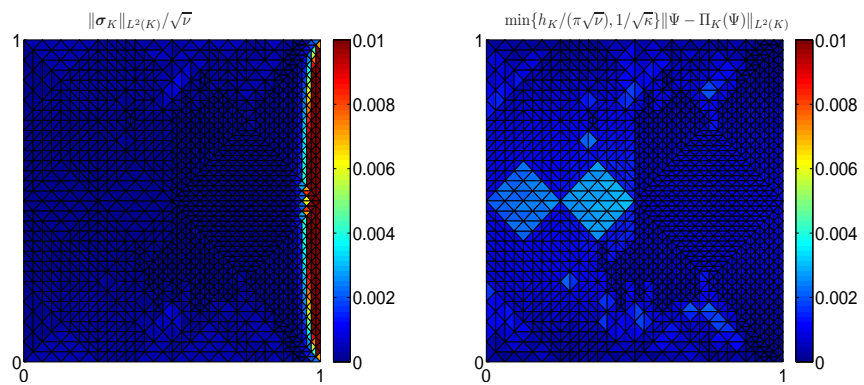


Figure 7.7: Local contribution of norm of σ_K and the oscillation term to the local error indicator for Example 2 taking $\nu = 10^{-3}$ and $\kappa = 1$ on a fixed mesh with 1678 elements.

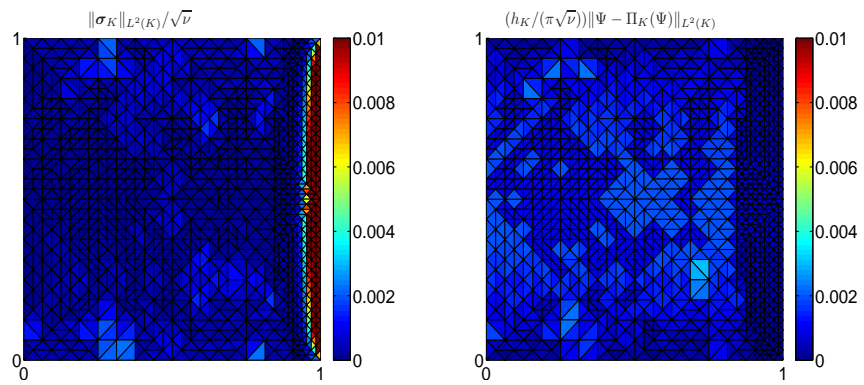
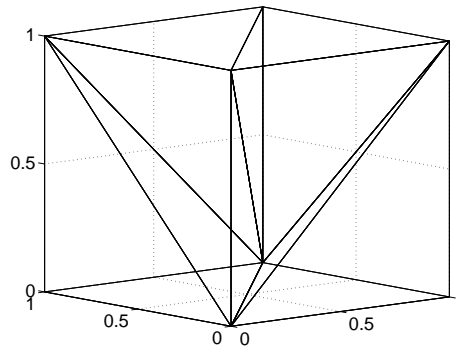
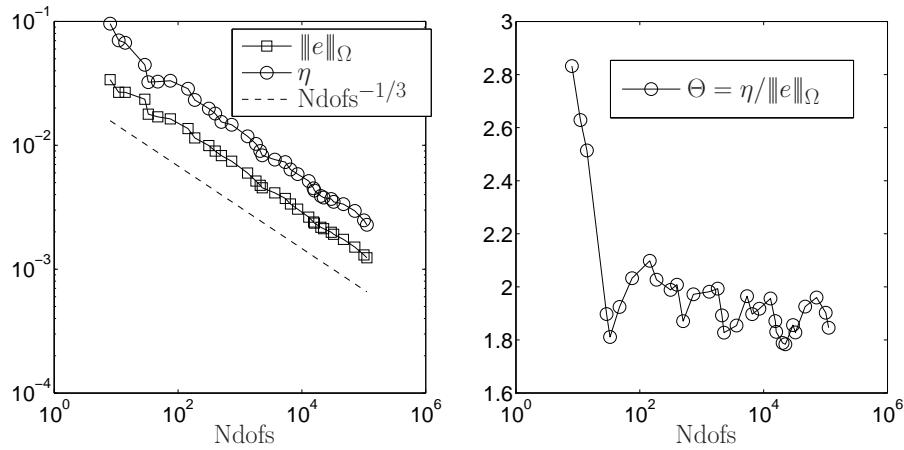


Figure 7.8: Local contribution of norm of σ_K and the oscillation term to the local error indicator for Example 2 taking $\nu = 10^{-3}$ and $\kappa = 0$ on a fixed mesh with 1678 elements.

Figure 7.9: Initial mesh $\mathcal{P}_{(0)}$ for Example 4 and 5.Figure 7.10: Accuracy (left) and effectivity index (right) for Example 4, using adaptive refinement over the mesh $\mathcal{P}_{(0)}$ from Figure 7.9, based on the AMRA-CDR algorithm (see Table 7.1).

From Figures 7.10 and 7.11 and Table 7.4 we can see that the error estimators also provides an accurate guaranteed upper bound for Example 4. This accuracy is also presented in Example 4 whenever the boundary layer is resolved.

7.11 Conclusions.

In this chapter we proposed and analysed a fully computable a posteriori error estimator, providing a guaranteed upper bound for the advection-reaction-diffusion problem discretized with a SUPG stabilized finite element method.

The results presented in this chapter are going to be presented and extended to consider

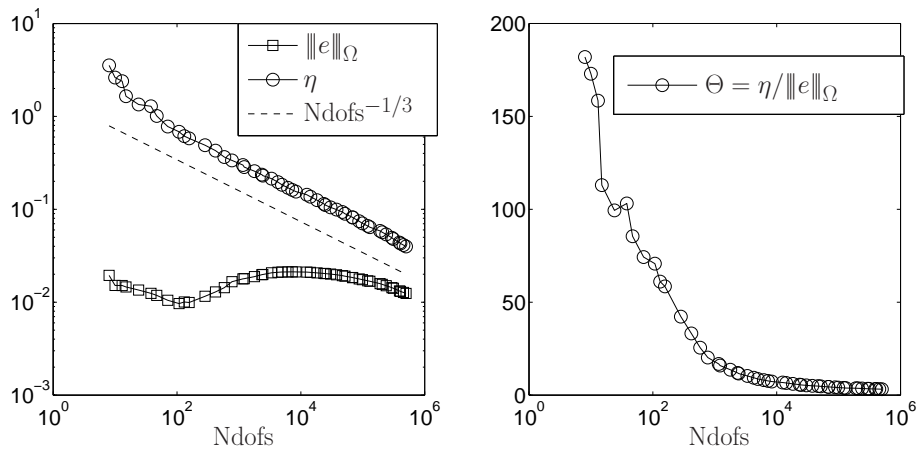


Figure 7.11: Accuracy (left) and effectivity index (right) for Example 5 taking $\nu = 10^{-3}$, using adaptive refinement over the mesh $\mathcal{P}_{(0)}$ from Figure 7.9, based on the AMRA-CDR algorithm (see Table 7.1).

Ndofs	Θ	Ndofs	Θ	Ndofs	Θ	Ndofs	Θ
8	181.97	581	25.51	12474	6.795	130097	3.82
10	172.99	771	20.22	14238	6.522	190479	3.69
13	158.46	1160	16.77	18230	6.060	205717	3.64
15	113.03	1219	15.90	23542	5.599	239152	3.56
24	99.41	1780	13.65	24783	5.467	295470	3.44
38	103.14	2339	11.91	30190	5.223	311214	3.39
47	85.47	2432	11.59	37654	5.023	390755	3.31
71	74.29	3360	10.32	46831	4.83	405401	3.27
108	70.74	4262	9.336	51533	4.70	453903	3.23
131	61.07	4950	8.683	68225	4.44	500134	3.2
157	58.48	6200	8.043	87535	4.18		
283	42.25	7249	7.623	98462	4.03		
419	33.19	8344	7.314	120094	3.89		

Table 7.4: Effectivity indices from Figure 7.11 right.

nonhomogeneous Dirichlet and Neumann conditions in [7].

Chapter 8

Conclusions and future work.

In this manuscript we have presented fully computable a posteriori error estimators, providing two-sided bounds in errors measured in energy or natural norms, for a Stokes, Poisson and an Advection-Reaction-Diffusion problems. More remarkably, the error estimators provide guaranteed fully computable upper bounds, which allows to establish a stopping criterion for adaptive refinement algorithms.

The treatment to obtain these error estimators was mainly based on the study of the error equation. In order to obtain fully computable upper bounds, the key step was to rewrite the error functionals as a local Neumann problem, for which explicit solutions can be obtained. For the Fortin–Soulie nonconforming finite element approximation this was achieved by the construction of a proper projection operator preserving constant functions. For conforming and stabilized conforming finite element approximations the equilibrated residual method allows such rewriting. Now, in the case of the Stokes problem, in order to improve the accuracy of the error estimators the gradient of the velocity field is orthogonally decomposed. Finally the local efficiency of the error estimators follows by classical bubble function arguments.

In terms of future work we would like to address the following topics:

- A study of the convergence of adaptive algorithms using our a posteriori error estimator, especially when boundary fluxes are used.
- Extend our results to anisotropic mesh adaptation and curved domains.
- Incorporate nonhomogeneous Dirichlet and Neumann conditions into the a posteriori error analysis in a more general framework.

In the case of incompressible fluid flow problems, we would also like to achieve:

- Fully computable a posteriori error estimators for Stokes/Oseen/Darcy and coupled Stokes-Darcy/Oseen-Darcy three-dimensional problems for inf-sup stable conforming and stabilized conforming finite element approximations.
- Study the time-dependent version of the previous problems.

In the case of the convection-diffusion-reaction problem, we would like to address the following topics:

- Obtain a fully computable error estimator being robust in the sense that the ratio of the upper and lower bounds should be uniformly bounded with respect to the size of the convection and dissipation coefficient and the error being measured in a pure energy norm. The method of the minimum energy extension for the equilibrated residual method, first introduced in [9], already provides a fully computable and robust error estimator for a singularly perturbed reaction-diffusion problem in [17], and it can be a starting point in order to obtain the desired robustness.
- Extend the analysis for a wider family of stabilized methods like the ones given in [73,76,81].

Finally we would like to extend the a posteriori analysis for the Navier-Stokes equations.

Bibliography

- [1] R.A. Adams. *Sobolev Spaces*. Academic Press, New York, 1975.
- [2] M. Ainsworth. Robust a posteriori error estimation for nonconforming finite element approximation. *SIAM J. Numer. Anal.*, 42:2320–2341, 2005.
- [3] M. Ainsworth. A synthesis of a posteriori error estimation techniques for conforming, non-conforming and discontinuous Galerkin finite element methods. *Contemp. Math.*, 383:1–14, 2005.
- [4] M. Ainsworth. A posteriori error estimation for discontinuous Galerkin finite element approximation. *SIAM J. Numer. Anal.*, 45:1777–1798, 2007.
- [5] M. Ainsworth. A framework for obtaining guaranteed error bounds for finite element approximations. *J. Comput. Appl. Math.*, 234:2618–2632, 2010.
- [6] M. Ainsworth, A. Allendes, G.R. Barrenechea, and R. Rankin. Computable error bounds for nonconforming Fortin–Soulie finite element approximation of the Stokes problem. *IMA J. Numer. Anal.*, to appear.
- [7] M. Ainsworth, A. Allendes, G.R. Barrenechea, and R. Rankin. Fully computable a posteriori error bounds for stabilized FEM approximation of Advection-Reaction-Diffusion problems in three dimensions. *in preparation*.
- [8] M. Ainsworth, A. Allendes, G.R. Barrenechea, and R. Rankin. On the adaptive selection of the parameter in stabilized finite element approximations. *Research Report, Department of Mathematics and Statistics University of Strathclyde, #7*, 2011.
- [9] M. Ainsworth and I. Babuška. Reliable and robust a posteriori error estimation for singularly perturbed reaction-diffusion problems. *SIAM J. Numer. Anal.*, 36:331–353, 1999.

- [10] M. Ainsworth, L. Demkowicz, and C.W. Kim. Analysis of the equilibrated residual method for a posteriori error estimation on meshes with hanging nodes. *Comp. Methods Appl. Mech. Engrg.*, 196:3493–3507, 2007.
- [11] M. Ainsworth and J.T. Oden. *A Posteriori Error Estimation in Finite Element Analysis*. Pure and Applied Mathematics, Wiley-Interscience. John Wiley & Sons, New York, 2000.
- [12] M. Ainsworth and R. Rankin. Guaranteed computable bounds on quantities of interest in finite element computations. *Int. J. Numer. Meth. Eng. (to appear)*.
- [13] M. Ainsworth and R. Rankin. Fully computable bounds for the error in nonconforming finite element approximations of arbitrary order on triangular elements. *SIAM J. Numer. Anal.*, 46:3207–3232, 2008.
- [14] M. Ainsworth and R. Rankin. Robust a posteriori error estimation for the nonconforming Fortin–Soulie finite element approximation. *Math. Comput.*, 77:1917–1939, 2008.
- [15] M. Ainsworth and R. Rankin. Guaranteed computable error bounds for conforming and nonconforming finite element analysis in planar elasticity. *Int. J. Numer. Meth. Eng.*, 82:1114–1157, 2010.
- [16] M. Ainsworth and R. Rankin. Realistic computable error bounds for three dimensional finite element analyses in linear elasticity. *Comput. Methods Appl. Mech. Engrg.*, 200:1909–1926, 2011.
- [17] M. Ainsworth and T. Vejchodský. Fully computable robust a posteriori error bounds for singularly perturbed reaction–diffusion problems. *Numer. Math.*, 119:219–243, 2011.
- [18] L. El Alaoui, A. Ern, and E. Burman. *A nonconforming finite element method with face penalty for advection-diffusion equations, Proceedings EnuMath 2005*. Numerical mathematics and advanced applications, Springer-Verlag, 2006.
- [19] L. El Alaoui, A. Ern, and E. Burman. A priori and a posteriori error estimates of nonconforming finite elements with face penalty for advection-diffusion equations. *IMA J. Numer. Anal.*, 27:151–171, 2007.
- [20] R. Araya, G. Barrenechea, and A. Poza. An adaptive stabilized finite element method for the generalized Stokes problem. *J. Comput. Appl. Math.*, 214:457–479, 2008.

- [21] R. Araya, G.R. Barrenechea, and F. Valentin. Stabilized finite element methods based on multiscale enrichment for the Stokes problem. *SIAM J. Numer. Anal.*, 44:322–348, 2006.
- [22] R. Araya, G.R. Barrenechea, and F. Valentin. A stabilized finite-element method for the Stokes problem including element and edge residuals. *IMA J. Num. Anal.*, 27:172–197, 2007.
- [23] R. Araya, E. Behrens, and R. Rodríguez. An adaptive stabilized finite element scheme for the advection-reaction-diffusion equation. *Appl. Numer. Math.*, 54:491–503, 2005.
- [24] R. Araya, E. Behrens, and R. Rodríguez. Error estimators for advection-reaction-diffusion equations based on the solution of local problems. *J. Comput. Appl. Math.*, 206:440–453, 2007.
- [25] R. Araya, A.H. Poza, and E.P. Stephan. A hierarchical a posteriori error estimate for an advection-diffusion-reaction problem. *Math. Models Methods Appl. Sci.*, 15:1119–1139, 2005.
- [26] I. Babuška and W.R. Rheinboldt. A-posteriori error estimates for the finite element method. *Internat. J. Numer. Methods Engrg.*, 12:1597–1615, 1978.
- [27] I. Babuška and W.R. Rheinboldt. Error estimates for adaptive finite element computations. *SIAM J. Numer. Anal.*, 15:736–754, 1978.
- [28] I. Babuška and T. Strouboulis. *The finite element method and its reliability*. Numerical mathematics and scientific computation. Oxford University Press, Oxford, 2001.
- [29] C. Baiocchi, F. Brezzi, and L.P. Franca. Virtual bubbles and Galerkin-least-squares type methods (Ga. L. S.). *Comput. Methods Appl. Mech. Engrg.*, 105:125–141, 1993.
- [30] W. Bangerth and R. Rannacher. *Adaptive finite element methods for differential equations*. Lectures in Mathematics ETH Zürich, Birkhäuser Verlag. Basel, 2003.
- [31] G.R. Barrenechea and F. Valentin. Consistent local projection stabilized finite element methods. *SIAM J. Numer. Anal.*, 48:1801–1825, 2010.
- [32] T. Barth, P.B. Bochev, M. Gunzburger, and J. Shadid. A taxonomy of consistently stabilized finite element methods for the Stokes problem. *SIAM J. Sci. Comput.*, 25:1585–1607, 2004.

- [33] M.A. Bebendorf. A note on the Poincaré inequality for convex domains. *Z. Anal. Anwendungen*, 22:751–756, 2003.
- [34] R. Becker and M. Braack. A finite element pressure gradient stabilization for the Stokes equations based on local projections. *Calcolo*, 38:173–199, 2007.
- [35] C. Bernardi, V. Girault, and V. Hecht. A posteriori analysis of a penalty method and application to the Stokes problem. *Math. Model. Meth. Appl. Sci.*, 13:1599–1628, 2003.
- [36] S. Berrone. Robustness in a posteriori error analysis for FEM flow models. *Numer. Math.*, 91:389–422, 2002.
- [37] P.B. Bochev, C.R. Dohrmann, and M.D. Gunzburger. Stabilization of low-order mixed finite elements for the Stokes equations. *SIAM J. Numer. Anal.*, 44:82–101, 2006.
- [38] D. Boffi, F. Brezzi, L.F. Demkowicz, R.G. Durán, R.S. Falk, and M. Fortin. *Mixed finite elements, compatibility conditions, and applications*. Springer-Verlag, 2006.
- [39] R.P. Bonet. Numerical stabilization of convection-diffusion-reaction problems. *Technical report*, 2006.
- [40] S.C. Brenner and L.R. Scott. *The Mathematical Theory of Finite Element Methods, 15 of Texts in Applied Mathematics*, volume 3. Springer-Verlag, New York, 1994.
- [41] H. Brezis. *Functional Analysis, Sobolev Spaces and Partial Differential Equations*. Springer-Verlag, New York, 2010.
- [42] F. Brezzi. On the existence, uniqueness, and approximation of saddle point problems arising from Lagrangian multipliers. *R.A.I.R.O.*, 2:129–151, 1974.
- [43] F. Brezzi and M. Fortin. *Mixed and Hybrid Finite Element Methods*. Springer-Verlag, 1991.
- [44] F. Brezzi, T.J.R. Hughes, L.D. Marini, A. Russo, and E. Süli. A priori error analysis of finite element method with residual-free bubbles for advection-dominated equations. *SIAM J. Num. Anal.*, 36:1933–1948, 1999.
- [45] F. Brezzi and J. Pitkäranta. On the stabilization of finite element approximations of the Stokes equations. *Efficient Solution of Elliptic Systems*, (W. Hackbush ed.). Braunschweig: Vieweg:11–19, 1984.

- [46] A. Brooks and T.J.R. Hughes. Streamline upwind Petrov-Galerkin formulations for convection dominated flows with particular emphasis on the incompressible Navier-Stokes equations. *Comput. Methods Appl. Mech. Engrg.*, 32:199–259, 1982.
- [47] E. Burman. A posteriori error estimation for interior penalty finite element approximations of the advection-reaction equation. *SIAM J. Numer. Anal.*, 47:3584–3607, 2009.
- [48] E. Burman and P. Hansbo. Edge stabilization for Galerkin approximations of convection-diffusion-reaction problems. *Comput. Methods Appl. Mech. Engrg.*, 193:1437–1453, 2004.
- [49] E. Burman and P. Zunino. A domain decomposition method based on weighted interior penalties for advection-diffusion-reaction problems. *SIAM J. Numer. Anal.*, 44:1612–1638, 2006.
- [50] G.F. Carey and R. Krishnan. Penalty approximation of Stokes flow. *Comput. Methods Appl. Mech. Engrg.*, 35:169–206, 1982.
- [51] C. Carstensen and J. Hu. A unifying theory of a posteriori error control for nonconforming finite element methods. *Numer. Math.*, 107:473–502, 2007.
- [52] P.G. Ciarlet. *The Finite Element Method for Elliptic Problems*. North-Holland, 1978.
- [53] R. Codina. On stabilized finite element methods for linear systems of convection-diffusion-reaction equations. *Comput. Methods Appl. Mech. Engrg.*, 188:61–82, 2000.
- [54] A. R. Conn, K. Scheinberg, and L. N. Vicente. Global convergence of general derivative-free trust-region algorithms to first and second order critical points. *SIAM J. Optim.*, 20:387–415, 2009.
- [55] A. R. Conn, K. Scheinberg, and L. N. Vicente. *Introduction to Derivative-Free Optimization*. Mps-Siam, Series on Optimization 8. 2009.
- [56] A.R. Coon, K. Scheinberg, and Ph.L. Toint. *On the convergence of derivative-free methods for unconstrained optimization*. In *Approximation Theory and Optimization, Tributes to M. J. D. Powell*, edited by M. D. Buhmann and A. Iserles Cambridge University Press, Cambridge, pages 83–108, 1997.
- [57] A.R. Coon, K. Scheinberg, and L.N. Vicente. Geometry of interpolation sets in derivative free optimization. *Math. Program., Ser. B*, 111:141–172, 2008.

- [58] M. Crouzeix and P.A. Raviart. Conforming and nonconforming finite element methods for solving the stationary Stokes equations. *RAIRO Anal. Numér.*, 7:33–76, 1973.
- [59] E. Dari, R. Durán, and Padra. Error estimators for nonconforming finite element approximations of the Stokes problem. *Math. Comp.*, 64:1017–1033, 1995.
- [60] E. Dari, R. Durán, C. Padra, and V. Vampa. A posteriori error estimators for nonconforming finite element methods. *RAIRO-Modél. Math. Anal. Numér.*, 30:385–400, 1996.
- [61] P.J. Davis. *Interpolation and Approximation*. Dover, New York, 1976.
- [62] P. Destuynder and B. Métivet. Explicit error bounds in conforming finite element method. *Math. Comp.*, 228:1379–1396, 1999.
- [63] M. Dobrowolski. On the LBB condition in the numerical analysis of the stokes equations. *Appl. Numer. Math.*, 54:314–323, 2005.
- [64] C.R. Dohrmann and P.B. Bochev. A stabilized finite element method for the Stokes problem based on polynomial pressure projections. *Int. J. Numer. Meth. Fluid*, 46:183–201, 2004.
- [65] W. Dörfler. A convergent adaptive algorithm for Poisson’s equation. *SIAM J. Numer. Anal.*, 33:1106–1124, 1996.
- [66] W. Dörfler and M. Ainsworth. Reliable a posteriori error control for nonconforming finite element approximation of Stokes flow. *Math. Comput.*, 74:1599–1616, 2005.
- [67] J. Douglas and J. Wang. An absolutely stabilized finite element method for the Stokes problem. *Math. Comput.*, 52:495–508, 1989.
- [68] K. Eriksson, D. Estep, P. Hansbo, and C. Johnson. *Introduction to adaptive methods for differential equations*. Acta numerica, 1995, Acta Numer., Cambridge Univ. Press. Cambridge, 1995.
- [69] A. Ern and J-L. Guermond. *Theory and Practice of Finite Elements*, volume 159. Springer-Verlag, New York, 2004.
- [70] A. Ern, A.F. Stephansen, and M. Vohralík. Guaranteed and robust discontinuous Galerkin a posteriori error estimates for convection-diffusion-reaction problems. *J. Comput. Appl. Math.*, 234:114–130, 2010.

- [71] M. Fortin and M. Soulie. A non-conforming piecewise quadratic finite element on triangles. *Internat. J. Numer. Methods Engrg.*, 19:505–520, 1983.
- [72] L.P. Franca, S.L. Frey, and T.J.R. Hughes. Stabilized finite element methods I: Application to the advective-diffusive model. *Comput. Methods Appl. Mech. Engrg.*, 95:253–276, 1992.
- [73] L.P. Franca and F. Valentin. On an improved unusual stabilized finite element method for the advection-reactive- diffusive equation. *Comput. Methods Appl. Mech. Engrg.*, 190:1785–1800, 2001.
- [74] V. Girault and P.A. Raviart. *Finite element methods for Navier-Stokes equations: theory and algorithms*, volume 5 of *Series in Computational Mathematics*. Springer, New York, 1986.
- [75] A. Hannukainen, R. Stenberg, and M. Vohralík. A unified framework for a posteriori error estimation for the Stokes problem. *Numer. Math.*, to appear.
- [76] G. Hauke. A simple subgrid scale stabilized method for the advection-diffusion-reaction equation. *Comput. Methods Appl. Mech. Engrg.*, 191:2925–2947, 2002.
- [77] T.J.R. Hughes and A.N. Brooks. *A multidimensional upwind scheme with no crosswind diffusion*, volume 34 of AMD. ASME. In T.J.R. Hughes, editor, *Finite Element Methods for Convection Dominated Flows*, New York, 1979.
- [78] T.J.R. Hughes, G.R. Feijoo, L. Mazzei, and J. Quincy. The variational multiscale method - a paradigm for computational mechanics. *Comput. Methods Appl. Mech. Engrg.*, 166:3–24, 1998.
- [79] T.J.R. Hughes and L.P. Franca. A new finite element formulation for computational fluid dynamics: VII. The Stokes problem with various well-posed boundary conditions: symmetric formulations that converge for all velocity/pressure spaces. *Comput. Methods Appl. Mech. Engrg.*, 65:85–96, 1987.
- [80] T.J.R. Hughes, L.P. Franca, and M. Balestra. A new finite element formulation for computational fluids dynamics: V. Circumventing the Babuška–Brezzi condition: a stable Petrov–Galerkin formulation of the Stokes problem accommodating equal-order interpolations. *Comput. Methods Appl. Mech. Engrg.*, 59:85–99, 1986.

- [81] T.J.R. Hughes, L.P. Franca, and G.M. Hulbert. A new finite element formulation for fluid dynamics: VIII. The Galerkin/least-squares method for the advection-diffusive equations. *Comput. Methods Appl. Mech. Engrg.*, 73:173–189, 1989.
- [82] V. John, P. Knobloch, and S. Savescu. A posteriori optimization of parameters in stabilized methods for convection-diffusion problems - Part I. *Comput. Methods Appl. Mech. Engrg.*, 200:2916–2929, 2011.
- [83] D Kay and D. Silvester. A posteriori error estimation for stabilized mixed approximations of the Stokes equations. *SIAM J. Sci. Comput.*, 21:1321–1336, 1999.
- [84] N. Kechkar and D. Silvester. Analysis of locally stabilised mixed finite element methods for the Stokes problem. *Math. Comp.*, 58:1–10, 1992.
- [85] K-Y. Kim. Flux reconstruction for the $P2$ nonconforming finite element method with application to a posteriori error estimation. *Preprint*, 2010.
- [86] J.L. Lions and E. Magenes. *Problèmes aux limites non-homogènes et applications*. Dunod, Paris, 1968.
- [87] R. Luce and B.I. Wohlmuth. A local a posteriori error estimator based on equilibrated fluxes. *SIAM J. Numer. Anal.*, 4:1394–1414, 2004.
- [88] Y. Maday. Relèvements de traces polynomiales et interpolations hilbertiennes entre espaces de polynômes. *C.R Acad. Sci. Paris Sér. I Math.*, 309:463–468, 1984.
- [89] P. Morin, R.H. Nochetto, and K.G. Siebert. Data oscillation and convergence of adaptive FEM. *SIAM J. Numer. Anal.*, 38:466–488, 2000.
- [90] J. Nečas. *Les méthodes directes en théorie des équations elliptiques*. Masson, Paris, 1967.
- [91] A. Papastavrou and R. Verfürth. A posteriori error estimators for stationary convection-diffusion problems: a computational comparison. *Comput. Methods Appl. Mech. Engrg.*, 189:449–462, 2000.
- [92] L.E. Payne and H.F. Weinberger. An optimal Poincaré inequality for convex domains. *Arch. Rational Mech. Anal.*, 5:286–292, 1960.
- [93] A. Quarteroni and A. Valli. *Numerical Approximation of Partial Differential Equations*. Springer-Verlag, 1994.

- [94] P.A. Raviart and J.M. Thomas. *A mixed finite element method for 2nd order elliptic problems. In Mathematical aspects of finite element methods*, volume 606 of *Lecture Notes in Math.* Springer, Berlin, 1977.
- [95] P.A. Raviart and J.M. Thomas. *Introduction á L'Analyse Numérique des Equations aux Dérivées Partielles.* Masson, 1983.
- [96] S. Repin. *A Posteriori Estimates for Partial Differential Equations.* Volume 4 of Radon series on computational and applied mathematics. Berlin, 2008.
- [97] S. Repin and S. Sauter. Functional a posteriori estimates for the reaction-diffusion problem. *C. R. Math. Acad. Sci. Paris*, 5:349–354, 2006.
- [98] H. Roos, M. Stynes, and L. Tobiska. *Robust numerical methods for singularly perturbed differential equations.* Springer Series in Computational Mathematics, Springer-Verlag, Berlin Heidelberg, 2008.
- [99] G. Sangalli. Robust a-posteriori estimator for advection-diffusion-reaction problems. *Math Comp.*, 77:41–70, 2007.
- [100] D. Silvester. Optimal low order finite element methods for incompressible flow. *Comput. Methods Appl. Mech. Engrg.*, 111:357–368, 1994.
- [101] R. Stevenson. Optimality of a standard adaptive finite element method. *Foundations of Computational Mathematics.*
- [102] G. Stoyan. Towards discrete Velté decompositions and narrow bounds for the inf-sup constants. *Comp. Math. Appl.*, 38:243–261, 1999.
- [103] R. Verfürth. *A Review of A Posteriori Error Estimation and Adaptive Mesh-Refinement Techniques.* Wiley-Teubner, Chichester, 1996.
- [104] R. Verfürth. A posteriori error estimators for convection-diffusion equations. *Numer. Math.*, 80:641–663, 1998.
- [105] R. Verfürth. Robust a posteriori error estimates for stationary convection-diffusion equations. *SIAM J. Numer. Anal.*, 43:1766–1782, 2005.

- [106] M. Vohralík. A posteriori error estimates for lowest-order mixed finite element discretizations of convection-diffusion-reaction equations. *SIAM J. Numer. Anal.*, 45:1570–1599, 2007.
- [107] M. Vohralík. A posteriori error estimation in the conforming finite element method based on its local conservativity and using local minimization. *C. R. Math. Acad. Sci. Paris*, 346:687–690, 2008.
- [108] J. Wang, Y. Wang, and X. YE. A posteriori error estimate for stabilized finite element methods for the Stokes equations. *Inter. J. Model. Comp. Inf.*, 9:1–16, 2012.